Chapter 5
Gas Flow and Transport
(Wilson, Barnard)

Gaseous releases of ^{14}C in the form of $^{14}CO_2$ are expected to be important for a partially saturated repository (see, e.g., Park and Pflum, 1990; Van Konynenburg, 1991). A significant amount of ^{14}C is in the spent-fuel inventory. In Chapter 4 it is pointed out that the radionuclide source model being used assumes rapid releases (higher than the NRC containment criterion in 10 CFR Part 60 would allow) of the highly soluble species from the EBS because of oxidation alteration of the spent-fuel matrix. ^{14}C also falls into the alteration-limited release category and, because gas transport times tend to be much shorter than water transport times, there is potential for large (in terms of EPA ratio) releases of ^{14}C to the accessible environment.

Figure 5-1 shows schematically some of the important factors that go into the gaseous flow and transport calculations.

The analysis of gaseous release and transport is very similar to the analysis of

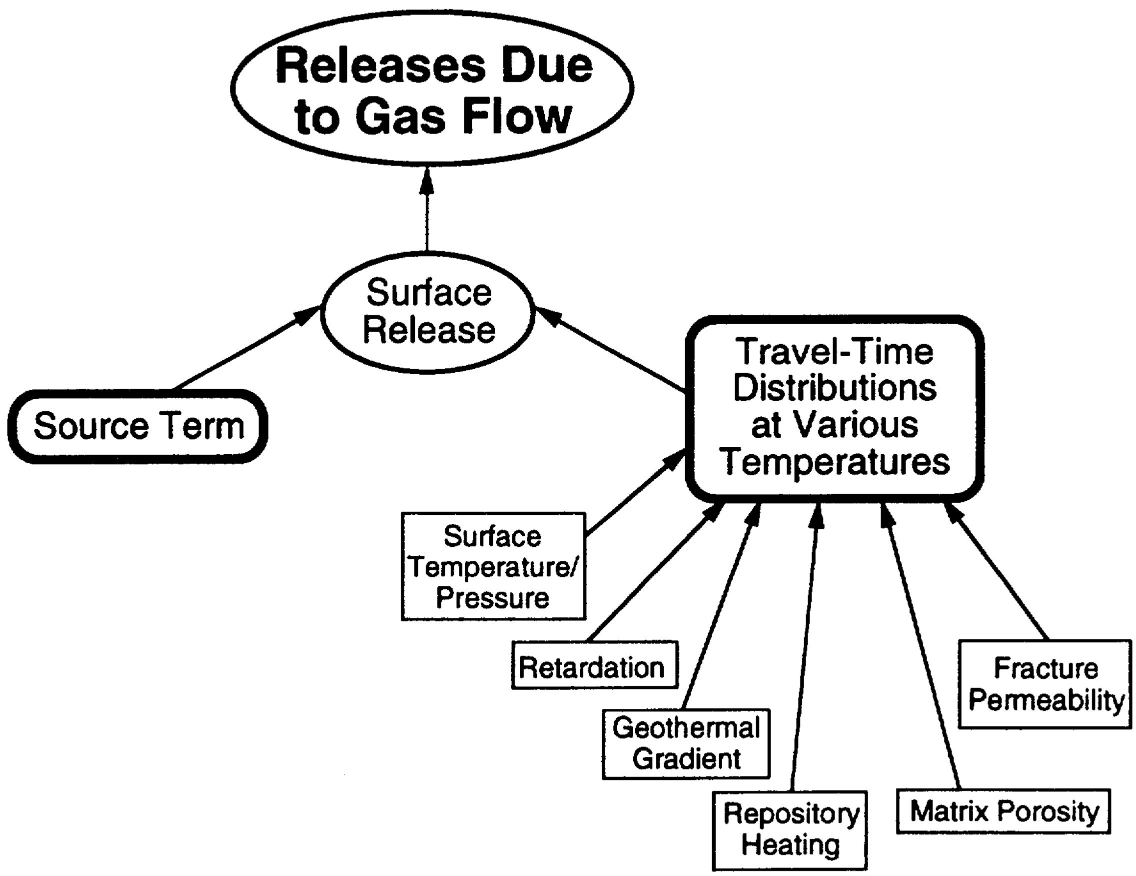

Figure 5-1. Factors included in the gas-flow problem.

aqueous release and transport in Chapter 4. Models are needed for release of ^{14}C from the EBS, for gas flow, and for transport of $^{14}CO_2$. These models are discussed in the following sections. The models are combined with probability distributions of their input parameters to generate probability distributions of the performance measures (the EPA ratio and the NRC ratio), which are then compared to the prescribed limits.

The probabilistic calculations were performed using the Monte Carlo method, in which "realizations" of the system are successively generated by random sampling from the input probability distributions. For each realization, the releases of radionuclides to the accessible environment in 10,000 years were calculated. The results from all realizations were used to determine the probability distributions of the releases.

As for aqueous releases, the Monte Carlo simulation of gaseous releases was done with the TSA computer program (Wilson et al., 1991; Wilson, 1992). A flow diagram of the method is shown in Figure 5-2. As shown in the figure, there are two separate calculations of gaseous releases, corresponding to the two conceptual models of unsaturated-zone water flow (the composite-porosity model and the weeps model—see Chapter 4). Even though water flow is not directly of interest in the gas-flow calculation, it influences the gaseous releases from the EBS because waste mobilization and release from the waste containers is dependent on contact of liquid water with the waste containers. For simplicity, the gas- and water-flow calculations in this TSPA were performed separately. In a more sophisticated treatment, gas and water flow would be coupled.

5.1 Problem development and scenario screening

The scenario describing the TSPA gas flow and transport analysis was developed from the same FEP diagram as was used for the groundwater-flow problem. The upper-level FEPs for this scenario are the same as for groundwater flow, e.g., "Distributed Infiltration" and "Imbibition into Matrix Near Surface," and are shown in Figure 4-1. As with the groundwater-flow problem, the composite-porosity and weeps models are considered to be the two mechanisms important to release of radionuclides from the EBS. All the branches of the FEP diagram in Figure 4-1 end with the FEP "Interaction with the Repository." Figure 5-3 shows the subsequent FEPs; no distinction is made here between container failure occurring in the composite-porosity model and that occurring in the weeps model.

As Figure 5-3 shows, the same two conditions for the repository—"Hot Repository" and "Cold Repository"—appear in the gas-flow FEP diagram as in the water-

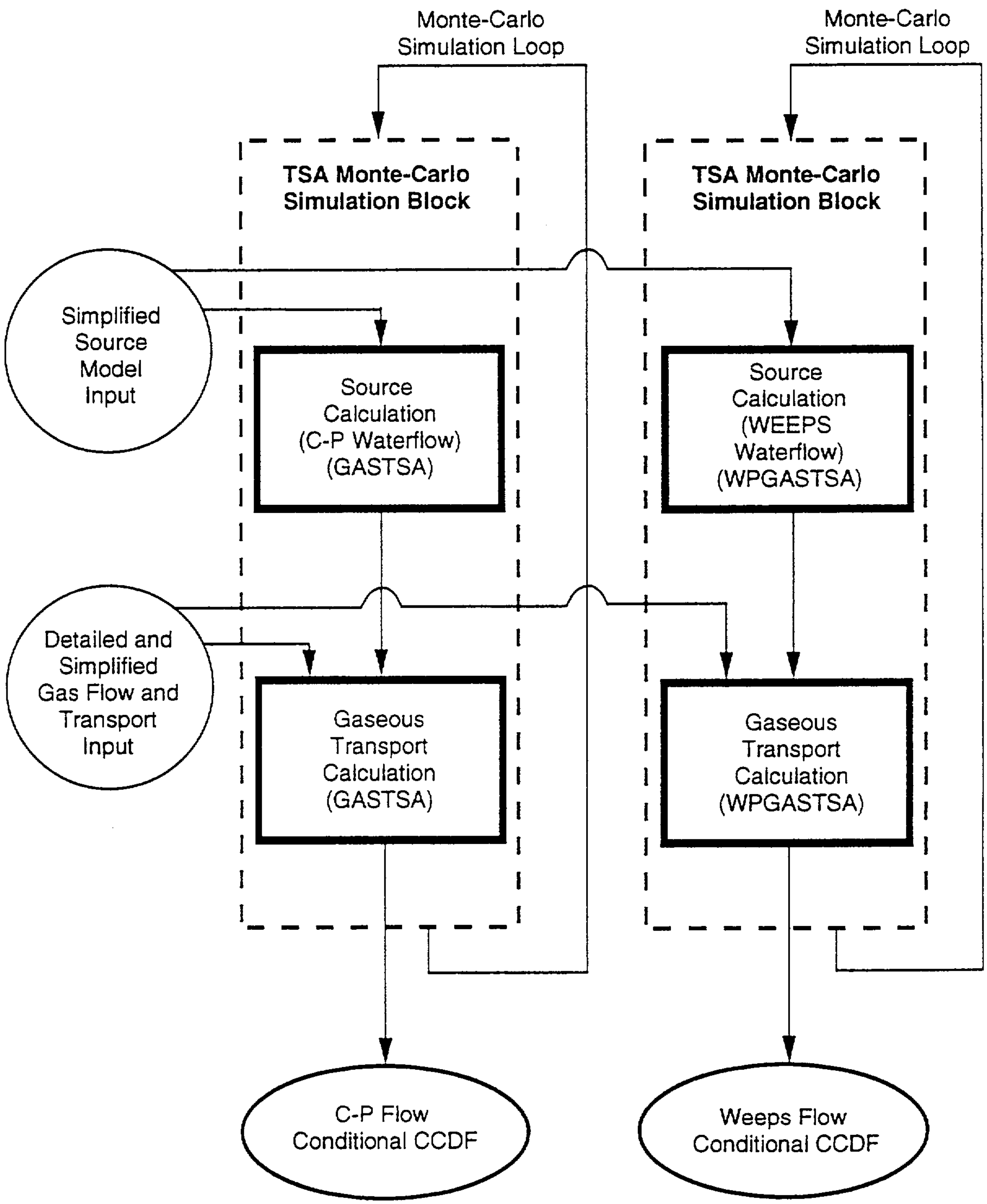

Figure 5-2. Flow diagram for the two TSA gaseous-transport simulations, one for composite-porosity water flow and one for weeps water flow. (Only the source calculations are different; the transport calculations in GASTSA and WPGASTSA are identical.)

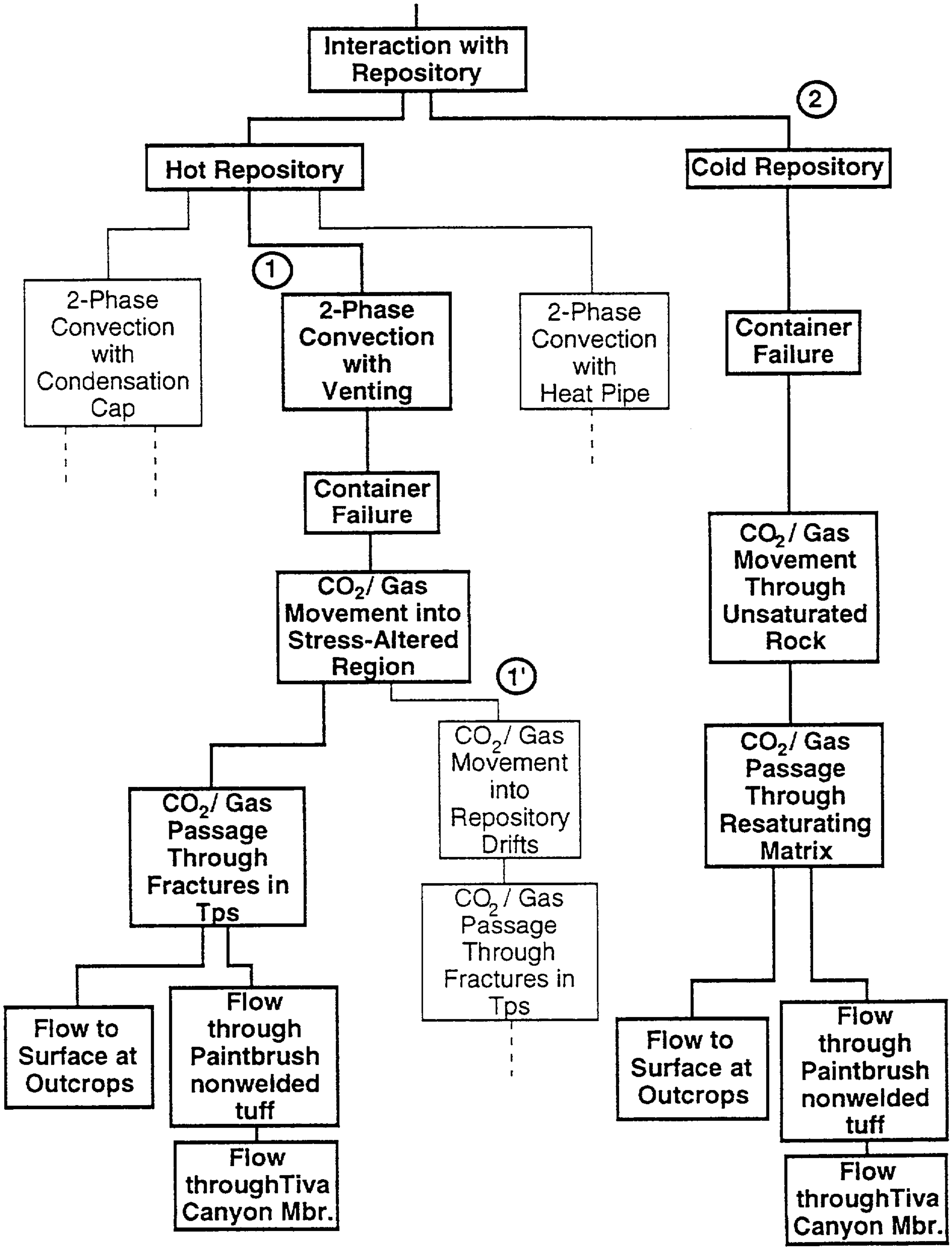

Figure 5-3. FEP diagram for nominal gas flow.

flow FEP diagrams (Figures 4-2 and 4-3). For the "Hot Repository" FEPs, the same two-phase processes are included as for groundwater flow. The gas-flow and water-flow FEPs are both part of the same FEP diagram, but Figure 5-3 shows only the gas-flow part and Figures 4-2 and 4-3 show only the water-flow part. The paths applicable to the TSPA gas-flow analysis are shown as 1 and 2 in Figure 5-3. The scenario that would most likely produce fast and large releases would occur from venting gas to the surface.

The TSPA gas-release calculation considers only the release of ^{14}C, in the form of $^{14}CO_2$. It is assumed that the $^{14}CO_2$ has formed in the spent fuel from chemical and radiolytic processes occurring since discharge of the fuel from the reactors. The gas inventory includes that available at the time the waste package is breached and that formed later due to alteration of the fuel. Gas is released to the rock surrounding the waste packages by failure of those packages. It is assumed that either unsaturated or saturated groundwater conditions could cause these failures. After a waste package is breached, the $^{14}CO_2$ escapes into the surrounding rock. The rock surrounding the waste packages will be disturbed by the construction of the repository. The most likely effect of this disturbance is to alter the stress fields such that there could be more or larger fractures. In addition, the backfilled repository drifts represent rock volumes that are considerably different from the country rock. The gas can be expected to move into this volume.

The mechanism specified in the TSPA analysis for gas to move from the repository to the surface is flow through connected fractures or faults. Flow through the Topopah Spring Formation (Tps), the Paintbrush nonwelded tuff, and the Tiva Canyon Member are listed separately because of the likely differences in the flow rates. The Paintbrush nonwelded tuff is probably much less fractured than the Tps Formation and therefore would have lower gas-flow rates. The Tiva Canyon Member is probably similar to the Tps. In addition, the Topopah Spring has outcrops in Solitario Canyon, so it is possible that some of the gas flow can avoid the Paintbrush and Tiva Canyon entirely.

The radionuclide release-vs.-time has a component for the promptly released fraction, and one for the gas released due to fuel-matrix alteration. In addition, the curve shape depends on the assumptions made about what happens to the gas when it first escapes from the waste packages. If it goes directly into the connected fractures, the release will be as described above. If it goes into the repository drifts before moving into the fractures, the prompt-release fraction can be damped, and the alteration-release fraction can occur over a longer time. This process is not considered in the TSPA analysis, but is shown in Figure 5-3 as path 1′.

5.2 Radionuclide source term for gaseous releases

The radionuclide source term for gaseous releases is essentially the same as the source term for aqueous releases, which was already described in Sections 4.3 and 4.4.4 (for composite-porosity water flow and weeps water flow, respectively). This TSPA includes two different Monte Carlo simulations of gaseous release, flow, and transport. The flow and transport calculations are the same for the two simulations, but different assumptions are used in calculating the source releases because the source model is dependent on the choice of groundwater-flow model. The parts of the source model that are the same as given in Chapter 4 will not be repeated; only the additional information needed to complete the specification of the gaseous source term will be presented.

Table 5-1 gives inventory and general information for ^{14}C in spent fuel. The data sources are the same as given previously for Table 4-1 and additionally Park and Pflum (1990). Note that ^{14}C is the only radionuclide considered to be transported in gaseous form (Van Konynenburg, 1989). In the release calculations, there is no attempt to distinguish between gaseous and aqueous mobilization of ^{14}C in the waste container. One of the basic assumptions in the transport calculations is that carbon dioxide in the air is in equilibrium with bicarbonate in the water (and other aqueous carbon species; at the pH of groundwater in Yucca Mountain, bicarbonate is expected to be the predominant form of dissolved carbon). This implies that, whether the ^{14}C is initially released in gaseous or aqueous form, it will quickly come to equilibrium and be transported primarily via the gas flow. This assumption will be discussed more fully in the next section.

The inventory figures in Table 5-1 could be high. Van Konynenburg (1991) re-examined the assumptions of Roddy et al. (1986) regarding ^{14}C production during reactor operation, and he suggested the following revised inventory numbers

Table 5-1. Some ^{14}C data.

Quantity	Value
Inventory (Ci/MTHM)	1.54
Inventory in fuel matrix (Ci/MTHM)	0.58
Inventory in cladding (Ci/MTHM)	0.51
Inventory in assembly hardware (Ci/MTHM)	0.45
Half-life (yr)	5729
Activity (Ci/mol)	62.4
NRC limit (Ci/MTHM-yr)	1.67×10^{-5}
EPA limit (Ci/MTHM)	0.1
Release type	alteration-limited

(his figures for PWR and BWR inventories have been combined in a 60%/40% ratio, consistent with the other inventory numbers used for this study): fuel-matrix inventory, 0.58 Ci/MTHM (unchanged); cladding inventory, 0.26 Ci/MTHM (about half the value in Table 5-1); and assembly-hardware inventory, 0.17 Ci/MTHM (about 38 percent of the value in Table 5-1). Van Konynenburg's revised inventories were not adopted for this TSPA, but should be considered for use in future TSPA studies.

Aside from the gaseous nature of the ^{14}C releases, the other major difference between ^{14}C releases and releases of the other nuclides being modeled (see Table 4-1) is that ^{14}C has a significant fraction of its inventory outside the fuel pellets. As shown in the table, there are significant amounts of ^{14}C in the fuel-rod cladding and in the fuel-assembly hardware in addition to the UO_2 fuel matrix. As already mentioned in Section 4.3, ideally there would be source submodels to describe releases from the cladding and the fuel-assembly hardware, but they are not included at the present time. For this TSPA, the releases from cladding and hardware were neglected except for the important quick-release part of the cladding releases (Park and Pflum, 1990; Wilson, 1991). It should be reasonable to neglect these releases because they should be small compared to releases from the fuel matrix (Wilson, 1991, estimated the time scales for releases from cladding and fuel-assembly hardware to be greater than 60,000 yr—much greater, in the case of cladding releases—whereas the fuel-matrix-alteration time scale used in this study to determine the rate of releases from the fuel matrix varies from 1,000 yr to 20,000 yr—see Table 4-2).

The quick-release fraction of the ^{14}C inventory comes from an oxidation layer on the surface of the fuel-rod cladding (Van Konynenburg et al., 1985, 1987). The ^{14}C comes off in gaseous form and is available for release as soon as the waste container has failed (release does not require cladding failure because it is on the outside of the cladding). The quick-release inventory of ^{14}C should be released earlier than the gap/grain-boundary inventory, but the source model being used has no provision for including the cladding as a barrier (i.e., the cladding-failure time is being neglected), so for these calculations the quick-release ^{14}C and the gap/grain-boundary ^{14}C were lumped together into the "prompt" inventory fraction f_p. It is uncertain how much of the ^{14}C inventory might come off in the initial pulse upon container failure, but a recent review by Park and Pflum (1990) suggests that it might be as much as 5 percent of the ^{14}C inventory. The gap/grain-boundary fraction is also uncertain, but the aqueous-release calculations assumed it to be 2 percent. For compatibility, 2 percent was also assumed for ^{14}C, but only 2 percent of the fuel-matrix portion rather than 2 percent of the whole inventory.

As a result of the assumptions discussed above, the following numbers were adopted. The quick-release fraction of the ^{14}C inventory was assumed to vary between 0.5 percent and 5 percent of the total inventory; i.e., between 0.0077 Ci/MTHM and 0.077 Ci/MTHM, since a total inventory of 1.54 Ci/MTHM is being assumed (Table 5-1). The gap/grain-boundary fraction was assumed to be 2 percent of the fuel-matrix inventory of 0.58 Ci/MTHM; this amount comes to 0.012 Ci/MTHM. The combination of quick-release and gap/grain-boundary inventories thus varies from 0.019 Ci/MTHM to 0.089 Ci/MTHM. The fuel-assembly-hardware part of the inventory (0.45 Ci/MTHM) is neglected entirely and most of the cladding inventory (0.51 Ci/MTHM) is also neglected, except for the quick-release part of the cladding inventory. The total modeled ^{14}C inventory consists of the matrix part (0.58 Ci/MTHM) plus the quick-release part (from 0.0077 Ci/MTHM to 0.077 Ci/MTHM), so the ^{14}C inventory varies from 0.58 Ci/MTHM to 0.65 Ci/MTHM. The prompt fraction is the quotient of the combined quick-release and gap/grain-boundary inventories, and the total inventory; therefore, the prompt fraction varies from 0.03 to 0.14 ($0.019/0.58 \approx 0.03$ and $0.089/0.65 \approx 0.14$). Uniform probability distributions were used and a correlation was built into the sampling so that if a high prompt fraction was chosen for a realization then a high value for the inventory was also chosen. This information is summarized in Table 5-2.

The source-term calculation proceeds exactly as described in Sections 4.3 and 4.4.4, with the following exception: The time scales for transport out of the waste container ($t_{i,t,x}$, where $i = 0, 1, 2$ and $x = s, d, c, dm$, or dw) are set to zero. That is, the amount of time it takes the ^{14}C to get out of the waste container after it has been mobilized is neglected. This change is not significant because the transport times, as defined in Section 4.3, are small in most cases anyway, so that the other time scales (for container failure, for fuel-matrix alteration, etc.) determine the behavior. The reason for making the change is that the time for gas to get out of a waste container is probably small compared to the time for liquid to get out of a waste container. Some work has been done on modeling diffusion of gases, including carbon dioxide, out of a breached waste container (Light et al., 1990; Pescatore,

Table 5-2. Probability distributions assumed for ^{14}C inventory.

Model parameter	Distribution	Distribution parameters[a]	Mean value
^{14}C inventory, I_0 (Ci/MTHM)	uniform	0.58, 0.65	0.0615
^{14}C prompt fraction, f_p	uniform	0.03, 0.14	0.085

Note: a rank correlation of 0.9 was assumed between I_0 and f_p.

[a] Parameters for the uniform distribution are minimum, maximum.

1990), but that work generally assumes that the container is mostly intact except for a few pinholes or cracks. That assumption is not consistent with the assumptions made for the aqueous-release source model in Section 4.3, where the waste container as a barrier was neglected after failure. To be consistent, it is neglected here, for gaseous releases, as well. Clearly, though, future work should include more realistic container models for both aqueous and gaseous releases.

5.3 The gas-flow model

Benjamin Ross and his coworkers at Disposal Safety Incorporated have been developing a gas-flow model of Yucca Mountain under contract to Sandia National Laboratories. The most comprehensive calculations to date of gas flow within Yucca Mountain are reported by Ross et al. (1992). The TSPA calculation of ^{14}C transport uses their results directly. In this section, an overview of the gas-flow model and its major assumptions will be given; a discussion of how those results are used within the TSA will be given in the following section.

The Ross et al. computer model, called TGIF, is a two-dimensional, steady-state model of gas flow within Yucca Mountain. The major assumptions that go into the gas-flow model are:

- Thermodynamic equilibrium exists among air, water vapor, and water.
- The gas is saturated with water vapor.
- Changes in partial pressure of water vapor are accommodated by changes in gas composition, with the total pressure remaining nearly constant.
- Molecular diffusion resulting from gradients of water-vapor partial pressure has a negligible effect on gas flow.
- The porous matrix and fractures could be treated together as an equivalent porous medium.
- The presently available results assume steady-state conditions. There are at least two important implications of this assumption. First, there must be a steady water source (presumably surface infiltration) to replenish the water that the moist underground air carries out into the atmosphere. Second, atmospheric temperature, humidity, and pressure are assumed constant (in time, not in space) in the calculations. The diurnal and annual variations are neglected and average values are used.

See Ross et al. (1992) for additional details.

In addition to describing the model, Ross et al. present results of a series of detailed calculations of gas flow in Yucca Mountain, both under ambient conditions and with a repository present, providing additional thermal driving force. For the detailed calculations that were made, four east-west cross-sections were used. Figure 5-4 shows a plan view of the potential repository area with a grid superimposed. The four east-west grid lines that cross the potential repository area indicate the locations of the four model cross-sections. Figures 5-5 through 5-8 show the four cross-sections. The most important features affecting the gas flow are:

- The assumed repository. Repository heating is very important in driving the gas flow.
- The layer of nonwelded tuff, labeled PTn in the figures. It is between two layers of welded tuff labeled TSw and TCw; TSw corresponds to "welded" in Figure 4-16. The nonwelded tuff probably has lower permeability than the welded tuff because it is not as heavily fractured. Because of the lower permeability it could act as a confining layer, slowing flow to the surface.
- The surface topography. Under ambient conditions, the temperature, humidity, and pressure differences between the atmosphere and the subsurface gas are important in driving the gas flow. At high repository temperatures, repository-induced thermal driving tends to overwhelm the topographic effects, but they are never negligible.

The lower boundary of the welded tuff (TSw in the figures) is used as the lower boundary of the calculational mesh because there is probably a permeability reduction there, too, leading to little gas flow downward into the nonwelded tuff. The western boundary of the calculational mesh is at the trough of Solitario Canyon, which is probably a natural flow boundary; the eastern boundary of the calculational mesh is set far away from the assumed repository so that that boundary condition will have little effect on the solution near the repository.

Figures 5-9 and 5-10 show examples of the calculational results for the predicted gas-flow pathlines, Figure 5-9 for ambient conditions and Figure 5-10 for a repository heated to a uniform temperature of 330 K (approximately 30 K above ambient). The calculations show air being drawn in at lower elevations and then expelled at higher elevations. Repository heating can cause large convection cells to form. In the simulations shown, the permeability of the nonwelded tuff (shown as a narrow shaded band) was set to 1 percent of the permeability of the welded

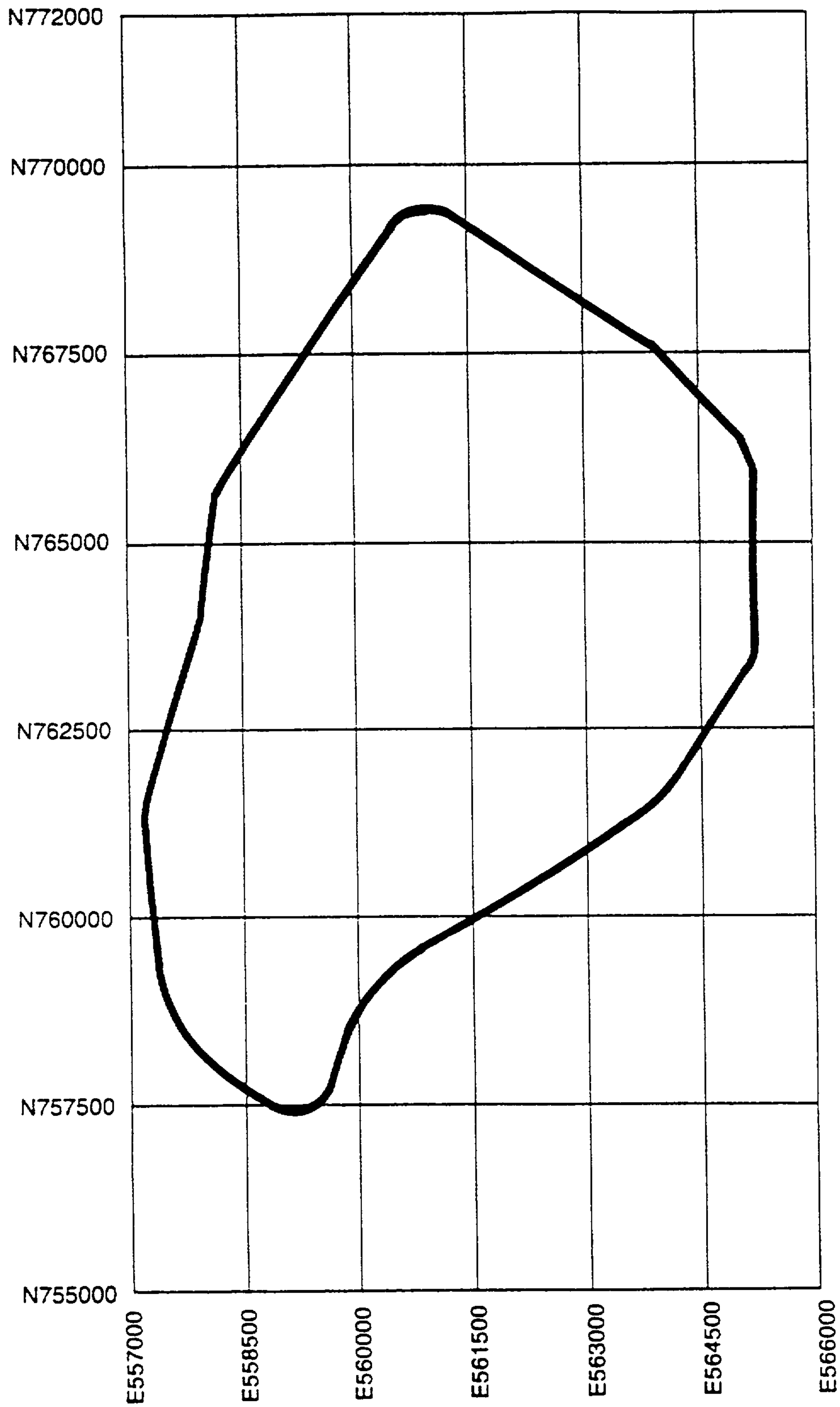

Figure 5-4. Map of the repository (taken from Figure 6-1 of Ross et al., 1992).

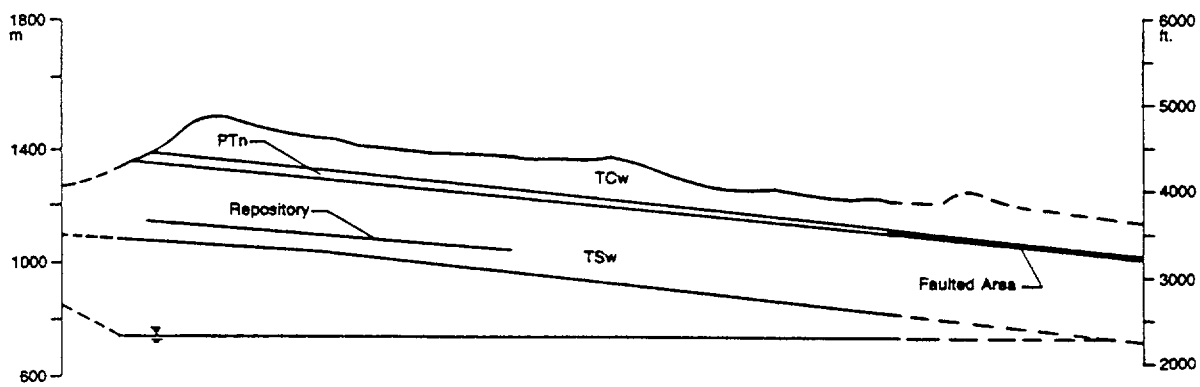

Figure 5-5. Geometry of cross-section N760000 (taken from Figure 6-2 of Ross et al., 1992).

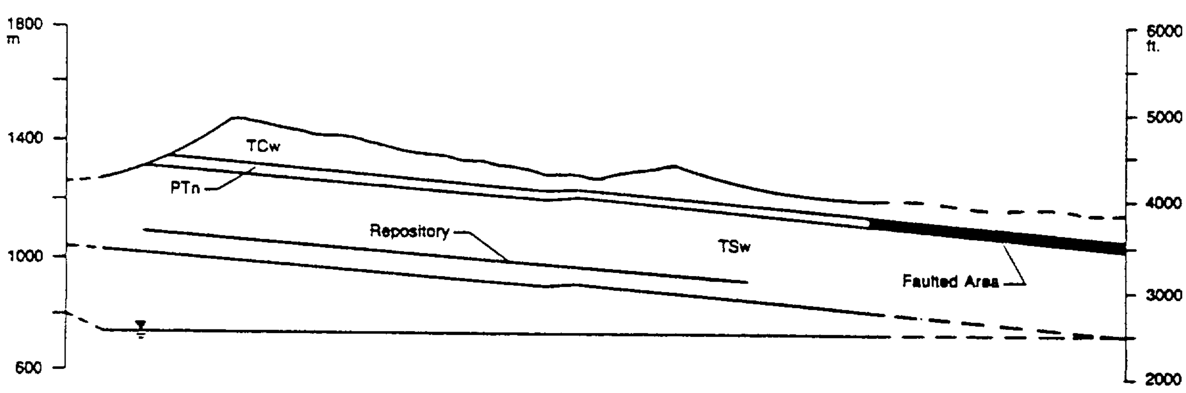

Figure 5-6. Geometry of cross-section N762500 (taken from Figure 6-3 of Ross et al., 1992).

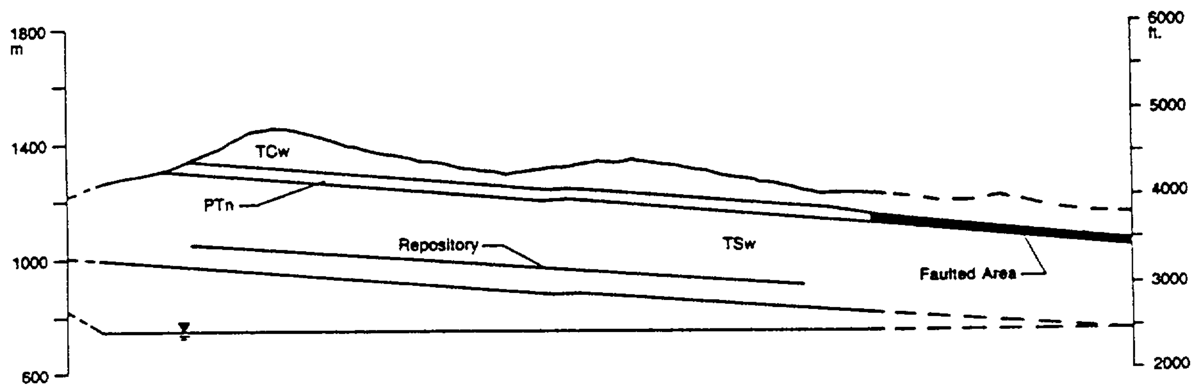

Figure 5-7. Geometry of cross-section N765000 (taken from Figure 6-4 of Ross et al., 1992).

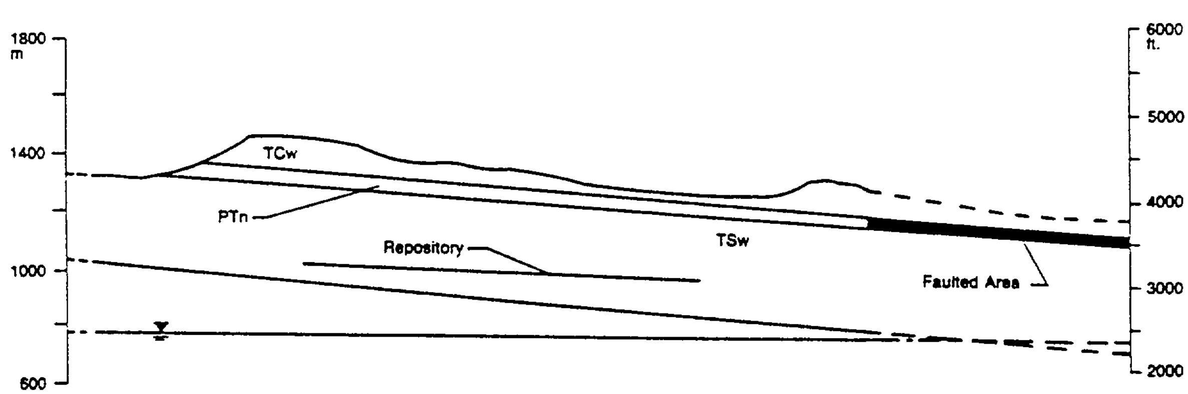

Figure 5-8. Geometry of cross-section N767500 (taken from Figure 6-5 of Ross et al., 1992).

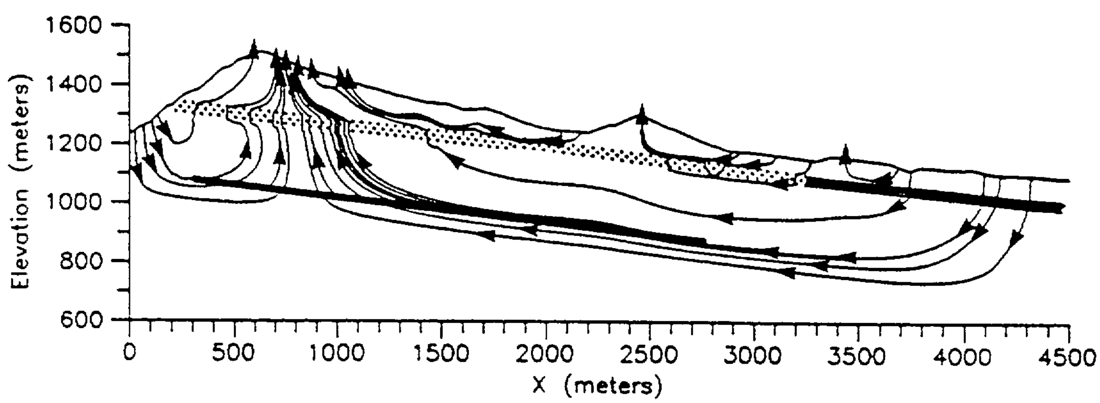

Figure 5-9. Path lines with ambient temperature and nonwelded/welded permeability ratio of 0.01 (0.1 in faulted area). Cross-section N762500. (Taken from Figure 6-13 of Ross et al., 1992.)

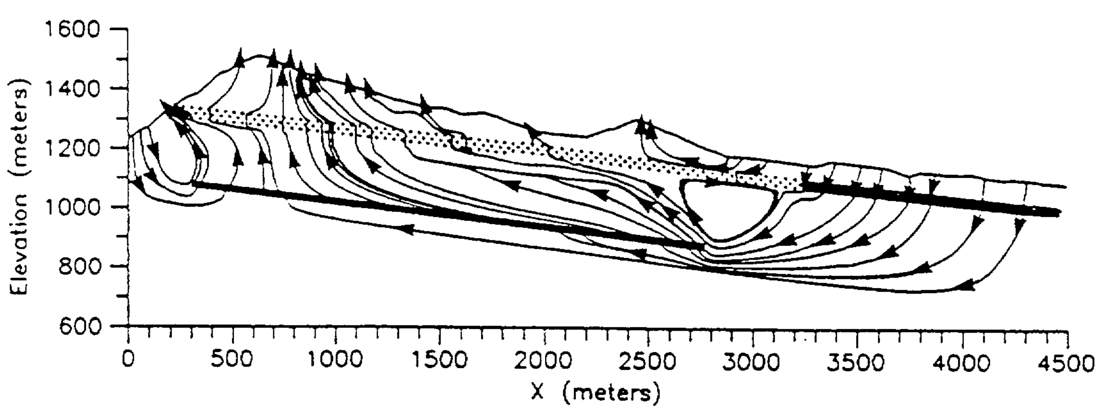

Figure 5-10. Path lines with the repository heated to 330 K and nonwelded/welded permeability ratio of 0.01 (0.1 in faulted area). Cross-section N762500. (Taken from Figure 6-14 of Ross et al., 1992.)

tuff. This choice is somewhat arbitrary, and simulations were also performed using other values for the permeability ratio (Ross et al., 1992; Lu et al., 1991). The results for permeability ratio of 1 percent were used as the base case in the transport calculations described in the next section. This choice was made because Thorstenson (1991) observed that naturally occurring ^{14}C abundances differ above and below the nonwelded unit (at drill hole USW UZ-1), which implies that the air-flow systems above and below are fairly independent. In the simulations, the nonwelded layer is fairly effective as a semi-confining layer that separates the mountain into two flow systems, but more so as the permeability ratio decreases. Thorstenson's measurements of ^{14}C abundance also provide some qualitative validation of the gas-flow model, because the measurements found ^{14}C abundances of a fourth to a half of the modern abundance, and the calculated ^{14}C travel times for ambient conditions are a few times the half-life of 5700 yr. Permeability will be discussed more later, but for now let us note that the gas-flow equations used are linear in the permeability, so the absolute value does not affect the pathlines shown in Figures 5-9 and 5-10, but only the relative values for the different layers.

Additional considerations enter into the calculation of transport of carbon dioxide to the surface. The ^{14}C travel time from repository to surface is sensitive to the permeability values chosen for the rock layers and to the assumptions made concerning geochemical retardation, so those two topics will be discussed next. Note that transport of ^{14}C is assumed to be entirely by advection; i.e., diffusion is neglected. With the values used for permeability, this assumption is reasonable, but if a much lower value were used for permeability then it would be necessary to include diffusion.

Montazer et al. (1986) measured air permeabilities in two boreholes, USW UZ-1 and UE-25a#4. The permeabilities were derived from an analysis of air-pressure fluctuations in the boreholes; they represent large-scale field measurements and should be applicable to the large-scale flow calculations of interest. Values of 7×10^{-13} m^2, 8×10^{-13} m^2, and 1×10^{-11} m^2 in the Topopah Spring welded unit and 2×10^{-11} m^2 in the Tiva Canyon welded unit were reported. Ross et al. adopted a value of 10^{-11} m^2 for their calculations. Thordarson (1983) reported a permeability of 1×10^{-12} m^2 for Topopah Spring welded tuff, from pump tests on well J-13, where the Topopah Spring unit is in the saturated zone (these are also large-scale field measurements, but less applicable because of possible differences between the saturated zone and the unsaturated zone). Tsang and Pruess (1987) made site-scale gas-flow calculations for Yucca Mountain. They used a permeability of 2×10^{-14} m^2, but the source of that number was not stated. Buscheck and Nitao (1988), in a study of hydrothermal effects for EBS design, used a permeability of 3×10^{-13} m^2, but the origins of the number are unclear. The mean of the distribution used for fracture permeability (the matrix permeability being negligible in comparison) of the "welded" layer in the water-flow calculations for this TSPA is 5×10^{-14} m^2. (To calculate this value requires information on fracture conductivity from Table 3-14 and information on fracture density from Table 3-23.) In using different permeability in this chapter than in the previous chapter we are not necessarily being inconsistent, because the appropriate value for unsaturated water flow could be different from the appropriate value for gas flow. Such a difference could occur because the gas flow is primarily through the largest fractures while the water flow is primarily through smaller fractures. It is important to reconcile these numbers in the future, though, by acquiring more data on the distribution of fracture apertures. Clearly, there is quite a bit of uncertainty about the correct permeability to use. In the TSPA calculations, this uncertainty is partially taken into account by use of a "retardation/permeability factor" that will be discussed in the next section.

The permeability of the nonwelded layer is also important to the calculation of ^{14}C travel time. As mentioned earlier, Ross et al. made calculations for several values of the nonwelded/welded permeability ratio, but we have adopted as our base case the simulations that had a nonwelded permeability that was 1 percent of the welded permeability, or 10^{-13} m^2. Montazer et al. (1986) reported permeability values for the Paintbrush nonwelded unit from 2×10^{-14} m^2 to 7×10^{-12} m^2. It was decided that for this TSPA no variations on the permeability ratio would be included, so all of our gas-release results assume that the nonwelded tuff has a permeability two orders of magnitude smaller than the welded tuff. Variations on this parameter are left to future work.

For retardation, Ross et al. made some theoretical calculations of the geochemistry of carbon dioxide in air in equilibrium with bicarbonate in water. They found retardation factors in the range of 30 to 75, depending on the type of tuff and the temperature (see Figure 5-11). They used the calculated temperature-dependent retardation factors in their calculation of travel times for ^{14}C from repository to surface. There are several uncertainties in the retardation-factor calculation, including uncertainty about the dominant chemical reactions, uncertainty about the water composition in the unsaturated zone, and uncertainty about the pH of unsaturated-zone water. Also, it has been suggested that precipitation of calcite could provide a significant retardation factor (Codell and Murphy, 1992) and it is quite possible that there is some sorption of the carbon dioxide on the rock in addition to the reaction with the water; strong sorption has been observed on iron and aluminum oxides

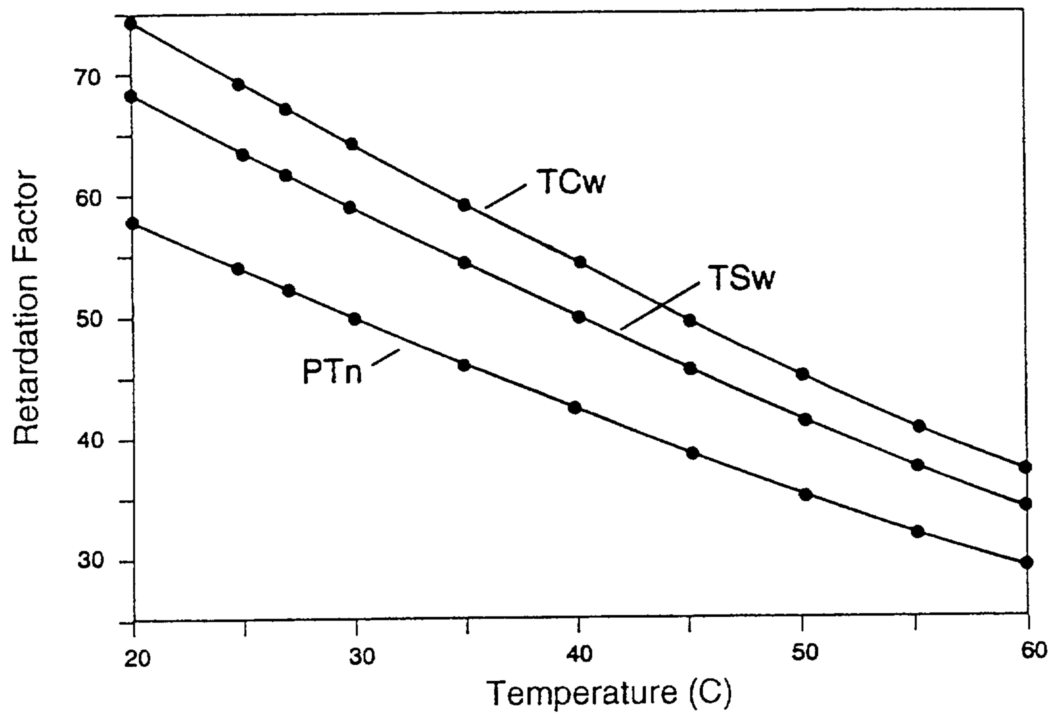

Figure 5-11. Retardation factor as a function of temperature for all units (taken from Figure 4-2 of Ross al., 1992).

(Russell et al., 1975; Schulthess and McCarthy, 1990). The amount of uncertainty in retardation is unclear, but some account of the uncertainty will be taken in defining the "retardation/permeability factor" referred to above.

5.4 Adaptation of gas flow and transport for the TSA

The method used in the TSA for calculating gaseous releases has been described briefly elsewhere (Wilson, 1992); it will be presented in somewhat more detail here. The gaseous transport calculation is based directly on results from Ross et al. (1992). That report includes distributions of ^{14}C travel time from the repository to the earth's surface calculated using the gas-flow model described in the previous section. The report includes travel-time distributions for three steady-state repository temperatures, 300 K (ambient temperatures), 315 K, and 330 K. Ross et al. have also calculated the travel-time distribution for 360 K; those results are not included in the report, but were used for this study along with the other three distributions. The four travel-time distributions are shown in Figure 5-12. It can be seen that the travel-time distribution is bimodal—the cumulative distribution function rises, then levels off, then rises again. The first rise (or lower travel times) represents ^{14}C that originates near the western end of the repository and has a relatively short travel

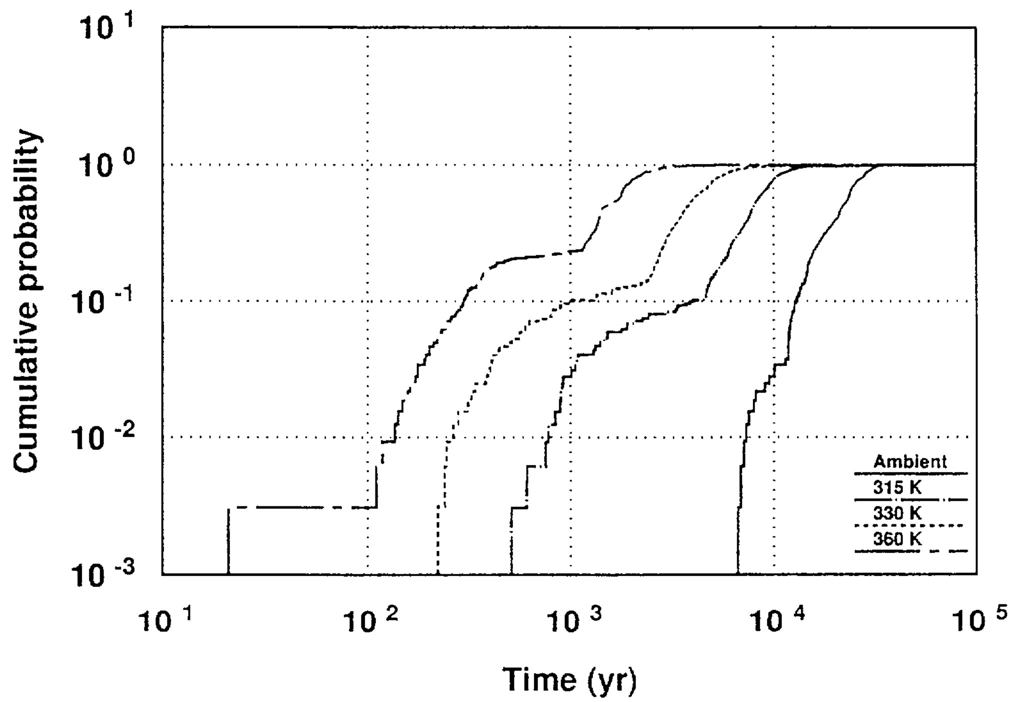

Figure 5-12. The four ^{14}C travel-time distributions.

path out the face of Solitario Canyon without having to go through the nonwelded layer. See the short pathlines at the left of Figure 5-10. Note also that Figure 5-9, for ambient conditions, has none of those short pathlines, and correspondingly the first mode in the ambient curve of Figure 5-12 occurs at a lower cumulative probability and is much less prominent than it is in the heated-repository curves. The second mode, which contains most of the probability in all four cases, represents the majority of the ^{14}C, which has longer pathlines and has to go through the nonwelded layer to reach the surface.

A number of approximations are necessary to use these results for a calculation of ^{14}C release in the TSA. The repository temperature is not in steady state, but declines slowly with time as the radioactivity decays away. To represent this process with four steady-state travel-time distributions entails a certain amount of error. To mitigate this error, approximations were made in such a way as to err on the conservative side (that is, in such a way as to increase releases). The first step was to identify the points in time corresponding to the four repository temperatures. This was accomplished by using results of Tsang and Pruess (1987). The Tsang and Pruess results are not directly comparable to the Ross et al. results because a number of different assumptions were made. In particular, as has already been mentioned, Ross et al. use a value of gas permeability that is three orders of magnitude higher than that used by Tsang and Pruess (for the welded tuff; Tsang and Pruess used the same permeability for welded and nonwelded tuff). The higher permeability leads to higher gas velocities in the Ross et al. calculations. One effect of the higher velocities should be a greater rate of repository cooling, so that for a given time the Tsang and Pruess temperature is expected to be higher than the Ross et al. temperature would be. Therefore, associating the Ross et al. temperatures with the Tsang and Pruess temperatures is inconsistent, but should be conservative. (Conservative because the temperature at a given time is taken to be higher than it would be if the temperature were calculated using the Ross et al. values, and higher temperatures imply higher gas velocities and therefore shorter ^{14}C travel time to the surface.) It is possible that repository cooling is primarily dominated by heat conduction through the rock, in which case the Tsang and Pruess temperature could be a good approximation of the Ross et al. temperature.

The temperature history of the repository, as reported by Tsang and Pruess (1987) is shown in Figure 5-13. Also shown in the figure is a dashed line indicating the temperature history assumed for the TSPA gas-release calculations. Since ^{14}C travel-time distributions were only available for four temperature values, the dashed line is a "stair-step" curve. The 360-K travel-time distribution was used from the beginning of the calculation until a time of 2400 yr, the 330-K distribution was used from 2400 yr until 4800 yr, and the 315-K distribution was used after 4800 yr. If calculations were extended beyond 10,000 yr, the 300-K distribution would be used for times past 10,000 yr. It would be preferable to have distributions for additional temperatures so that the temperature discretization would not be as gross, but by always taking the travel-time distribution from a higher temperature than is expected at a given time, conservatism is maintained. The first part of the calculation may not be entirely conservative, since the Tsang and Pruess temperature goes above 360 K for a time. However, the transport calculation is conservative in another way, too. The temperature field should be declining with time rather than remaining constant. The decline in temperature has two effects: (1) During the course of transport from repository to surface, temperatures could decline significantly; the method being used for the transport calculations instead assumes that the temperature field remains fixed as it was at the time of release. This choice was made only for pragmatic reasons—travel-time distributions including effects of cooling *en route* were not available. (2) Using steady-state temperature profiles overestimates the spatial extent of the temperature field. That is, when the repository temperature is at 360 K, the high-temperature region has not spread out as far from the repository

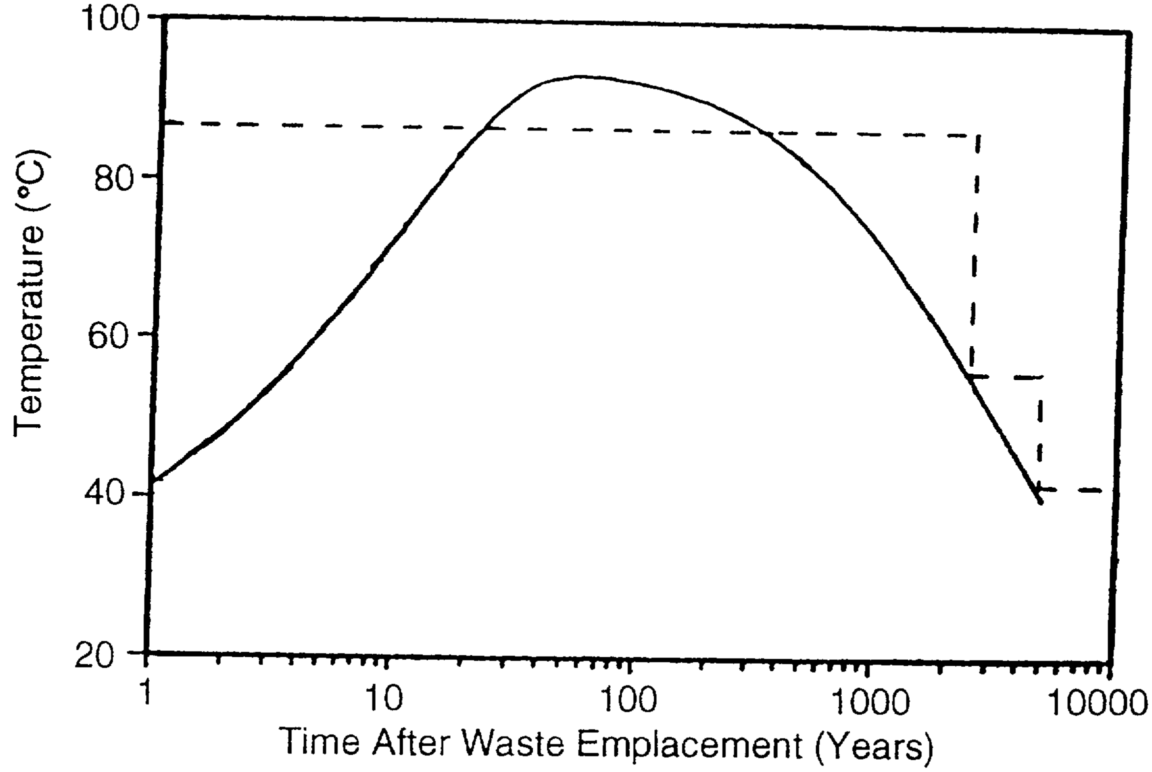

Figure 5-13. Temperature vs. time after waste emplacement at the center of the repository (taken from Figure 4 of Tsang and Pruess, 1987). Dashed line shows the TSA approximation.

as a steady-state temperature field with the repository at 360 K. The consequence of this effect is similar to that of the first effect: the ^{14}C, during its migration to the surface, should see lower temperatures than we are assuming. This shortcoming is another result of using steady-state calculations to determine the travel-time distributions.

The calculation of ^{14}C gaseous release proceeds as follows. The release rate from the source, $\Sigma(\tau)$, is calculated using the radionuclide source model described in Section 5.2; τ is the time of release from the source. At each time τ, there is a distribution of travel times, $P(t;\tau)$, where t is the travel time to the surface (see Figure 5-12). Of the ^{14}C released at time τ, the fraction that escapes to the atmosphere within the EPA time period is calculated as an integral over the travel-time distribution. The formula used for the calculation can be written as

$$R = \int_0^T d\tau \, \Sigma(\tau) \int_0^{T-\tau} dt \, P(t;\tau) e^{-\lambda t} \, , \tag{5.1}$$

where R is the cumulative release to the accessible environment, T is the EPA time period (10,000 yr), and λ is the decay rate of ^{14}C. As indicated in the equation and as discussed above, the travel-time distribution P depends on the release time τ. P

is normalized so that $\int_0^\infty P(t;\tau)\,dt = 1$.

In calculating the integral over the travel-time distributions, the distributions were regarded as discrete rather than continuous. That is, each of the four travel-time distributions consisted of a list of 323 ^{14}C travel times; rather than do some sort of smoothing or interpolation, the travel-time density function was taken to be a sum of 323 delta functions. (This is why the cumulative distribution functions in Figure 5-12 are stair-steps instead of smooth curves.) Then, for example,

$$\int_0^T P(t;\tau)e^{-\lambda t}\,dt = \sum_{n=1}^{N} \tfrac{1}{323}e^{-\lambda t_n} \ , \tag{5.2}$$

where $\{t_n, n = 1,\ldots,323\}$ are the calculated travel times for release-time τ, and $\{t_n, n = 1,\ldots,N\}$ are the travel times smaller than T (only travel times t between 0 and T contribute to the integral.)

To take into account the uncertainties in permeability and retardation discussed in the previous section, a "retardation/permeability factor" is introduced; let us denote the factor by F. This factor is a multiplication factor for the travel-time distributions. The travel times are directly proportional to the retardation factor (remember, though, that the retardation is not a simple constant; see Figure 5-11) and inversely proportional to the permeability (permeability is not a simple constant, either, but varies from geologic unit to geologic unit). The factor F represents the deviation from the "base" values:

$$F = (R/R_b)\cdot(k_b/k) \ , \tag{5.3}$$

where R is the retardation factor, R_b is the base retardation factor, k is the permeability, and k_b is the base permeability. If the retardation is multiplied by some factor everywhere and the permeability is multiplied by some other factor everywhere, then F is the ratio of those two factors. F is used by multiplying all the travel times by it. For example, for the travel-time distribution $\{t_n, n = 1,\ldots,323\}$ of Equation 5.2, the adjusted travel-time distribution would be $\{Ft_n, n = 1,\ldots,323\}$.

We wanted to assign a distribution to F that would represent the uncertainty in k and R. A log-uniform distribution from 0.5 to 10 was chosen. The reason for selecting a maximum of 10 is that some of the field-measured permeability values for the Topopah Spring welded tuff are as small as about one tenth of the base value of 10^{-11} m^2. It could be that the lower values (longer travel times) are more representative, but additional data are needed. For now, a log-uniform distribution is used to represent the great uncertainty. The lower bound of 0.5 for F is less based on hard data; it is intended to represent the possibility of retardation factors lower than the base values. (Also, the permeability could be higher than the base value.) In fact, higher retardation factors are probably more likely than lower ones, and if ^{14}C retardation is better quantified in the future it could move the F distribution upward.

The important factors going into the gas flow and transport calculation are summarized in Table 5-3.

5.5 Results

For each of the conceptual models of groundwater flow, composite-porosity and weeps, a Monte Carlo simulation of 1000 realizations was performed, using the models and parameter distributions described above. For the gaseous-release calculations associated with composite-porosity water flow, the repository was not divided into six columns, as it was for the aqueous-release calculations (Section 4.4.2). For both gaseous-release simulations, the repository was treated as a whole.

The conceptual model of groundwater flow enters in because interaction of groundwater with the waste containers could be an important element in the mobilization of ^{14}C. The "quick-release" part of the ^{14}C inventory can be released without water being present (Van Konynenburg et al., 1985, 1987), and the fuel-matrix alteration process that liberates the ^{14}C in the UO_2 matrix could be able to proceed without water being present (but perhaps at a lower rate; little is known about the effect of water on the matrix-alteration rate). Regardless of whether water is important to ^{14}C mobilization, it certainly is important to the processes that lead to container failure.

Figure 5-14 shows the conditional CCDFs for normalized gaseous releases to the accessible environment for the two Monte Carlo simulations. Aqueous releases in the weeps model were higher than in the composite-porosity model (Figure 4-44), so it is

Table 5-3. Probability distributions assumed for ^{14}C transport.

Model parameter	Distribution	Distribution parameters[a]	Mean value
Base permeability for welded (m^2)	—	—	10^{-11}
Base permeability for nonwelded (m^2)	—	—	10^{-13}
Base retardation factors	see Figure 5-11		
Times for 360-K travel-time dist. (yr)	—	0 to 2400	—
Times for 330-K travel-time dist. (yr)	—	2400 to 4800	—
Times for 315-K travel-time dist. (yr)	—	4800 to 10,000	—
Times for 300-K travel-time dist. (yr)	—	over 10,000	—
Retardation/permeability factor, F	log-uniform	0.5, 10	3.2

[a] Parameters for the log-uniform distribution are minimum, maximum.

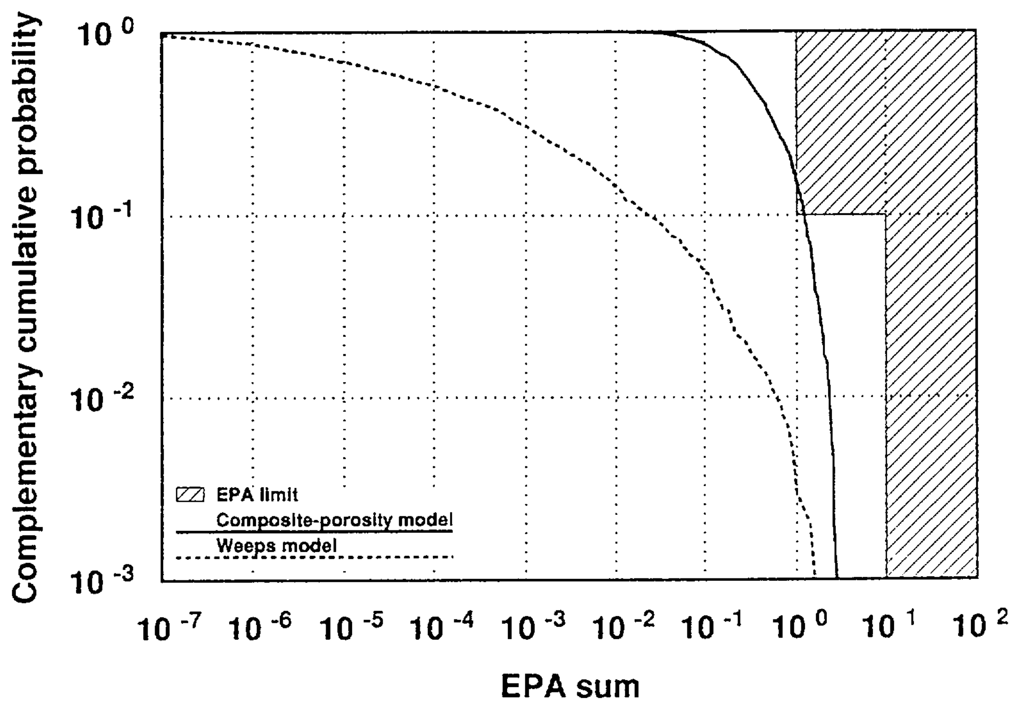

Figure 5-14. Conditional CCDFs for gaseous releases. Shown are the distributions for the composite-porosity model and for the weeps model.

surprising at first that for gaseous releases they are reversed—gaseous releases in the composite-porosity model are higher than in the weeps model. The reason for this has already been mentioned in another context in Section 4.7: In the weeps model it is assumed that only a subset of waste containers is contacted by flowing water, and only that subset fails and releases radionuclides. In the composite-porosity model, more waste containers are contacted by water and fail, releasing radionuclides. In realizations with high values of the fuel-matrix alteration rate, it is possible for all of the ^{14}C to be released from the waste containers within 10,000 yr and for most of it to be released to the surface. It is also possible for all waste containers to be contacted by water and release all of their ^{14}C in a weeps realization, but with the parameter distributions being used (see Table 4-5) the probability of that occurrence is fairly low.

It can be seen from Figure 5-14 that the calculated gaseous releases assuming the composite-porosity water-flow model exceed the 1985 EPA limits (represented by the shaded region). This result should be kept in perspective. Remember that, for this first attempt at a total-system performance assessment, a number of conservative assumptions have been made. Some of the assumptions (e.g., neglecting the container and cladding as barriers in the source-release calculation, using the simple stair-step approximation of repository temperature in the transport calculation) are merely pragmatic and could be handled better in future calculations as better modeling capabilities are developed. Other assumptions (e.g., use of the simple matrix-alteration model of waste mobilization, use of a mean water flux of 1 mm/yr) require additional data to determine their validity or to determine the appropriate parameter values. In cases like these, we often feel that the choices made were conservative, but we will not know for sure until more data become available.

Some additional information helps to provide a better understanding of the results. Figure 5-15 shows the CCDFs for NRC ratio (ratio of peak release rate from the EBS to the NRC release-rate limit in 10 CFR 60.113). It can be seen that the NRC release-rate limit is exceeded almost 80 percent of the time for the composite-porosity model and about 3 percent of the time for the weeps model (with the assumptions used). This shows that source release rates are relatively high. This clearly shows that the source model being used is overly conservative; these high NRC ratios could be reduced to a more realistic estimate by improving the model. Some possibilities for improvement include improved modeling of the container and cladding barriers, applying different container-failure distributions to "wet" and "moist" containers, and determining whether the matrix-alteration model of waste mobilization is correct. Note also that the percolation-rate distribution assumed could be unrealistically high for the composite-porosity model (see Section 4.7.1), which increases composite-porosity releases by putting more waste containers in "wet" conditions. It is likely that, if the number of high NRC ratios were reduced, then the number of high EPA sums would be reduced, so that the composite-porosity curve in Figure 5-14 would no longer exceed the EPA limits. To complete the discussion of the NRC containment requirements of 10 CFR 60.113, note that the "substantially complete containment" requirement is met because the source model being used has no releases before 300 yr.

Figure 5-16 shows conditional CCDFs for gaseous releases from the EBS and gaseous releases to the accessible environment (i.e., without and with transport to the surface included) assuming the composite-porosity water-flow model. The corresponding curves for the weeps water-flow model are shown in Figure 5-17. In these figures, the curves for releases to the accessible environment are the same as the curves in Figure 5-14. Figures 5-16 and 5-17 show that little is gained by the transport to the surface. The ^{14}C travel times are too short to reduce the releases significantly. As was mentioned in the description of the transport calculations in the preceding section, a number of approximations were made (using the Tsang and Pruess temperature history when the Ross et al. temperatures would probably be

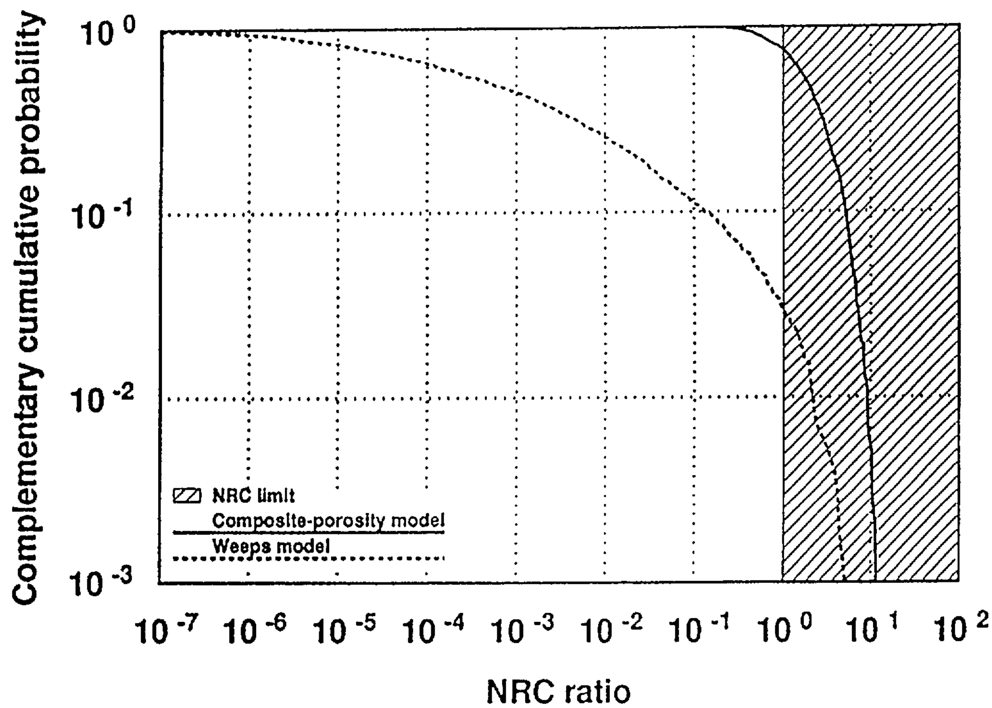

Figure 5-15. Probability distributions of the NRC ratio, calculated for the composite-porosity model and for the weeps model.

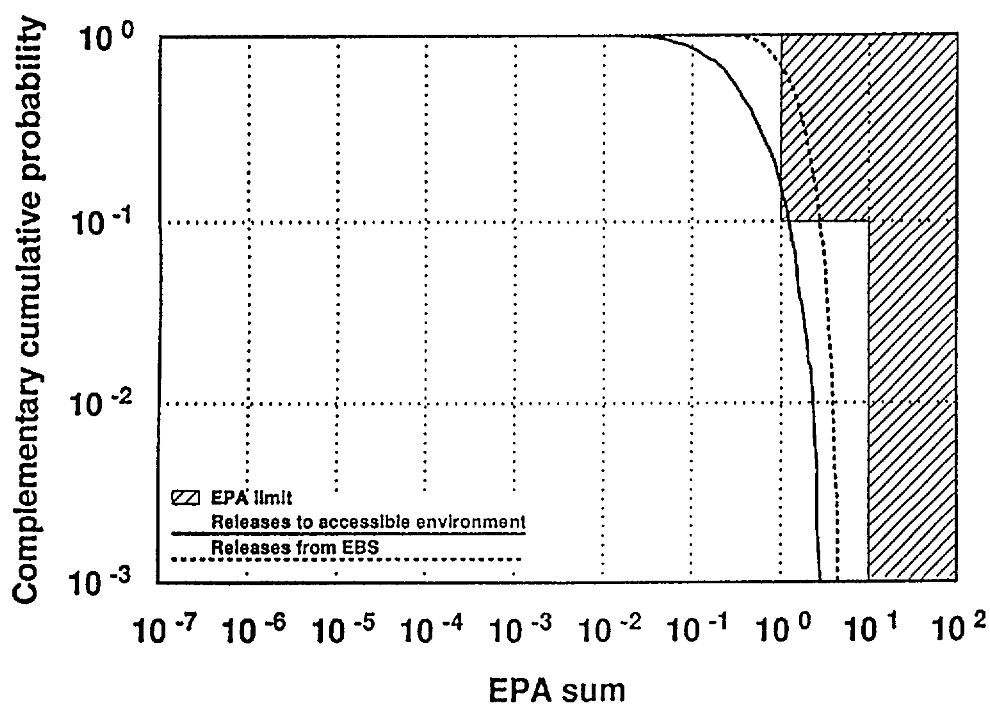

Figure 5-16. Conditional CCDFs for gaseous releases, calculated using the composite-porosity model for water flow. Shown are partial EPA sums calculated using releases from the EBS and releases to the accessible environment.

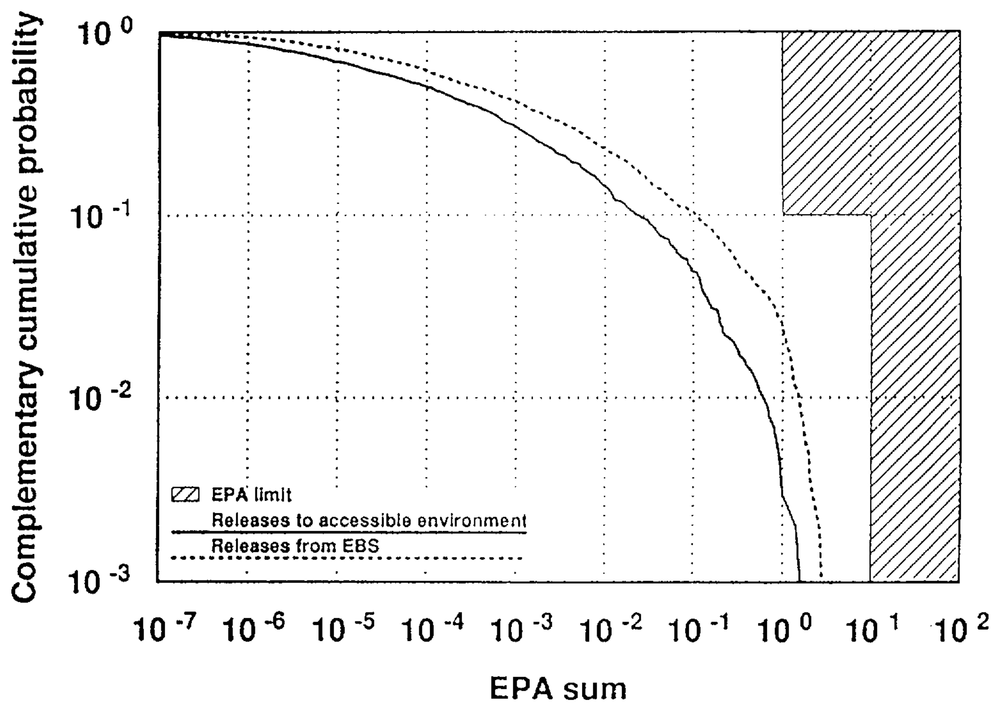

Figure 5-17. Conditional CCDFs for gaseous releases, calculated using the weeps model for water flow. Shown are partial EPA sums calculated using releases from the EBS and releases to the accessible environment.

lower, using a ^{14}C travel-time distribution for a higher temperature at each time, using travel-time distributions calculated for steady-state conditions), each of them in such a way as to overestimate the releases. Refining the transport model would undoubtedly reduce the EPA ratios for releases to the accessible environment (which would increase the separation between the EBS and accessible-environment curves), but there is probably much more potential for reducing the EPA ratios by refining the source model (which would move both curves to the left).

To conclude, Park and Pflum (1990) and Van Konynenburg (1991) have argued that, for a partially saturated repository, it will be difficult (i.e., expensive) to meet the EPA and NRC release criteria for ^{14}C, because heavy reliance must be placed on the EBS to reduce ^{14}C releases. They also point out that even the entire ^{14}C inventory would be negligible compared to the natural ^{14}C background. From the results presented in this section, it seems quite likely that more realistic release and transport models for ^{14}C would reduce releases to the accessible environment to below the EPA limits. To reduce EBS release rates below the NRC limit could require adding additional barriers to ^{14}C releases in the EBS. However, such considerations should be studied using more realistic release models than were used here.

5.6 Analysis of the average case

To go along with the average-case aqueous-release calculations reported in Section 4.8, corresponding calculations were made for gaseous releases. As stated before, the "average" case is the case for which all the parameters are assigned the means of their respective probability distributions; it is not intended to represent the expected state of a repository at Yucca Mountain. The reasons for investigating the average case are given in Section 4.8. The results are shown in Figures 5-18 through 5-23. Gaseous releases were only calculated for 20,000 yr rather than for 10^6 yr as the average-case aqueous calculations were. Nothing is lost by this reduction because the half-life of ^{14}C is only 5700 yr, which means that most of it will decay away within 20,000 yr. (The average-case aqueous calculations were extended to such a large time so that the peak release rates to the accessible environment could be observed for some of the nuclides. The peak release rate for ^{14}C occurs within 20,000 yr.) The "wiggles" in the accessible-environment-release curves (Figures 5-18 and 5-19) are artificial, caused by the switches from one ^{14}C travel-time distribution to another. These switches occur at 2400 yr, 4800 yr, and 10,000 yr (see Table 5-3).

As with the probabilistic calculations, releases are higher for the composite-porosity model than for the weeps model. For the composite-porosity model, the

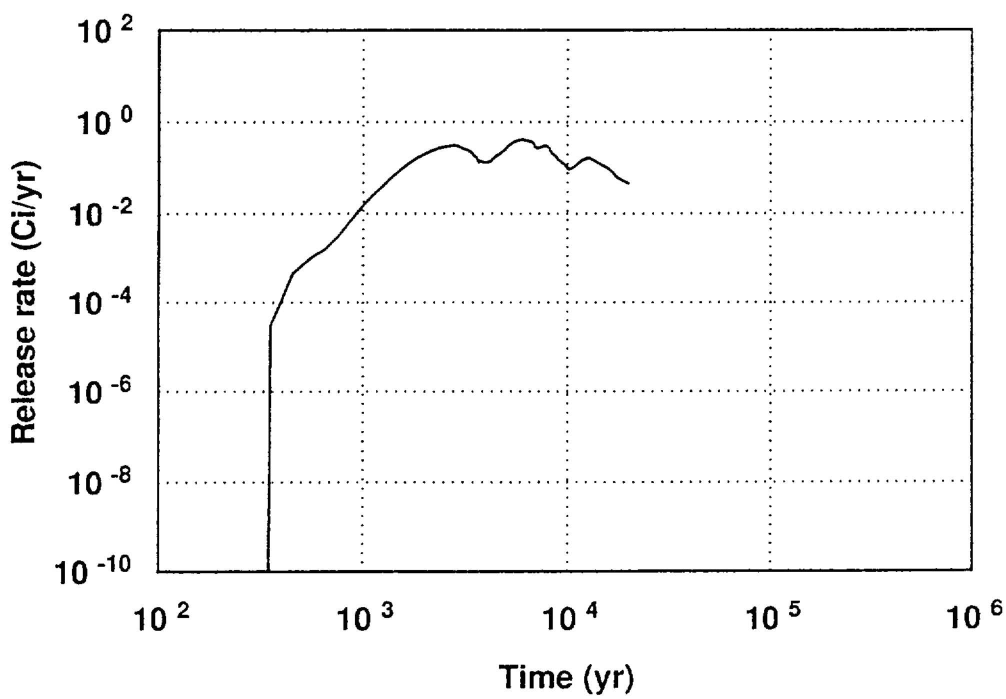

Figure 5-18. Release rate to the accessible environment for gaseous ^{14}C, using the composite-porosity model for water flow and mean values for all parameters.

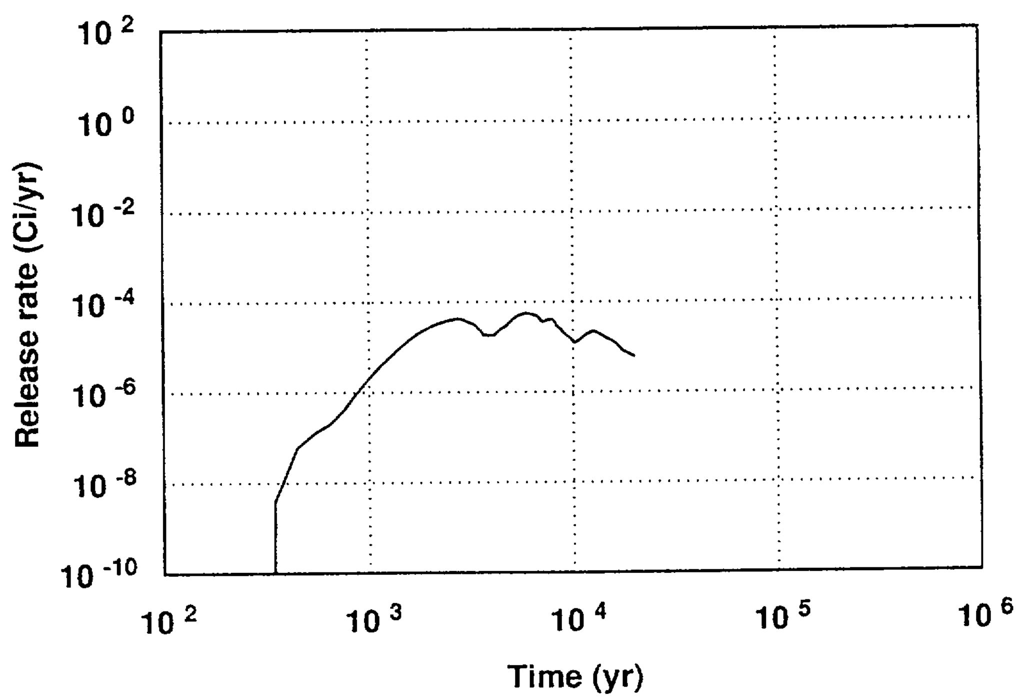

Figure 5-19. Release rate to the accessible environment for gaseous ^{14}C, using the weeps model for water flow and mean values for all parameters.

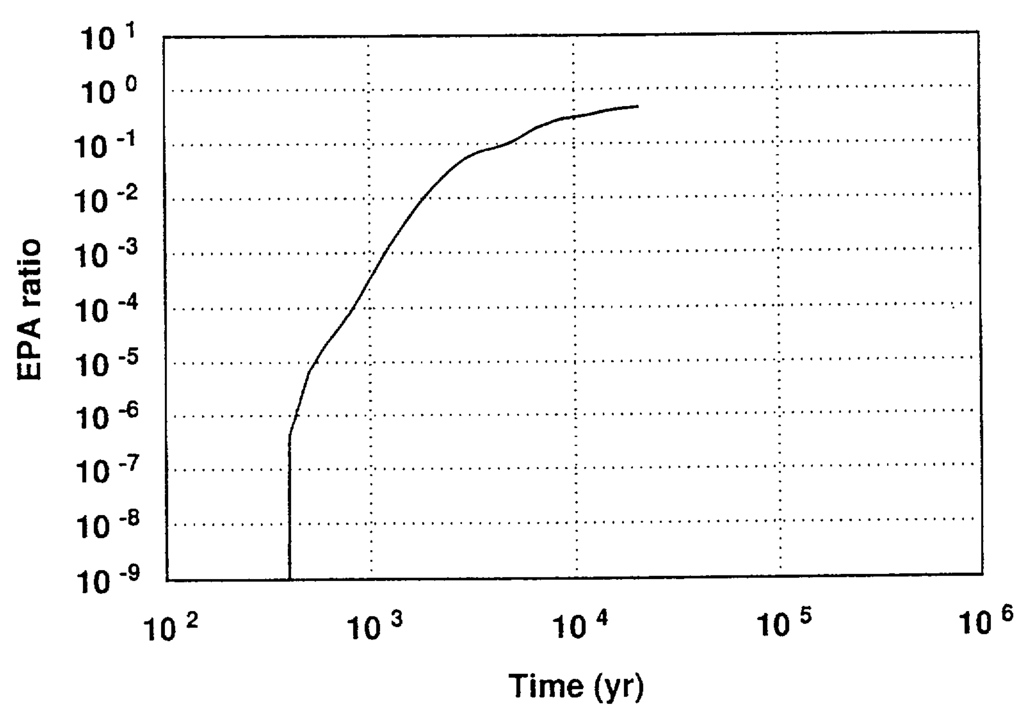

Figure 5-20. ^{14}C EPA ratio as a function of time for the composite-porosity model, using mean values for all parameters.

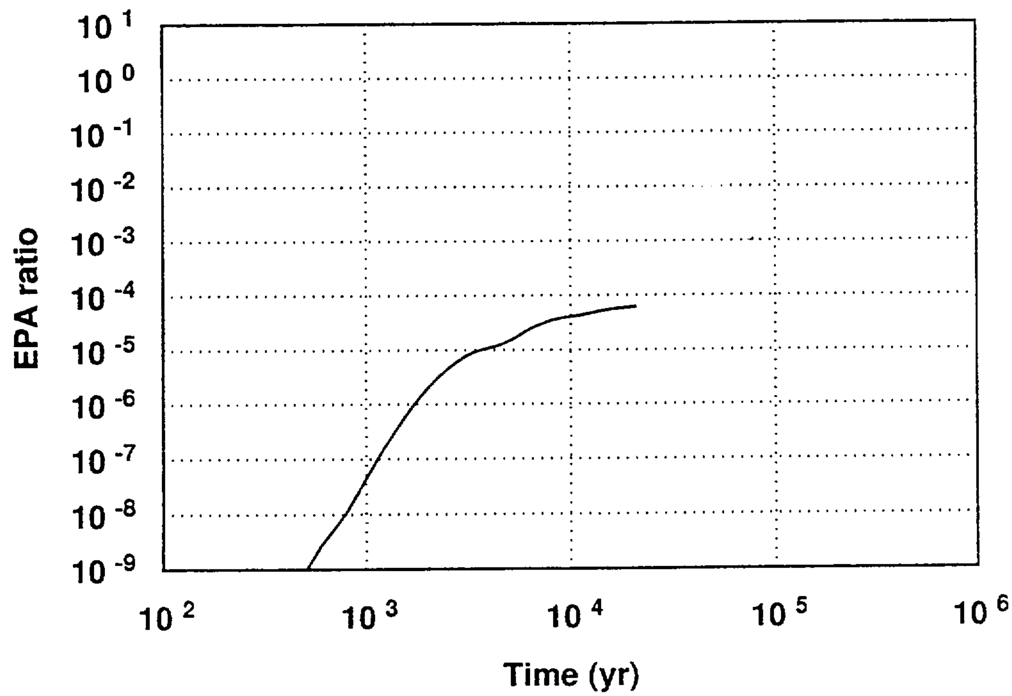

Figure 5-21. ^{14}C EPA ratio as a function of time for the weeps model, using mean values for all parameters.

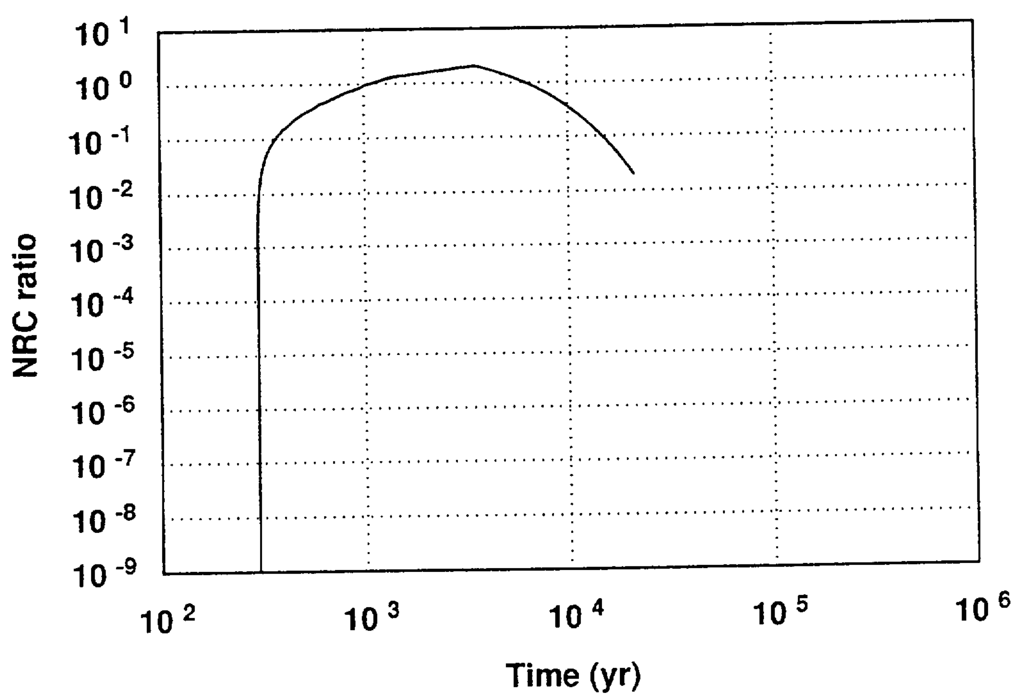

Figure 5-22. ^{14}C NRC ratio as a function of time for the composite-porosity model, using mean values for all parameters.

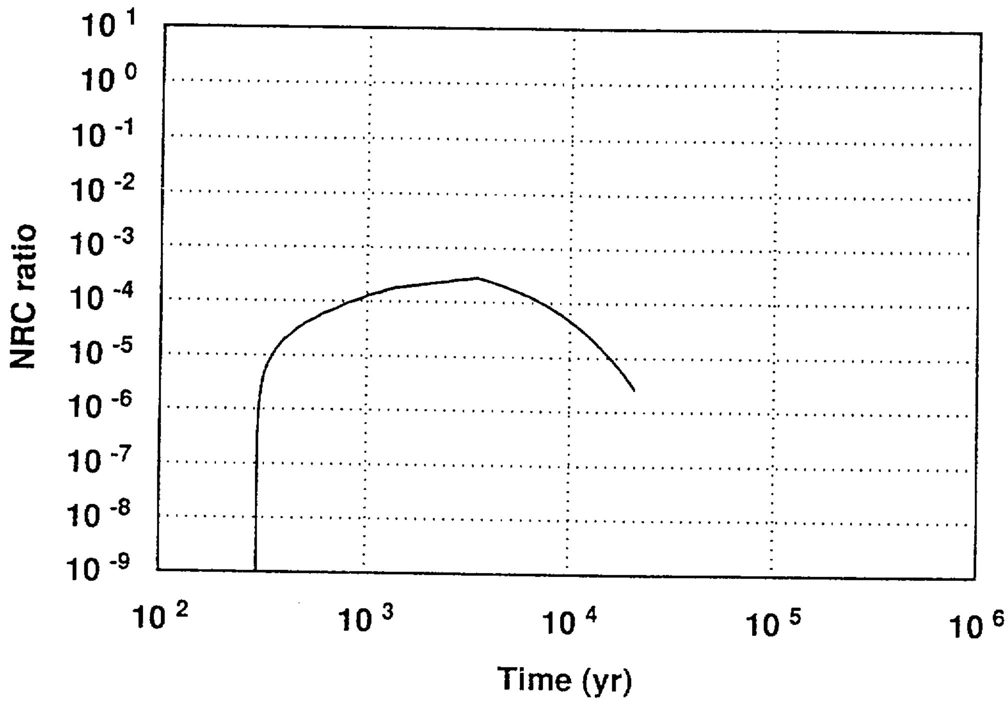

Figure 5-23. ^{14}C NRC ratio as a function of time for the weeps model, using mean values for all parameters.

release rate to the accessible environment peaks at approximately 0.4 Ci/yr at 6000 yr. The EPA ratio (at 10,000 yr) is about 0.3. Also, for the composite-porosity model the NRC release-rate limit is exceeded, with the peak release rate reached at about 3000 yr. The peak release rate for the weeps model occurs at about the same time, but is four orders of magnitude lower. The reason for this, as has been stated before, is that only a small fraction of the waste containers release their radionuclides in the weeps calculation. For the weeps model, the EPA ratio is only 4×10^{-5} and the peak release-rate to the accessible environment is 6×10^{-5} Ci/yr at 6000 yr.

Chapter 6
Human Intrusion

(Barnard, Dockery, Wilson)

6.1 Introduction

This component of the TSPA analysis considers releases of radionuclides that might occur because of postclosure drilling operations into a potential repository in Yucca Mountain. Releases are calculated at the earth's surface and at a subsurface regulatory boundary. The time period of this analysis spans the 10,000-year regulatory period specified by the EPA in 40 CFR Part 191 (EPA, 1985). The analyses of releases due to drilling are simplified representations of only a few human-intrusion scenarios.

The philosophy of this component of the TSPA is to attempt to represent complex scenarios by simple analyses that capture the essence of the processes. Specifically, this is accomplished by simplifying the treatment of the radionuclide source term, simplifying the estimation of the geometric probability of intersecting containers during intrusion, and by reducing a multi-dimensional problem to one dimension.

6.2 Problem definition

The scenario describing this TSPA analysis was developed from the FEP diagram for human intrusion (Barr et al., 1991). Figure 6-1 shows the portion of the FEP diagram that includes the FEPs captured in the calculation. The TSPA analysis considers only drilling events (the bold paths in Figure 6-1). The specification of the FEP "Exploratory Drilling", rather than "Production", has implications for the number and density of drillholes—exploratory drilling holes are random in space and time. Specifying "Hydrocarbon and Mineral Exploration", rather than "Scientific Exploration", has implications about the size of the holes that are drilled.

The human-intrusion scenario can be stated as follows: At various times in the future, one or more boreholes are drilled from the surface of Yucca Mountain through the potential repository. Twentieth-century exploratory-drilling technology is assumed. The drilling processes are assumed to break open any intersected waste containers. Releases are assumed to occur through direct transport either to the surface or into the saturated zone.

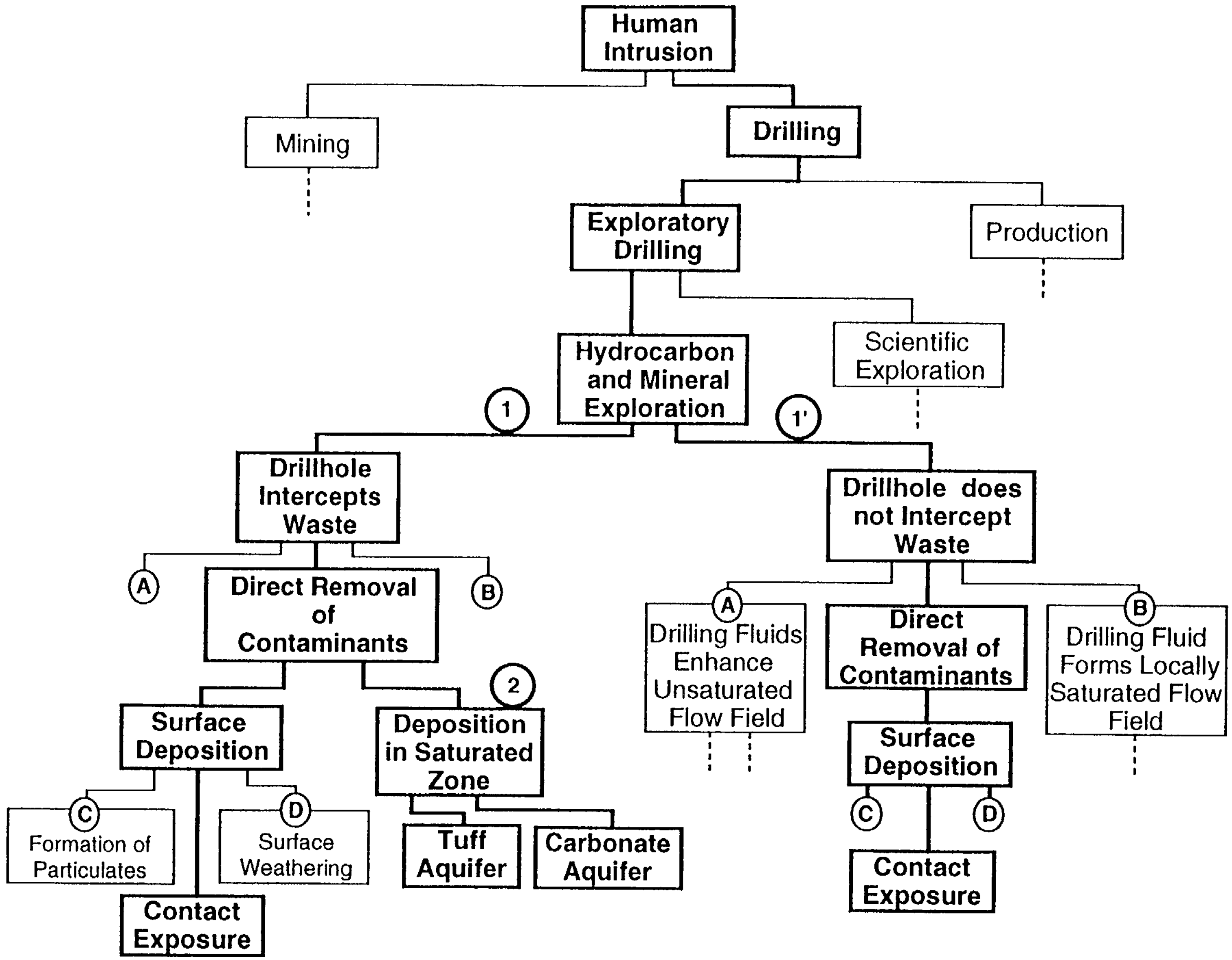

Figure 6-1. FEP diagram for human-intrusion scenarios

Surface release occurs under two circumstances. In the first (direct hits), waste is lifted to the surface by entrainment in the drilling fluid or by contamination of the drill string (indicated as path 1 in Figure 6-1). Figure 6-2 illustrates this process. In the second (near misses), the drill hole passes through rock that has been contaminated by migrating radionuclides from nearby containers (indicated as path 1' in Figure 6-1); as in the first circumstance, contaminated rock is lifted to the surface by drilling fluid or the drill string. Release for both of these circumstances is defined as occurring when the radioactive waste reaches the earth's surface (indicated by the FEPs "Contact Exposure" in Figure 6-1).

Because the Yucca Mountain site is underlain by a saturated zone thought to have two distinct components, two variations of release to the saturated zone were considered (shown as path 2 in Figure 6-1). The first entails drilling to the water table and into the saturated-tuff zone. The second variation includes drilling to tag the basement rock; in this case, into the Paleozoic carbonate aquifer. For both cases, waste is assumed to fall down the drill hole into the saturated zone, where it can dissolve and be transported to the accessible environment by saturated-zone flow. Figure 6-3 illustrates this event.

The scenario descriptions include every FEP in the appropriate paths in Figure 6-1, although the processes modeled have generally been simplified. Some of the assumptions and simplifications made for this analysis follow. Waste packages are assumed to be emplaced vertically. It is assumed that a conventional drill bit can penetrate a waste package. Oil-field veterans have expressed some skepticism that the drill string would penetrate the waste package instead of veering away*, so this assumption is probably conservative. For the surface-release scenario, it is assumed that the working fluid for the drilling operation would be liquid (water or drilling mud) with sufficient density and viscosity to entrain the fragments of waste. The entrainment process is assumed to occur when waste from a ruptured package falls down the borehole and is ground up by the drill bit. The fines and small particles are then carried in the drilling mud to the surface. Figure 6-2 simplifies the details of the entrainment mechanism. It is further assumed that the entrained waste travels directly through the drill hole to the surface. For vertically emplaced waste packages, this implies that the hole drilled through the emplacement drift above the waste package has been cased or grouted to prevent loss of circulation. For the saturated-zone release scenario, it is assumed that it is possible for the contents of an

---

* D. Chesnut, Lawrence Livermore National Laboratory, personal communication.

entire waste package to fall over 200 m to the saturated tuff (and even farther to the carbonate aquifer). Other assumptions specific to the modeling of the problems will be stated later in this report.

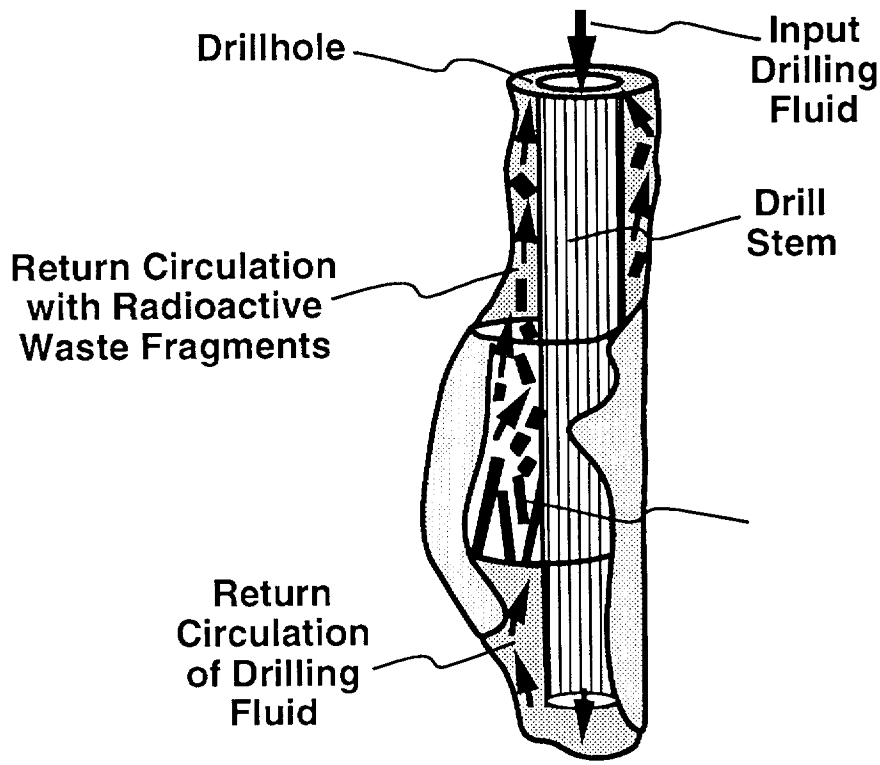

Figure 6-2. Schematic of mobilization process for surface-release scenario

6.3 Estimation of probability of occurrence

The probability of occurrence for this scenario is composed of two components. First, there is the probability that drilling operations would be conducted at Yucca Mountain. Second is the probability that, if drilling occurs, a waste package or contaminated rock will be intersected by the drill string.

6.3.1 Natural resources

The scenario used as the basis for this calculation assumes that exploratory drilling is the reason for human intrusion. Therefore, the probability that drilling will occur at Yucca Mountain depends on the attractiveness of the subsurface resources. The question of the known presence of economic natural resources or of geologic features indicating a greater-than-normal probability that natural resources may exist has been addressed previously in the Environmental Assessment (EA) (DOE, 1986). The EA stated that no economic minerals are present at Yucca Mountain and that it is unlikely that intrusion based on the search for valuable natural resources would occur (see also Younker et al., 1992). In numerous studies since the EA, there have been no data to refute this claim. For instance, Castor et al. (1989) performed geochemical analyses to identify any significant deposits of base or precious metals. Their report states that there are no identified mineral resources at Yucca Mountain, and they assessed the potential for metals to be very low, especially for surficial or near-surface deposits. The same report rates the petroleum potential of Yucca Mountain as low. People have, however, thought exploration worthwhile as demonstrated by the history of claims in the area. Also, gold is currently being extracted from the Bare Mountain area, and several petroleum explor-

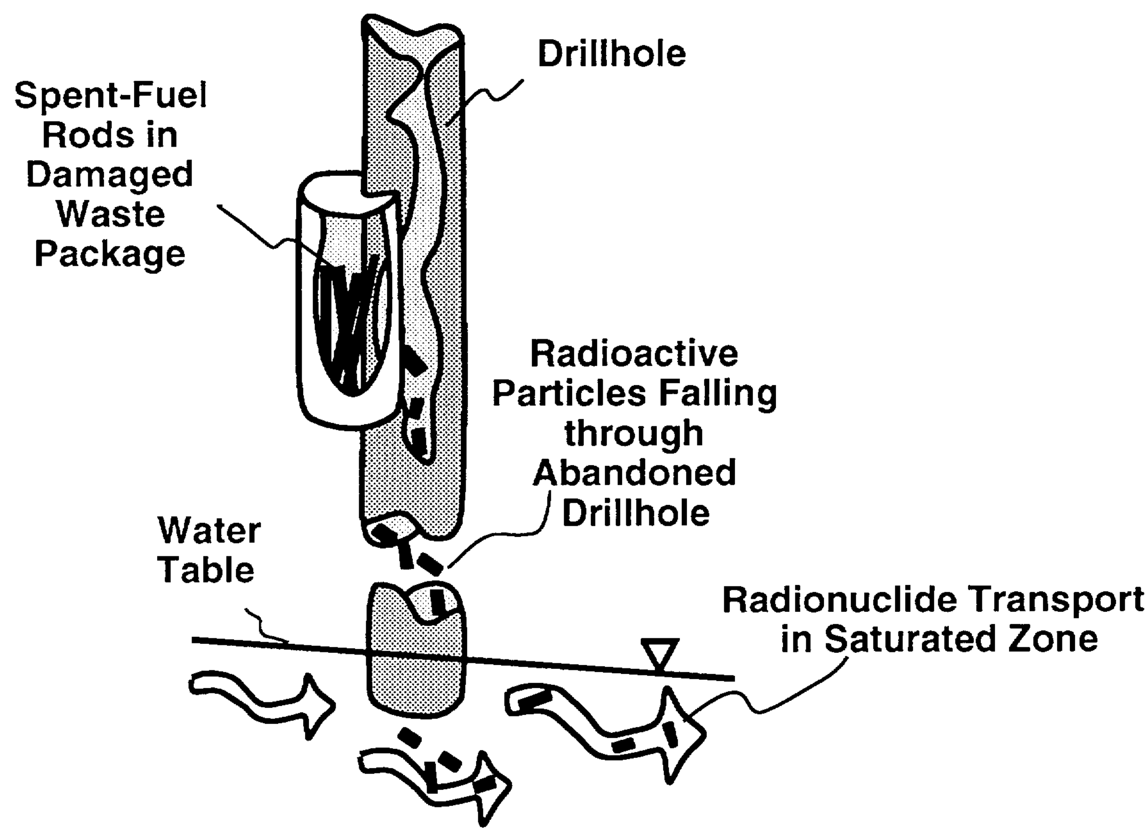

Figure 6-3. Schematic of mobilization process for saturated-zone-release scenario.

ation wells have been drilled in the Amargosa Valley (Figure 6-4). Thus, this report concurs with the judgment of the Early Site Suitability Evaluation (Younker et al., 1992) that no defensible probability can be assigned to the presence of natural resources until site characterization is performed. Lacking any further information for this analysis, we have assigned a probability of 1 to the likelihood that there will be human-intrusion activities at the site over 10,000 years.

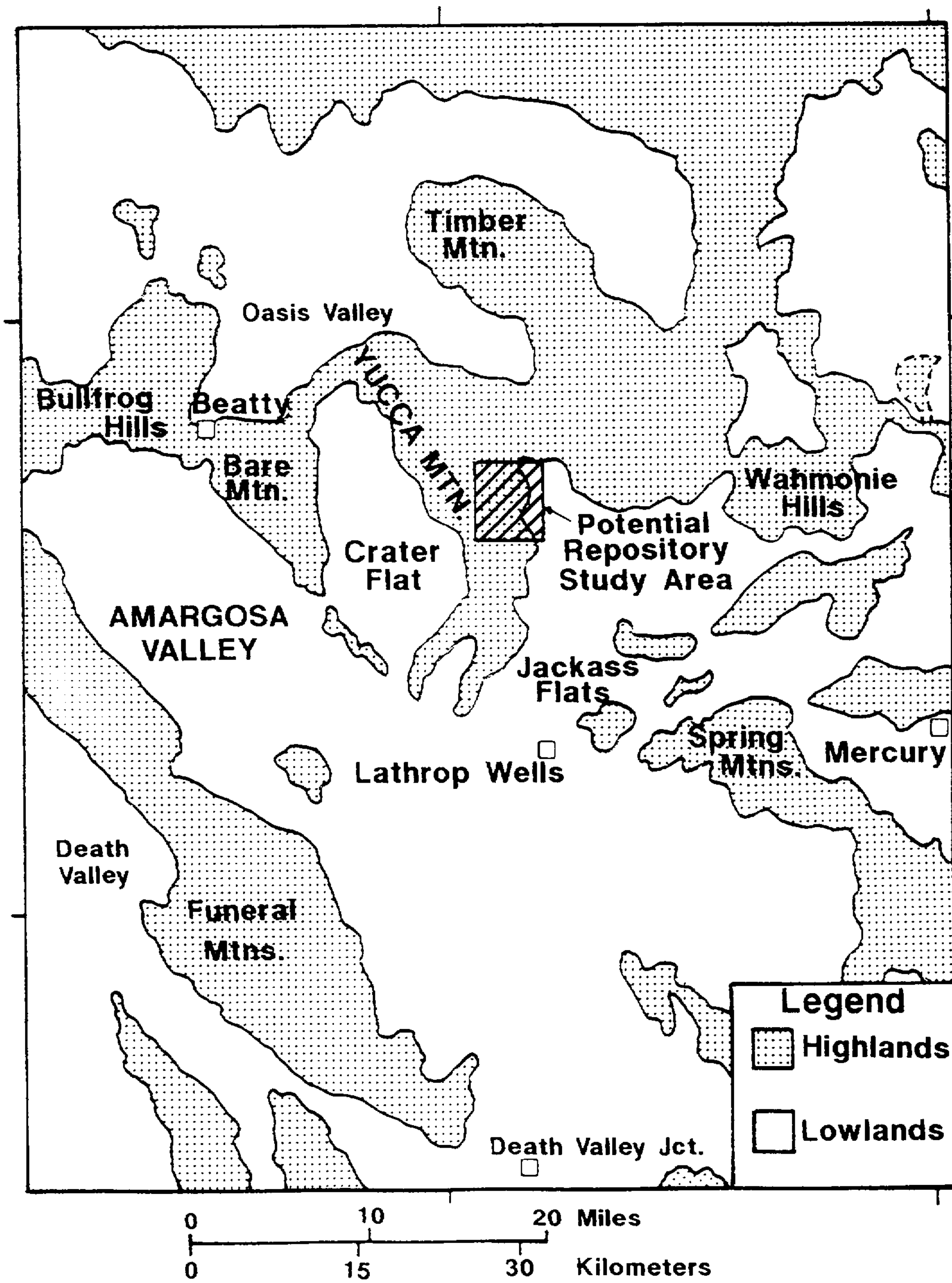

Figure 6-4. Resource-exploration areas near Yucca Mountain

6.3.2 Geometric probability

The probability that a drill bit will intersect a waste package or contaminated rock can be determined from geometric considerations. The probability per drilling event for hitting one waste package in the repository depends on the area of the drill bit and the area of waste container perpendicular to the drill string.

One of the major uncertainties in this scenario concerns the likely number of boreholes that might be drilled at the site over the regulated 10,000-year containment period. Guidance for drilling rate for areas not underlain by sedimentary rocks given in 40 CFR Part 191 is 3 drillholes/km^2/10,000 years (EPA, 1985). The basis for this estimate has not been well established, although it appears that the number is derived from drilling densities for exploratory drilling in the Delaware Basin, New Mexico (Apostolakis et al., 1991). A study of the drilling in this basin gives an estimate of 30 drillholes/km^2/10,000 years. This number is suggested by the regulations for use in sedimentary basins. An arbitrary "factor of ten" decrease was used to derive a suggestion for nonsedimentary environments, such as Yucca Mountain.

The geometric-probability analysis (given in detail in Appendix I) used the EPA estimate of 3 boreholes/km^2/10,000 years to calculate the probabilities of hitting one, two, or three vertically or horizontally emplaced waste packages. To calculate the probability (assuming vertical emplacement of the waste packages), the "enhanced" area of the waste package is first determined. The enhanced area includes the combined areas of the waste package (characterized by r_{wp}), and the area of the drill bit (characterized by r_{bh}). For a single drilling event over the repository, any one of the N_{wp} packages could be hit (the packages are assumed to be uniformly distributed in the repository.) Thus, the probability of a direct hit is given by the total enhanced area divided by the area of the repository (A_{rep}):

$$P_{hit} = \frac{N_{wp}[\pi(r_{wp} + r_{bh})^2]}{A_{rep}} \qquad (6.1)$$

The parameters used in the probability calculation are given in Table 6-3 (Section 6.4.3). Using these numbers, the probability for a hit from a single drilling event is 0.0075. To calculate the probability for the estimated 17 drilling events over 10,000 years (3 boreholes/km^2/10,000 years * 5.61 km^2), one must estimate the frequency of getting a hit during the expected number of trials. Either a binomial distribution or a Poisson distribution may be used for this estimate.

The binomial formula for the probability of getting r hits in n trials is:

$$P[r] = \binom{n}{r} p^{n-r} q^r, \tag{6.2}$$

where q is the probability of a hit (P_{hit}), and $p = 1 - q$. This formula gives the probabilities shown in Table 6-1.

Whereas the binomial formulation assumed that 17 boreholes would always be drilled over 10,000 years, the uncertainty in that number can be accounted for by specifying 17 boreholes as the mean number drilled, and assuming that the frequency of drilling follows a Poisson distribution. In this case, the probability of r hits is given by

$$P[r] = \frac{e^{-\mu P_{hit}} (\mu P_{hit})^r}{r!}, \tag{6.3}$$

where μ is the mean number of boreholes and μP_{hit} is the expected number of hits. The probabilities are shown in Table 6-2.

Table 6-1
Probabilities of hits for binomial distribution

Number of Hits	Probability over 10,000 years
0	0.880
1	0.113
2	.00683
3	2.58×10^{-4}

Table 6-2
Probabilities of hits for Poisson distribution

Number Of Hits	Probability Over 10,000 Years
0	0.880
1	0.112
2	.00716
3	3.04×10^{-4}

The probabilities arising from the two distributions are quite similar. The main difference between them is that with the Poisson distribution, the likelihood of having two or more hits is slightly increased.

The definition of the enhanced area for the waste package is quite generous, because any intersection of the drill bit and the waste package—ranging from coaxial to tangential—is considered a direct hit. This definition somewhat overestimates the geometric probability. The use of different diameters for the borehole would also change the probability of a hit.

Calculation of the probability of a near miss is based on the same assumptions as for a direct hit—using the ratio of the area of contaminated rock (calculated in Section 6.4.1) to the total repository area.

6.4 Modeling assumptions

The source term appears to be one of the most important factors, and the outcomes for the saturated-zone transport are highly dependent on the parameter values chosen because of the assumptions about the nature of the processes involved. The substantiations underlying these observations and their implications are discussed in the following subsections.

6.4.1 Source term for surface releases

It is assumed that the waste mobilized by drilling incidents is immediately carried to the surface; no further releases due to groundwater transport are considered. Therefore, the extent of releases is described strictly by the radionuclide inventory present in and around the waste package at the time of the drilling incident. Temporal variation in the inventory due to decay is described by the Bateman chain-decay relationships (Bateman, 1910).

As time progresses and the waste containers degrade, groundwater can transport nuclides into the rock surrounding the waste package. As a calculational simplification for this analysis, it is assumed that the transport mechanism is molecular diffusion. (The groundwater-flow and transport calculations used in Chapters 4 and 5 were too complex to be included in this analysis.) This assumption, and the extent of the transport over 10,000 years, is based on the PACE-90 nominal-case analyses (Barnard and Dockery, 1991). Furthermore, only radionuclides that have little retardation are assumed to diffuse into the rock surrounding the waste package. A more sophisticated analysis would include a coupling between the near-miss calculation and the nominal-flow calculations, but that coupling is probably a second-order effect, and is probably not significant.

The area for near misses is calculated as follows. The line of waste packages in an emplacement drift is considered to be an instantaneous line source. (The spacing between the waste containers in a drift is 5 m, and the spacing between drifts is approximately 40 m, so a line source is a reasonable approximation.) For an instantaneous source, the fractional concentration as a function of time and distance is given by

$$C(x,t)/C_0 = \frac{1}{4\pi Dt} e^{-x^2/4Dt}, \tag{6.4}$$

(taking into account the symmetry along the line of the source), where C_0 is a reference concentration, x is the radial distance from the source, and D is the diffusion coefficient. A solution to this diffusion problem is given in Crank (1956). The diffusion coefficient is determined by evaluating the diffusion equation with $C(x,t)/C_0 = 10^{-5}$ at 35 m from the waste container after 100,000 years. These values are derived from the PACE-90 TOSPAC results for ^{129}I and ^{99}Tc (Barnard and Dockery, 1991). In the PACE-90 analysis, the transport is influenced by both diffusion and advection; for this analysis, an effective diffusion coefficient is used to represent the transport results. A fractional concentration of 10^{-3} is used to define the boundary of contaminated rock. The location of the 10^{-3} fractional concentration is determined at the time of the specified drilling event (after accounting for the time for which no containers had failed—300 years). Figure 6-5 shows the diffusion concentration profiles for several time periods. The area of contamination is then computed from the product of the location of the 10^{-3} fractional concentration (as one axis of an ellipse) and the half-spacing of the waste packages in the emplacement drift (as the other axis).

Figure 6-6 schematically illustrates the geometric relationships between containers, the surrounding areas of contaminated rock, and the drill holes. The waste containers are assumed to be distributed uniformly throughout the repository, so that releases from direct hits or near misses can be expressed as a fraction of the entire inventory.

Only waste in the form of spent fuel has been considered for this analysis. Had glass waste been included, a different treatment of the groundwater-induced transport processes would have been necessary. Although ^{14}C is included in the inventory, its releases are not treated differently from those of the less mobile isotopes. When a direct hit occurs, all (or a portion) of the affected waste package is assumed to be available for transport to the surface. All radionuclide transport is assumed to occur solely by mechanical means.

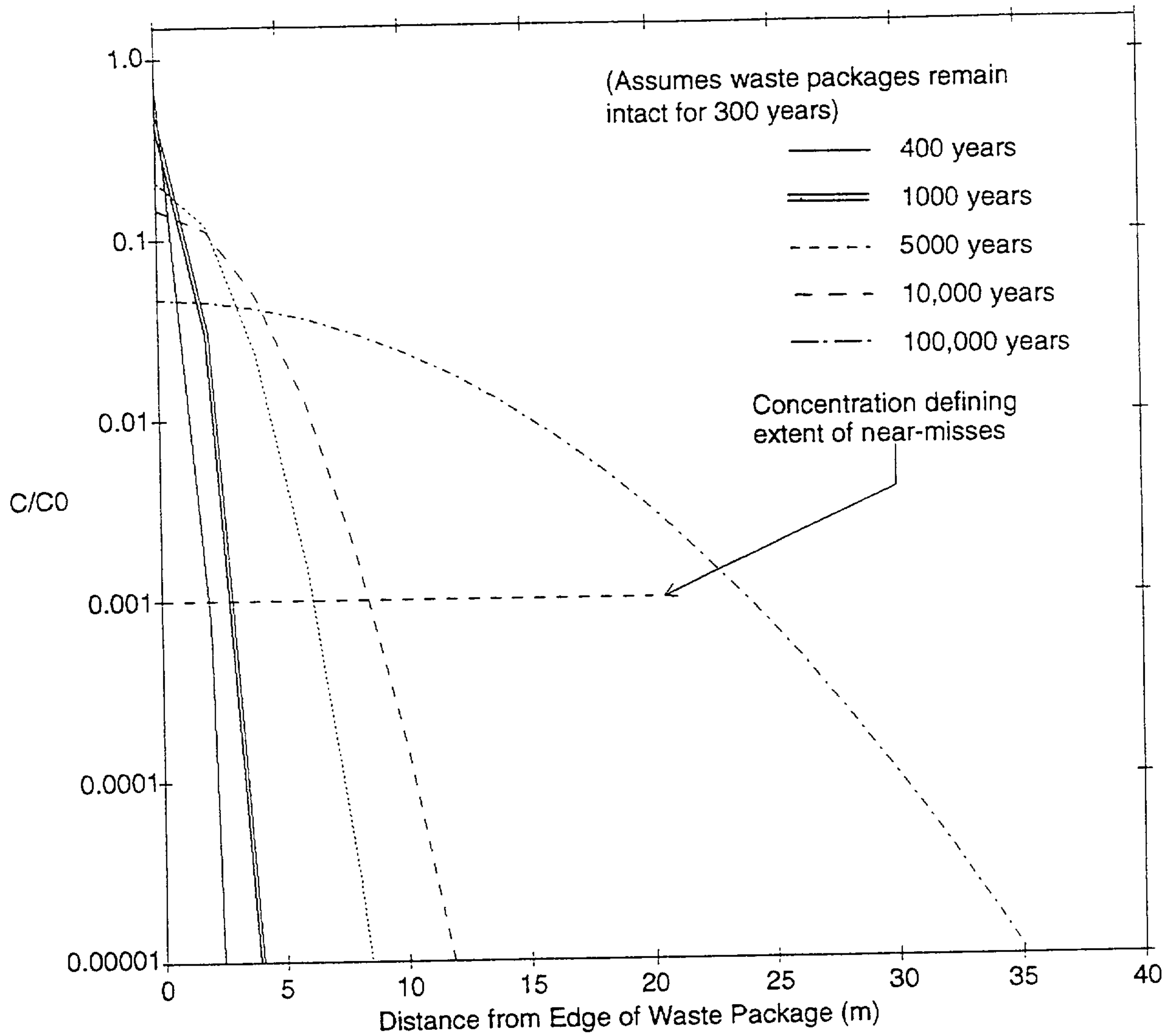

Figure 6-5. Diffusion profiles vs time

Previous analyses have used a radionuclide inventory based on average characteristics of the spent fuel, i.e., the average mix of spent fuel from boiling-water reactors (BWRs) and pressurized-water reactors (PWRs), and the average burnup of the fuel from those reactors. For this analysis, such an inventory is called a lumped-source inventory. One sensitivity study, to be described later in this chapter, investigates multiple-source inventories, where the repository is considered to be filled with spent fuel whose source (BWR or PWR), burnup, and ages since discharge from the reactor are all specified.

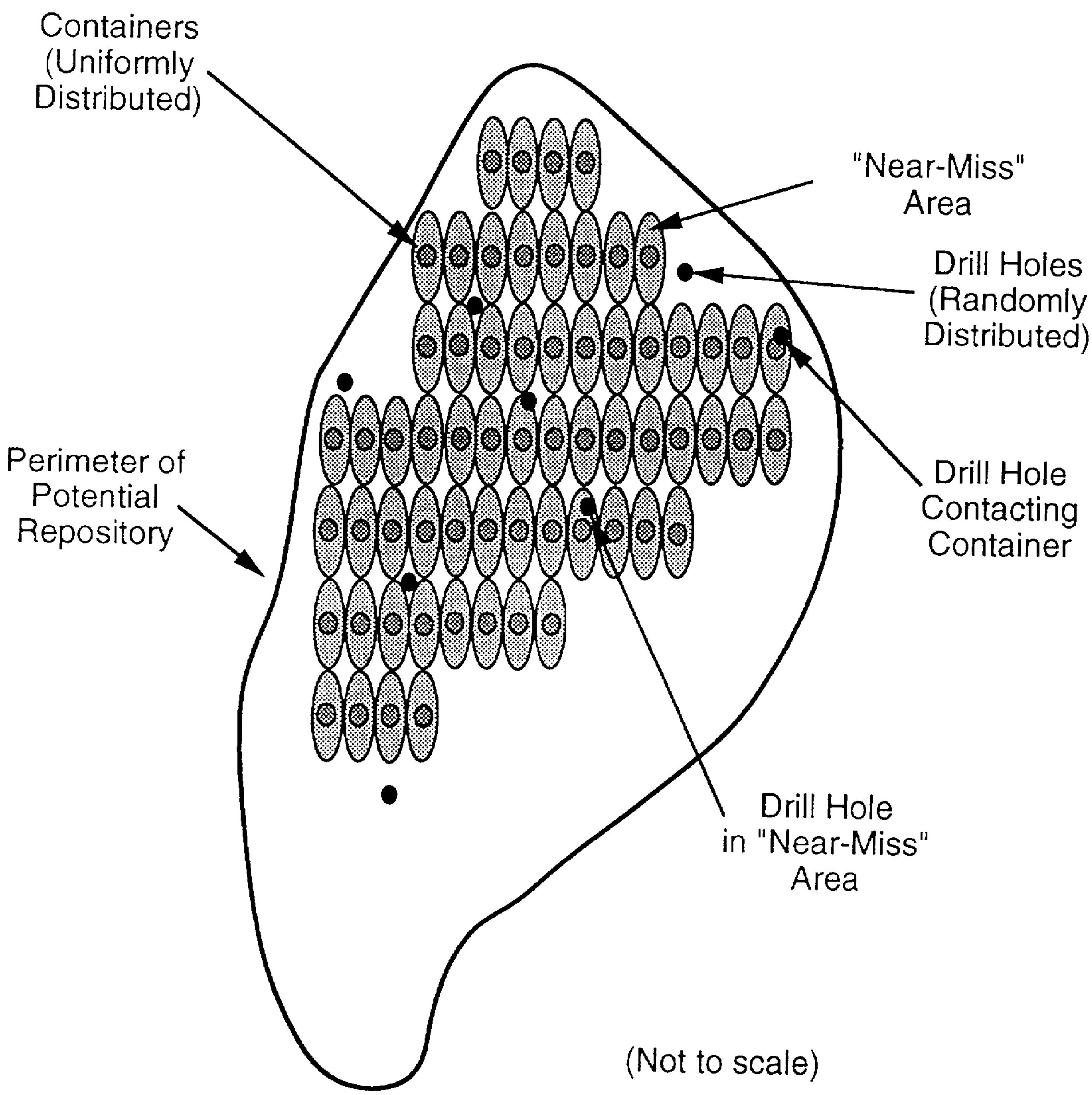

Figure 6-6. Geometric layout for drilling scenarios

6.4.2 Source term for saturated-zone releases

The saturated-zone problem assumes that aqueous processes transport the waste which has fallen down the drillhole to the aquifer. Because this transport mechanism is not "instantaneous", like the mechanical transport to the surface, factors such as geochemical retardation can influence which radionuclides reach the accessible environment. For this reason, the set of radionuclides used for the saturated-zone problem is smaller than for the surface-release case. Radionuclides with large retardations will not be transported to the accessible environment within the regulatory time period, so there is little value in calculating their releases. The resulting suite of isotopes included ^{243}Am, ^{241}Am, ^{240}Pu, ^{239}Pu, ^{237}Np, ^{234}U, ^{135}Cs, ^{129}I, ^{126}Sn, ^{99}Tc, ^{79}Se, and ^{14}C. This set of isotopes was expanded from the PACE-90 set (Barnard and Dockery, 1991), by the addition of radionuclides with high inventories and those which contribute significantly to dose calculations.

Some simplifying assumptions made about the radionuclide source term are as follows. The entire contents of one (and only one) waste package are deposited in the saturated flow field. The solubility of the waste has been chosen to be sufficiently high that it immediately dissolves when it enters the saturated zone. The actual inventories of each radionuclide are determined from the decay and chain ingrowth at the time at which the event occurred.

6.4.3 Parameters

Table 6-3 lists the parameters pertinent to the base-case drilling surface-release analysis. It also lists the alternative values for parameters varied in the sensitivity studies.

The fraction of the repository inventory contained in one waste package as listed in Table 6-3 is calculated from the contents of one waste package (2.1 MTHM) divided by the total inventory (70,000 MTHM). The fraction of the repository inventory available to diffuse (i.e., the source for near-misses) consists only of the fraction of the total inventory that consists of mobile species (i.e., ^{99}Tc and ^{129}I).

The radioisotopes used in the base-case source terms are listed in Table 6-4 (Wilson, 1991). The inventories are based on the parameters given in Table 6-3; these are called the "lumped" source terms in this section. Most of those isotopes for which an EPA limit is not defined (i.e., those for which the half-life is less than 20 years) were not included in the source term. The only isotopes with short half-lives that were included had high inventories that would affect the inventories of elements further down their decay chains. Some isotopes with very low inventories were also omitted. However, the inventory used for the surface-release problem includes more than 99% of the spent-fuel inventory in the potential repository. The list includes both actinides and fission products. Several decay chains are included. The "Inventory" column in Table 6-4 is the base-case lumped-parameter inventory and is typical of the values used for all inventories. The saturated-zone problem uses the isotopes (indicated by †) listed in Table 6-4 for the radionuclides included in that source term. Chain-decay ingrowth from nuclides not included in the source term have been included in the appropriate inventories.

Table 6-3

Parameters for surface-release scenario

Parameter	Value
General parameters	
Repository area	5.6×10^6 m^2
Number of waste packages (N_{wp})	33,333
Waste package orientation	vertical
Performance Time	10,000 years
Typical number of trials in a simulation	20,000
Base-case source term	
Fraction of repository in 1 waste package	3.0×10^{-5}
Diffusive fraction in 1 waste package	6.9×10^{-9}
Spent-fuel burnup (in MWd/MTHM)	33,000 (PWR) 27,500 (PWR)
PWR/BWR proportion	60/40
Number of radionuclides used in source	43
Probability factors	
Number of boreholes	17
Probability of hitting 1 waste package (P_{hit})	0.0075
Radius of waste package (r_{wp})	0.33 m
Radius of drill bit (r_{bh})	0.305 m
Spacing between containers in a drift	5 m
Time before first waste package fails	300 years
Diffusion coefficient	3.65×10^{-4} m^2/yr.
Variations in source term for multiple sources	
Fraction of BWR and PWR, and respective burnups	(See Table 6-6)
Variation in geometric probability	
Increased number of boreholes	170, 340
Variation in near-miss inventory	
Increased diffusive fraction of repository	6.9×10^{-7}
Variation in diffusion coefficient	
Increased diffusion coefficient	3.65×10^{-2} m^2/yr.

Table 6-4
Radioisotopes used in source term

Isotope	Half-life (years)	EPA Limit (Ci/MTHM)	Inventory (Ci/MTHM)
U-238	4.468×10^{9}	0.1	3.18×10^{-1}
Cm-246	4.731×10^{3}	0.1	2.58×10^{-2}
Pu-242	3.869×10^{5}	0.1	1.60×10^{0}
Am-242	1.520×10^{2}	0.1	7.46×10^{0}
Pu-238	8.774×10^{1}	0.1	2.12×10^{3}
U-234†	2.445×10^{5}	0.1	1.13×10^{0}
Th-230	7.700×10^{4}	0.01	1.29×10^{-4}
Ra-226	1.600×10^{3}	0.1	3.67×10^{-7}
Pb-210	2.230×10^{1}	1.0	4.71×10^{-8}
Cm-243	2.850×10^{1}	0.1	1.54×10^{1}
Am-243†	7.380×10^{3}	0.1	1.55×10^{1}
Pu-239†	2.406×10^{4}	0.1	3.08×10^{2}
U-235	7.038×10^{8}	0.1	1.68×10^{-2}
Pa-231	3.277×10^{4}	0.1	1.94×10^{-5}
Ac-227	2.177×10^{1}	0.1	5.19×10^{-6}
Cm-245	8.499×10^{3}	0.1	1.26×10^{-1}
Pu-241	1.440×10^{1}	0.0	7.43×10^{4}
Am-241†	4.322×10^{2}	0.1	1.64×10^{3}
Np-237†	2.140×10^{6}	0.1	2.88×10^{-1}
U-233	1.585×10^{5}	0.1	2.54×10^{-5}
Th-229	7.339×10^{3}	0.1	1.40×10^{-7}
Cm-244	1.811×10^{1}	0.0	1.15×10^{3}
Pu-240†	6.537×10^{3}	0.1	5.08×10^{2}
U-236	2.341×10^{7}	0.1	2.40×10^{-1}
U-232	7.200×10^{1}	0.1	2.50×10^{-2}
Sm-151	8.999×10^{1}	1.0	3.18×10^{2}
Cs-137	3.000×10^{1}	1.0	7.66×10^{4}
Cs-135†	2.300×10^{6}	1.0	3.50×10^{-1}
I-129†	1.570×10^{7}	0.1	2.95×10^{-2}
Sn-126†	1.000×10^{5}	1.0	7.17×10^{-1}
Sn-121	4.997×10^{1}	1.0	9.04×10^{-1}
Ag-108	1.270×10^{2}	1.0	1.19×10^{-2}
Pd-107	6.496×10^{6}	1.0	1.05×10^{-1}
Tc-99†	2.130×10^{5}	10.0	1.23×10^{1}
Mo-93	3.498×10^{3}	1.0	1.60×10^{-2}
Nb-94	2.030×10^{4}	1.0	7.93×10^{-1}

Table 6-4, continued
Radioisotopes used in source term

Isotope	Half-life (years)	EPA Limit (Ci/MTHM)	Inventory (Ci/MTHM)
Zr-93	1.530×10^6	1.0	1.88×10^0
Sr-90	2.912×10^1	1.0	5.32×10^4
Se-79†	6.496×10^4	1.0	3.81×10^{-1}
Ni-63	9.200×10^1	1.0	4.55×10^2
Ni-59	8.000×10^4	1.0	3.56×10^0
Cl-36	3.010×10^5	1.0	1.19×10^{-2}
C-14†	5.729×10^3	0.1	1.54×10^0

†Isotopes also used for the saturated-zone source term.

The parameters used in the saturated-zone analyses are listed in Table 6-5. This analysis employed the same parameter values for the saturated-tuff zone as those discussed in Chapters 3 and 4. As was described in Section 4.5, the water velocity in the saturated tuff was calculated from the regional hydrology model of Czarnecki (1985). Parameters for the carbonate aquifer were taken from McGraw et al. (1991). These latter values are known with considerably less confidence. Table 6-5 reiterates the characteristic values of the hydrologic parameters used.

Derivations of PDFs for the geochemical sorption coefficients have been discussed in Section 3.4. Table 3-25 (Section 3.4) lists the PDFs used for the distribution coefficients. The shapes of the PDFs have been shown in Figures 3-11 through 3-18.

Table 6-6 lists the parameters used to construct the multiple-source inventory. Using the spent-fuel "LWR Quantities Data Base" (DOE, 1987, v. 4), the amounts of spent fuel from 1969 through the year 2040 (the predicted end of light-water reactor (LWR) operations) are determined. These amounts are listed according to type of reactor (BWR or PWR) and amount of burnup (in MWd/MTHM). To determine the isotopic composition of these inventories at the year 2040, the decay of the radioisotopes from time of discharge from the reactor to the year 2040 is calculated using the ORIGEN computer code (Roddy et al., 1986). The inventories are then lumped into roughly 10-year intervals. The entries in Table 6-6 describe inventories consisting of individual radionuclides that have decayed for the times listed in column 1. The inventories are weighted by the proportion of BWR fuel (column 2) to

Table 6-5

Parameters for saturated-zone release problems

Parameter	Value
General parameters	
Distance to accessible environment	5000 m
Typical number of trials in a simulation	1000
Source term	
Spent-fuel burnup (in MWd/MTHM)	33,000 (PWR) 27,500 (BWR)
PWR/BWR proportion	60/40
Number of radionuclides in source	12
Solubility of radionuclides	1000 kg/m^3
Probability factors	
Number of boreholes	17
Probability of hitting 1 waste package in 10,000 years with 17 boreholes	0.113
Hydrologic parameters (mean values)	
Saturated velocity (tuff zone)	4.07 m/yr.
Saturated velocity (carbonate aquifer)	230. m/yr.
Saturated porosity (tuff zone)	0.175
Saturated porosity (carbonate aquifer)	0.05
Saturated dispersivity (tuff zone)	195 m
Saturated dispersivity (carbonate aquifer)	195 m

PWR fuel (column 4) and by the amount of burnup for each reactor for that year (columns 3 and 5). Because the potential Yucca Mountain repository is designed to hold 70,000 MTHM, which is less than the total spent fuel to be generated, the table was cut off when 70,000 MTHM was reached. The percentage of the entire repository represented by fuel of a given year grouping is listed in the last column of Table 6-6. The actual inventories used for the multi-source analyses consist of six separate lists of radionuclides similar to Table 6-4.

6.5 Description of TSPA Calculation

The TSPA analysis included several simulations of human-intrusion drilling incidents. The base-case simulation used the parameters listed in Tables 6-3 and 6-4 above. In addition, several simulations investigating the sensitivities of the releases to parameter variations were completed. Each simulation consists of numerous trials, where a trial represents a 10,000-year history of drilling events at the site.

From each simulation a CCDF relating releases and the associated probabilities can be generated. The CCDFs represent the different models being investigated (i.e., the base case, and the sensitivity studies).

Table 6-6
Multiple-source inventory parameters

Decay Years	% BWR Inventory	BWR Burnup	% PWR Inventory	PWR Burnup	% of Total Inventory
70	55.1	15,000	44.9	25,000	1.46
60	39.7	25,000	60.3	30,000	14.63
50	33.1	27,500	66.9	35,000	26.01
40	32.9	40,000	67.1	45,000	25.77
30	34.5	40,000	65.5	50,000	24.97
25	31.2	40,000	68.8	45,000	7.17

The calculation combines numerous trials to create a probabilistic representation of the releases. After all the trials in the simulation have been completed, the EPA sums are sorted and a conditional CCDF is prepared. Conditional CCDFs show the probabilities of release given that the human-intrusion scenario has occurred. Because of the uncertainties mentioned above regarding the probability of human intrusion, using conditional CCDFs allows the probabilities of the consequences to be separated from the overall probabilities of occurrence. In addition, the distributions of release values are presented in the form of histograms. The surface-release and saturated-transport problems treat the probabilities of occurrence of the releases slightly differently, as described in Sections 6.5.1 and 6.5.2.

6.5.1 Surface-release calculations

For each trial, the following steps are performed. For each of the boreholes expected to be drilled over the 10,000 years (i.e., 17 holes in the base case), the time of occurrence of the drilling incident is randomly selected (from a uniform PDF). Then the probability of hitting (P_{hit}) anywhere within the entire contaminated area around the waste package (i.e., including both the waste package itself and the surrounding contaminated rock) is selected from another uniform PDF. If P_{hit} for a given realization is greater than the probability of having a near miss, then no release occurs. If the probability selected is between the probability of a direct hit and that of a near miss, the latter is assumed to occur. Finally, if P_{hit} is less than the probability for a direct hit, the waste package is considered to be breached. The amount of waste available to be released is described by another uniform PDF ranging from 0 to the entire waste package.

To establish the number of curies released, the radioactive decay from the start-time of the trial (0 years) to the time of the incident is determined. Both decay and ingrowth from decay chains are included. From the separate inventories of the isotopes in the source term, the EPA ratio for each isotope is constructed. The EPA ratio is constructed from the amount released for each element divided by the EPA limit for that element (listed in Table 6-4). For each trial, the program sums the EPA ratios in case more than one drill hole has contributed to the releases. Finally, the EPA ratios are combined to give the normalized EPA sum.

For both direct hits and near misses, the amount of radionuclides released does not vary with the location where the drill string penetrates the waste package or the contaminated rock. Thus, for this analysis, the entire contents of a waste package are available to be released if there is a direct hit. Also, if there is a near miss, the concentration of mobile species is assumed to be constant within the halo of contaminated rock. However, to reflect the fact that the concentration actually decreases with distance away from the waste package (shown in Figure 6-5), the amount available to be released for a near miss has been specified as a random variable ranging over the three orders of magnitude that the concentration can vary.

6.5.2 Saturated-zone calculations

The saturated-zone analyses also consisted of numerous trials, each representing a 10,000-year history of the repository. Because the calculations for this problem are much more complicated than for the surface-release problem, fewer trials were done. Additionally, rather than using the analysis involving the geometric probability of occurrence of a drilling incident (i.e., P_{hit}, described above) to determine the probabilities of releases, releases were calculated for each trial and then multiplied by the probability of occurrence to obtain a conditional CCDF consistent with the surface-release analysis.

The calculation of saturated-zone releases is performed with the code TOSPAC (Dudley et al., 1988). This code is a one-dimensional, time-dependent groundwater flow and solute transport code that can include the effects of advection, dispersion, and radionuclide decay and ingrowth. The code models the same physical processes for saturated flow and transport as for the unsaturated zone, except that the rock moisture content is not a function of the pressure head. Using a steady-state groundwater flow field, the code calculates the concentrations of each radionuclide in the source term at every point along the flow path at specified time steps. TOSPAC has been set up to perform stochastic analyses by calculating releases for each of the realizations drawn from the parameter distributions.

The saturated-zone analysis for the saturated-tuff zone has been based on detailed analyses made by Czarnecki (1985), as modeled by the STAFF2D code (Huyakorn et al., 1991). The flow field for the tuff zone described by Czarnecki attempts to be consistent with the observed regional saturated-zone data at Yucca Mountain, and no variations are reported in the saturated water velocities in the region. To provide a range of outcomes, the TSPA analysis assumes that variations in travel time for radionuclides from the points of injection under the repository to the 5-km boundary of the accessible environment are primarily due to the distances the contaminants must travel. Thus, the variations in the water velocity input to TOSPAC are simply a means of describing differences in travel distance, and do not represent variations in the expected value of the regional saturated flow field (see section 4.5).

For the carbonate aquifer, there are far fewer data. Water velocities were taken from a report prepared for the Early Site-Suitability Evaluation (McGraw et al., 1991). The velocities were calculated using the code EPASTAT (Eslinger and Sagar, 1988). The same calculational procedure was followed as for the tuff problem.

6.5.3 Sensitivity studies for surface-release calculations

Several alternative assumptions and variations in parameter values were investigated during a number of sensitivity studies. The various sensitivity studies are as follows:

- Subdividing the inventory according to degree of burnup of the fuel, percentage of the inventory produced by BWRs and PWRs, and decay since discharge of the fuel from the reactors. This produces a multiple-source inventory instead of a lumped-parameter descriptor for the spent fuel in the radioactive waste inventory.

- Calculating the effects of drilling ten and twenty times the EPA-recommended number of boreholes over 10,000 years.

- Varying the fraction of the inventory available to be brought to the surface through near-misses.

- Varying the diffusion coefficient associated with movement of radionuclides into the rock surrounding the waste containers.

- Weighting the occurrence of drilling events to later times in the 10,000-year period to investigate the consequences of loss of institutional control.

Because of the simplifying assumptions made for this analysis, the sensitivity studies should be interpreted more in terms of the response of the model than in terms of the actual response of the potential repository site.

6.6 Results

6.6.1 Surface-release calculations

For most of the simulations, 20,000 trials were run. Figure 6-7 shows the distribution of the 20,000 releases calculated for the base case. The releases fall into three groups: direct hits, with average EPA sums of the order of 10^{-1}; near misses, with EPA sums of about 10^{-5} to 10^{-6}; and complete misses, shown as releases of 10^{-10}. The conditional CCDF for the base case (Figure 6-8) shows that the surface releases do not exceed the EPA limits (the shaded area in Figure 6-8). The effect of including near-misses in the simulation can be seen from the conditional CCDFs shown in Figure 6-9. The "step" in the CCDF at releases of about 10^{-5} represents the contribution of near misses. For the base case, the amount of waste assumed to be released has been treated as a uniform random value from 0 to 100% of the waste package. Figure 6-10 shows the effect of assuming that the entire contents of a waste package are released if the package is breached. As expected, this affects only the high-release, low probability part of the CCDF.

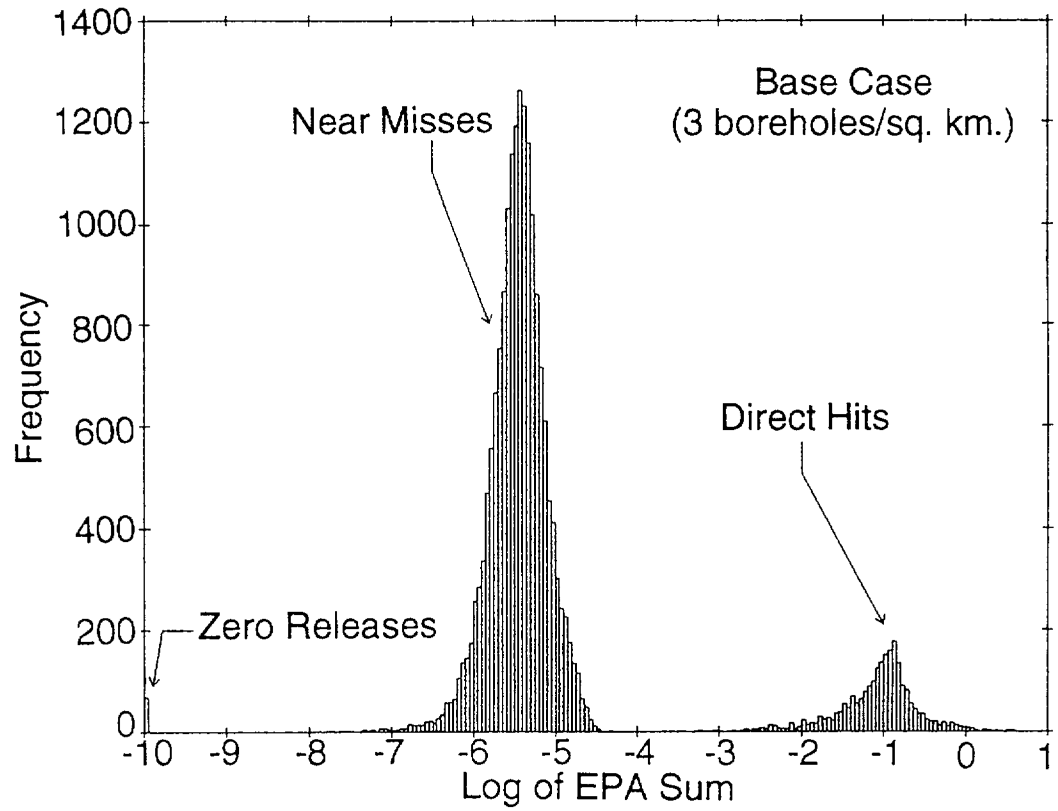

Figure 6-7. Distribution of surface releases from drilling (base case)

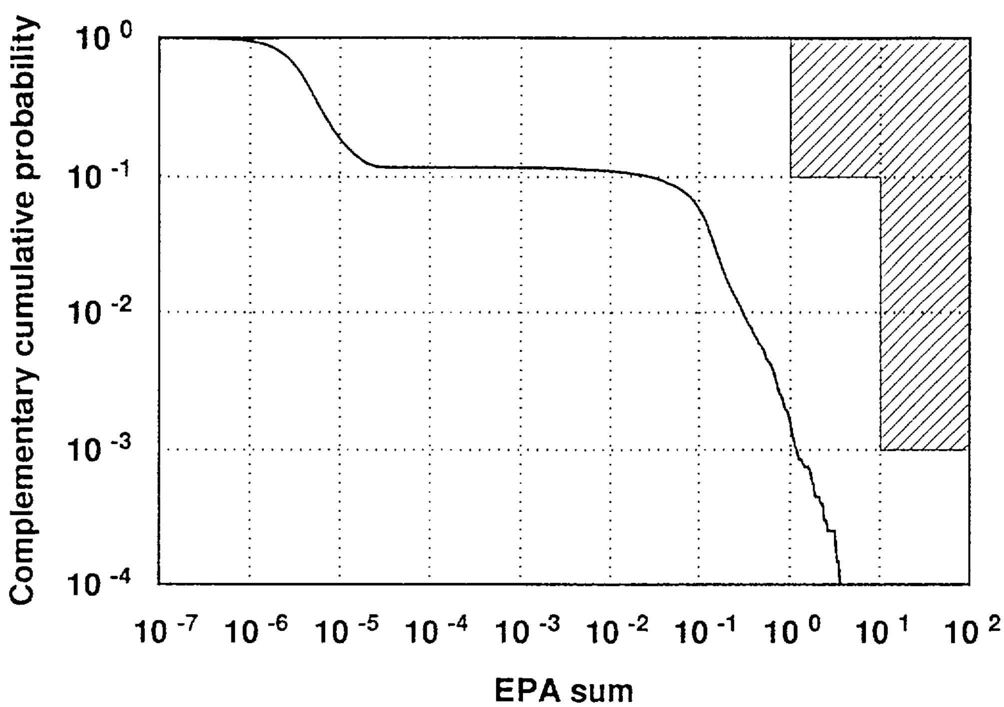

Figure 6-8. Conditional CCDF for surface releases due to drilling

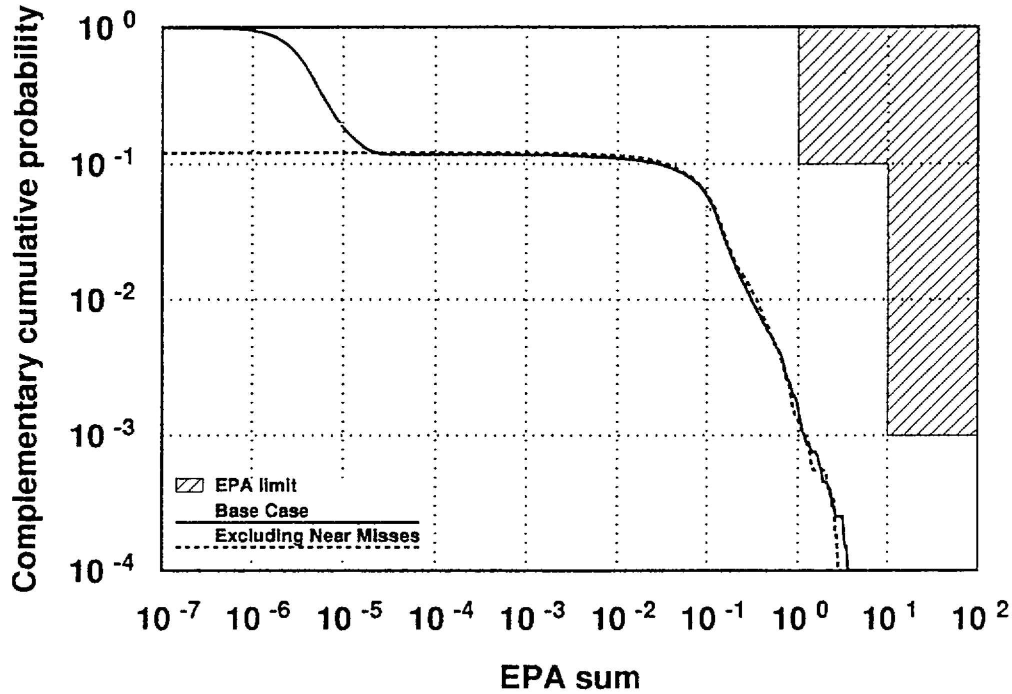

Figure 6-9. Conditional CCDF showing contributions of near misses

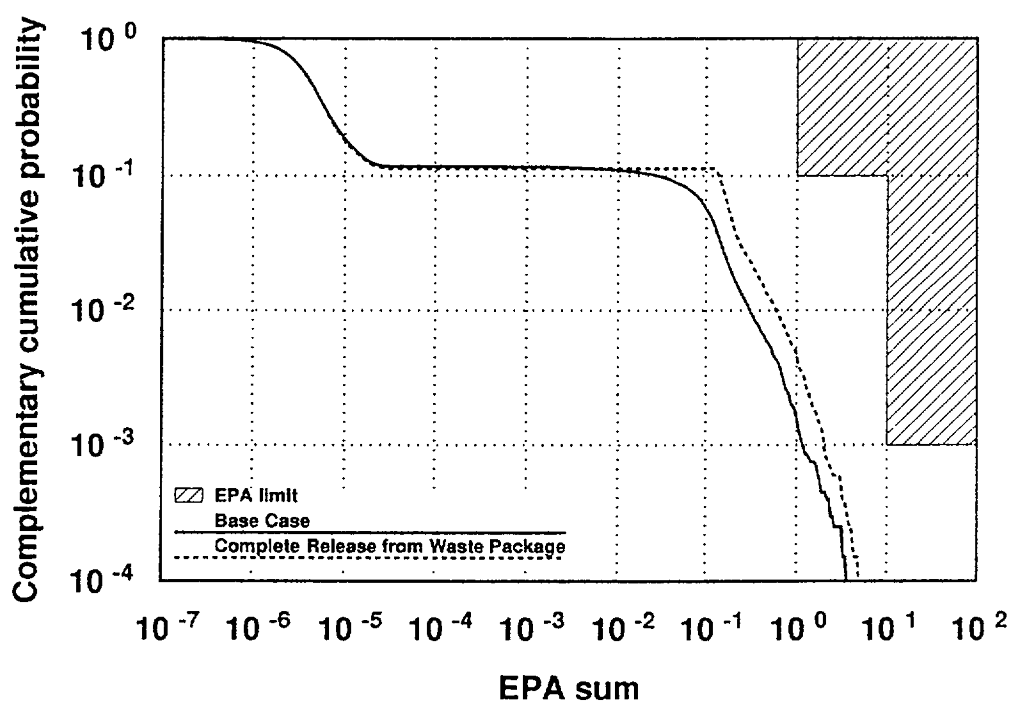

Figure 6-10. Conditional CCDF showing effect of releasing entire waste package

Figure 6-11 shows the distribution of the number of waste packages hit in 20,000 trials. For the base case of 17 boreholes (i.e., 3 boreholes/km^2) drilled in each trial, most trials have no direct hits. However, there are five trials in which three waste packages were hit. The figure also shows the prediction of the binomial formula for 17 trials and a P_{hit} of 0.0075.

Using 17 boreholes as the mean number drilled with the frequency of drilling following a Poisson distribution (instead of always drilling 17 boreholes) gives the results shown in Figure 6-12. The releases are almost identical with those of the base case, as expected from the similarity of the P_{hit} values listed in Tables 6-1 and 6-2. The conditional CCDFs (Figure 6-13) also show essentially the same response.

Figure 6-14 shows the distribution of hits on waste packages for the trials using the Poisson distribution. As with the base case, most trials do not have direct hits. In this simulation, however, twelve trials have three packages that were hit, and in one trial four packages were intersected.

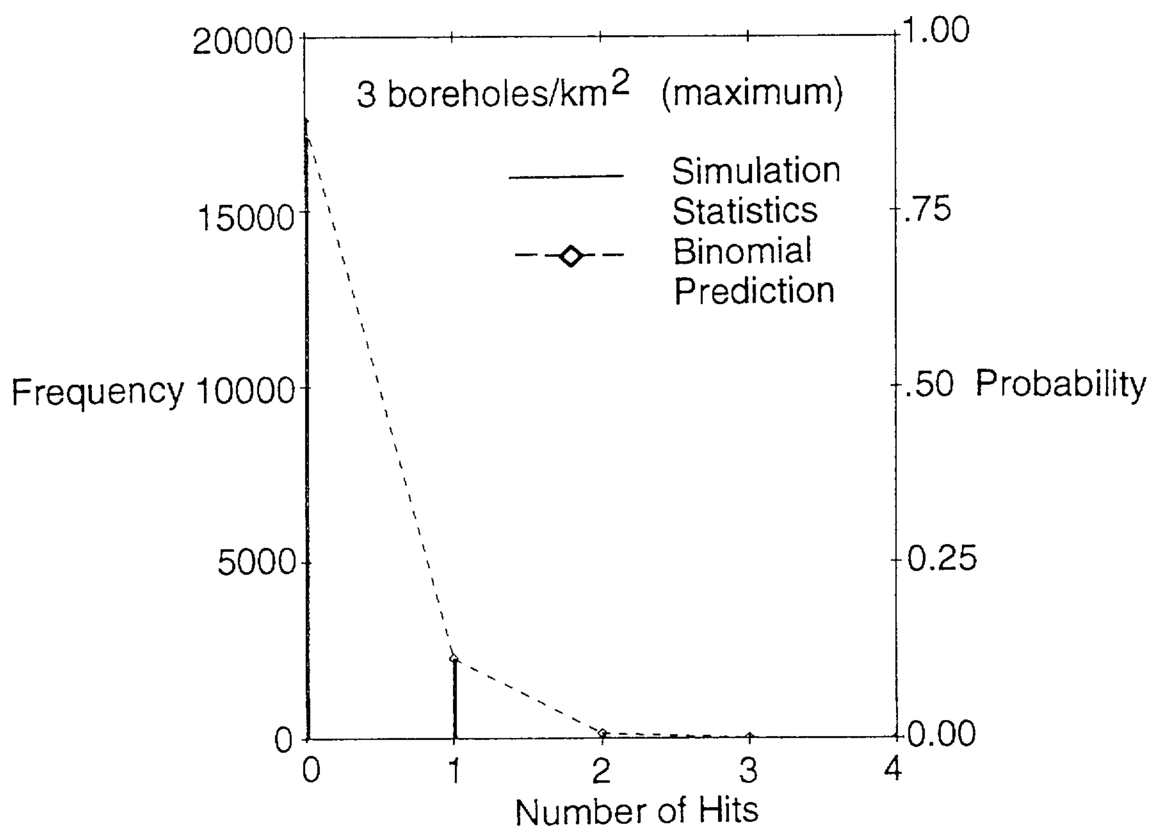

Figure 6-11. Distribution of hits on waste packages for base-case drilling density

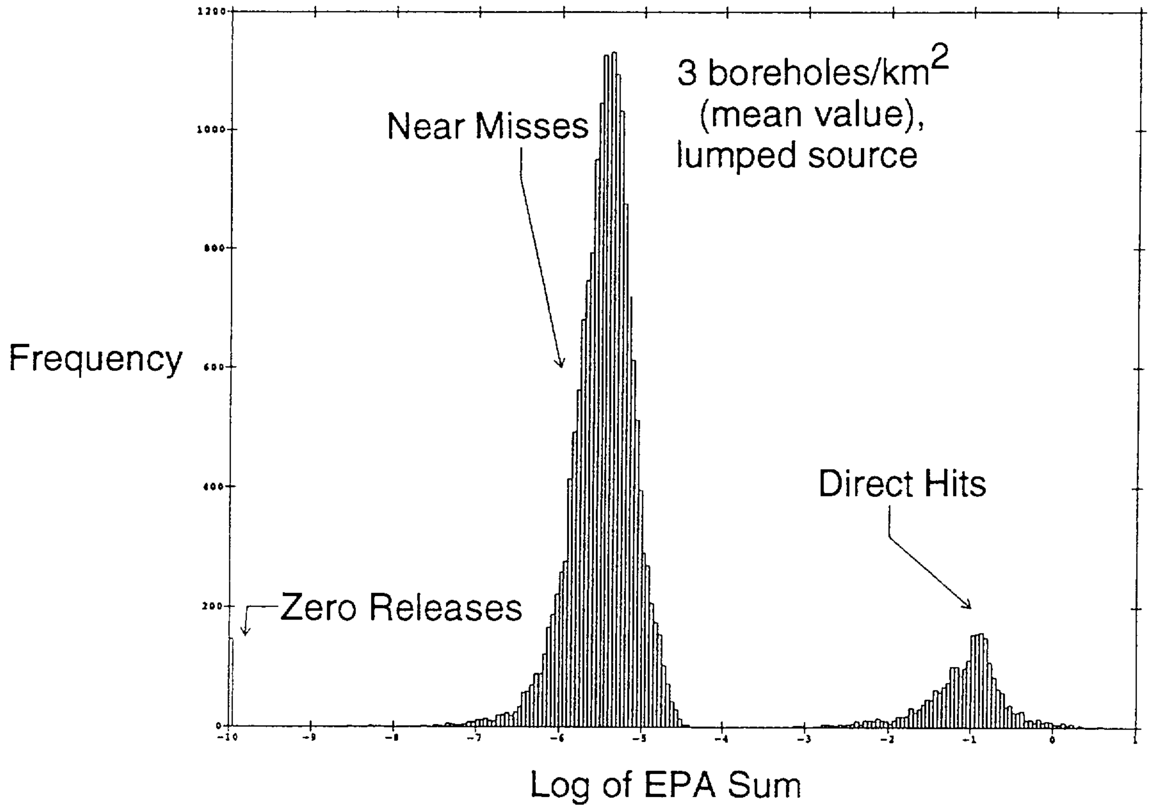

Figure 6-12. Distribution of releases for mean drilling density of 3 holes/km^2

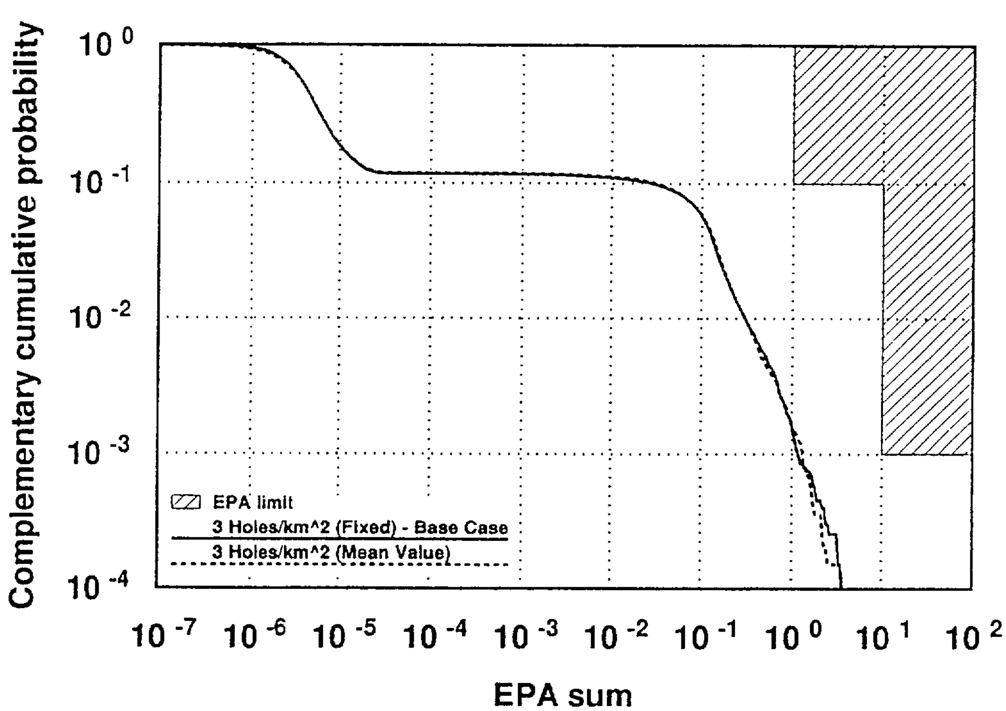

Figure 6-13. Comparison of conditional CCDFs for different assumptions for drilling density

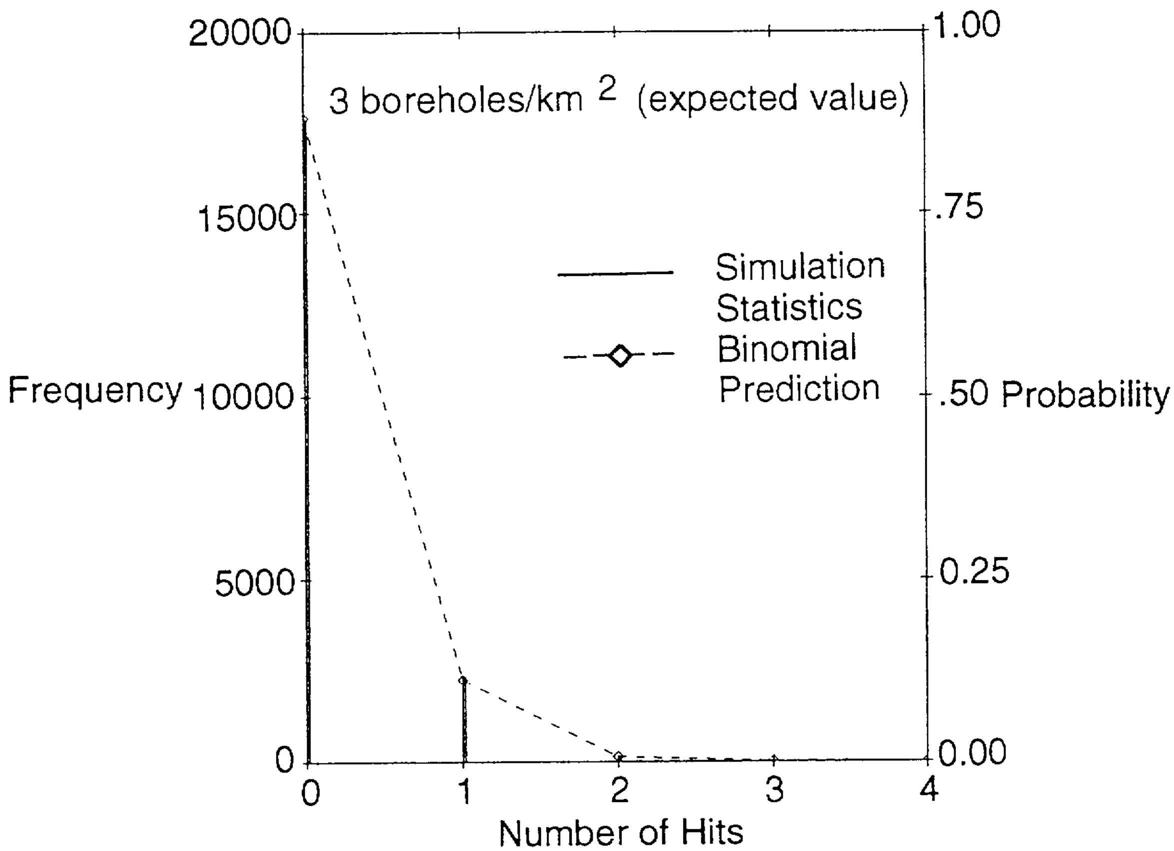

Figure 6-14. Distribution of hits on waste packages for mean drilling density of 3 boreholes/km^2

6.6.2 Surface-release sensitivity studies

Using multiple sources instead of the lumped source has very little effect on the outcomes. Figure 6-15 compares the releases for the two types of sources. The histograms can be seen to be essentially coincident. Furthermore, Figure 6-15 shows that the ranges of the distributions are roughly the same and that there are no greater occurrences of extreme values for the multi-source simulation than for the lumped-source analysis.

The greatest differences occur when the number of boreholes drilled over 10,000 years is set to either 170 (ten times the base case), or 340. The first number would be consistent with the maximum number of drillholes postulated by the EPA to be drilled in a heavily explored sedimentary basin with the areal extent of Yucca Mountain, over the course of 10,000 years. For this simulation, the conditional CCDFs show greater releases for both near misses and direct hits and show greater probabilities for both types of events (Figure 6-16). Because of the greater number of holes drilled, each trial has a greater potential to have a nonzero outcome. As Figure 6-17 shows, one hit per trial is the most likely occurrence when exactly 30 boreholes/km^2 are drilled, but as many as 7 hits per trial can occur. (With 30 boreholes/km^2 as the expected number for a Poisson drilling model, the shape of the distribution is substantially the same, except that 8 hits occur in two of the trials.) When exactly 60 boreholes/km^2 per trial are drilled, the distribution of hits and the prediction of the binomial formula are shown in Figure 6-18. Now, two hits per trial is the most likely, with a maximum of ten hits in one instance. Using 60 boreholes/km^2 as the expected number of hits for a Poisson drilling model gives a very similar distribution, with 11 hits occurring in one instance. The releases, for ten times as many boreholes, are not ten times those of the base case. While drilling ten times the number of boreholes does increase the frequency of events leading to a release, the actual amount of the releases also varies with time because of the variation in the amounts brought to the surface and because of different amounts of decay. Furthermore, the maximum values for the releases occur when there are multiple direct hits in a trial. Increasing the number of drillholes only increases the opportunity for multiple hits. It does not directly increase the number of multiple-hit outcomes.

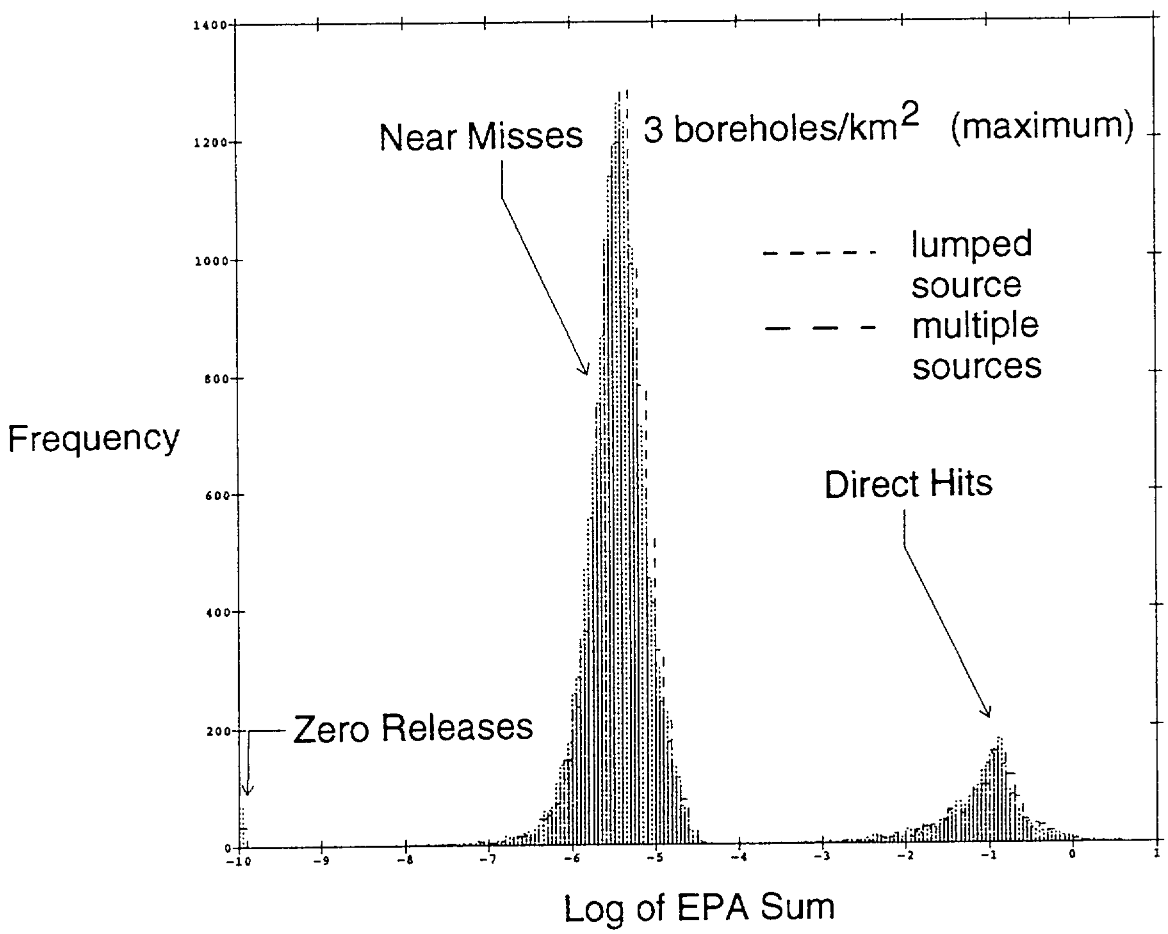

Figure 6-15. Comparison of lumped-inventory and multiple-inventory source terms

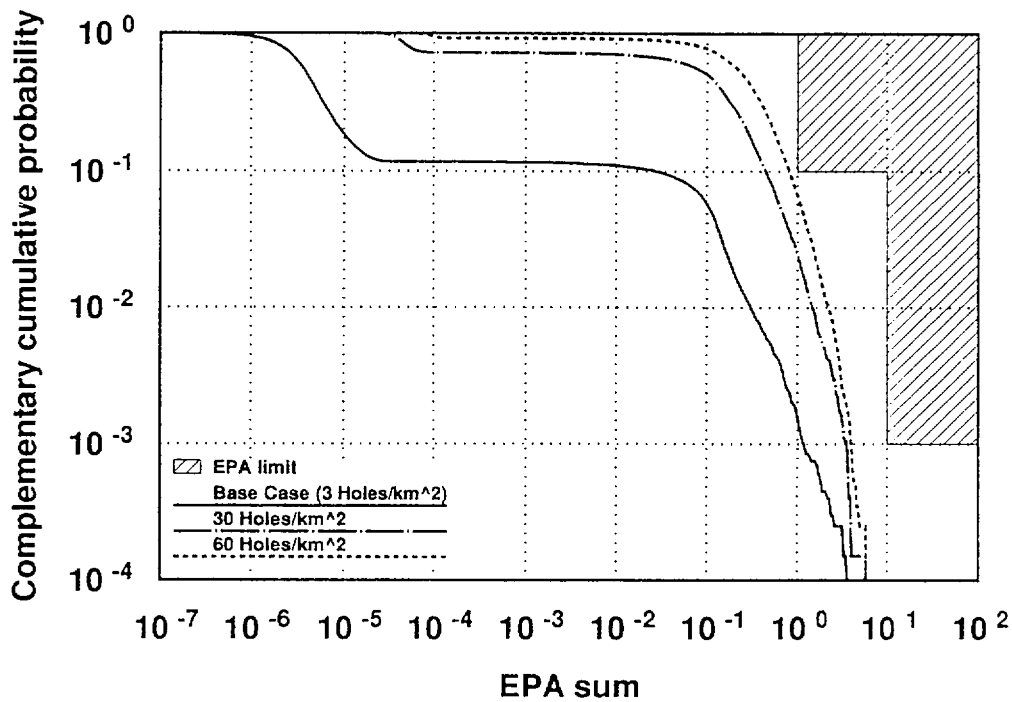

Figure 6-16. Conditional CCDF showing increases in surface releases due to increasing the number of holes drilled over 10,000 years

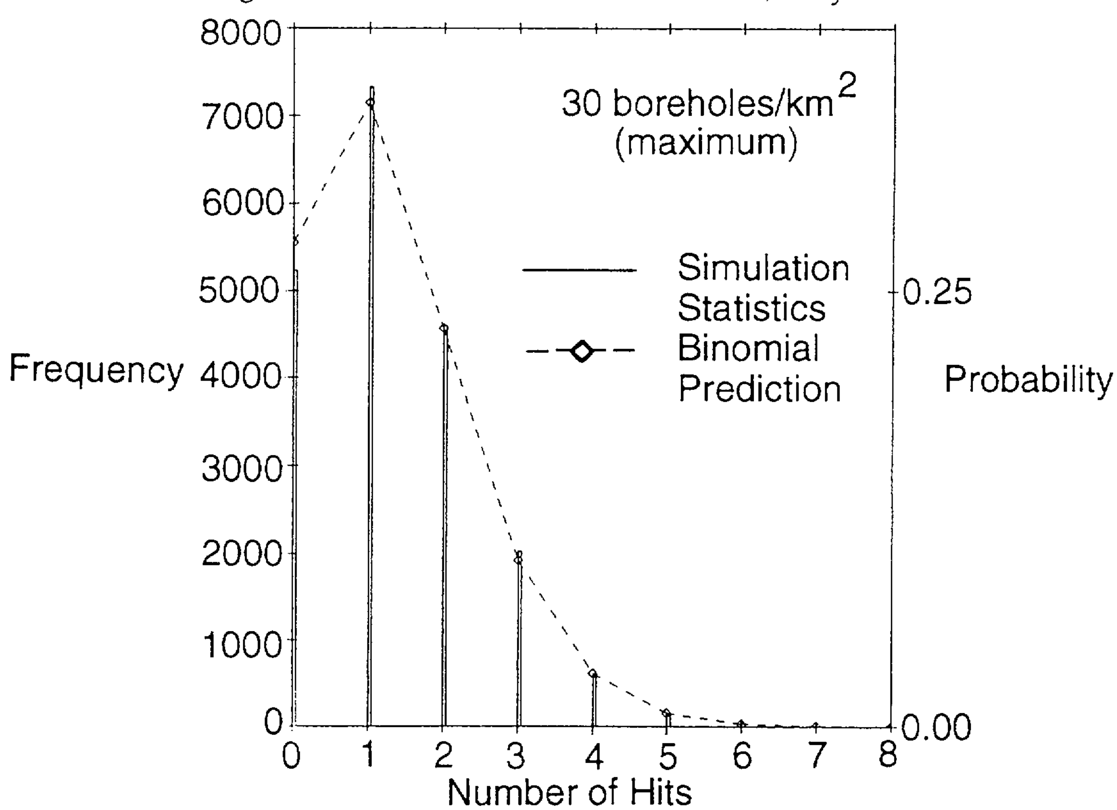

Figure 6-17. Distribution of hits on waste packages for drilling density of 30 boreholes/km^2

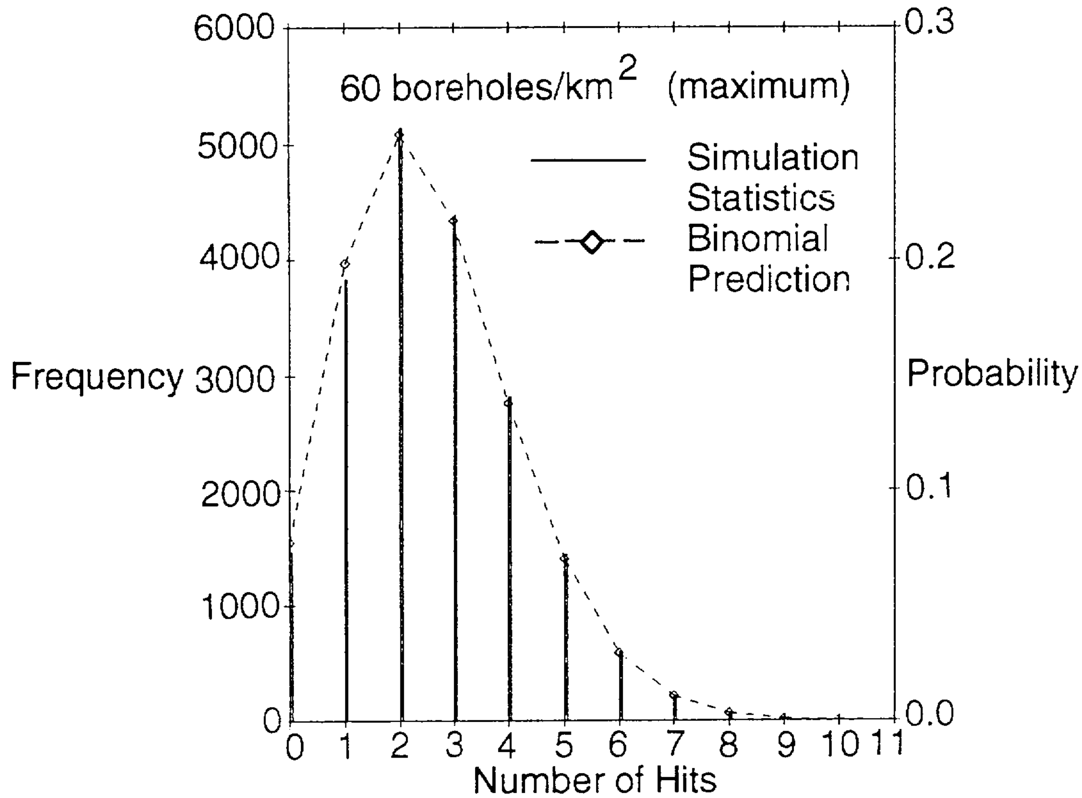

Figure 6-18. Distributions of hits on waste packages for drilling density of 60 boreholes/km^2

The result of performing the calculation with the inventory of radionuclides available in the near-miss zone two orders of magnitude greater than the base case is shown in Figure 6-19. There is a shift in the releases of two orders of magnitude for near misses only; otherwise the shapes of the curves are almost the same. In view of the linear dependence of the near-miss releases on the inventory, these results are not unexpected.

The effective diffusion coefficient used to calculate the area of contaminated rock for the near misses was taken from prior work (Barnard and Dockery, 1991), The value, 3.65×10^{-4} m^2/yr., is about two orders of magnitude below the molecular self-diffusion coefficient in pure water. The lower value was selected to account for the rate of movement expected in a material with the tortuosity and porosity expected for the rock in the repository horizon. The results of increasing the diffusion coefficient by two orders of magnitude are shown in Figure 6-20. The figure compares the distributions of releases for the base case with those for the increased-diffusion case. As expected, the direct-hit releases are essentially identical, and there

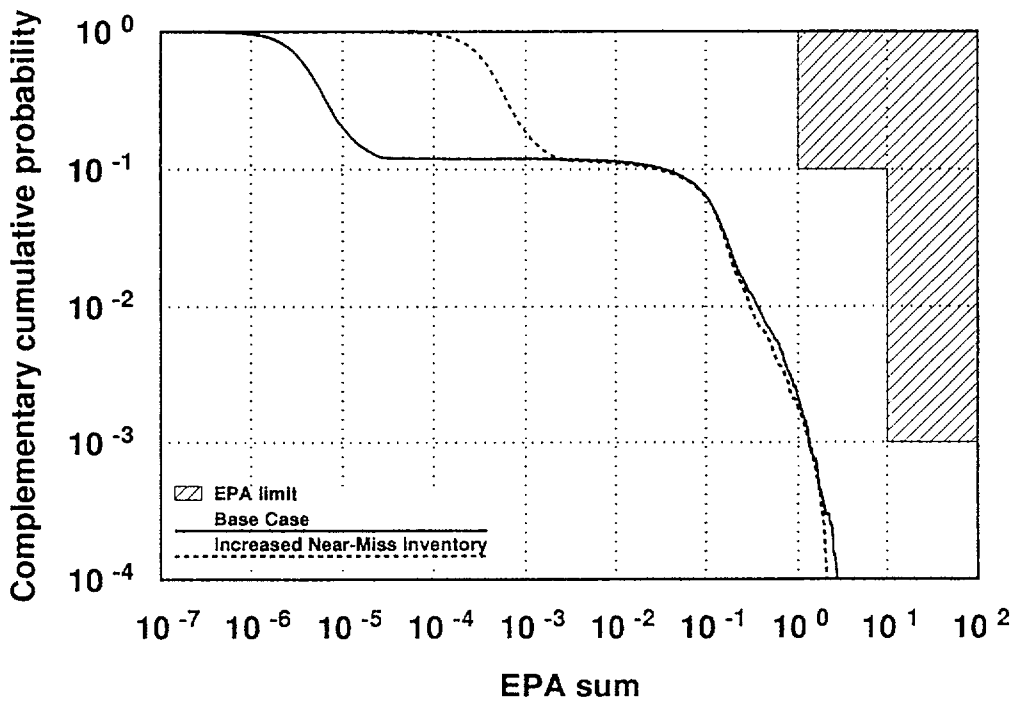

Figure 6-19. Conditional CCDF showing increases in surface releases due to increasing the near-miss inventory

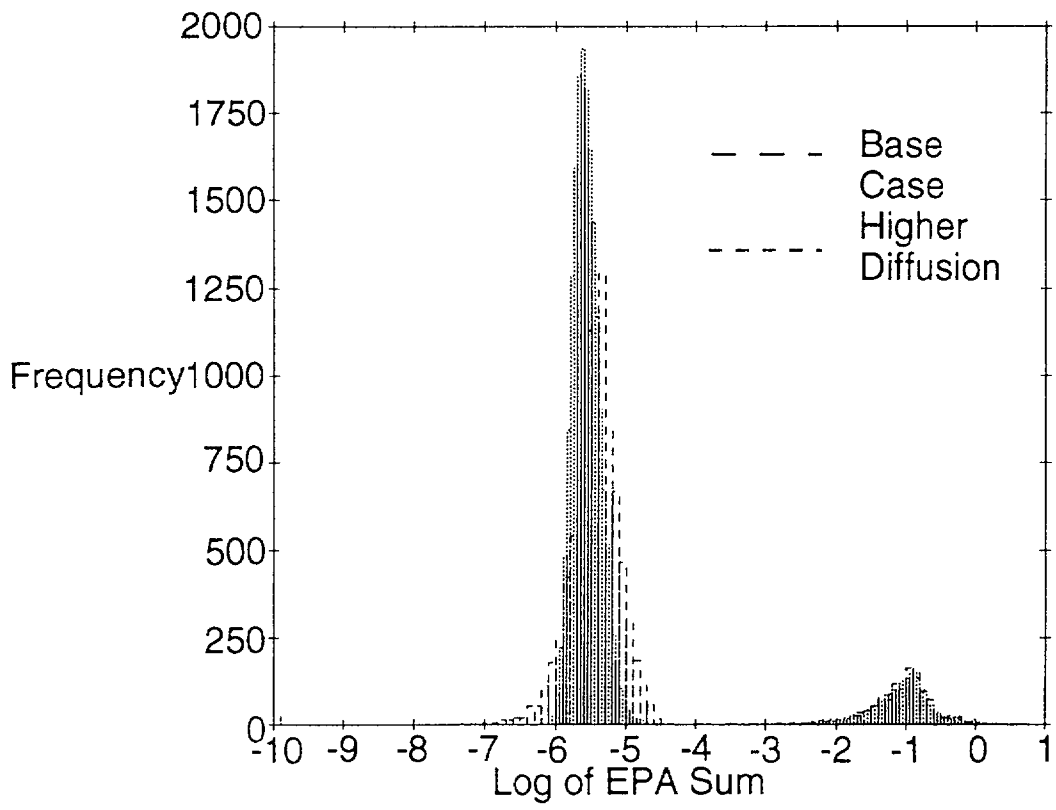

Figure 6-20. Comparison of distributions of releases for base case and 100-fold increase in diffusion coefficient

are no zero-releases for the enhanced-diffusion case. When the diffusion coefficient is increased, a larger area for near misses to encounter is created. For a constant diffusion source, this larger area results in a smaller concentration. As can be noted from the figure, the median of the near misses for the enhanced-diffusion case is lower than that for the base case, but the range is broader.

In one study, the distribution for the time of drilling was biased to occur primarily in the later part of the 10,000-year time period (using a beta distribution with a mean time of drilling of 7500 years) to account for the effect of institutional control at early times. The major effect on the outcome is a decrease in the number of events that have the highest values for release (Figure 6-21). This is, of course, due to the greater decay time that occurs prior to more of the interceptions. Because the program limits the number of values it can accept from a beta-distribution input, only 1000 trials were run for this simulation. Comparisons with other analyses may not be statistically meaningful.

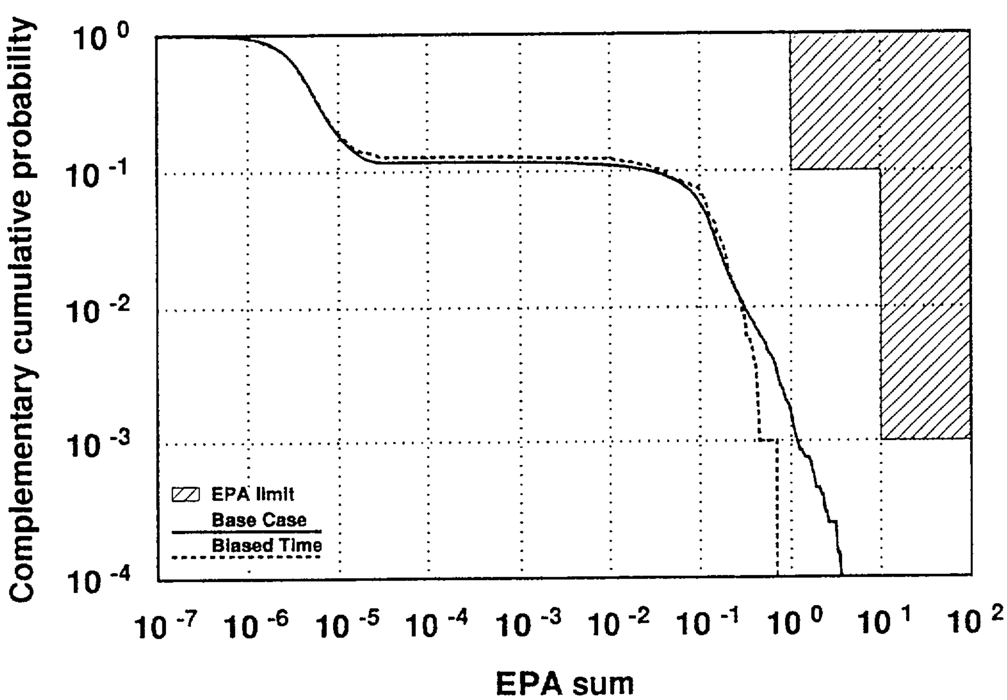

Figure 6-21. Conditional CCDF showing change in surface releases due to biasing drilling events to later in performance period

6.6.3 Saturated-zone calculations

The conditional probabilities of releases of radionuclides through the saturated tuff zone over 10,000 years are shown in Figure 6-22. (These conditional probabilities do not include the probabilities that a hit has occurred.) The radionuclides form two groups—those with low retardation (^{14}C, ^{99}Tc, and ^{129}I), and those with slightly higher retardation (^{237}Np, ^{234}U, and ^{79}Se). In this simulation (1,000 trials), the maximum releases, of about 5×10^{-4} of the EPA sum, are each produced by carbon, neptunium and uranium. The plutonium and americium isotopes, and tin and cesium do not have measurable releases in this period. As Figure 6-23 shows, for the particular realization shown, cesium and tin do not reach the accessible environment until more than 250,000 years have passed, and plutonium and americium either take longer or have decayed away. For these analyses, the ^{14}C is assumed to be transported entirely by aqueous means. Figure 6-24 shows the major contributors to the releases averaged over 10,000 years. Carbon contributes over 60% of the radioactive release, with neptunium contributing about 15%.

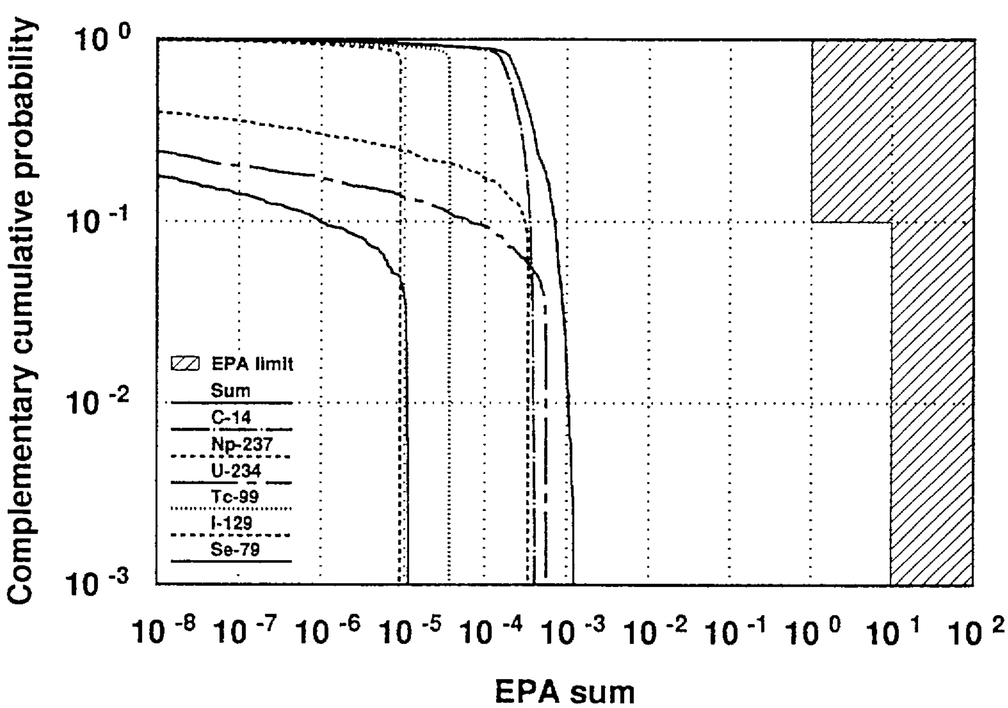

Figure 6-22. Conditional CCDF for releases to accessible environment through saturated-tuff zone due to human intrusion

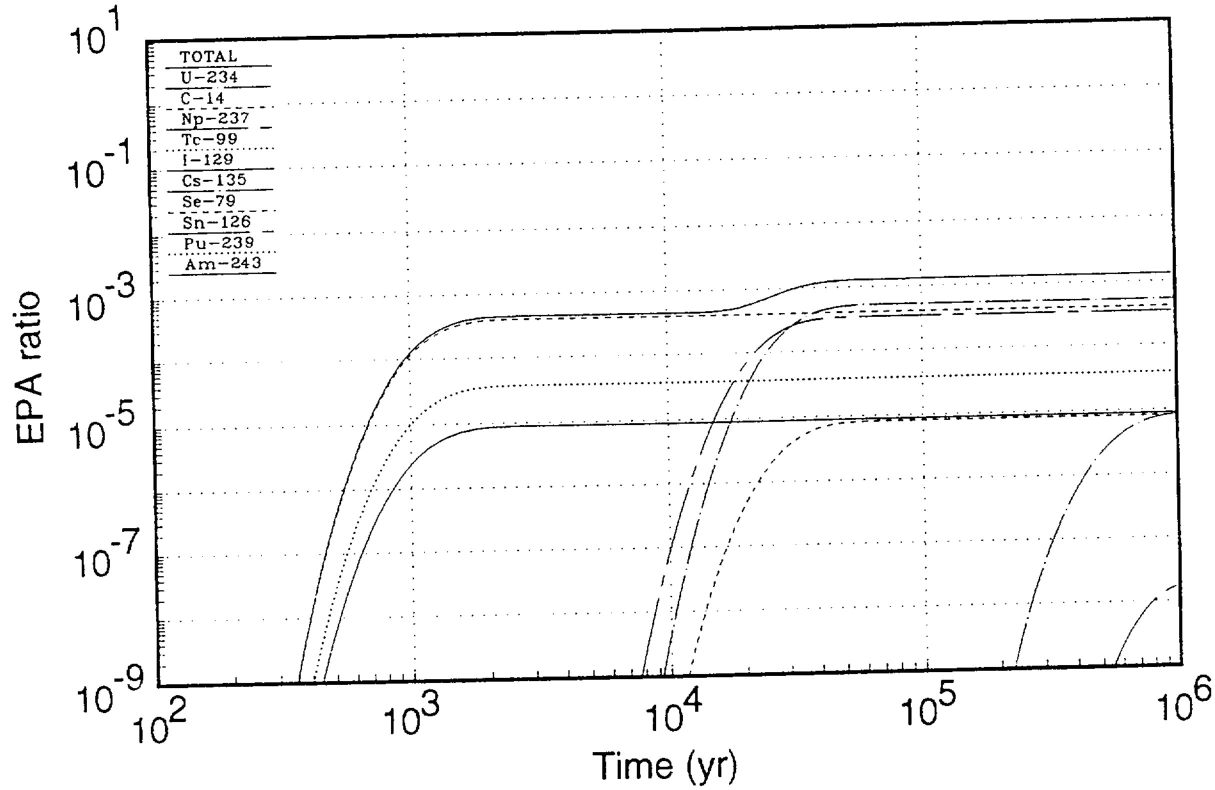

Figure 6-23. Cumulative releases to accessible environment through saturated-tuff zone

Because of the shorter travel times specified for the carbonate aquifer, the releases through it are greater. Figure 6-25 shows the total releases and several of the component releases over 10,000 years. Now, the two plutonium isotopes have the highest probabilities of large releases. Because of a short half-life, the ^{241}Am has a reduced probability of releases for the entire 10,000-year period. However, it produces the highest releases of all the radionuclides used. Figure 6-26 shows the expected values of the major components of the releases over 10,000 years. The two plutonium isotopes contribute over 90% of the total. Figure 6-27 shows the cumulative releases as a function of time for one realization. Although Figure 6-27 implies that ^{239}Pu does not contribute significantly to the total release until almost 30,000 years have passed, it is only a single realization. The average ^{239}Pu contribution for all trials is given in Figure 6-26.

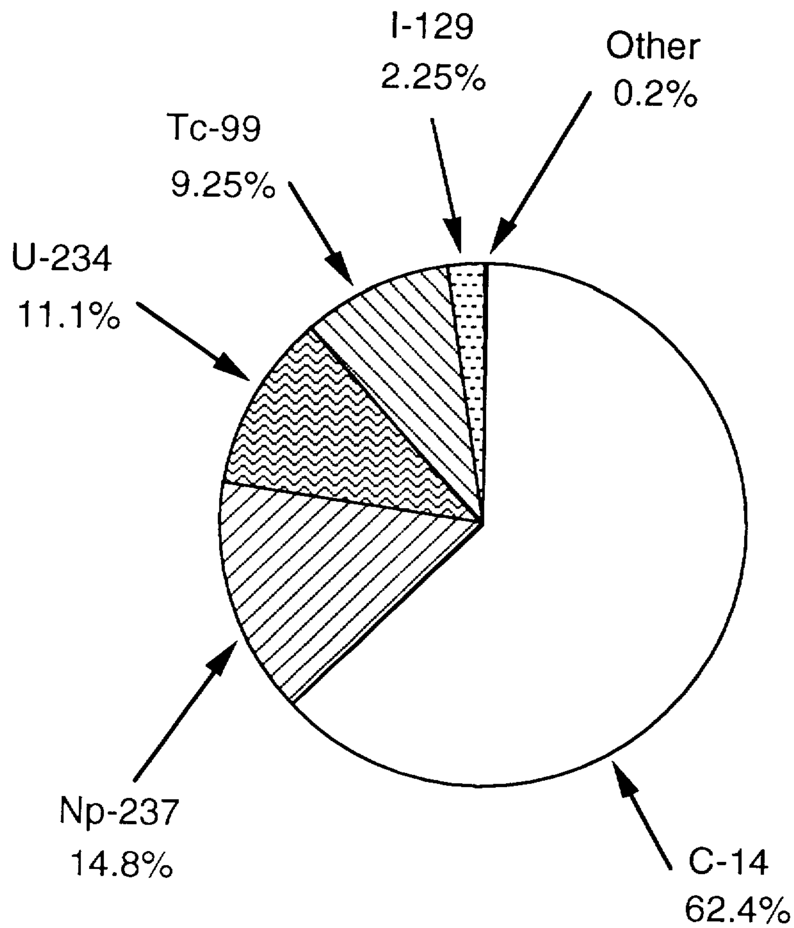

Figure 6-24. Average percentages of radionuclides released through saturated-tuff zone

Comparing the total releases through the two saturated-zone pathways (Figures 6-23 and 6-27), about 6% of the releases in the carbonate aquifer occur within the first 100 years. (The maximum EPA sum is about 0.009; at 100 years the sum is $5x10^{-4}$.) In contrast, releases in the saturated-tuff zone at 100 years are more than six orders of magnitude below the maximum. This difference can be explained by considering the travel times in the two pathways from the repository to the accessible environment: the saturated-tuff zone and the carbonate aquifer. Figure 6-28 compares these travel times for a nonsorbing particle. The curves in the figure relate the times at which given percentages of the released radionuclides reach the respective boundaries. For this comparison, a fixed number of particles are instantaneously released into steady-state flow fields. Because travel times in the carbonate aquifer are considerably shorter than the other two pathways, the figure shows that about 10% of the particles reach the boundary in one year.

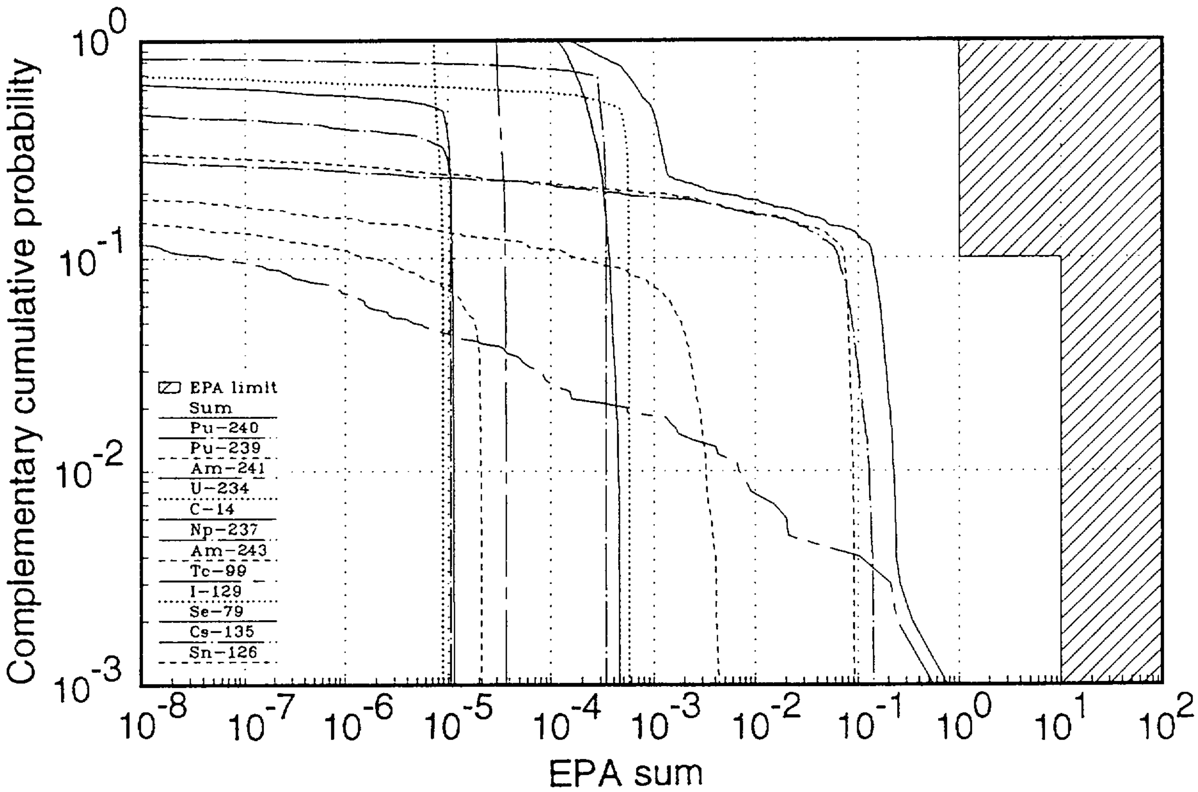

Figure 6-25. Conditional CCDF for releases to accessible environment through carbonate aquifer due to human intrusion

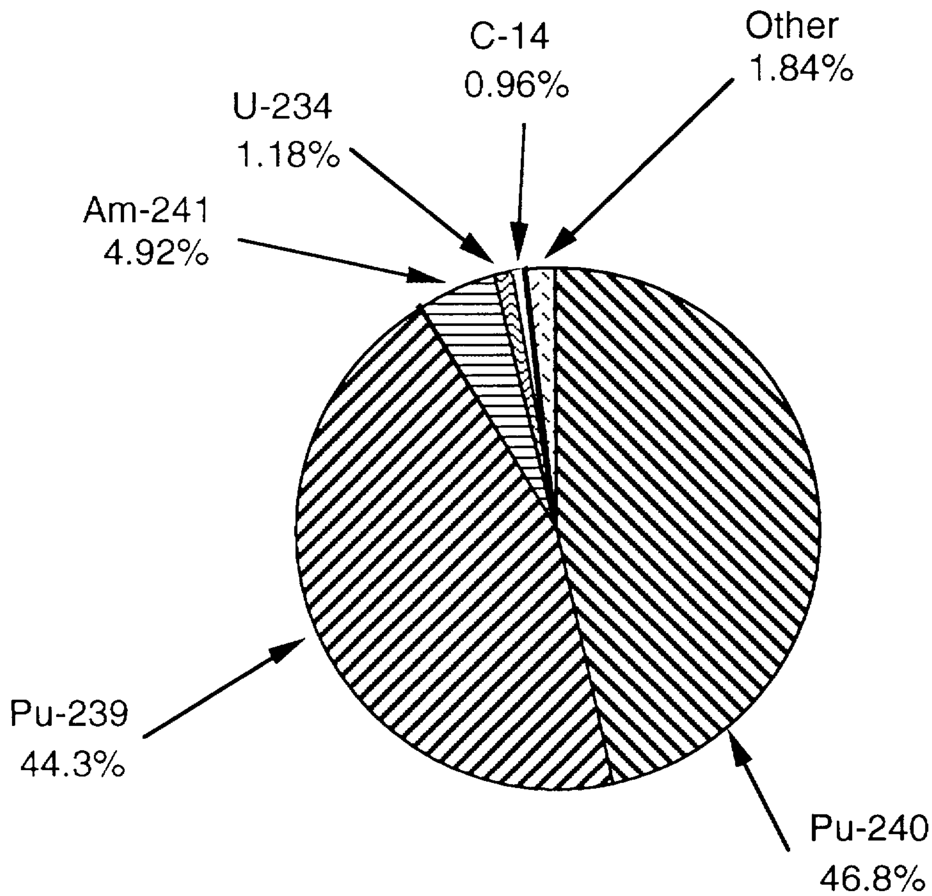

Figure 6-26. Average percentages of radionuclides released through carbonate aquifer

The relative magnitudes of the releases from the three drilling scenarios are compared in Figure 6-29. In order to compare the conditional CCDFs for saturated-zone releases (where the probabilities of drilling hits are not included), with the CCDF for surface release (where the probabilities are included), the probability of intersecting a waste package for the surface-release scenario, was set to 1.0; the entire contents were released at random times. The magnitudes of surface releases are consistently above those of the groundwater-based processes. Maximum releases from the saturated tuff are about three orders of magnitude below those from the carbonate aquifer primarily because the lower velocity and higher retardation in the tuff keep plutonium and americium from reaching the accessible environment in 10,000 years.

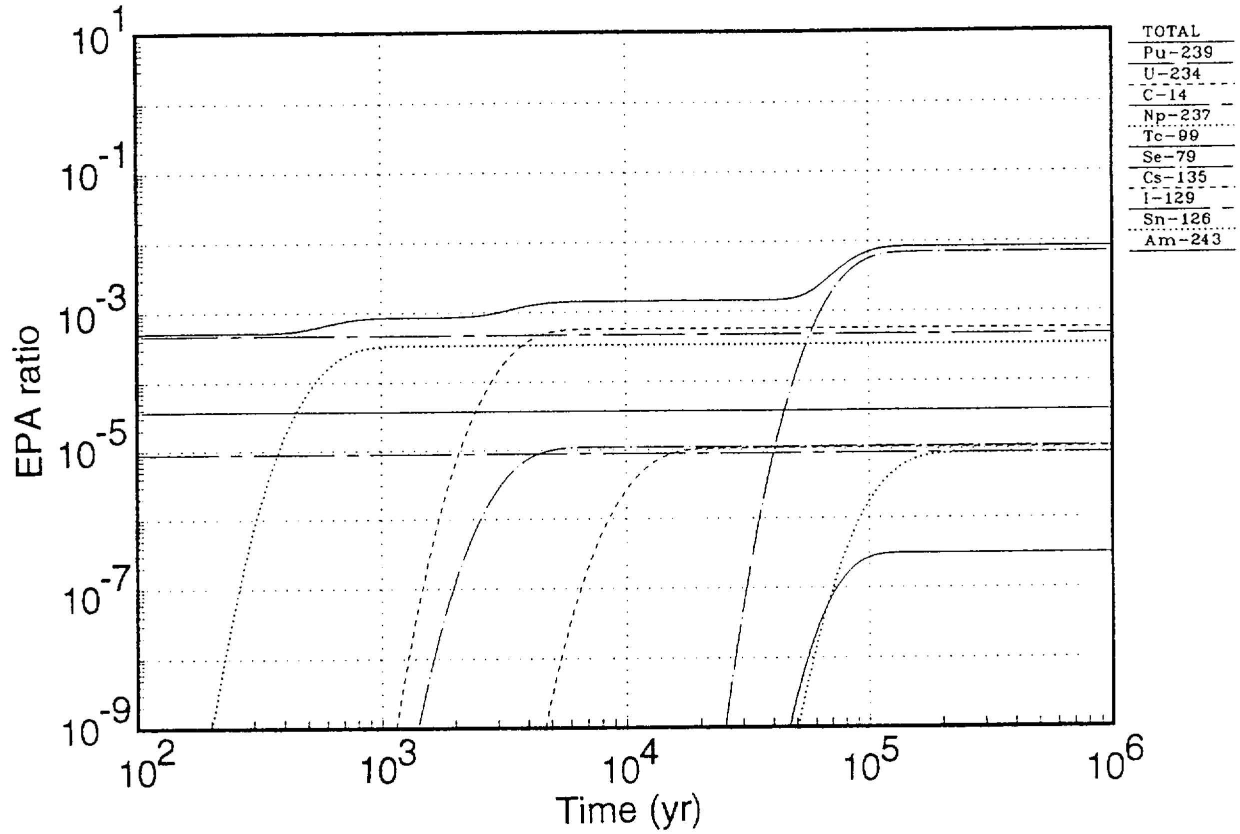

Figure 6-27. Cumulative releases to accessible environment through carbonate aquifer

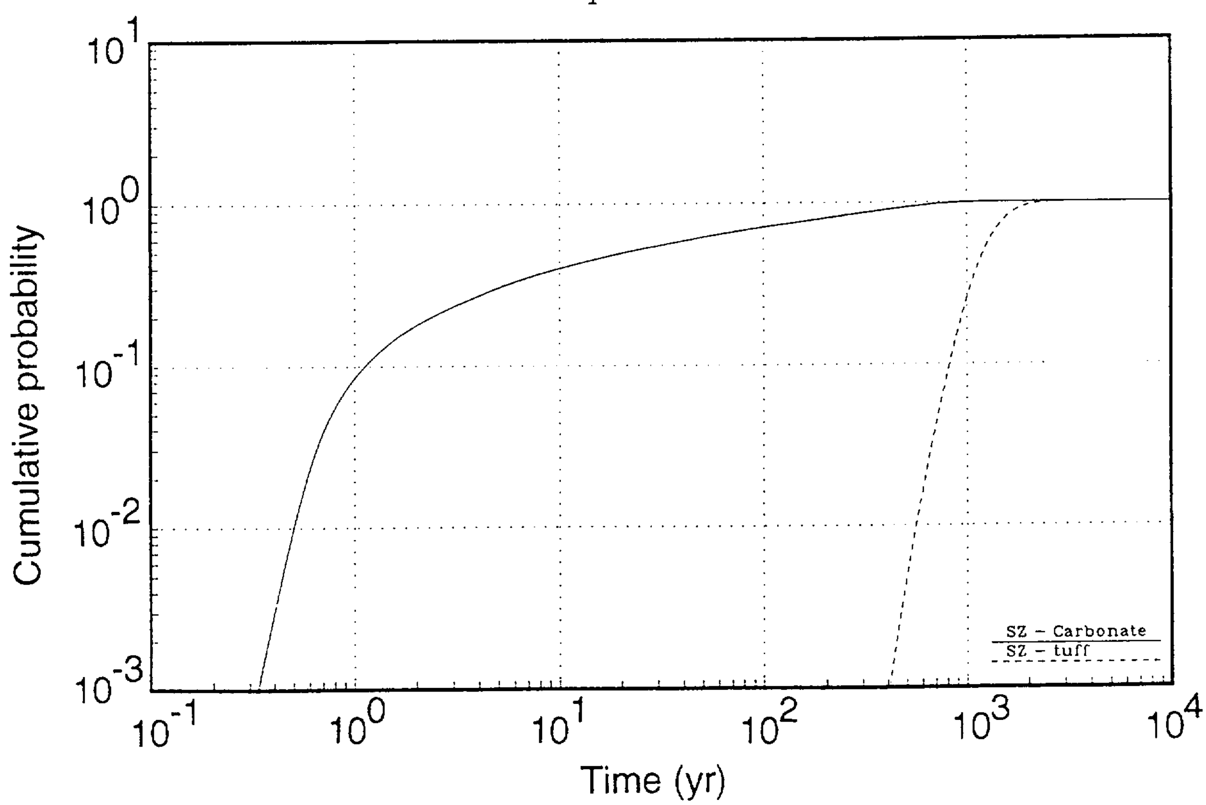

Figure 6-28. Distributions of tracer travel times

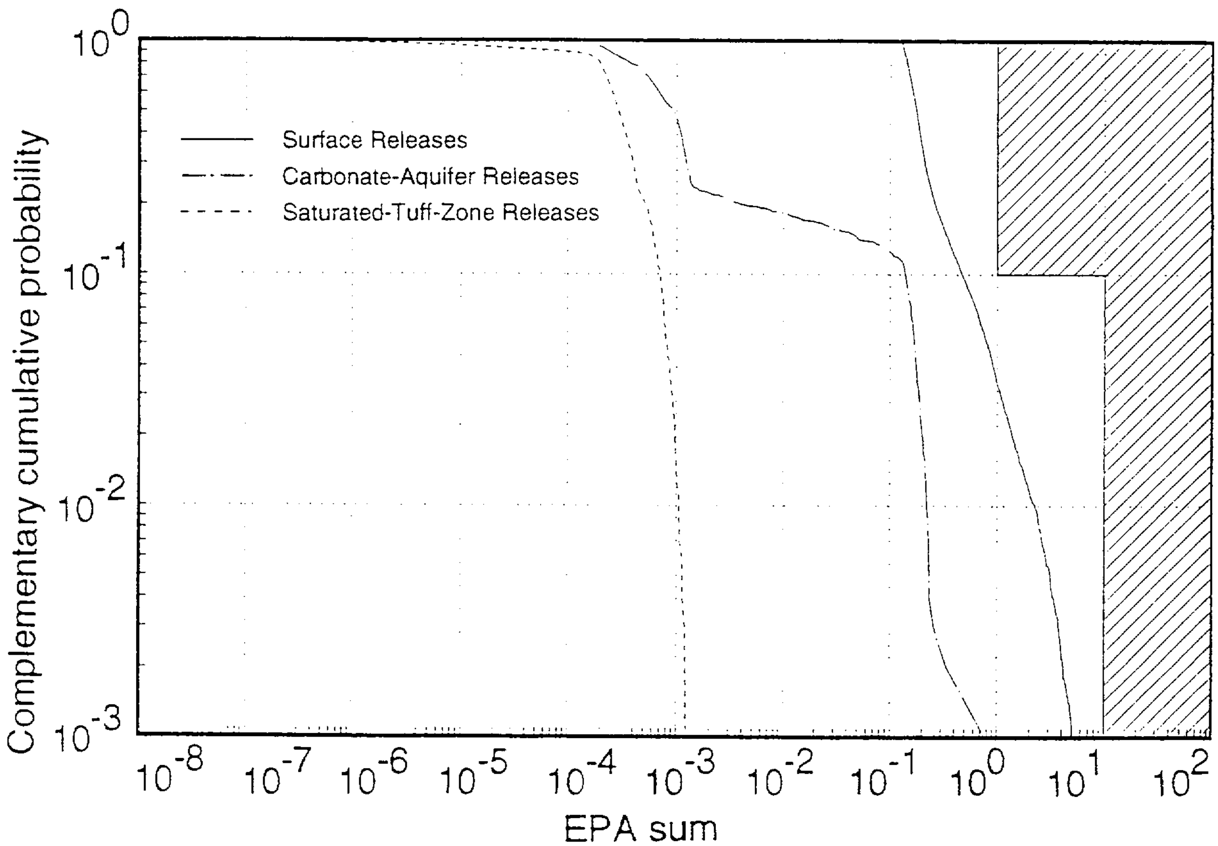

Figure 6-29. Comparison of CCDFs for releases for three drilling scenarios

A composite CCDF showing the probabilities of releases if any of the three scenarios occurs is shown in Figure 6-30. To combine the conditional CCDFs for surface release and the two saturated-zone releases, it was assumed that the three scenarios are mutually exclusive. As is shown in Tables 6-1 or 6-2, the probability of a waste package being hit by drilling events over 10,000 years is about 0.12. Because the three scenarios are considered to be mutually exclusive, the probability for direct hits was equally apportioned to each. Thus, to calculate a combined CCDF reflecting the probability of having any of the three releases occur, the direct-hit portions of each component CCDF (for surface, tuff, and carbonate releases) were multiplied by 0.04. (The probability of having releases due to near misses approaches 1 (e.g. Figure 6-9), so this portion of the surface-release CCDF was not scaled.) This combined CCDF is still conditional on the probability that drilling events occur at the site at all. The curve is dominated by the surface releases, as would be expected from the comparisons of the magnitudes in Figure 6-29. There is no discernible change to the highest releases (i.e., above an EPA sum of 0.1) from the addition of the aqueous scenarios. The contribution from the aqueous releases occurs for EPA sums in the range of about 0.0002 - 0.001. Because near misses can occur whenever drilling is done, their releases take the CCDF to a probability of 1.0.

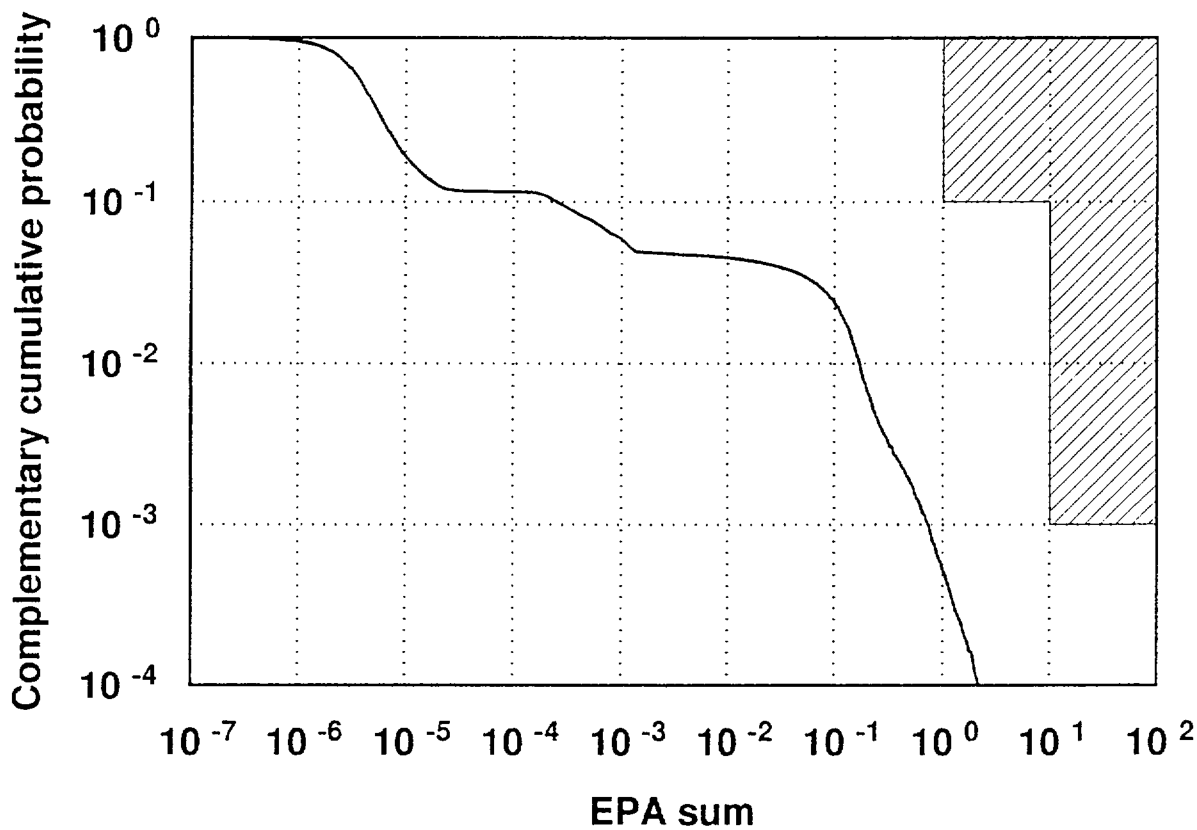

Figure 6-30. Combined conditional CCDF for three drilling scenarios

6.7 Summary

The TSPA analyses of releases due to drilling are simplified representations of a few human-intrusion scenarios. The base-case analyses show that, ignoring the fact that the probability of human intrusion at the site is probably small, the releases as a result of drilling do not have a significant probability of exceeding the EPA standard. For the surface-release scenario, varying some of the parameters, such as the source term or distribution of drilling of boreholes, does not significantly alter the outcomes. The increase in releases due to varying the strength of the near-miss portion of the source term is directly proportional to the variation. The most dramatic effect occurs when the maximum number of boreholes is increased; however, even a twenty fold increase still does not cause the CCDF to exceed the EPA standard.

Many of the assumptions made in this analysis were quite conservative. Therefore, refining the simplifying assumptions with better site-specific data may not result in increased releases. However, such refinements may make it possible to interpret the human-intrusion results in terms of the actual response of the repository rather than in terms of the response of the model.

For aqueous releases, the conditional CCDFs also do not exceed the EPA standards. As the problem was set up, the water velocity in the carbonate aquifer was considerably higher than the velocity for the saturated-tuff zone. Releases through the former aquifer were consequently over two orders of magnitude higher at the 1% probability level. Because of the faster travel time in the carbonate aquifer, plutonium is able to reach the accessible environment. The release of ^{14}C is roughly the same for both the aquifers, but the plutonium and americium releases increased greatly in the carbonate aquifer.

The composite conditional CCDF is dominated by the surface-release component. The highest releases all come from surface release, and any aqueous contribution is about three orders of magnitude below the maximums.

Chapter 7
Basaltic Igneous Activity

(Dockery, Barnard)

7.1 Introduction

This component of the TSPA study considers releases at the earth's surface of radionuclides from a potential repository in Yucca Mountain. These releases are postulated to occur due to postclosure basaltic igneous activity resulting in volcanism at Yucca Mountain. The time period of this analysis spans the 10,000-year regulatory period specified by the EPA (EPA, 1985).

The complexity of a scenario involving a basaltic dike intersecting the repository, then erupting mechanically entrained waste at the surface is greatly simplified. We attempted to capture the essence of the processes by simplifying both the treatment of the radionuclide source term and the interaction between a hypothetical dike and the radioactive waste in the repository.

7.2 Problem definition

The scenario describing this TSPA analysis was developed from the FEP diagram for basaltic igneous processes (Barr et al., 1991). Figure 7-1 shows the portion of the FEP diagram that includes the FEPs captured in the calculation. These FEPs are described in more detail below.

There is a finite probability that a basaltic igneous body might intrude the waste-emplacement horizon of a potential repository at Yucca Mountain. Such an occurrence could possibly mobilize waste by rupturing waste packages and entraining the waste in a moving magmatic body (Figure 7-2). The eruption of this body at the surface would allow the entrained waste to reach the surface (Figure 7-3).

For this problem, release to the accessible environment is defined to occur when radioactive material reaches the surface. We have assumed that bare spent fuel will be erupted at the surface, even though, in a more realistic assumption, the waste would be encapsulated in a hardened basalt coating. Also, potential areal concentrations due to erosion, transport, and deposition are not considered.

The current estimates of the probabilities for the occurrence of basaltic igneous activity within the repository block are very small, as discussed in Section 7.3.3. Therefore, the consequences of the igneous activity are calculated first, without regard to their probabilities of occurrence, to obtain a conditional CCDF. The final

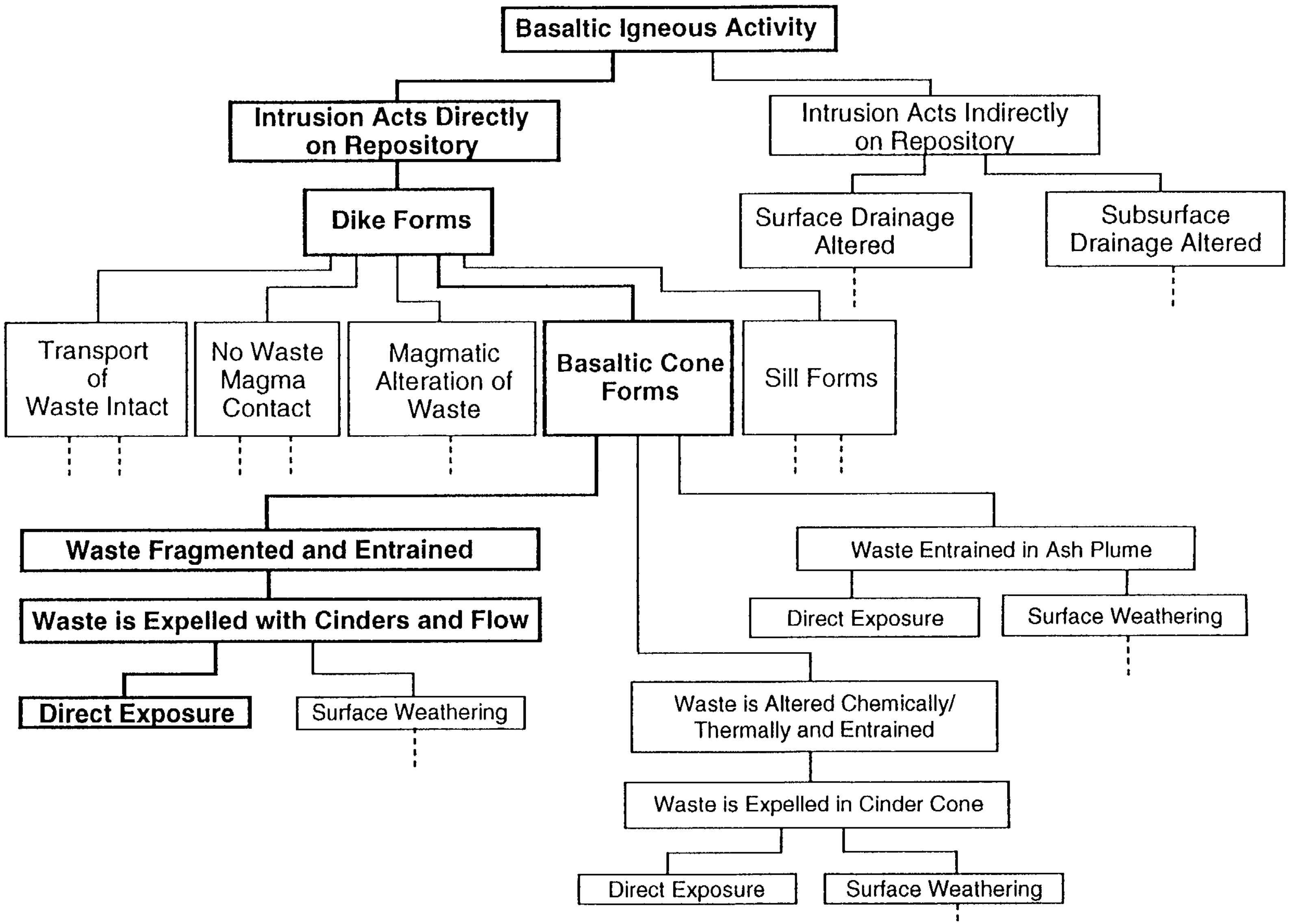

Figure 7-1. FEP diagram for basaltic igneous activity

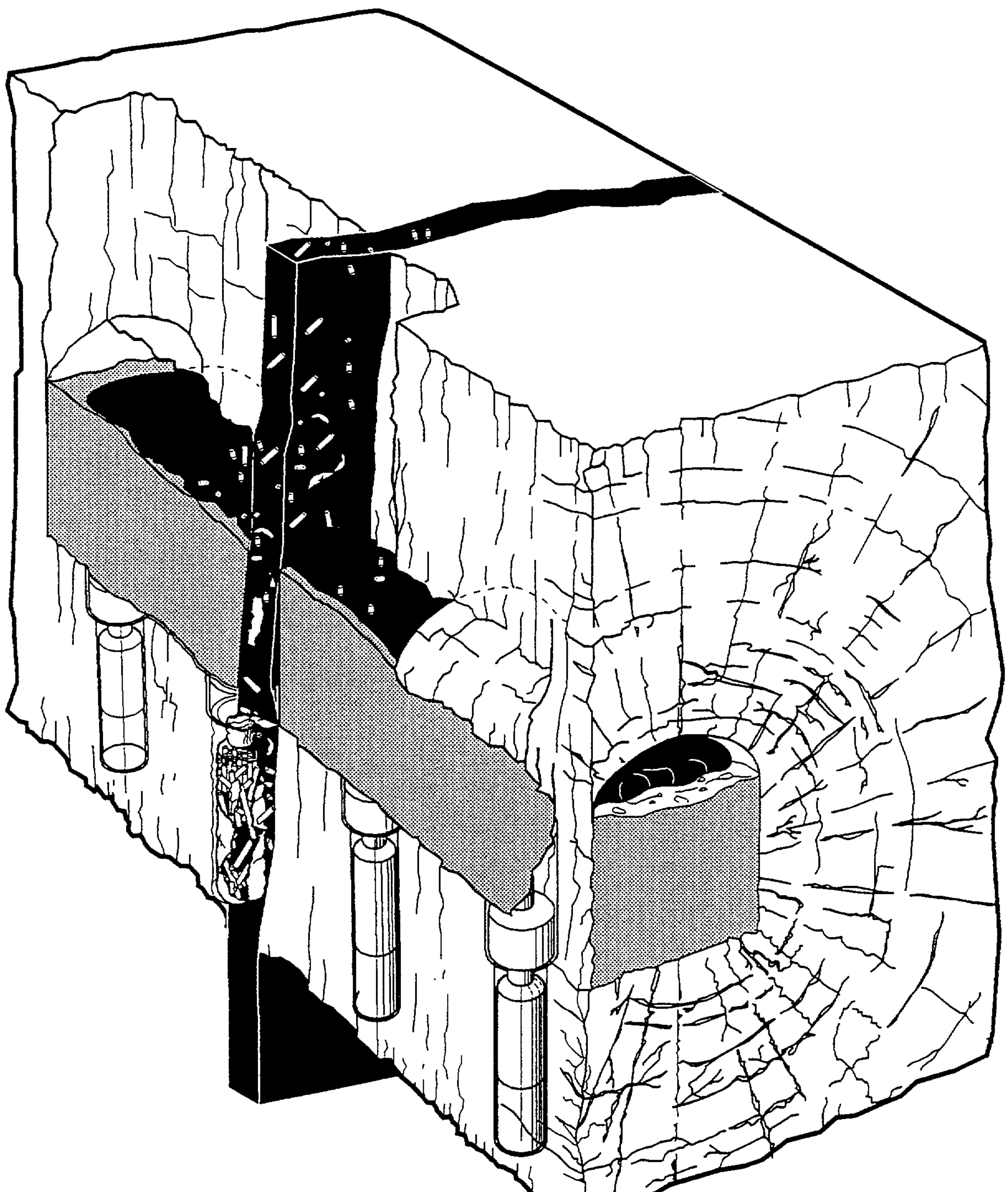

Figure 7-2. Interaction of dike with waste package

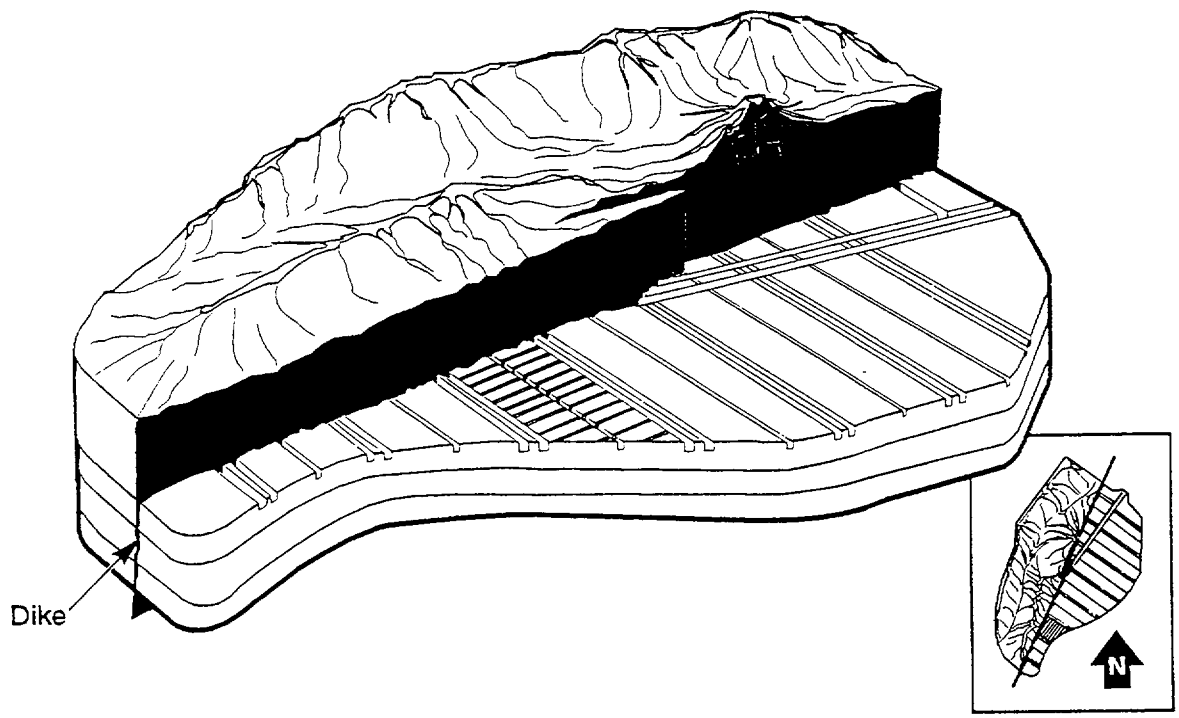

Figure 7-3. Distribution mechanism for waste at surface

CCDF is obtained by multiplying the conditional CCDF by the probability of occurrence of a dike intrusion within the repository.

Details of the scenario for these calculations are simplified from assumptions contained in Crowe et al. (1983). Parameter values for processes associated with an igneous intrusion are from Valentine et al. (1992). A summary of the simplified model includes:

- a basaltic intrusion interacts directly with the radioactive waste,
- the waste is fragmented and entrained in the upward flow of basalt in the dike as a result of the thermo-mechanical effects,
- the fragments are erupted as part of the cinder cone or lava sheet at the surface.

We assume that the dike intrudes along a plane behind an upwardly propagating stress crack. Thus, the country rock at the propagating tip is pushed laterally by the compression caused by dike intrusion. The entire volume of the country rock displaced by the dike is not expected to be engulfed and entrained in the upward-flowing magma (Valentine et al., 1992). Entrainment of the wall rock is assumed to occur after the dike pathway is formed. Entrainment is accomplished when turbulence in the magma, primarily induced by exsolution of the volatile phases, results in erosion of the wall rock.

We have used two methods for determining the amount of waste expelled at the surface by an upward flowing dike. For both methods, the amount of waste that reaches the surface is proportional to that part of the dike that interacts with the repository. Method 1 uses geometrical arguments. It models the interaction volume defined by the periphery of a dike inside the repository and an erosion depth into the rock next to the dike. This method requires information on the length, width, and erosion depth for each dike in the simulation. Method 2 uses data on observed eruptive events. The process is modeled by assuming that the amount of waste entrained is proportional to the amount of wall rock derived from the repository horizon. Data required for this model include observed volumes for basaltic events, the relative fraction of xenoliths in those eruptive volumes, and the dike path length from the repository to the surface divided by the dike length in the repository.

These analyses make several other simplifying assumptions about the processes involved. Chemical effects, which may mobilize waste differently than thermo-mechanical processes, are not considered. Any transport mechanisms for the mobilized waste other than thermo-mechanical entrainment by the dike are not considered. A number of other detailed assumptions and simplifications are discussed in the following sections.

7.3 Estimation of probability of occurrence

The probabilistic treatment of the basaltic volcanism problem includes three parts: probability of volcanism within the general region that includes the repository, probability of volcanism within the repository, and consequences of the intrusion. The overall probability of release due to volcanic activity during the existence of a potential repository at Yucca Mountain can be expressed as the product of two conditional probabilities (Crowe et al., 1992):

$$P[E_1E_2E_3] = P[E_1]*P[E_2 \mid E_1]*P[E_3 \mid E_1E_2], \tag{7.1}$$

where $P[E_1E_2E_3]$ is the probability of exceeding EPA radioactive release limits, E_1 is the occurrence of a volcanic eruption in the region, E_2 is an eruption in the repository, and E_3 is the consequence of the eruption. $P[E_1]$ is the probability of occurrence of an eruption in the region; $P[E_2 \mid E_1]$ represents the probability of an eruption in repository, given that E_1 occurs; and $P[E_3 \mid E_1E_2]$ represents the probability of exceeding EPA limits for radioactive releases from a dike intrusion, given the occurrence of E_1 and E_2.

7.3.1 Frequency of an eruption in the region

Information on the frequency of occurrence ($F[E_1]$) of basaltic volcanism in the southern Great Basin near the Nevada Test Site that includes Yucca Mountain was excerpted from Crowe et al. (1983) and Crowe (1991). $F[E_1]$ has been represented by a log-normal distribution whose parameter values are:

$$\begin{aligned} \text{mean} &= 4.0\text{x}10^{-6} \text{ events/year} \\ \text{minimum} &= 2.0\text{x}10^{-6} \text{ events/year} \\ \text{maximum} &= 1.0\text{x}10^{-5} \text{ events/year} \\ \text{standard deviation} &= 1.2\text{x}10^{-6} \text{ events/year.} \end{aligned}$$

The value given for the minimum rate of occurrence is half that of the current rate. Because the present rate of occurrence is extremely low, it was assumed that this rate is unlikely to decrease to less that half of that currently observed (Crowe, 1991). The maximum rate is based on the rate of recurrence for Lunar Crater (Crowe et al., 1983), which is among the highest rates observed in the Great Basin. Higher rates would be atypical of continental basaltic volcanism and would be more indicative of rates similar to those of the Hawaiian shield volcanoes.

The Poisson probability distribution (e.g., Equation 6.3) can be used to determine the probabilities of occurrence over 10,000 years for a specified number of events using either the mean or the maximum for $F[E_1]$ (Crowe et al., 1992). Using the mean recurrence rate, we get a probability $P[E_1]$ of $3.8\text{x}10^{-2}$ for one eruption over 10,000 years; using the maximum for $F[E_1]$ gives a $P[E_1]$ of $9.0\text{x}10^{-2}$.

7.3.2 Probability of an eruption in the repository

The probability distribution provided for $P[E_2 \mid E_1]$, in Crowe (1991) is Gaussian and uses the following values:

$$\begin{aligned} \text{mean} &= 2.7\text{x}10^{-3} \\ \text{standard deviation} &= 8.0\text{x}10^{-4} \end{aligned}$$

The distribution for $P[E_2 \mid E_1]$ incorporates information on the work done by YMP volcanologists, as well as that by workers at University of Nevada, Las Vegas (UNLV) (Ho, 1991). The latter group advocates a model in which the area of most probable volcanism extends along a line north from the Lathrop Wells cone to the repository block. Because this line trends directly toward the repository block, the UNLV model would lead to a higher likelihood of eruption in the block than does the YMP model.

Using the maximum value for $P[E_1]$ and the mean value of the distribution for $P[E_2 \mid E_1]$, the probability of volcanism occurring within the repository, taken over 10,000 years, ($P[E_1E_2]$) is therefore 2.4×10^{-4}. This value is based on the assumptions discussed above of an extremely high eruption rate, combined with the more conservative UNLV structural model. Therefore, the frequency assumed for eruption at the repository site exceeds the EPA limit of 10^{-8} events/year, below which disruptive events need not be considered (EPA, 1985).

7.3.3 Conditional probability of releases $P[E_3 \mid E_1E_2]$

In a stochastic simulation of this volcanism problem, given this very small value for probability of occurrence, so few realizations would occur in a reasonable number of trials that statistics would be very poor. Therefore, for this set of calculations, we chose to first obtain a conditional CCDF based only on the consequence models $P[E_3 \mid E_1E_2]$, then subsequently to multiply this CCDF by $P[E_1E_2]$. In this way, we can better understand the contribution of the consequence portion to the total CCDF for volcanism.

7.4 Consequence of release from the repository

The consequence portion of the model has been simplified to capture the major aspects of a release due to potential volcanic activity. Given the extremely low probabilities for occurrence estimated above, we have used what we believe to be a conservative, but still reasonable, approach for estimating consequence. If, even in a conservative representation, the EPA limits are not exceeded, then more comprehensive formulation of variations on this problem may not be warranted.

7.4.1 Consequence model

Because of the uncertainty associated with the actual configuration of the drifts and container placement within the repository, several simplifying assumptions were made. First, only the properties and inventories of spent-fuel waste were considered. Other waste forms, such as glass, could have important impacts due to mobilization by chemical processes. Second, the entire inventory of 70,000 MTHM is assumed to be uniformly distributed throughout the volume of rock containing the repository.

For Method 1, based on the assumptions listed above, the amount of waste released from the repository as a result of a dike intrusion can be calculated as follows: if we assume that the waste in the repository is uniformly distributed, then the "density" of the waste (in MTHM/m^3) is given by $N/A\ h$, where N is the repository inventory (70,000 MTHM), A is repository area, and h is repository height. For a dike of length l within the repository, width w, and the erosion depth d, the interaction volume is given by $2\ (l + w)\ d\ h$. Thus, the fraction of the inventory available to be entrained in the dike is $2\ (l + w)\ d/A$.

For Method 2, given the volume of an eruptive cone, V, the volume fraction of lithic fragments is $V\ W$, where W is the wall-rock fraction. The fraction of lithic fragments that could come from the repository horizon is given by $V\ W\ R$, where R is the fraction of the erupted xenoliths originating in the repository. The factor representing the fraction of that portion of the dike participating in the erosion within the repository is given by F. The fraction of waste entrained in the dike is $V\ W\ R\ F/A\ h$.

Given the assumption of uniform distribution of waste in the repository, the release fraction is applied to each radionuclide to establish the release of that nuclide. The ratio of the release of each nuclide to its allowable release limit is its EPA ratio. The sum of the EPA ratios is the EPA sum. An EPA sum greater than 1.0 indicates that the releases have exceeded the maximum allowable.

7.4.2 Estimates of parameter values

These analyses assume that a basaltic dike, of varying trend (orientation of the linear intersection of the dike with the surface), length, and width, intrudes the repository block and entrains waste. The entrained waste is then assumed to be carried to the surface. Two methods for determining the amount of waste entrained in the repository horizon are described in Section 7.4.3.

The parameter values used in this analysis are very uncertain. Consequently, these uncertainties were treated by assigning distributions to the parameter values. Each trial in a simulation used values of the parameters drawn from the appropriate distributions. Distributions of parameter values may be uniform across a range or may be biased toward certain values within a range. We used the formalism described in Chapter 3 to generate PDFs, which are intended to quantify expert judgment regarding parameter values and distributions.

7.4.3 Geologic features

Information needed for Method 1, such as dike length, width, and trend, were obtained using expert opinion, as discussed in Section 3.3.2. Surface observations show that dike lengths range from about 0 to 5 km (Crowe et al., 1983). Dike lengths were assumed in the PDF to be uniformly distributed. Dike widths range from nearly 0.0 to 4.5 m, with a mean of 1.5 m. The PDF used to describe variability of dike width is shown in Figure 7-4. Discussion of the development of all the PDFs, except the erosion depth used in the volcanism calculations, may be found in Section 3.3.2.

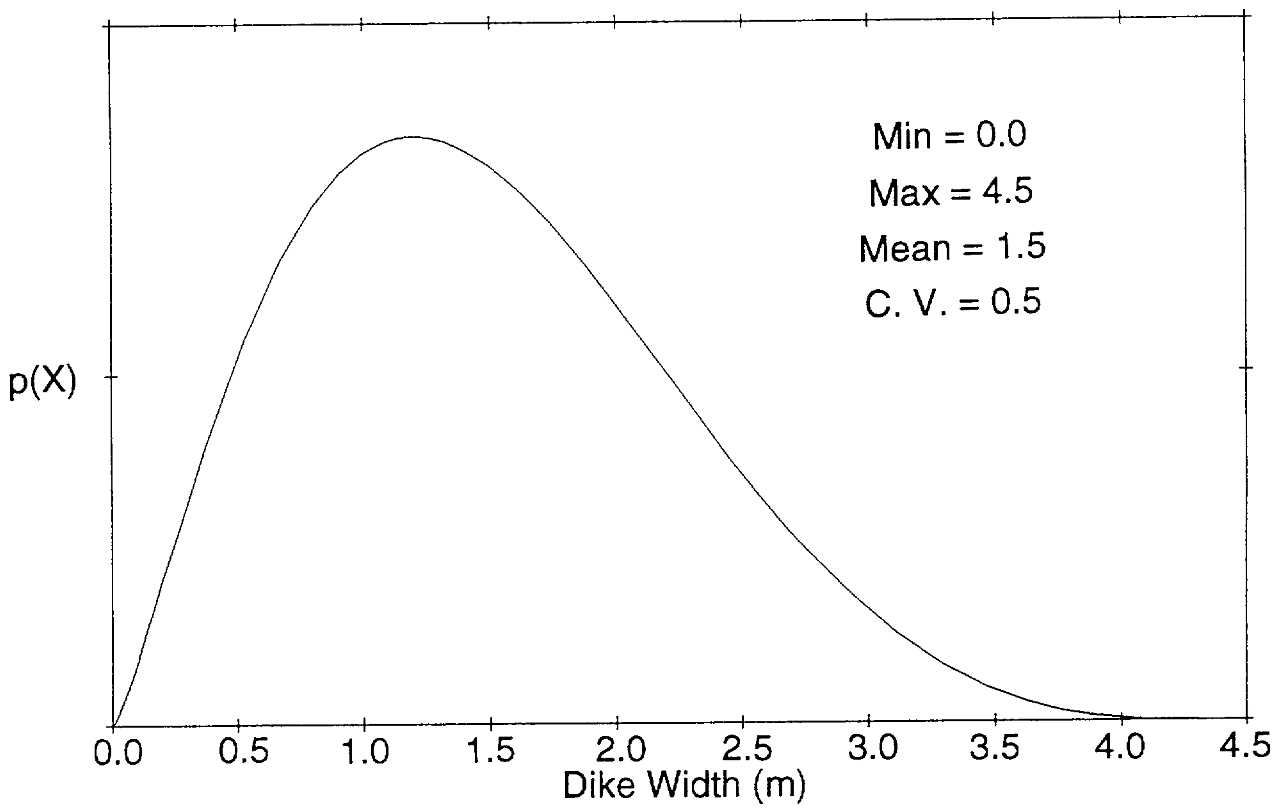

Figure 7-4. Probability density function for dike width

The distribution of dike trends was chosen to reflect the dominant pre-existing structural elements within the repository block. It was assumed that, at the depth of the repository, a dike would be most likely to follow pre-existing planes of weakness. The strike of the Ghost Dance Fault, N5°E, was viewed by the experts who developed the PDF as the mode of the distribution. The mean for this distribution is 15°. The PDF shown in Figure 7-5 reflects the predominance of north-north-easterly trends of the faults within the block. The extension direction in the present-day stress field has been identified as trending approximately N50°W in the region including Yucca Mountain (Carr, 1974; Ellis and Magner, 1980; Stock et al., 1985). Thus, the fault planes with trends more nearly normal to the extension direction will experience the highest tensile stresses and will, therefore, be the most likely to allow upward flow of magma. This PDF is a representation of the strong likelihood for dike emplacement to occur preferentially along the Ghost Dance fault zone, with some probability that such an event could occur along fault planes oriented favorably to the current extension direction.

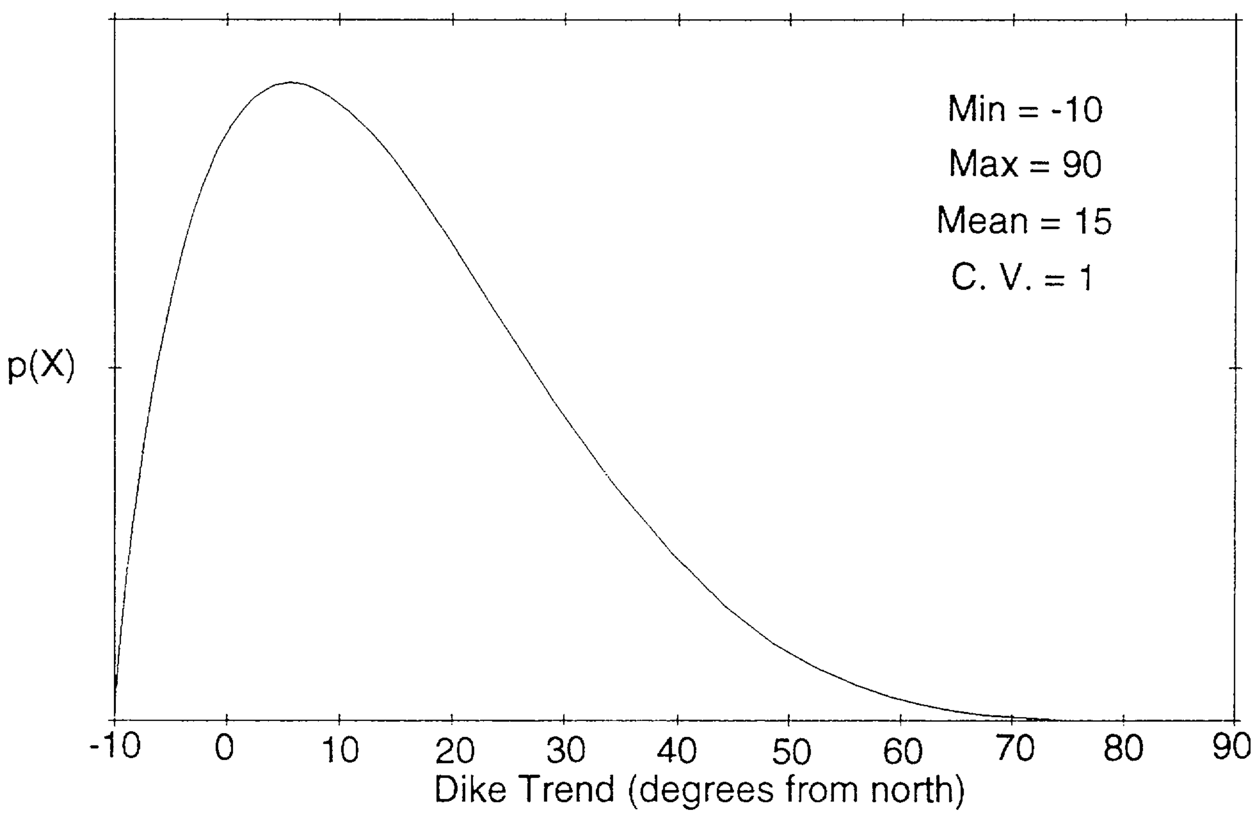

Figure 7-5. Probability density function for dike orientation

Information on the depth of erosion by a basaltic dike into the adjacent rock is not available for the Yucca Mountain area. The values for this parameter were determined based on the assumption that erosional depth would be no less than the observed diameters of xenolithic fragments in the Lathrop Wells cone. The median diameter of these fragments is reported as 4 mm (Crowe et al., 1983). The maximum xenolith diameter observed is about 5 cm. The largest blocks of basaltic lava observed forming scoria cones near NTS are 20 cm (Crowe et al., 1983). These values have been used here to attempt to constrain the range of values for an erosional depth. We assume that some resorption of the xenoliths occurs; the fragments at the surface are probably somewhat smaller than they were when they were plucked from the wall, even though they were carried to the surface very rapidly. Thus, the erosion depth is assumed to be somewhat larger than the fragment size. The range we have chosen for erosion depth has a minimum of 4 mm, based on the median observed xenolith size. The maximum value is set at 20 cm, based on the assumption that no xenolith will be larger than the largest block of lava observed. The mean value has been arbitrarily set at 5 cm, equal to the largest observed xenolith. The PDF for this parameter was chosen to be a beta function, with an arbitrary coefficient of variation of 0.1. It is shown in Figure 7-6.

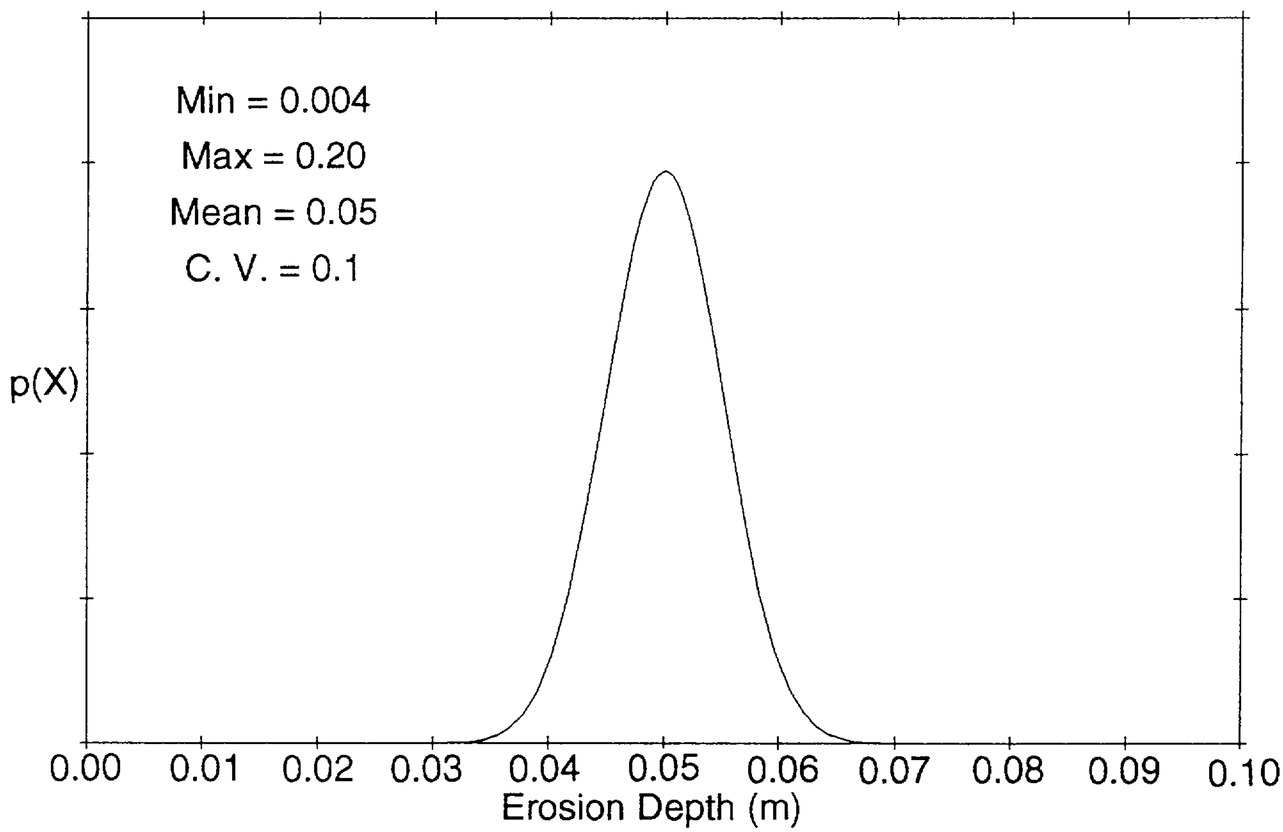

Figure 7-6. Probability density function for erosion depth

The information needed for Method 2 is the total erupted volume, and the fraction of that volume that represents rock from the repository horizon. The total volume of material erupted from the Crater Flat, Nevada, eruptive centers, including both the scoria cones and the associated lava flows, ranges from 3.4×10^5 to 1.0×10^8 m^3 (Crowe et al., 1983). The mean for this distribution was chosen to be the value observed for the total volume of cinder cones in the Crater Flat field, or 2.7×10^7 m^3 (Crowe et al., 1983). This PDF is shown in Figure 7-7.

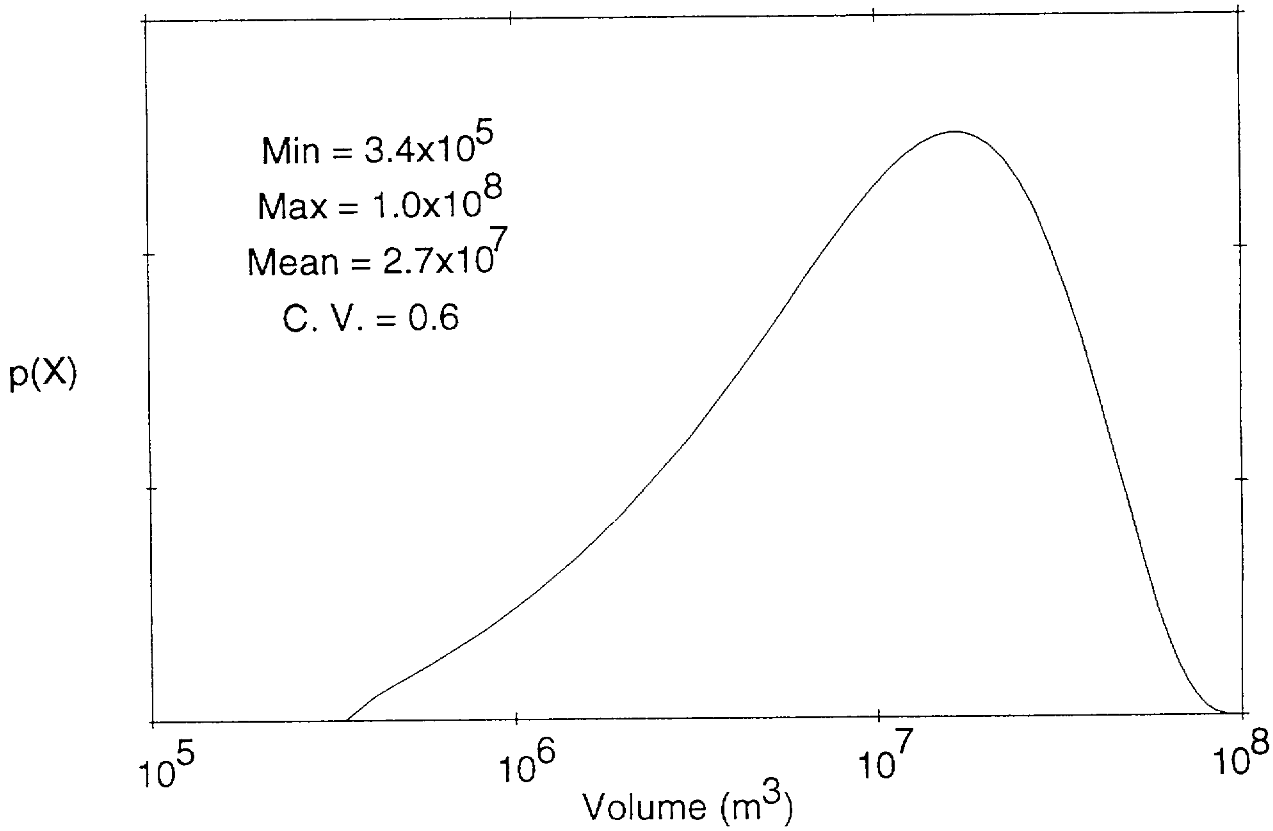

Figure 7-7. Probability density function for eruption volume

Estimations of the fraction of wall-rock xenoliths carried to the surface are based on the percentage of entrained fragments in basaltic scoria cones reported for a number of localities, including the Great Basin. For instance, studies of the San Francisco volcanic field in Arizona report that 0.03%-0.06% of the total volume of a scoriaceous cone is composed of material through which the magma erupted (Crowe et al., 1983). Similar studies for eruptive centers at Lathrop Wells show fractions of wall rock contained in the fragments making up a cinder cone as small as 0.009% (Crowe et al., 1983). Thus, values for the amount of wall rock in the surface volcanic rock range from 0.009% to 0.06%, with a mean of 0.03%, and were taken from Crowe et al. (1983). Figure 7-8 shows the PDF for the wall-rock fraction parameter.

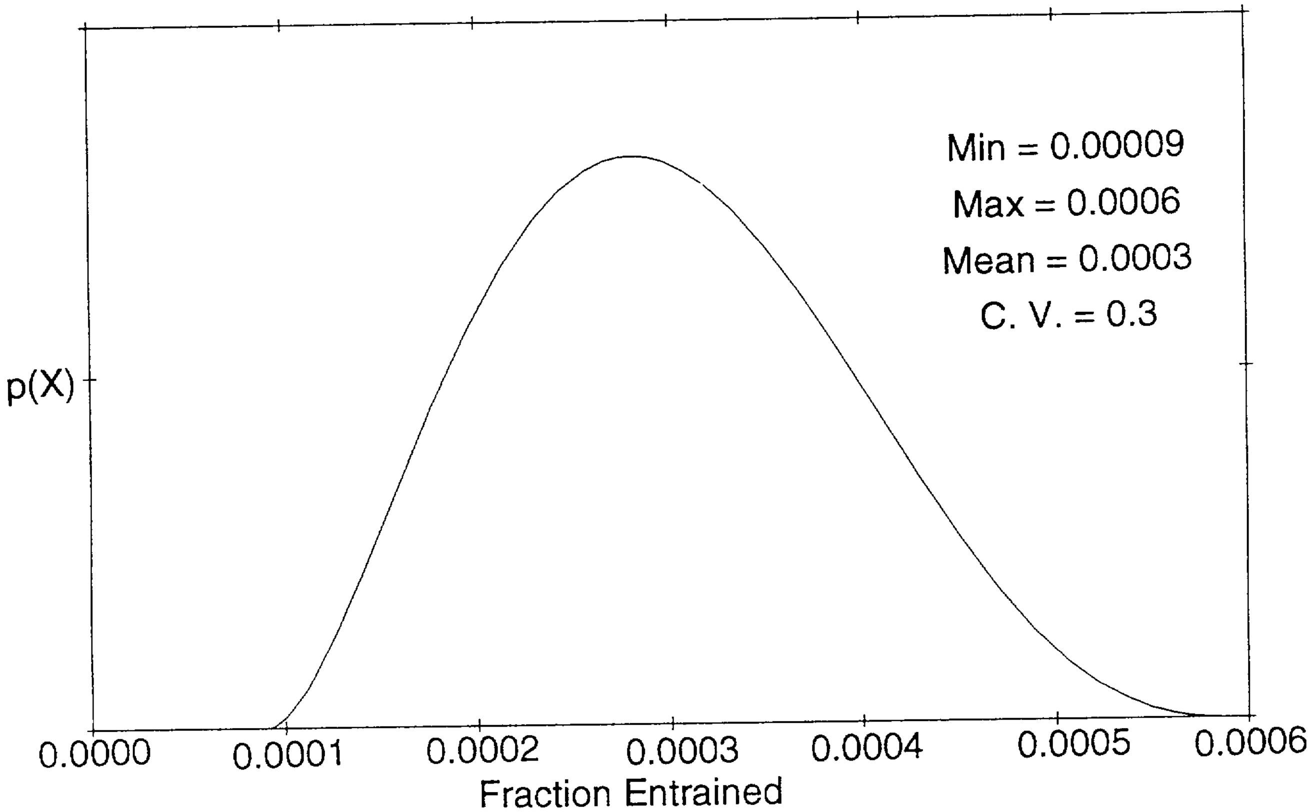

Figure 7-8. Probability density function for wall-rock fraction entrained

Most erosion of the wall rock at the Lathrop Wells location occurs within 10 to 50 m of the surface (Crowe et al., 1983, Valentine et al., 1992). This depth estimate is partially based on the observation that xenolithic fragments are probably derived entirely from the Tiva Canyon Member of the Paintbrush Tuff (the uppermost of the tuffs), which has a maximum thickness of 50 m (Byers et al., 1976). The erosion occurs because, as pressure from the overlying rock column decreases, volatiles begin to exsolve out of the magma (vesiculation). This induces turbulent flow that plucks rock from the conduit wall. For this problem, we assumed that wall rock is uniformly excavated by the magma from the walls along the entire length of the conduit from the repository to the surface. This is a conservative assumption, because the potential repository is expected to lie much deeper than the 50-m depth of expected wall-rock erosion. Also, below the zone of outgassing, other analyses indicate that the flowing magma may solidify along the margin of the conduit, essentially armoring the wall-rock against erosion (Bruce and Huppert, 1989; Carrigan and Eichelberger, 1990).

The height of the waste packages in the repository is approximately 5 m. Since only the area containing the waste packages is assumed to be contributing to the release fraction, for the formulation of this problem, the repository height is taken to be 5 m. The percentage of the dike's path length (from the surface to the depth at which wall-rock erosion begins) that intersects the repository ranges from 1.7% to 3.3% (Crowe et al., 1983). This fraction is used to model R, the fraction of xenoliths in the erupted volume. The variation in the path length occurs because the depth from the surface to the repository is variable, in part due to topography. This parameter was represented in the model by a uniform distribution.

The fraction of the dike that interacts with the repository is an unknown. There are too many considerations to be able to relate the erupted volume to the total dike volume. Additionally, the fraction of the dike length inside the repository is an unknown. Therefore, this uncertainty is represented by a uniform distribution that ranges in value from 0 to 100% of the amount of wall-rock xenoliths derived from the repository horizon.

7.4.4 Description of computations

A computer code was written to perform the multiple simulations to model a dike intrusion event through the repository, using either Method 1 or Method 2. The same stochastic techniques were used for this analysis as were used in the human-intrusion component. Because this intrusion event is so unlikely, only one intrusion per simulation was allowed to occur (in contrast to drilling, where multiple hits are possible in any simulation).

For each simulation for Method 1, values were selected for the dike width, trend, and starting point by sampling from the distributions. The starting point of the dike was chosen by randomly picking a point along an imaginary east-west-trending line south of the repository. The intersection of a northward projection from this point with the repository boundary was then taken as the starting point of the dike. Consequently, all the "dikes" constructed for this simulation begin at the southern boundary of the repository and extend in the directions sampled from the dike-trend distribution. Thus, the initiation of each dike at the southern boundary is only a modeling simplification. Figure 7-9 illustrates the locations of 32 dikes generated by this process. To simplify the calculation of the dike lengths, the repository shape has been modified so there are no concavities in the perimeter. The modified repository shape is shown with dashed lines in Figure 7-9. Dike lengths are calculated to be the shorter of the distance across the repository or the randomly chosen dike length (i.e., 0 to 5 km). This method of generating dikes probably over-estimates their lengths within the repository because the starting point for every dike is at the repository boundary.

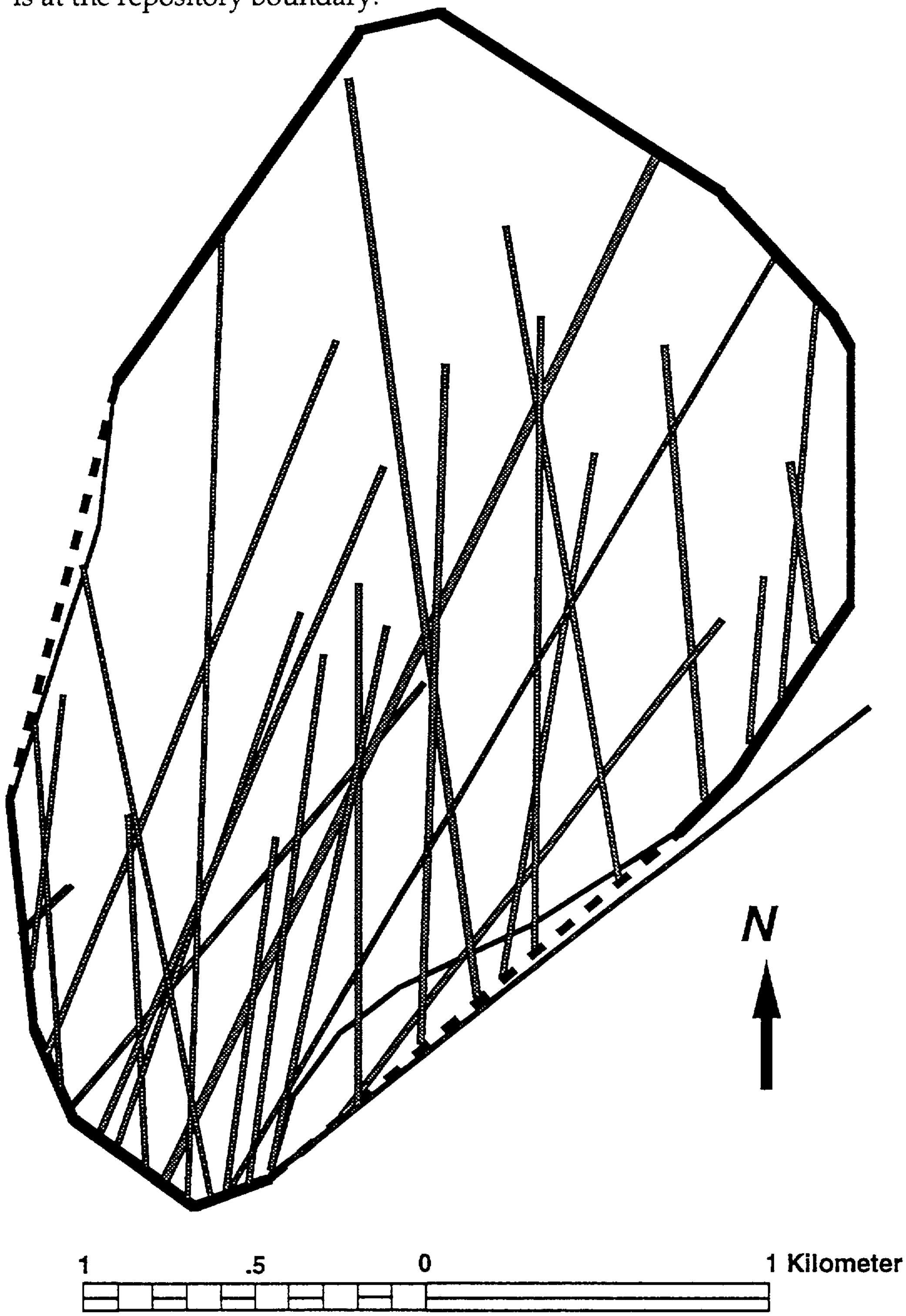

Figure 7-9. Modified repository shape with randomly placed dikes

After calculating the interaction volume from length, width, and erosion depth, this volume is expressed as a fraction of the total repository volume. The time at which the dike intrudes the repository is used to determine the radionuclide inventories, taking into account chain decay and ingrowth. The initial inventory used is the same as that used for the base-case human-intrusion calculations (see Table 6-4).

For Method 2, values were sampled from the distributions of eruptive volume (V), wall rock fraction (W), the fraction of the dike occurring within the repository (F), and the fraction of xenoliths from the repository (R). The amount of waste released at the surface was then calculated from the dike volume expressed as part of the total repository volume, as prescribed by the equations in Section 7.4.3.

7.5 Results

The distribution of surface releases due to basaltic intrusion for Method 1 (based on 1,000 trials) is shown in Figure 7-10. The mean value of the EPA sum is approximately 0.3, and the maximum release is about 8. The conditional CCDF for this process is shown in Figure 7-11; the releases do not exceed the EPA limits.

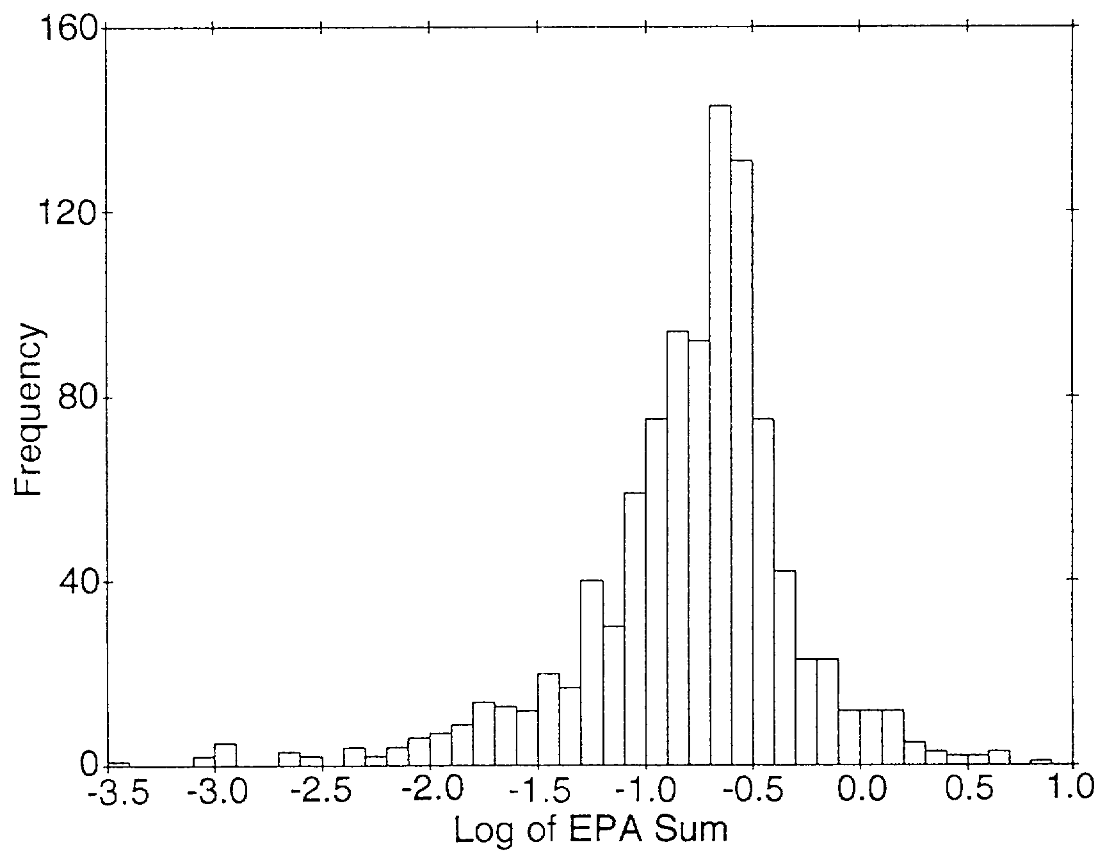

Figure 7-10. Distribution of surface releases due to igneous activity (method 1)

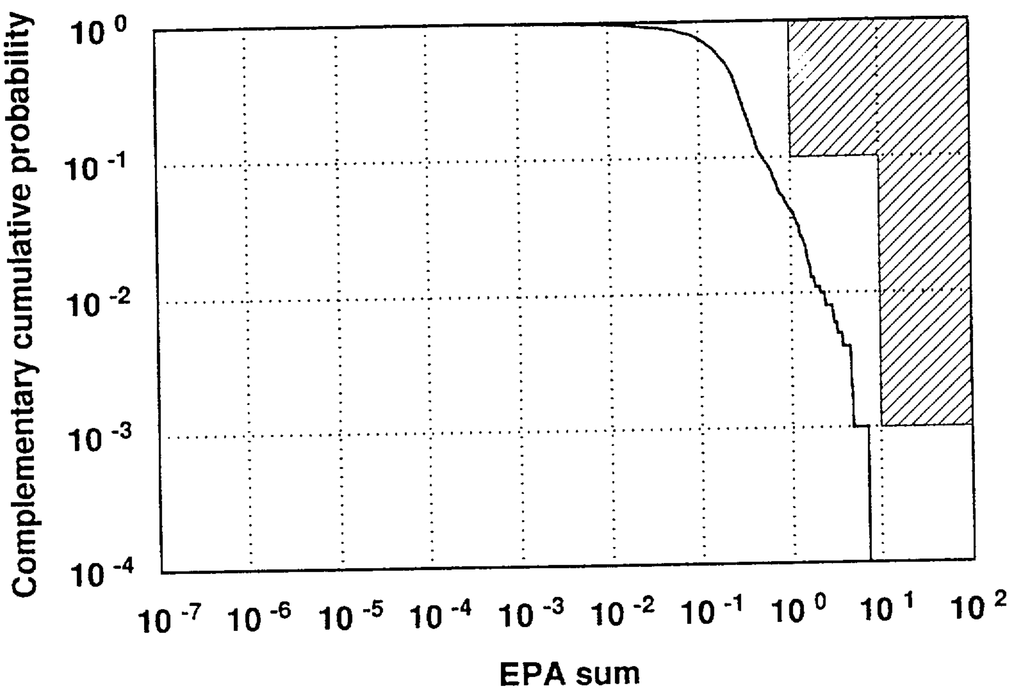

Figure 7-11. Conditional probability distribution for releases due to igneous activity (method 1)

The distribution of surface releases due to basaltic intrusion for Method 2 (also based on 1,000 trials) is shown in Figure 7-12. The mean value of the EPA sum is approximately 0.01, and the maximum release is about 1.0. The conditional CCDF for this process is shown in Figure 7-13, and shows a somewhat lower release than Method 1.

As a consistency check on these results, comparisons with prior work were done. The distribution of volumes of lithic fragments arising from the repository horizon (calculated by Method 2) is shown in Figure 7-14. The figure shows that the most likely volume of such fragments is about 20 m^3, and the mean is 35 m^3. In Crowe et al. (1982), 54 m^3 of material from the repository horizon is predicted to be deposited in a scoria cone.

The radionuclides that contribute most to releases (for both Methods 1 and 2) are shown in Figure 7-15. The figure shows the mean values (over 1,000 trials) of the EPA ratios for those elements. Approximately 90% of the releases are contributed by three radionuclides: ^{240}Pu, ^{239}Pu, and ^{241}Am. Furthermore, of the top seven radionuclides, five are actinides.

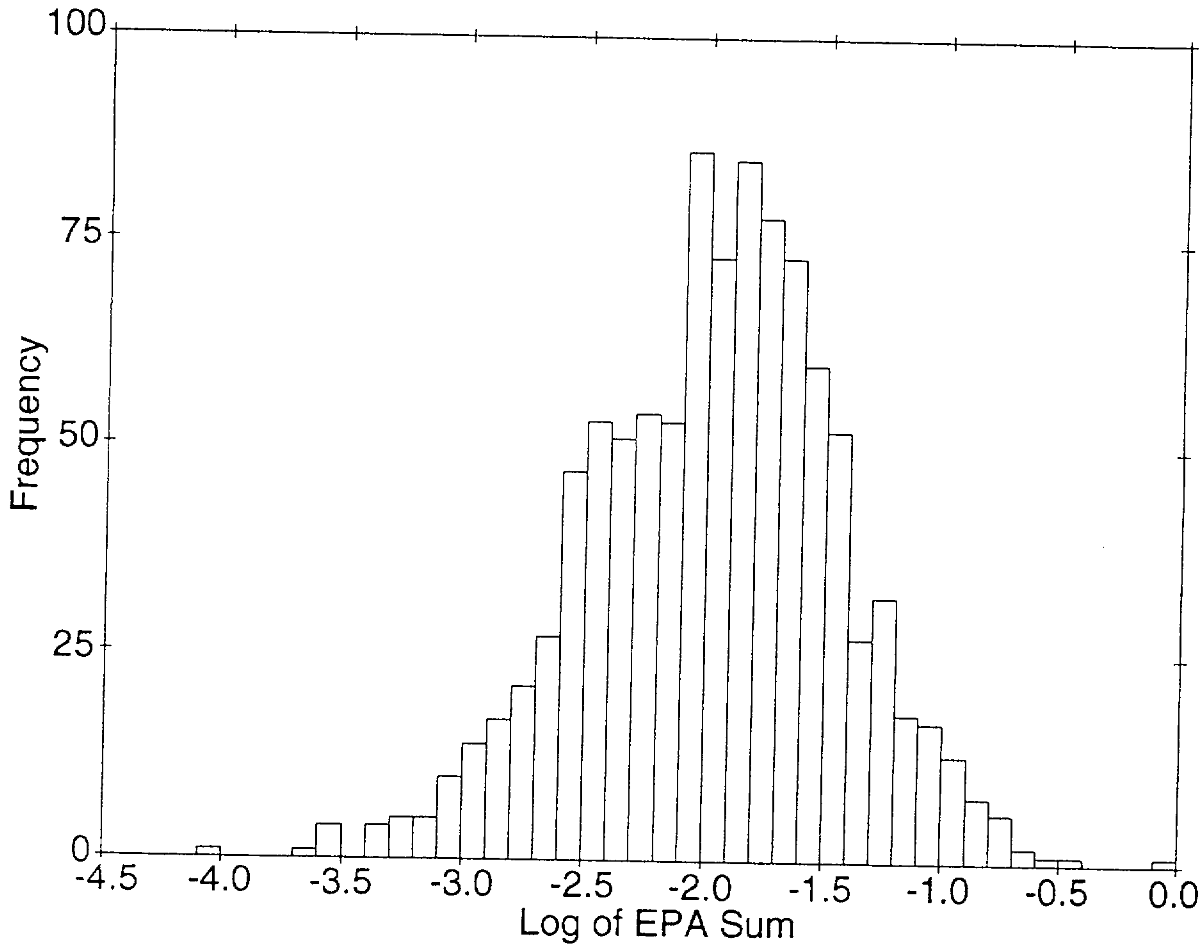

Figure 7-12. Distribution of surface releases due to igneous activity (method 2)

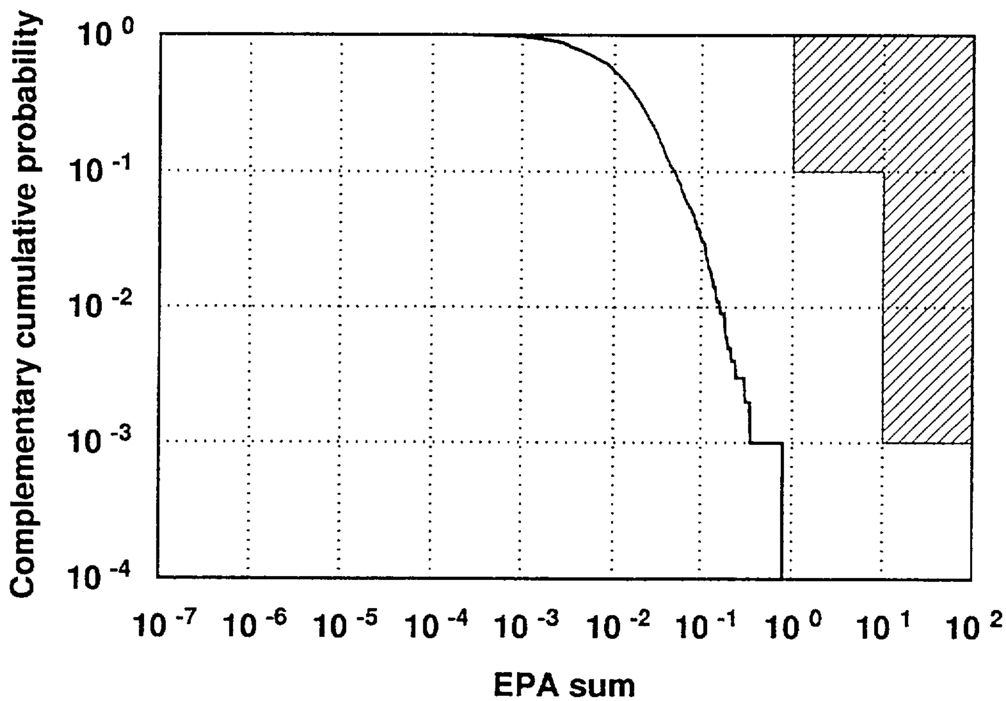

Figure 7-13. Conditional probability distribution for releases due to igneous activity (method 2)

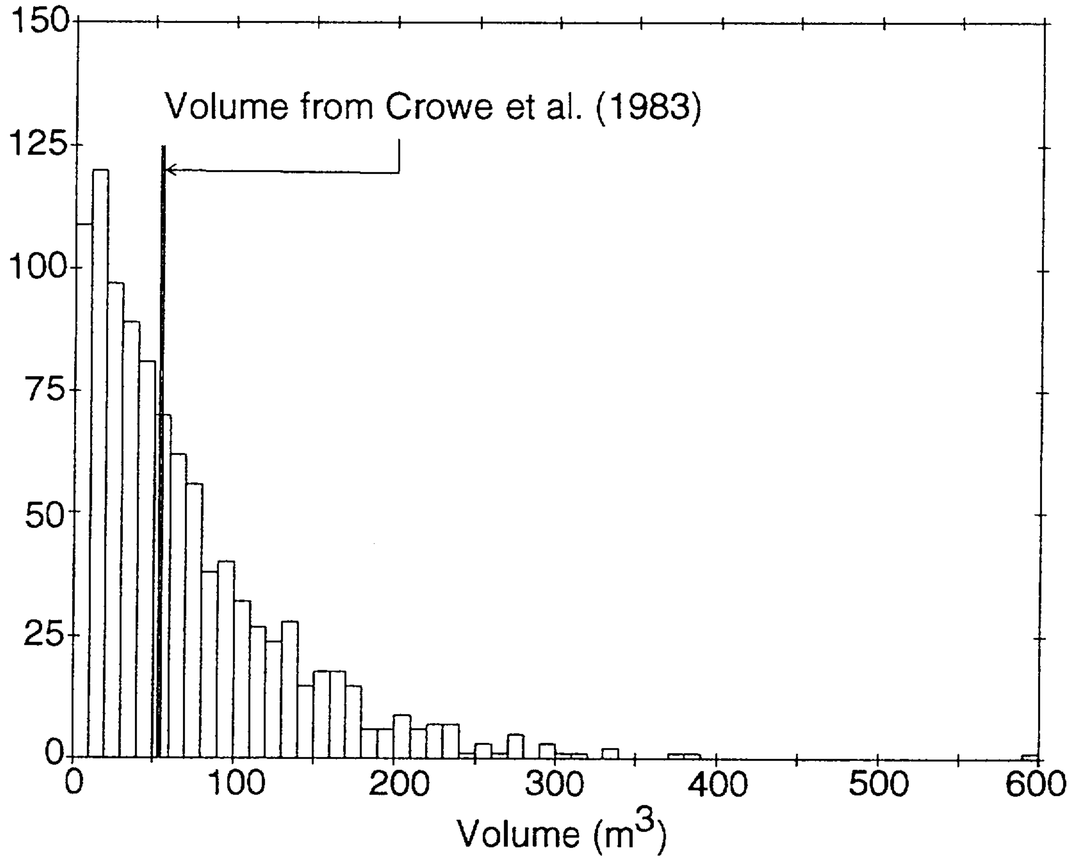

Figure 7-14. Distribution of volume of lithic fragments at surface originating in the repository

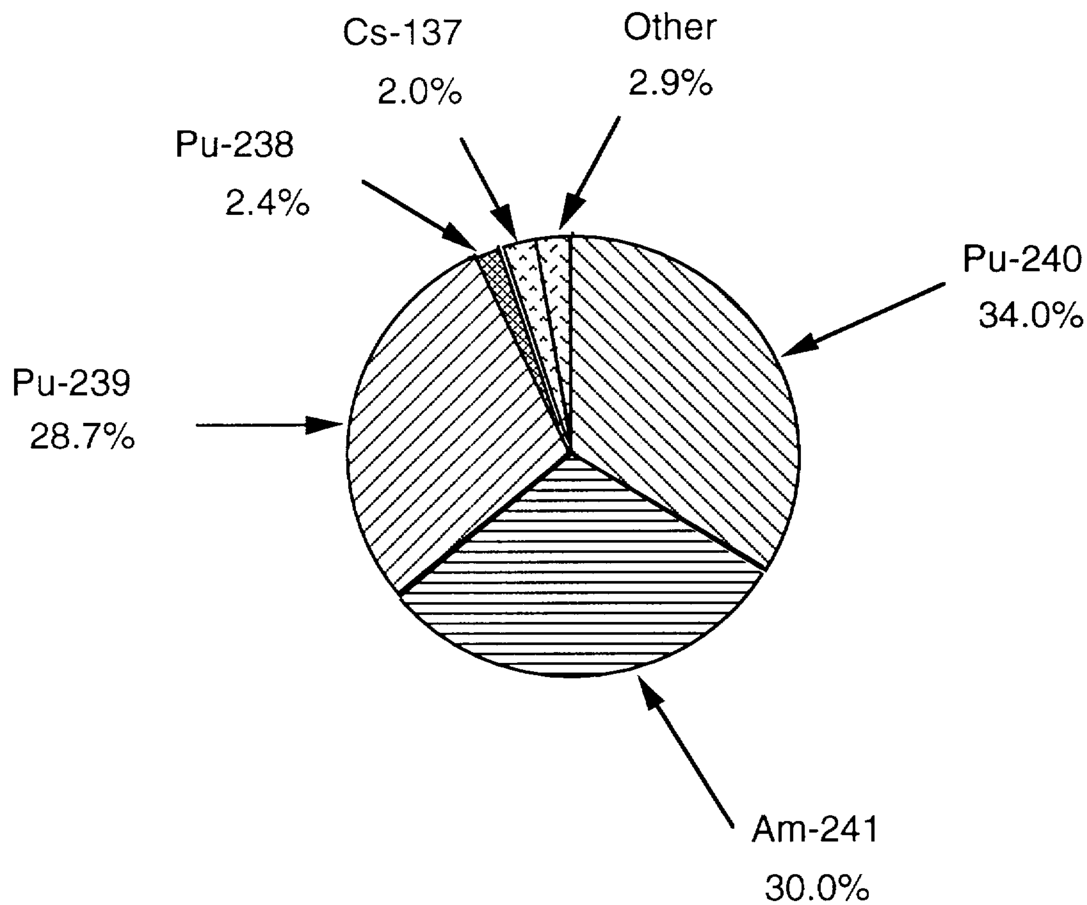

Figure 7-15. Average percentages of radionuclides released due to igneous activity

7.5.1 Sensitivity studies

Several types of sensitivity studies were done. For one category of sensitivity studies, the means and coefficients of variation were varied for parameters such as wall-rock fraction, dike width, and dike length while retaining the approximate shapes of the base-case PDFs. Another category of studies replaced the beta distributions with uniform distributions. The dike trend distribution was not varied. Table 7-1 lists the base-case parameters and the varied parameters, as used in both types of sensitivity studies. Figure 7-16 shows the three PDFs used for the variations of the beta distributions.

Table 7-1

Parameters varied for basaltic igneous activity sensitivity studies.

Case	Minimum	Maximum	Mean	Coefficient of Variation
Parameter:		**Wall-Rock Fraction**		
Base case	0.00009	0.0006	0.0003	0.3
Varied beta	0.00009	0.0010	0.0006	0.3
Uniform	0.00009	0.0006	0.000345	0.427
Parameter:		**Dike Width (m)**		
Base case	0.0	4.5	1.5	0.5
Varied beta	0.0	4.5	2.5	0.4
Uniform	0.0	4.5	2.25	0.577
Parameter:		**Erupted Volume (m^3)**		
Base Case	3.4×10^5	1.0×10^8	2.7×10^7	0.6
Varied beta	3.4×10^5	1.0×10^8	6.0×10^7	0.4
Uniform	3.4×10^5	1.0×10^8	5.0×10^7	0.563

Figures 7-17 through 7-19 compare the CCDFs for both types of sensitivity studies. For the studies in which different beta-distribution PDFs were used, only one parameter was changed for each study. As Figure 7-17 shows, changing either the eruption volume or the wall rock fraction produced an approximate five-fold increase in the releases calculated with Method 2. For Method 1, changing the dike width had essentially no effect on the releases shown in Figure 7-18. This is not unexpected, since dike length is generally much greater than dike width.

Uniform distributions were substituted for the beta distributions used in Method 2 to see whether making no assumptions about PDF shapes would change the outcomes significantly. As Figure 7-19 shows, with a uniform PDF, the releases are roughly the same as for the changed beta distributions in Figure 7-17.

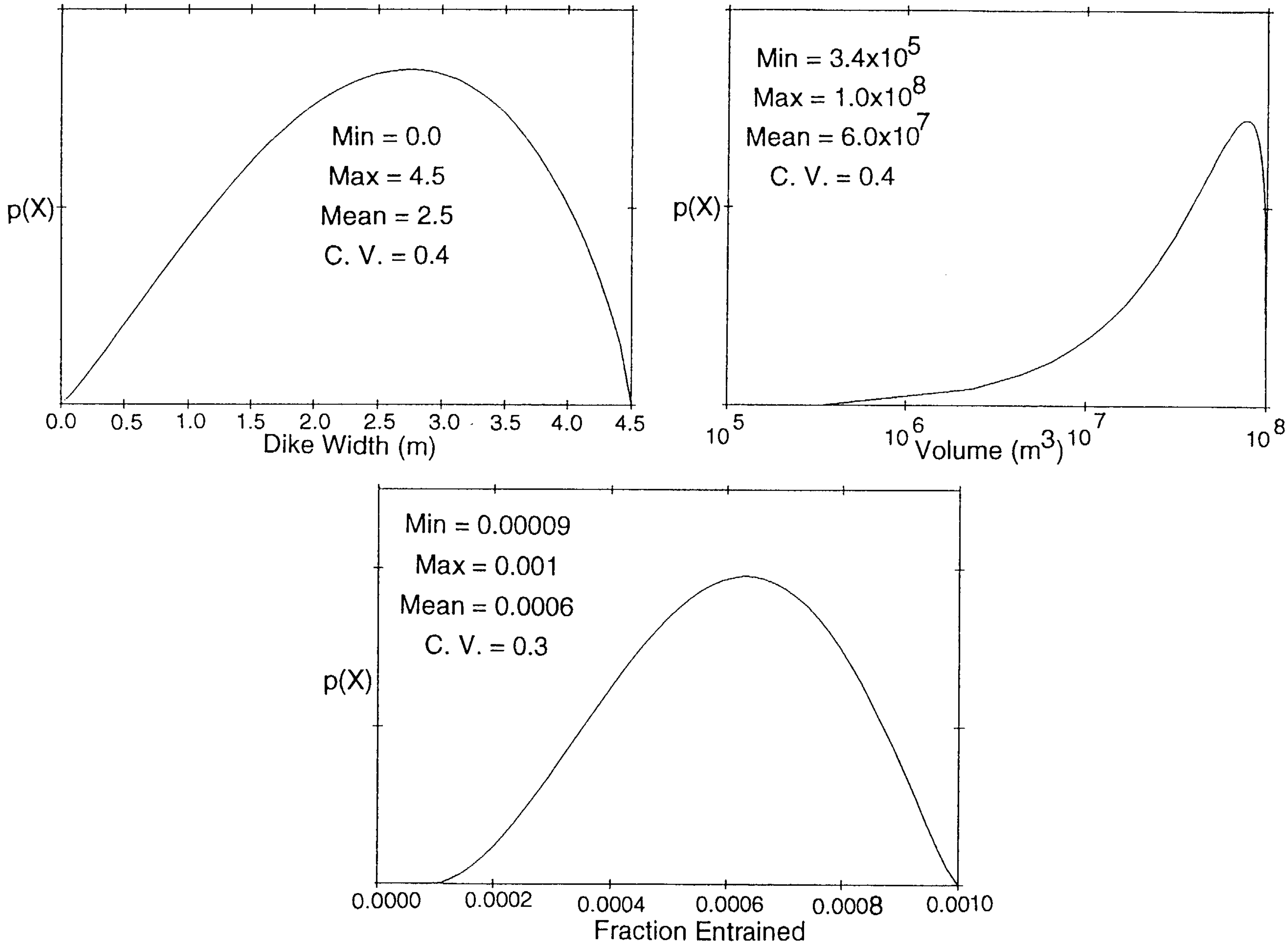

Figure 7-16. PDFs for parameters used in sensitivity studies

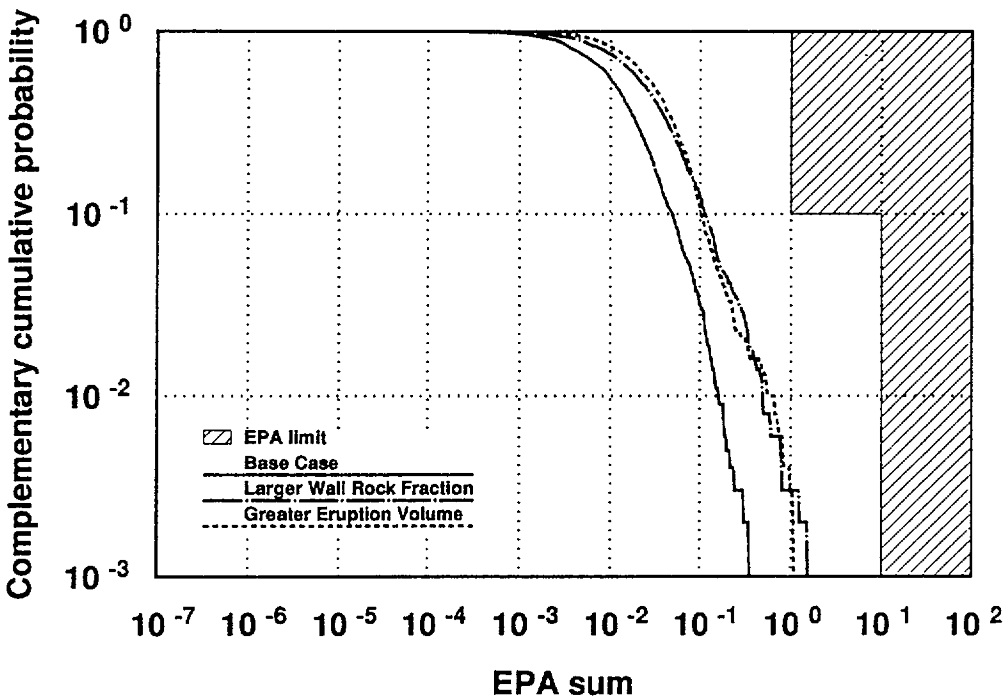

Figure 7-17. Comparison of releases for base-case and modified parameter PDFs (method 2)

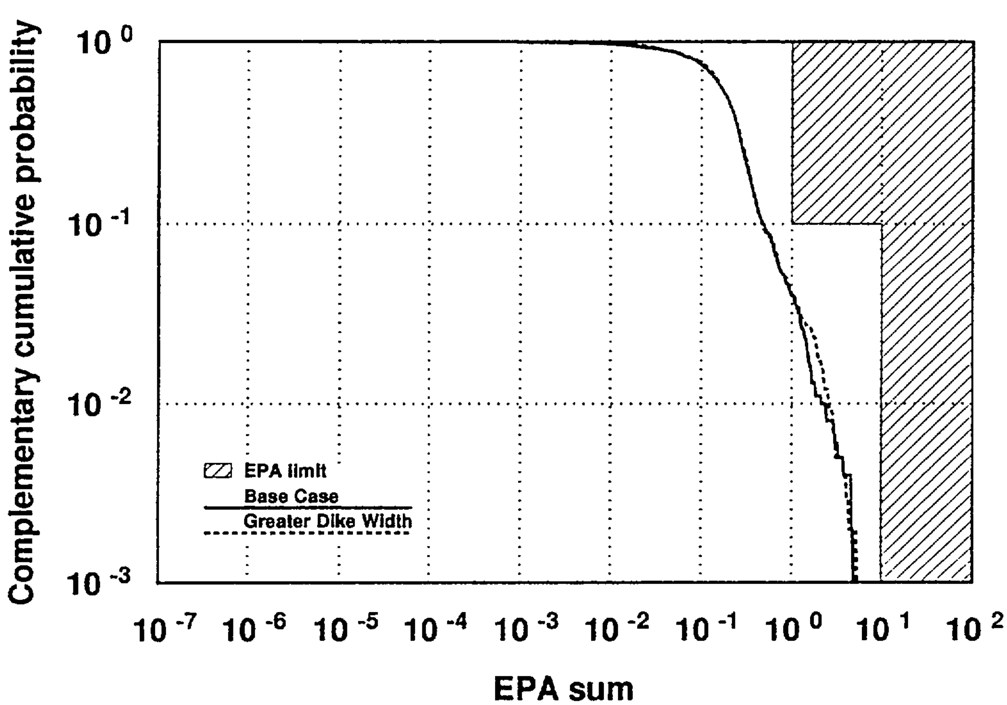

Figure 7-18. Comparison of base-case releases with releases for greater dike width (method 1)

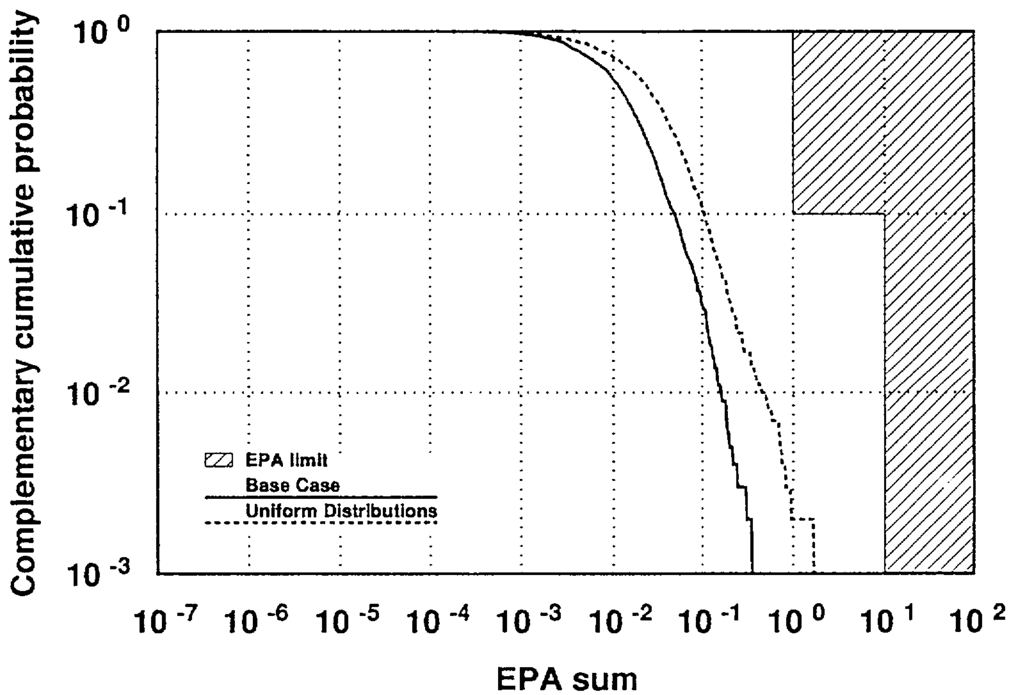

Figure 7-19. Comparison of base-case releases with releases for uniform parameter distributions

To see the effect of using a distribution for the factor, *F*, (the extent of interaction between the dike and the repository) in Method 2, a calculation was made with the value fixed at 1. Figure 7-20 shows the comparison with the base-case calculation, where *F* was allowed to vary by a uniform distribution. Releases are greater by about two times throughout, reflecting the fact that *F* always takes the value 1.0, instead of averaging 0.5.

7.5.2 Normalized CCDF for basaltic igneous activity

When the probability of occurrence for volcanic events is included, the CCDF is as is shown in Figures 7-21 and 7-22. The probabilities of the most likely occurrences are now about $3x10^{-4}$, and releases are below the EPA limit.

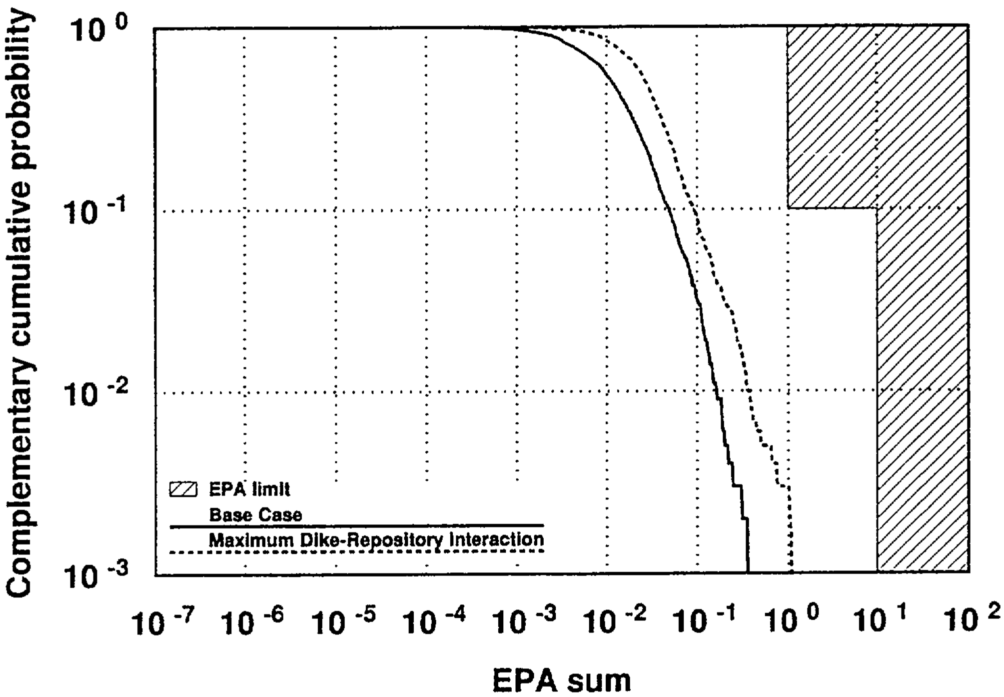

Figure 7-20. Effect of specifying that maximum dike length be in repository (method 2)

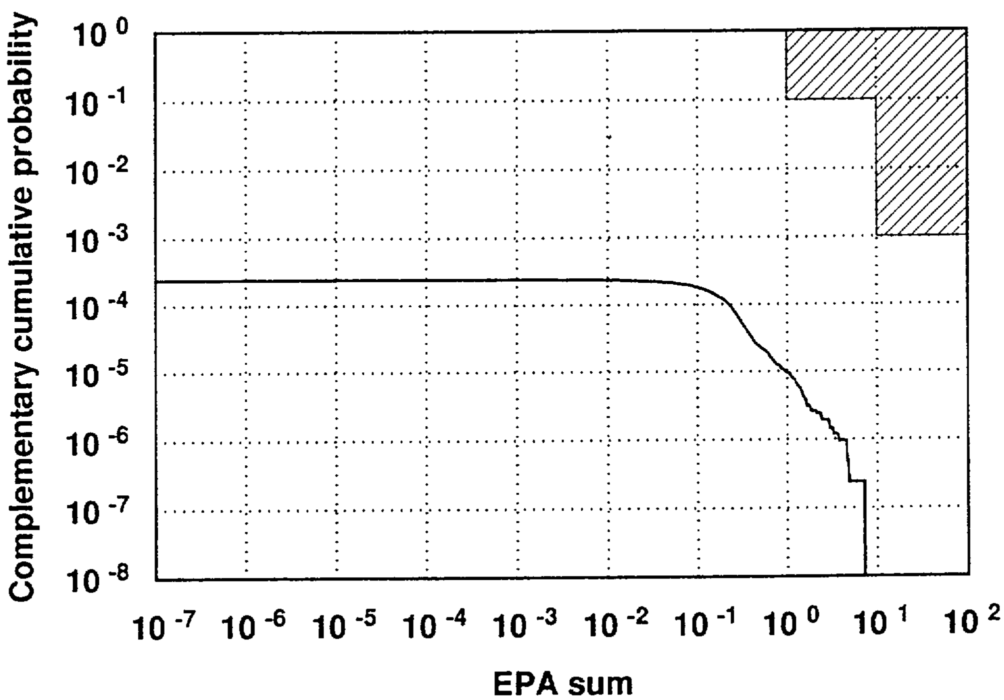

Figure 7-21. Conditional CCDF for surface releases from igneous activity, including probability of occurrence (method 1)

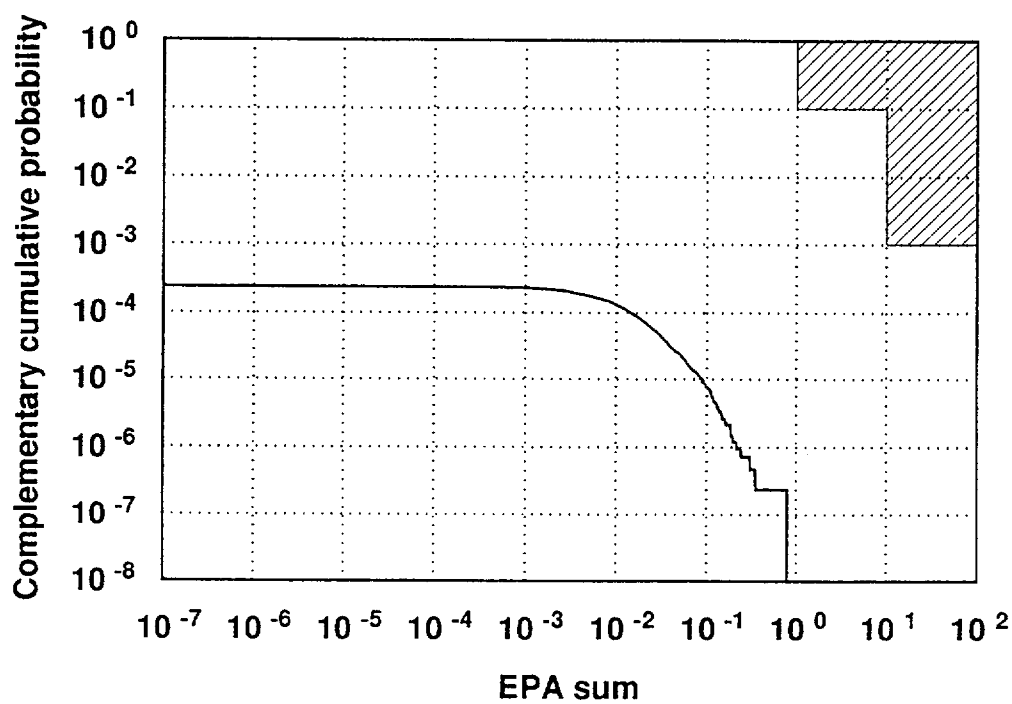

Figure 7-22. Conditional CCDF for surface releases from igneous activity, including probability of occurrence (method 2)

7.6 Discussion

This analysis shows that the consequences of igneous activity do not exceed the EPA limits for release of radionuclides (Figures 7-11 and 7-13). We further feel that the models used are quite conservative, so any reevaluation of the parameters would adjust the results downward. When probabilities of occurrence are considered, releases at the earth's surface from this basaltic volcanism scenario are even more insignificant.

Both the methods used to calculate releases give comparable results. We believe that the two methods used both lead to great overestimations of the amount of waste that could be released through the mechanism of mechanical entrainment. Certainly not all the material around the periphery of a dike is likely to be carried to the surface, although these models assume so. As stated above, the field evidence suggests that entrainment of wall rock probably does not even extend down to a depth as great as the repository horizon.

Because the model of this process has been simplified, and because there is considerable uncertainty in parameter values and processes, the range of releases is not known with any confidence. In this study, the relationships between the parameters of the release process are linear, so it would require orders-of-magnitude increases in the parameter values to cause the predicted releases to exceed the EPA limit. While the model parameter values are not known with great certainty, it is unlikely that they are all low by orders of magnitude. Method 2, which used field observations for the volcanic model parameters, involves one completely unknown factor—the fraction of the dike within the repository. Even if this parameter were specified to always be 1.0, the maximum releases are more than an order of magnitude below the EPA limit.

Perhaps the only simplification that could be a major factor in producing these low releases is the assumption that the waste in the repository is uniformly and homogeneously distributed across the repository horizon. If a dike of average width were to intrude the repository coincident with an emplacement drift, the density of waste available to be entrained would be roughly 20 times greater than the average value used in the TSPA analysis. Such an increase may cause the CCDF to approach the area of regulatory concern, although it will still be below the EPA limit because of the low probability of occurrence. Any additional analyses, if pursued, might investigate the effect of aggressive chemicals in the magma interacting with the waste material. The effect of a sill-like body intruding multiple drifts, thus altering fluid flow and directly affecting numerous waste packages also might be of interest.

Chapter 8
Combination of Conditional CCDFs
(Wilson)

In the preceding chapters, several components of the performance-assessment problem are presented. In this chapter, the parts are put together to look at the problem as a whole.

Combination of the conditional CCDFs presented in the preceding chapters is required for comparison with the (remanded) EPA standard. Appendix B of 40 CFR Part 191 offers the following guidance about how to apply the standard:

> The Agency assumes that, whenever practicable, the implementing agency will assemble all of the results of the performance assessments to determine compliance with §191.13 into a "complementary cumulative distribution function" that indicates the probability of exceeding various levels of cumulative release. When the uncertainties in parameters are considered in a performance assessment, the effects of the uncertainties considered can be incorporated into a single such distribution function for each disposal system considered. The Agency assumes that a disposal system can be considered to be in compliance with §191.13 if this single distribution function meets the requirements of §191.13(a).

From this passage it is clear that the EPA's intent is for all of the results to be combined into a *single* CCDF, which is then to be used for comparison with the limits in 40 CFR 191.13. Unfortunately, there is some controversy about this procedure. It is the NRC, not the EPA, that will evaluate the site license application, including the results of performance assessments. The NRC position is that, when multiple "alternative conceptual models" are considered, the results of the alternative models should not be combined, but should be kept separate. Using this logic, multiple CCDFs would be produced or, alternatively, a single CCDF using only the most conservative of the alternatives (NRC, 1989, Comment 98).

There is a logical difficulty in separating "alternative conceptual models" from simple parameter variation, because normally the alternative models are arrived at by choosing discrete, possibly extreme, values of some parameter or parameters. (See the discussion in Appendix A of Tierney, 1991.) For example, the two alternative models of unsaturated flow and transport that are discussed in this report (the composite-porosity model and the weeps model) could be regarded as two special cases of a more general model of flow and transport, one with an infinite value of a matrix/fracture coupling parameter and the other with a zero value for the coupling parameter. Similarly, many other branches of the FEP diagrams that have heretofore been called alternative conceptual models could also be parametric variations of more general models.

Our approach to dealing with this problem is to present the CCDFs both ways: CCDFs will be presented for each alternative model and for the combination.

8.1 Methods of generating an overall CCDF

Two methods have been described for generating an overall CCDF using Monte Carlo techniques (SCP Section 8.3.5.13; Tierney, 1991). In the first method, a single Monte Carlo simulation is made, in which all important FEPs are included. Some number of realizations of the repository system are calculated. Each realization is a possible future history of the system. For each realization, the appropriate probabilities are applied to determine whether a volcanic intrusion occurs and to determine percolation flux as a function of time, to take two examples. Each realization represents the whole system over the entire time of calculation, and a history of radionuclide releases over that time is produced. After all the realizations have been calculated, their associated normalized cumulative releases to the accessible environment are combined into a CCDF that can be compared directly to the EPA limits. Conceptually, this method is very simple, but there are practical problems with its application, especially for preliminary performance assessments such as this one. In preliminary work, study of repository subsystems individually makes it easier to understand the subsystems and to determine which FEPs are most important. Also, with this method, study of a low-probability event or feature would be very inefficient because the method requires calculation of a multitude of realizations, many of which would not incorporate the event or feature of interest.

These practical problems led to development of the second method, in which the set of all possible future histories, or scenarios, is subdivided into subsets, called "scenario classes." (The reader is cautioned that there is no standard terminology, and various authors use words like "scenario" to mean different things. We are following the terminology of SCP Section 8.3.5.13, and Tierney, 1991.) The parameter space is subdivided in such a way that the scenario classes are mutually exclusive (no scenario is counted twice) and exhaustive (any scenario belongs to one of the classes). A "conditional CCDF" (conditional upon the parameter values, etc., that define the scenario class) is calculated for each scenario class, and then the combined CCDF is a weighted sum of the conditional CCDFs:

$$G(m) = \sum_{j=1}^{N} p_j G_j(m) \, , \tag{8.1}$$

where m is the normalized release or EPA sum, $G_j(m)$ is the conditional CCDF for the jth scenario class, $G(m)$ is the overall CCDF, p_j is the weighting factor for the jth scenario class, and N is the number of scenario classes. The weighting factor p_j is the probability that scenario class j will occur. All of the probabilities must add up to one, so

$$\sum_{j=1}^{N} p_j = 1 \; . \tag{8.2}$$

G_j and G are complementary cumulative probability distribution functions and as such must follow the rules for such functions: $G(\infty) = 0$, $G(0) \leq 1$, and G must be monotonically nonincreasing. These rules are not normally of concern; if the CCDFs are calculated by means of a Monte Carlo method, they will automatically have the proper form.

Only one of the two Monte Carlo formalisms just described (the second) has actually been used up to now, and it is being used for performance assessments of the WIPP site (Bertram-Howery et al., 1990). Other methods, which do not use Monte Carlo techniques, are also possible. For example, McGuire et al. (1990) have demonstrated a method that uses a logic-tree formalism. Their method can be likened to the second method above, with discrete probability distributions rather than continuous probability distributions for the parameters.

The method used for this preliminary TSPA is unlike any of the methods described so far. The CCDF calculation is divided into parts, as in the second method above, but the division is made by calculating different processes separately rather than by defining mutually exclusive scenario classes. We will apply the term "scenario category" to our subdivisions to distinguish them from scenario classes. Scenario classes are mutually exclusive, but scenario categories are not. As has already been described, we made preliminary calculations for three basic scenario categories: "nominal" groundwater and gas transport, exploratory drilling, and basaltic igneous intrusion (volcanism). Some of these scenario categories were further subdivided into subcategories; for example, nominal conditions were modeled using two different models for unsaturated-zone groundwater flow and transport. The scenario categories modeled are not exhaustive, either. To achieve an exhaustive set of scenarios will require additional work on "scenario screening" to determine what FEPs are of such importance that they must be included in the calculations (see, e.g., Barr et al., 1991). The scenario categories used for this study were chosen because we believe them to be among the most important. Quantification of this belief will come with future work. Since we do not claim to have an exhaustive set of scenarios, the final CCDF that is generated is still a conditional CCDF, including only a subset of the important FEPs.

To discuss the issue of whether the scenario categories need to be mutually exclusive, let us consider our three top-level categories: nominal conditions, human intrusion, and volcanism. By definition, "nominal conditions" always occur. In our baseline human-intrusion case, exploratory drilling is always assumed to occur as well; in fact, it is assumed that 17 exploratory drill holes are drilled in the repository area in each realization (Section 6.5). Volcanism is the only one of the three that might or might not occur. A set of mutually exclusive scenario classes encompassing these assumptions would be as follows:

1) Nominal conditions and human intrusion occur, but volcanism does not.

2) Nominal conditions, human intrusion, and volcanism all occur.

It is much more convenient, at least at this preliminary stage of the performance assessment of Yucca Mountain, to calculate the three types of releases separately, as described in the preceeding chapters. The necessary assumption to be able to do this is *independence*. The three types of releases are assumed to be independent of each other. That is, we assume the following:

1) Exploratory drilling does not significantly affect groundwater or gas flow within the mountain.

2) Nominal groundwater and gas flow do not affect exploratory drilling.

3) Exploratory drilling does not affect volcanism.

4) Volcanism does not affect exploratory drilling.

5) Volcanism does not affect groundwater or gas flow.

6) Nominal groundwater and gas flow do not affect volcanism.

Some of these assumptions are not entirely valid, but in most cases the effects of interactions between these events or processes are of lower order (i.e., are less important) than the direct effects that we have modeled. Assumptions 3 and 6 seem likely to be valid. Assumption 1 is probably a good approximation because a drill hole probably will have a very small effect on the patterns of water and gas flow at Yucca Mountain; nonetheless, this is something that needs to be studied. Assumption 4 is probably not quite valid—if there were a volcanic event at Yucca Mountain, it would presumably suppress exploratory-drilling activity at least for a time. This seems like a very small effect that is reasonably neglected. Assumption 2 is partially true, in the sense that water and gas flow in the unsaturated zone probably do not have any influence on whether people decide to drill or where they drill (saturated-zone flow could influence drilling if the drilling is for water), but water flow can affect the *consequences* of a drilling event. The "near miss" part of the exploratory-drilling calculation should properly be coupled to the calculation of nominal groundwater flow and transport. In decoupling them we have made an approximation, the validity of which should be examined in the future. In the calculations that were made, the near-miss part of the exploratory-drilling CCDF was not very important; that seems likely to be true even for a more sophisticated, coupled calculation. The calculations of exploratory drilling followed by saturated-zone transport should properly be correlated with the saturated-zone transport part of the nominal-conditions calculations, but a noticeable effect on the results is unlikely. Lastly, assumption 5 was made for reasons of simplicity and is certainly not true. Effects of volcanic events on radionuclide transport need to be studied. The effect on the overall CCDF from these interactions would probably be minor, however, because of the low probability of having a volcanic event in the vicinity of Yucca Mountain within 10,000 yr. The probability would be higher than the 2×10^{-4} probability of an event that acts directly on the repository (Chapter 7) because a larger area has to be considered. However, it is likely that many types of volcanic events would have only a small effect on the regional groundwater flow.

To conclude this section, a comment on independence is in order. In the human-intrusion calculations for this TSPA, the "near miss" part of the calculation is an estimate of the effect of nominal flow and transport on releases due to exploratory drilling. Thus, in a sense, the nominal scenario category and the human-intrusion scenario category are not independent. However, in the present discussion we are using "independent" in a precise mathematical sense. If calculations can be performed for one scenario category without requiring knowledge of the corresponding calculations for another scenario category, then the first scenario category is independent of the second. If two scenario categories are independent of each other, we simply say that they are independent. The near-miss calculation is an estimate of the correlation between the nominal and human-intrusion scenario categories but, mathematically, the calculations assume that there is no correlation between the two scenario categories. This type of approach could suffice for some of the other correlations discussed above as well.

8.2 Combination of CCDFs for this study

In the course of this TSPA study, 14 conditional CCDFs were generated (not counting additional ones made for sensitivity studies). Figures 8-1 and 8-2 show

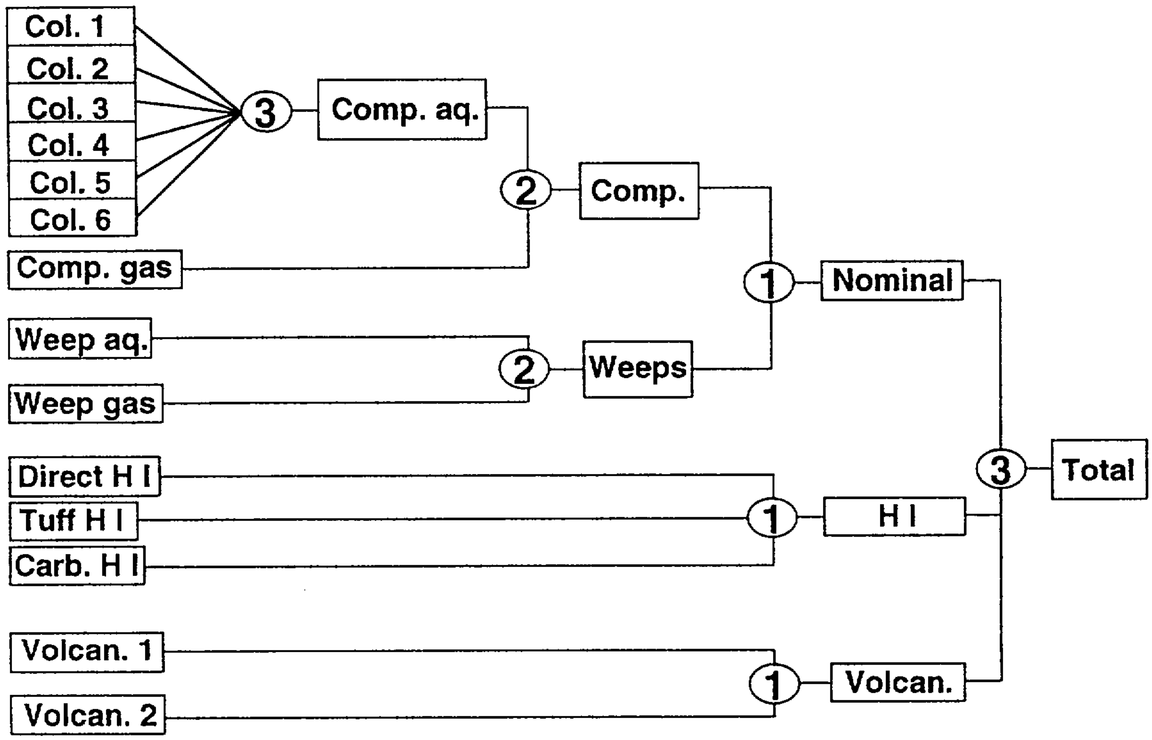

Figure 8-1. Schematic for combining 14 conditional CCDFs into 1.

schematically two possible ways of combining the CCDFs into a final conditional CCDF. Figure 8-1 shows the straightforward method that would be used if results of the two alternative unsaturated-zone-flow models were combined to form a combined CCDF for nominal conditions, the two alternative models of volcanism were combined to form a combined CCDF for volcanism, and those two combinations were then combined with the human-intrusion results to form a final overall CCDF. Note that the alternative models of volcanism are different in character than the alternative models of nominal conditions. The composite-porosity model and the weeps model represent different conceptualizations of nominal conditions. The two volcanism models, on the other hand, are based on the same conceptual model for releases caused by a basaltic intrusion, but calculate the releases in different ways, from different information. Note also that, although the three exploratory-drilling (human-intrusion) calculations appear in Figure 8-1 to be alternative models also, they are calculations of different aspects of the human-intrusion scenario category, as is discussed below.

Figure 8-2 shows the method that would be used if the alternative conceptual models were not combined, but rather overall CCDFs were produced for each flow

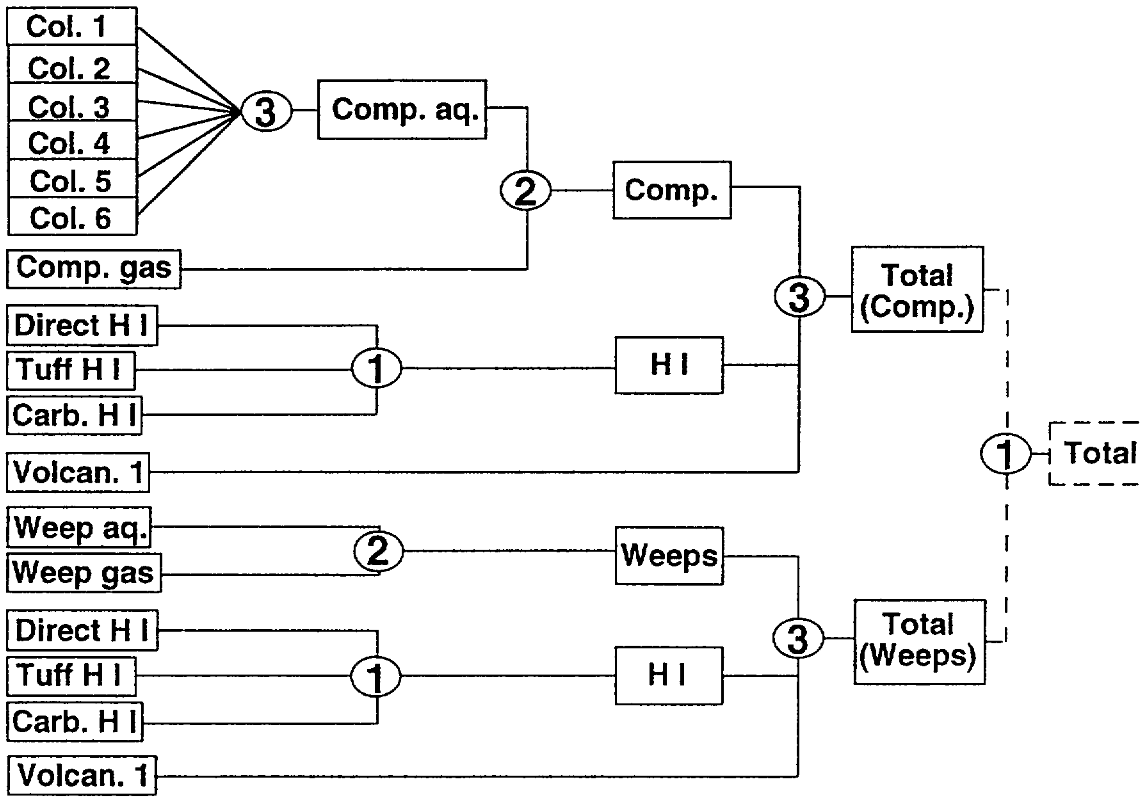

Figure 8-2. Schematic for combining the conditional CCDFs, keeping the "alternative conceptual models" separate.

model separately. The dashed lines show that the two "overall" CCDFs could still be combined at the end, and the resulting CCDF would then be the same as the one produced using the method in Figure 8-1. Because of the controversy over how to present results from alternative conceptual models, the second method (Figure 8-2) is used in the following discussion.

It is unclear how the two alternative models of volcanic releases should fit into the framework represented by Figure 8-2 since they are not really alternative *conceptual* models—they are both based on the same conception of the physical processes. Because of this distinction, it would perhaps be acceptable to combine the two volcanism CCDFs, though such a combination would have one of the same difficulties as a combination of conceptual models, the difficulty of justifying the relative weights of the two models. The two volcanism models could also be carried along separately, as is done for the alternative flow models, in which case there would be four "overall" CCDFs. Because of the low probability of the volcanism scenario and the relatively low consequences, the volcanism CCDF makes no significant contribution to the overall CCDF (except at very low probabilities), regardless of which method is used. Thus, in the following discussion, volcanic releases are simply represented by the releases calculated using Method 1, because they are higher than the releases calculated using Method 2 (see Chapter 7).

Nine of the fourteen CCDFs concern nominal aqueous and gaseous releases, three of the CCDFs concern releases due to exploratory drilling, and two of the CCDFs concern releases due to volcanism. There are two parts to "nominal" conditions because of the two alternative conceptual models of flow and transport that were used, the composite-porosity model and the weeps model. Of all the scenario categories, the most detail went into the calculations of nominal groundwater flow and transport for the composite-porosity model. This detail is present because that model is more "mature" than the others; it is reflected in the fact that 6 of the 14 CCDFs go into that category.

Three different methods were used in combining the component CCDFs. The nodes in Figures 8-1 and 8-2 are labeled with a 1, a 2, or a 3, depending on which method was used for that combination. The three methods are as follows.

1) "Weighted sum," for combining categories that are mutually exclusive. This is the classical method for combining scenarios that would be used for all CCDF combinations if we had a set of mutually exclusive, exhaustive scenario classes. The weighting referred to is just the probability of occurrence of the event or feature (it is harder to work processes into this framework, but it can be done—see Tierney, 1991). The probabilities could occasionally be deducible from hard data, but in practice they will most often be assigned on the basis of "expert opinion." The mathematical formulation of this method is given in Equation 8.1. An example of this combination type is given by the combination of the three human-intrusion CCDFs. This combination is described in Chapter 6. To reiterate, three different types of consequences for a drilling event were modeled: direct release to the surface, transport through the tuff aquifer to the accessible environment, and transport through the carbonate aquifer to the accessible environment. These three possibilities were assumed to be mutually exclusive—only one of them could occur for a given realization. This assumption is not necessarily true, of course, but was used to simplify the calculations. A realistic weighting of the three possibilities was not attempted; they were simply given equal weights for demonstration purposes. The resultant conditional CCDF for human intrusion is given in Figure 6-30. The other node where a type-1 combination is shown in Figure 8-2 is the (dashed) combination of the two alternative models of unsaturated-zone flow. That combination will be discussed below.

2) "Horizontal addition," for combining aqueous and gaseous releases. Ideally, for each realization of the system, aqueous and gaseous releases would be calculated and combined into the EPA sum for that realization, and thus the appropriate correlations between aqueous and gaseous releases would be preserved. For this study, to simplify the calculations, aqueous releases and gaseous releases were calculated separately, with no correlation between them. To combine them, the aqueous and gaseous EPA sums at the same probability level were added together to form the combined EPA sum. Mathematically, this is expressed as follows. Say that $G_a(m_a)$ is the conditional CCDF for aqueous releases and $G_g(m_g)$ is the conditional CCDF for gaseous releases. For a given probability g, find the aqueous partial EPA sum m_a such that $G_a(m_a) = g$ and the gaseous partial EPA sum m_g such that $G_g(m_g) = g$. Add the aqueous and gaseous partial EPA sums to get the combined EPA sum, $m = m_a + m_g$. Then the combined CCDF is such that $G(m) = g$. This combination method has no real theoretical justification, but is a good pragmatic choice when the correlations have not been preserved. It associates high aqueous releases with high gaseous releases and low aqueous releases with low gaseous releases. If both calculations had the same dominant parameter (for example, if the fuel-matrix-alteration rate were the key parameter), then this procedure would give nearly the right answer. With the assumptions made for this study, gaseous releases are significantly higher than aqueous releases, so the combination of the two is dominated by the gaseous part and including the correlations properly would make little difference. Figures 8-3 and 8-4 show the combined aqueous + gaseous conditional CCDFs for the composite-porosity model and for the weeps model. This method of combining CCDFs has been used by other researchers: for example, McGuire et al. (1990).

3) "Probabilistic sum," for combining independent categories. This method of CCDF combination is appropriate when the scenario categories being combined are completely independent (have no influence on each other). As discussed above, for this study we assume that the three basic scenario categories are independent of each other. This kind of CCDF combination is accomplished by making another Monte Carlo simulation. A sample (i.e., a partial EPA sum) is drawn from each of the distributions to be combined, and the partial EPA sums are added to get the combined EPA sum. This procedure is repeated many times (10,000 times was chosen as a suitably high number); the distribution of the combined EPA sums is recorded and becomes the combined CCDF. As shown in Figure 8-2, in addition to combining the three basic scenario categories by this method, the six columns in the composite-porosity unsaturated-zone calculation were combined this way. The underlying assumption is that parameter values in one column are completely un-

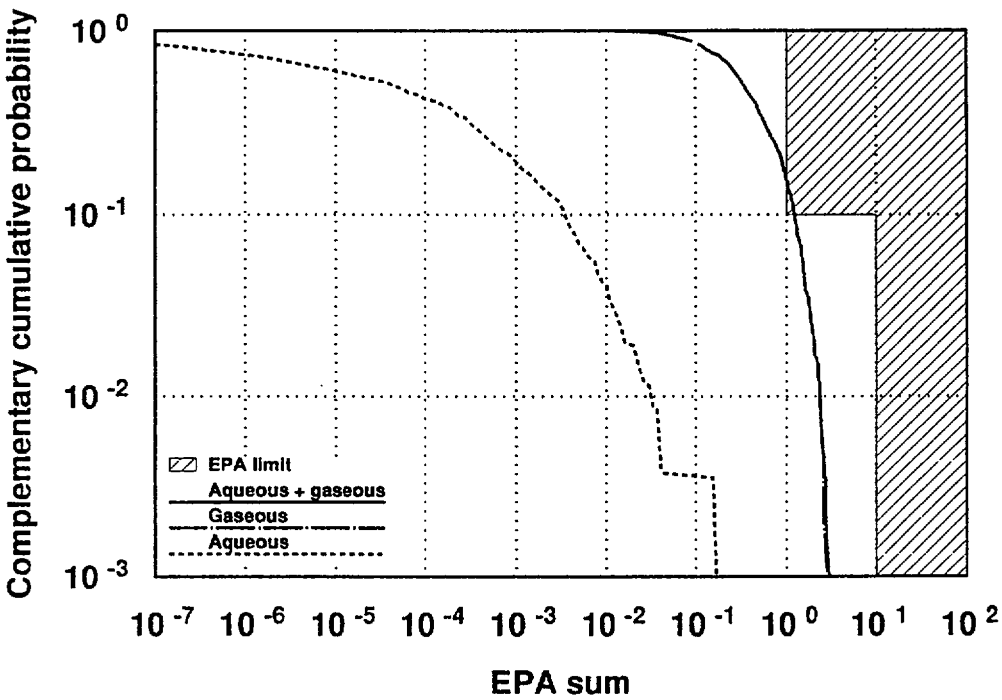

Figure 8-3. Combination of the aqueous and gaseous conditional CCDFs for the composite-porosity model.

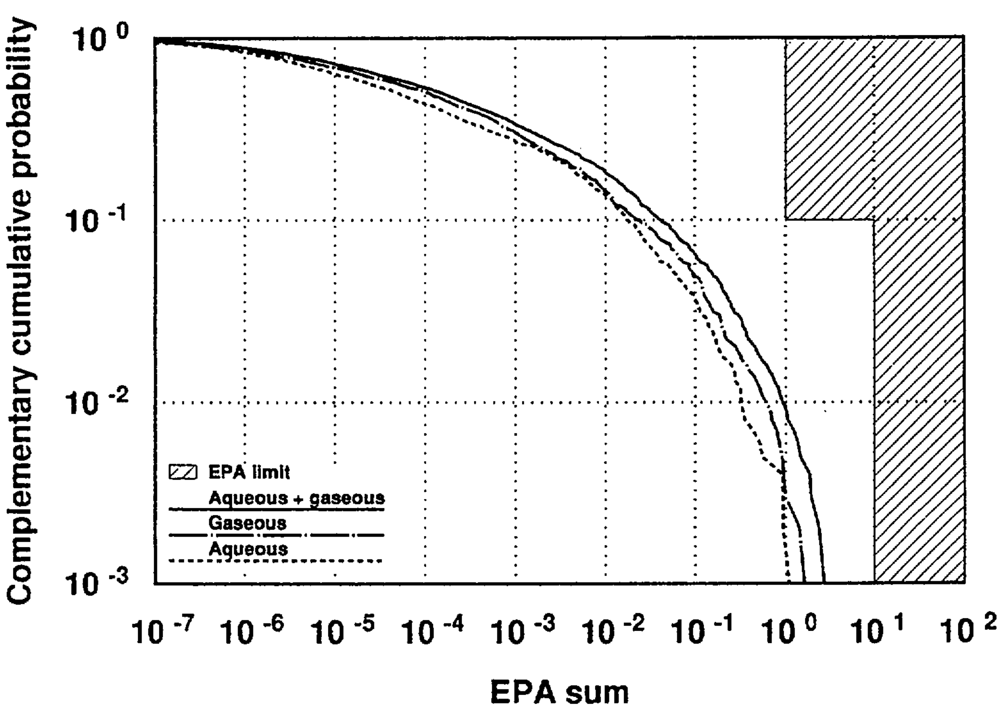

Figure 8-4. Combination of the aqueous and gaseous conditional CCDFs for the weeps model.

correlated with parameter values in the other five columns. Although this choice was made for reasons of convenience, to make the calculations easier, the choice is not completely unreasonable, because the spatial separation between the columns is large and there may well be little correlation. However, in future calculations it would be preferable to put in a better estimate of the expected correlation. Figure 8-5 shows the conditional CCDFs for the six columns (aqueous releases only) and the conditional CCDF for the combination. The fact that releases were usually significantly higher in Column 6 than in the other five columns reduces the possible effect of correlations. The inconsistency between the individual CCDFs and the combination CCDF at low probability values (for example, the CCDF for Column 1 sticks out beyond the combination CCDF) is a result of the statistics of low numbers (since the combination was done probabilistically rather than deterministically) and the way the range of EPA sums was divided into bins. The inconsistency should not be cause for concern; those low probability values have little statistical significance. (Some discussion of statistical significance in CCDFs can be found in Wilson et al., 1991.)

Next, let us turn to the combination of the three basic scenario categories. Because they are assumed to be independent of each other, the combination is done

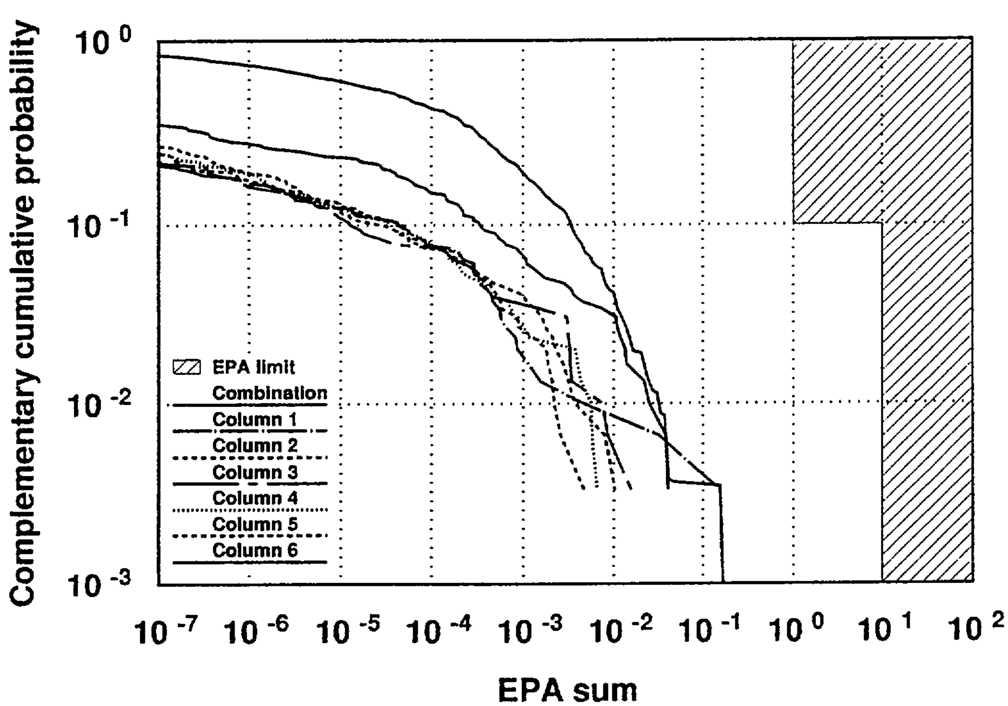

Figure 8-5. Conditional CCDFs for aqueous releases from the six columns, and the combination CCDF.

using method three. First, consider the combination of nominal conditions, human intrusion, and volcanism, with nominal conditions represented by the composite-porosity model (the upper part of Figure 8-2). This combination is shown in Figure 8-6. The "nominal" releases are much higher than the human-intrusion releases, so the combination curve is nearly the same as the nominal curve. The curve for volcanism is off the scale. If the same combination is made with nominal conditions represented by the weeps model (the lower part of Figure 8-2), the combination curve in Figure 8-7 results. This time, nominal conditions do not dominate human intrusion as much and the combination curve is noticeably different from the nominal curve. Once again, the volcanism curve is off the scale.

Finally, consider combining results for the two flow models (the dashed lines in Figure 8-2). For purposes of this study, the two flow models were considered to be mutually exclusive—either the composite-porosity model is right or the weeps model is right. This is a simplification of the real situation, in which it is possible for a combination of the two to be the right answer. However, we have no information about that possibility. To combine the CCDFs with the assumption of mutual exclusiveness, a linear combination of the two curves is taken, as discussed before. To do this, it is necessary to assign a relative weight to each of the models.

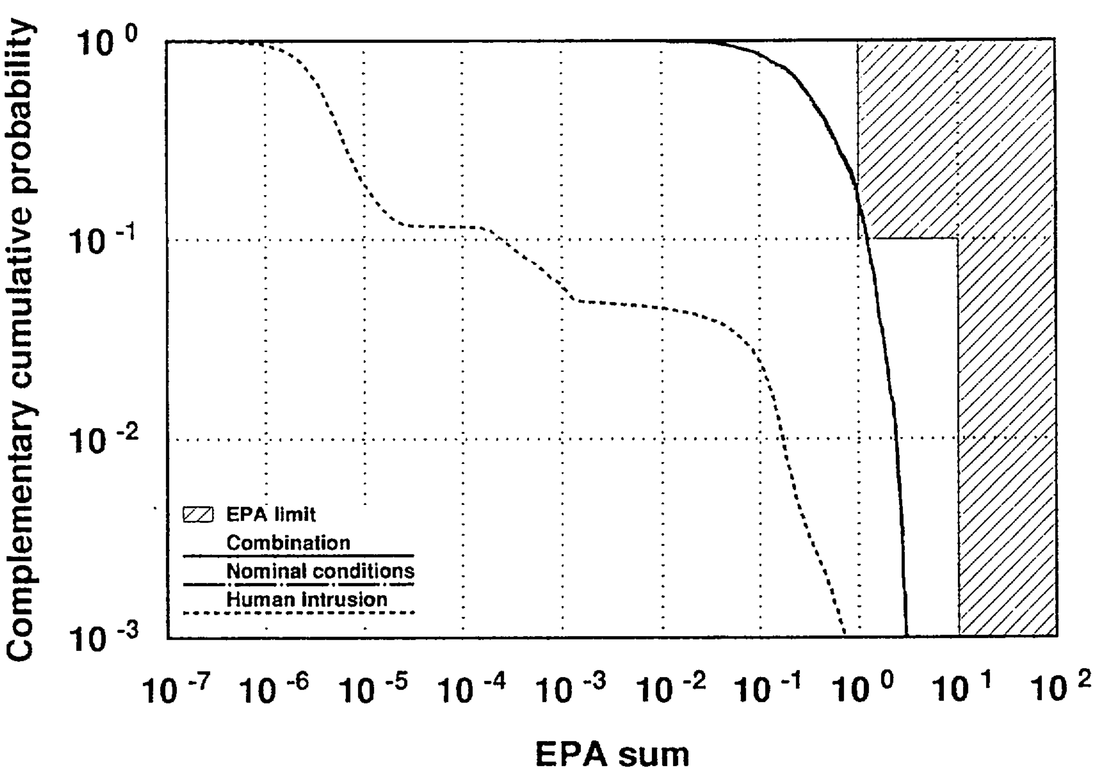

Figure 8-6. Overall conditional CCDF, with composite-porosity model assumed for unsaturated flow.

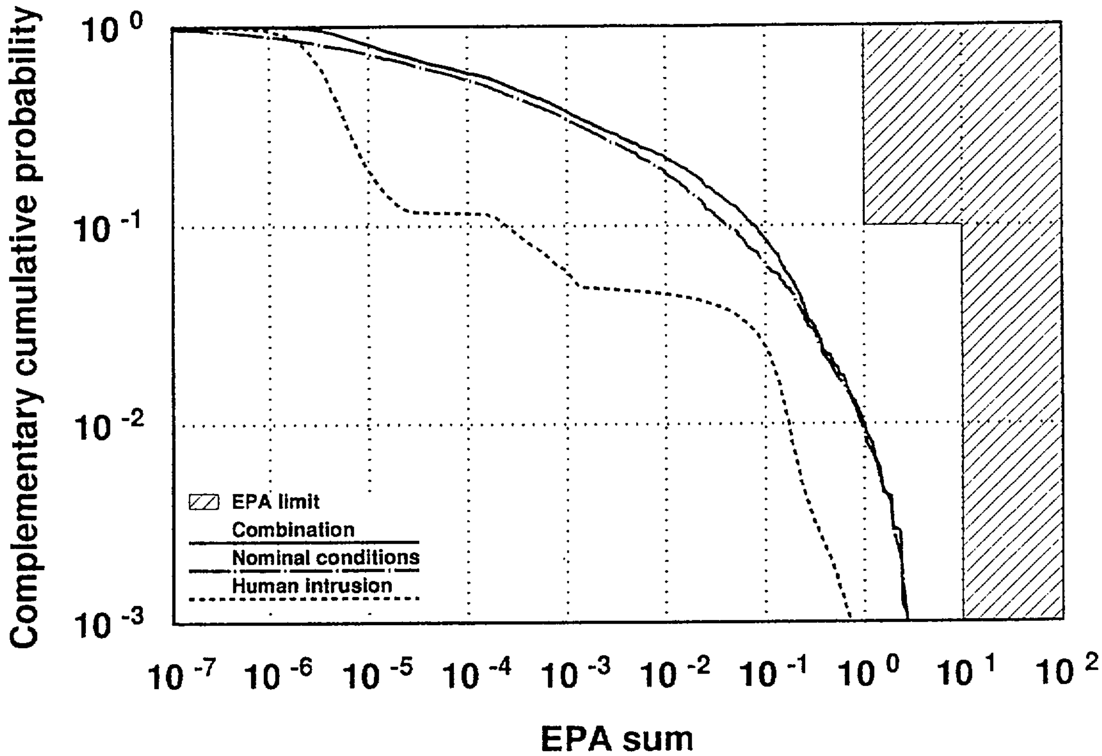

Figure 8-7. Overall conditional CCDF, with weeps model assumed for unsaturated flow.

Figure 8-8 shows three curves. Two of them have already been shown: they are the pure composite-porosity curve and the pure weeps curve. These two curves are the limiting cases of the possibilities for linear combinations; in one case the weighting would be $(1,0)$ and in the other the weighting would be $(0,1)$. The third curve is halfway in between, which is to say a weighting of $(0.5,0.5)$. Figure 8-8 has been duplicated in Figure 8-9 with a linear probability axis rather than the usual log probability axis, so that it can be seen more clearly that the middle curve is always halfway (vertically) between the other two curves. Equal weighting is the natural choice in the absence of any information favoring one model over the other. If some other weighting could be chosen, based on "expert opinion" or on objective information, then that weighting would define another curve. Clearly, any of the combination curves will always be between the two "pure" curves. As stated previously, whichever of these curves is regarded as the overall CCDF for this study, it is still not a total CCDF but only a conditional CCDF for the subset of the parameter space that we have considered.

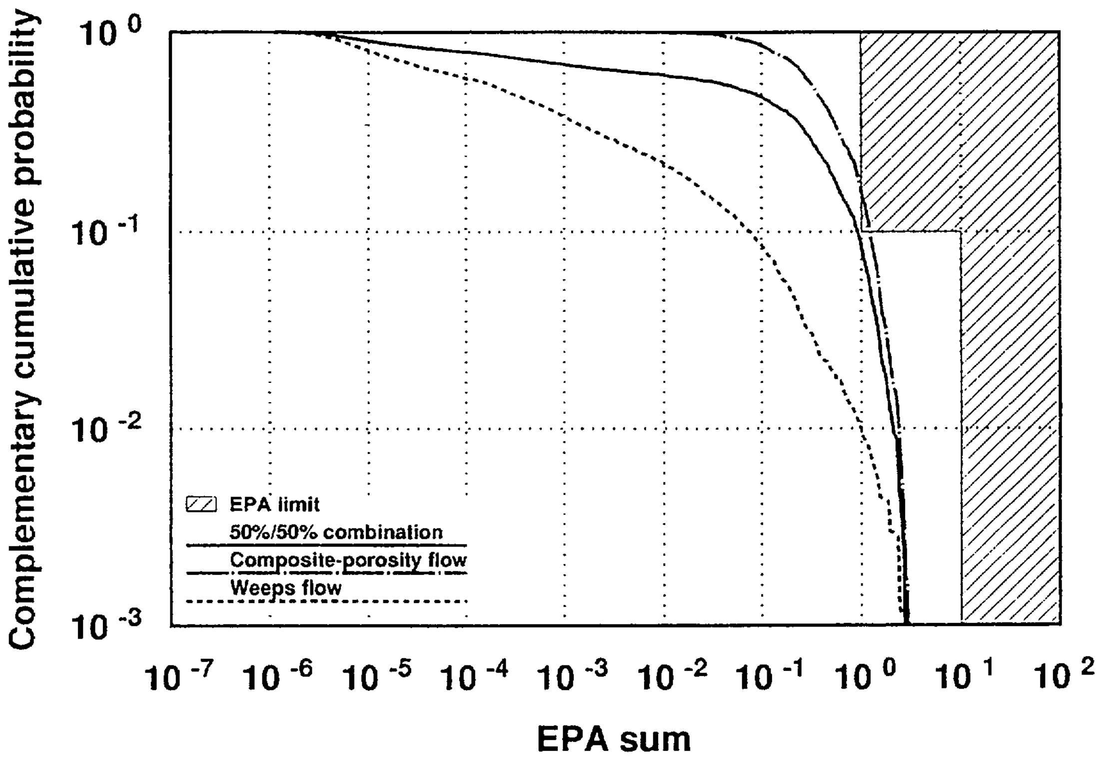

Figure 8-8. Overall conditional CCDF, with three weightings of composite-porosity and weeps models.

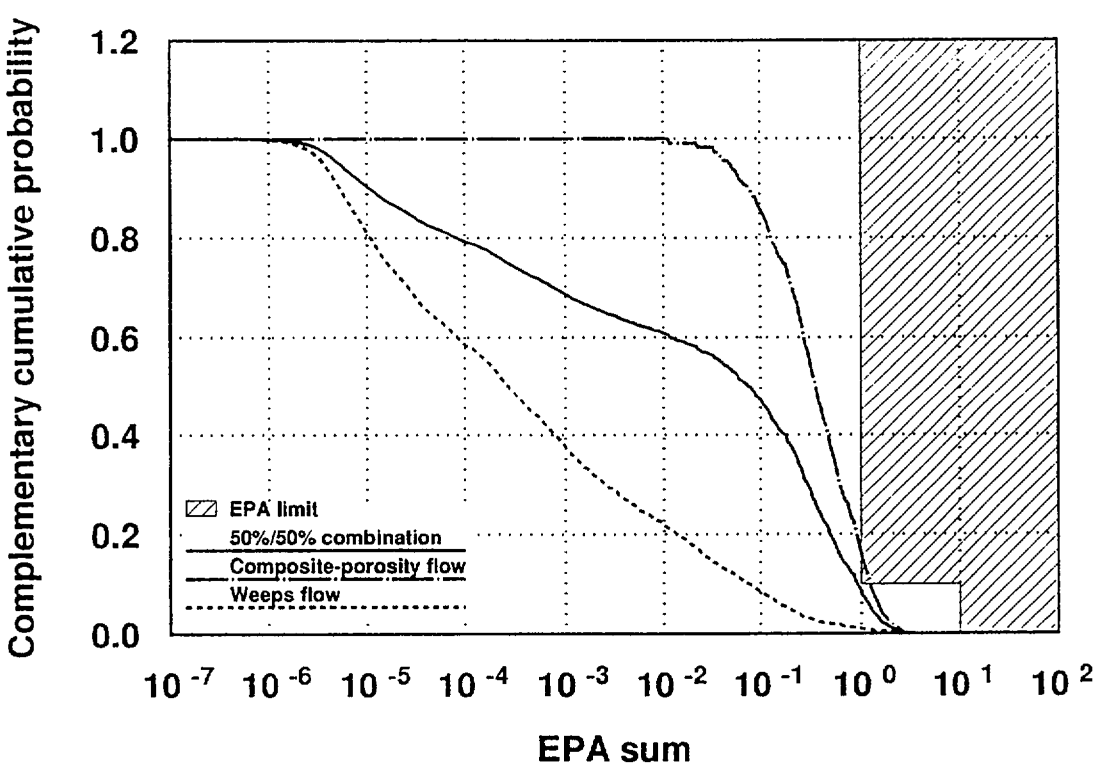

Figure 8-9. Same as Figure 8-8, but with linear probability axis.

Chapter 9
Comments and Comparisons

(Barnard, Eaton)

9.1 Comments on abstraction

The abstracted models used as a basis for this TSPA were developed from our current understanding of the Yucca Mountain site, analog sites, and from prior detailed analyses. They represent models near the top of the PA pyramid discussed in Chapter 2. The abstraction that produced these models was intended to capture the essential features of processes, concepts, and models, and possibly to permit their expression in a simpler fashion. It is quite possible that the abstracted models may not be simpler in concept than "detailed" models. They may only involve fewer calculational procedures. The abstracted models used in this study will change as the models lower in the pyramid receive further development.

Abstraction is not only done to facilitate complex analyses. Many processes are either so complex or so extensive that they cannot readily be comprehended. Abstraction, by grasping the essence of such processes, permits analyses of them to be more easily understood. It also is an important tool in the initial screening of scenarios, when it is not efficient to perform complex analyses of processes that can be shown to be insignificant. Abstracted models must strike a balance between being simple in construction and having sufficient sensitivity to the constituent parameters.

The abstractions done in this analysis fell into two categories. Some abstractions reduced the complexity of the processes being modeled—these abstractions were made by simplifying the description of the physics of the processes. Others were expedient—the amount of simplification in the descriptions was determined by the resources that could be committed to the work. In the former category was the use of the TGIF simulations for gas flow (Ross et al., 1992); in the latter category was the use of rather gross temperature bands for the relationship between travel time and temperature in the analysis of gas flow.

To properly do abstraction, it is necessary to use the results of the models located in the lower levels of the PA pyramid to avoid making excessively conservative assumptions. It is tempting to make conservative assumptions as a substitute for sufficiently detailed analyses. While each conservative assumption may not itself cause a serious overestimation of releases, multiple conservative assumptions can result in an excessively conservative result. When the process appears to be excessively conservative, an analysis of the assumptions that were used in the calculations may identify areas where further information would be most effective in making the assumptions and the calculations more realistic. Such an analysis can fruitfully be based on comparisons with detailed calculations. As the detailed models receive further development, conservatisms in the current study can be examined and perhaps relaxed.

The following table lists the supporting calculations for the various components of the TSPA analysis. The column listed "Examples of Conservatism Remaining" lists factors for which there were conservative assumptions made; it is not intended to be exhaustive. For each entry, the abstractions and conservatisms are discussed in the pertinent chapters.

Table 9-1

Resources for abstractions used in TSPA models

TSPA Component	Supporting Calculations for Model	Examples of Conservatism Remaining
Groundwater Flow and Transport	NORIA-SP and LLUVIA-II simulations for UZ composite model.	Water-flux distribution in model; source term.
	STAFF2D for SZ model.	Water-velocity flow field.
	Nonequilibrium fracture/matrix flow.	Absence of imbibition; source term.
Gas Flow and Transport	2-D TGIF simulations at various temperatures. Time-temperature profile.	Temperatures for travel times assumed hottest conditions; source term.
Human Intrusion	Expert opinion on drilling practices and phenomena.	Mobilization and transport probably overestimated.
Volcanism	Prior work on regional activity and occurrence.	Intrusion mechanism overestimates amount of waste entrained.

9.2 Comparisons with detailed calculations

Comparisons to validate the use of abstractions should be made against the models lower in the PA pyramid described in Chapter 2—those of limited scope, and with a more comprehensive treatment of the modeled processes. In this category, we can compare TSPA groundwater-flow analysis. The remaining TSPA components had no independently calculated detailed analyses against which to compare.

9.2.1 Comparisons for unsaturated flow

The justifications for the abstracted models for unsaturated groundwater flow were examined by calculations using the finite-element code NORIA-SP (Hopkins et al., 1991) and the finite-difference code LLUVIA-II (Eaton and Hopkins, 1992). These calculations are described in Appendix II. The calculations were run for four water percolation rates—0.01, 0.1, 1.0, and 3.0 mm/yr. The lowest flux was useful for confirming that saturation values were comparable for the 1-D and 2-D analyses. The higher percolation rates were important demonstrations that water flow was primarily one-dimensional downward in the problem domain, and that a one-dimensional abstraction was appropriate.

As has been observed previously for 2-D simulations, variations in the hydrologic material properties in adjacent geologic units can cause lateral flow by the percolating water. However, the analysis presented here showed that the relative amounts of lateral flow ($q_x$max/(percolation velocity)) decrease with increasing percolation. This is contrary to results obtained in the same percolation regime using other sets of material properties and geometries (Prindle and Hopkins, 1990). (Note that the lateral flow in Prindle and Hopkins is primarily above the repository horizon, and therefore out of the current problem domain.) Among the combinations of parameters sampled in the probabilistic simulations there are undoubtedly some that would lead to lateral diversion. However, given the assumptions made for the stratigraphy, material properties, and boundary conditions for this analysis, flow occurs dominantly in the vertical direction. Therefore, it is reasonable to assume that a 1-D simulation can approximate this behavior.

9.2.1.1 Results and comparisons

Appendix II describes the problem setup for the NORIA-SP and LLUVIA-II analyses. Figure 9-1 shows the near-steady-state results of the NORIA-SP calculation for the 3.0 mm/yr-flux boundary condition. Although appreciable vertical flow appears to be occurring in the Ghost Dance Fault, little lateral flow at the unit interfaces occurs. It should be noted that the NORIA-SP calculations were terminated before reaching a true steady-state because of the amount of computer time consumed. The flow is in steady state down through the top three layers. The flow in layers 4 and 5 did not reach steady-state.

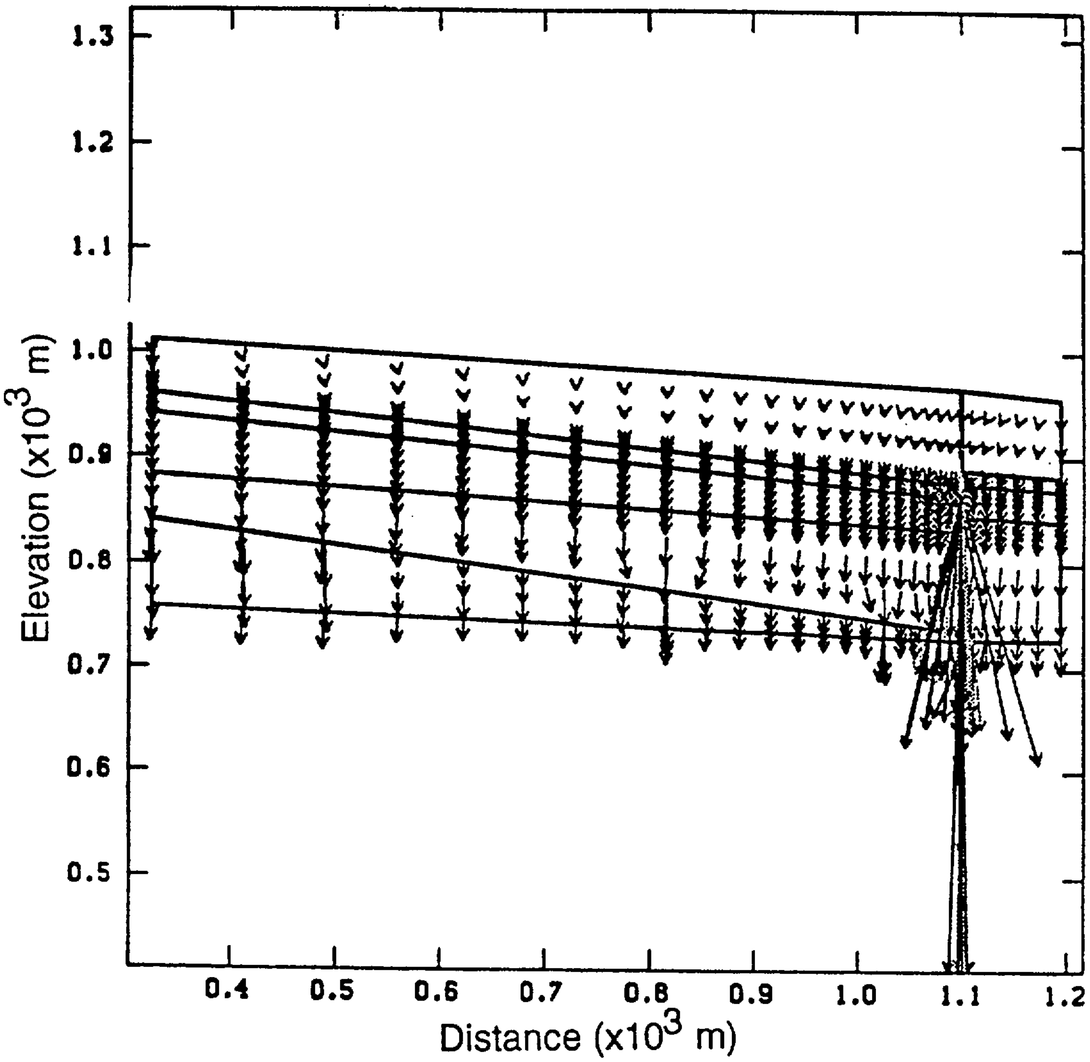

Figure 9-1. Darcy velocity vectors calculated by NORIA-SP

Figure 9-2 shows steady-state Darcy-velocity vectors calculated with LLUVIA-II for percolation rates (q_i) of 0.01, 0.1 and 1.0 mm/yr. It can be seen from the velocity-vector plots that the relative amount of lateral flow decreases as the boundary flux increases. Figure 9-3 shows particle pathlines for the 0.01 and 1.0 mm/yr cases. The plots show that the validity of the one-dimensional assumptions increases with percolation rate. Table 9-2 lists the ratio of the maximum lateral-flow fluxes to the boundary flux for the three cases. The table shows that while the magnitude of the lateral flow increases with increasing percolation the relative magnitude ($q_x$max/(percolation flux)) decreases. These relatively large amounts of lateral flow at the low fluxes are consistent with the TSPA groundwater-flow results obtained by PNL.

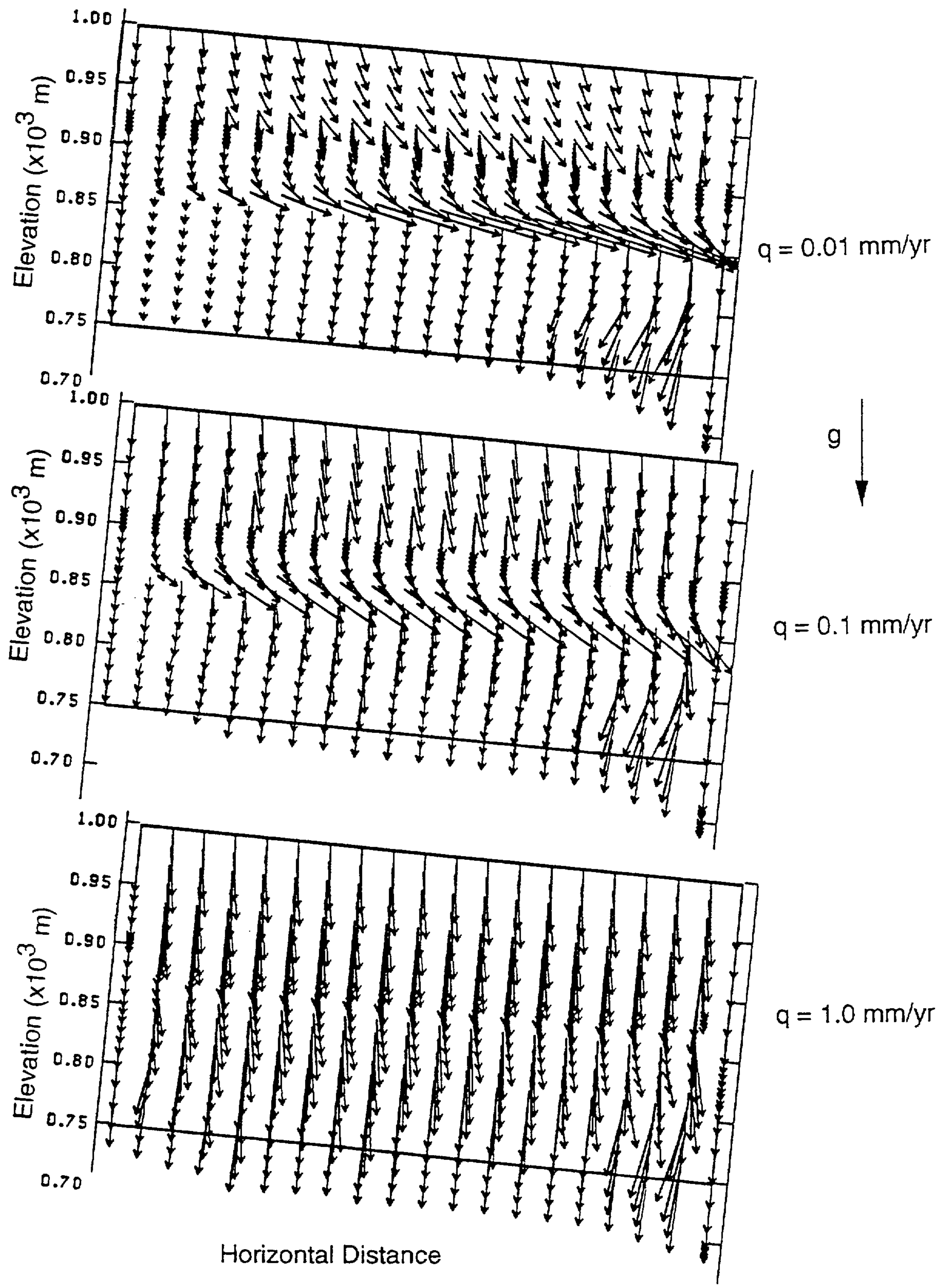

Figure 9-2. Darcy velocity vectors for three fluxes calculated by LLUVIA-II

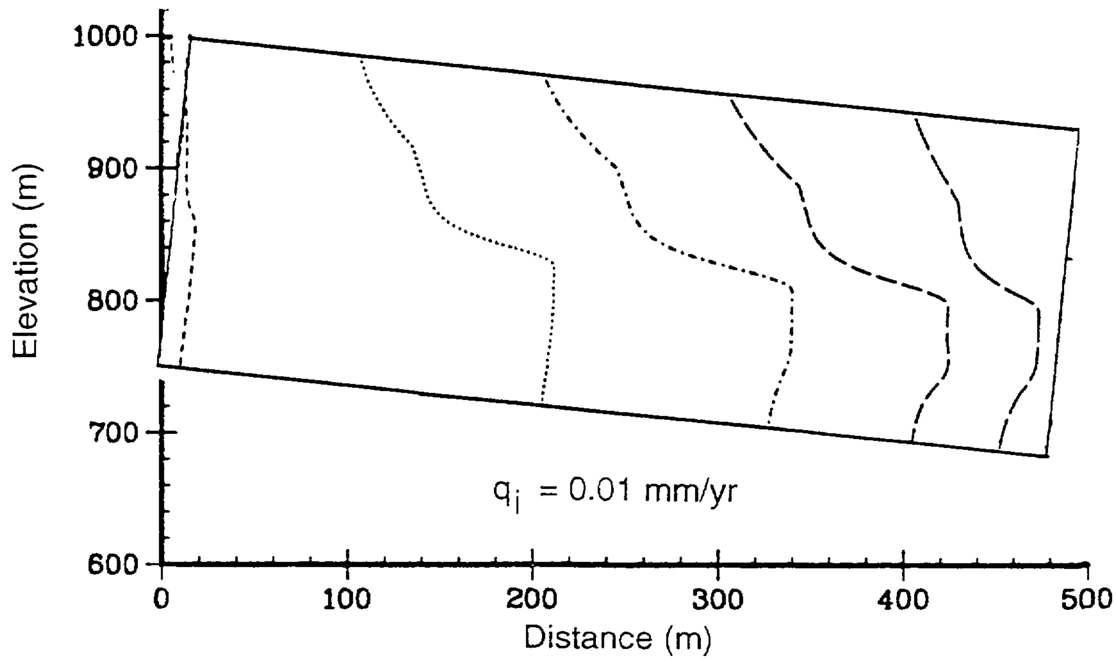

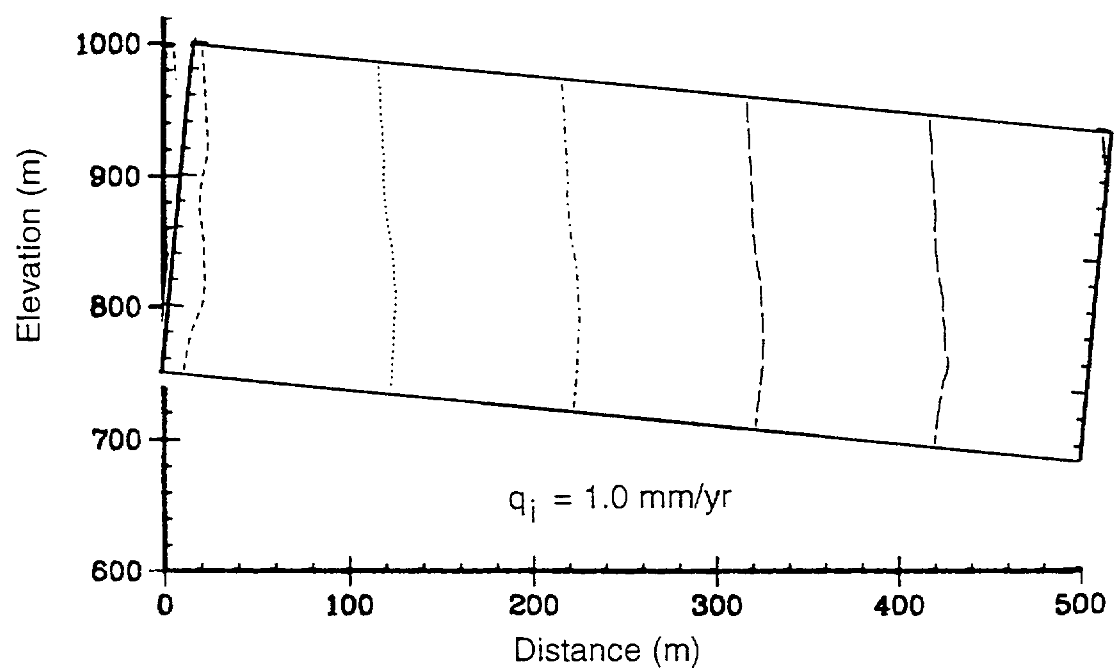

Figure 9-3. Particle pathlines for 0.01 and 1.0 mm/yr fluxes calculated by LLUVIA-II

Table 9-2
Relative lateral flow

Percolation (q_i) (mm/yr)	$q_x$max (mm/yr)	q_x/q_i
0.01	0.03	3.0
0.1	0.17	1.7
1.0	0.22	0.22

Lateral flow occurs when geologic units of relatively high permeability overlie units with lower permeabilities, or vice-versa. As the percolation rates are increased, the local negative pore pressure heads in all units increase toward zero, and the magnitudes of the pressure-dependent matrix conductivities approach their respective saturated values. The relative magnitudes of the conductivities vary as percolation rates are increased. For the materials used in this study, matrix conductivities at the interface of units 2 and 3 (zeolitic and vitric) differ by more than two orders of magnitude for the 0.01-mm/yr case. However, when the percolation is increased to 1.0 mm/yr, the conductivity ratio is less than a factor of 2. Consequently, the relative amount of lateral flow decreases.

Vertical and horizontal velocity profiles for a boundary flux of 0.1 mm/yr are shown in Figures 9-4 and 9-5. Figure 9-4 shows that at the water table, the downward velocity magnitude increases toward the down-slope end, as would be expected from gravitational effects. The spike in the lateral-velocity profile at elevation 870 m in Figure 9-5 is a result of the conductivity difference between units 4 and 5. Near this interface, there is over a 10-fold difference in the partially saturated conductivities. The ratio of the saturated conductivities at this material interface is $8{*}10^{-11}/3{*}10^{-12} = 27$. The larger conductivity with little change in pressure gradient gives the velocity spike.

Although the amount of lateral diversion at the lowest percolation fluxes is relatively large, it is still an absolutely small amount. This minor extent of lateral diversion helps to support the validity of using 1-D models for the groundwater-flow component of the TSPA. However, until the range of percolation is better defined, lateral flow cannot be ignored in calculations. The horizontal uniformity of the flow field implies that the use of several 1-D columns whose properties are spatially uncorrelated is not inappropriate for modeling extended regions, such as the repository. For further examination of the validity of 1-D simulations, 2-D transport runs should be done to compare with the 1-D simulations.

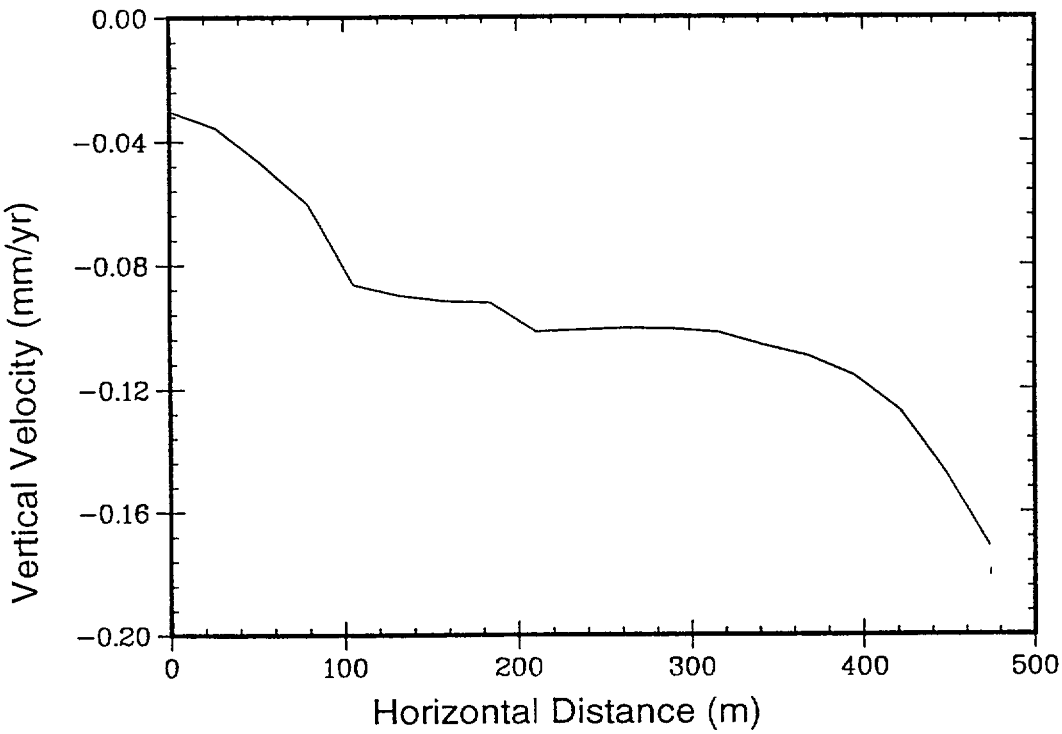

Figure 9-4. Vertical groundwater velocities at the water table

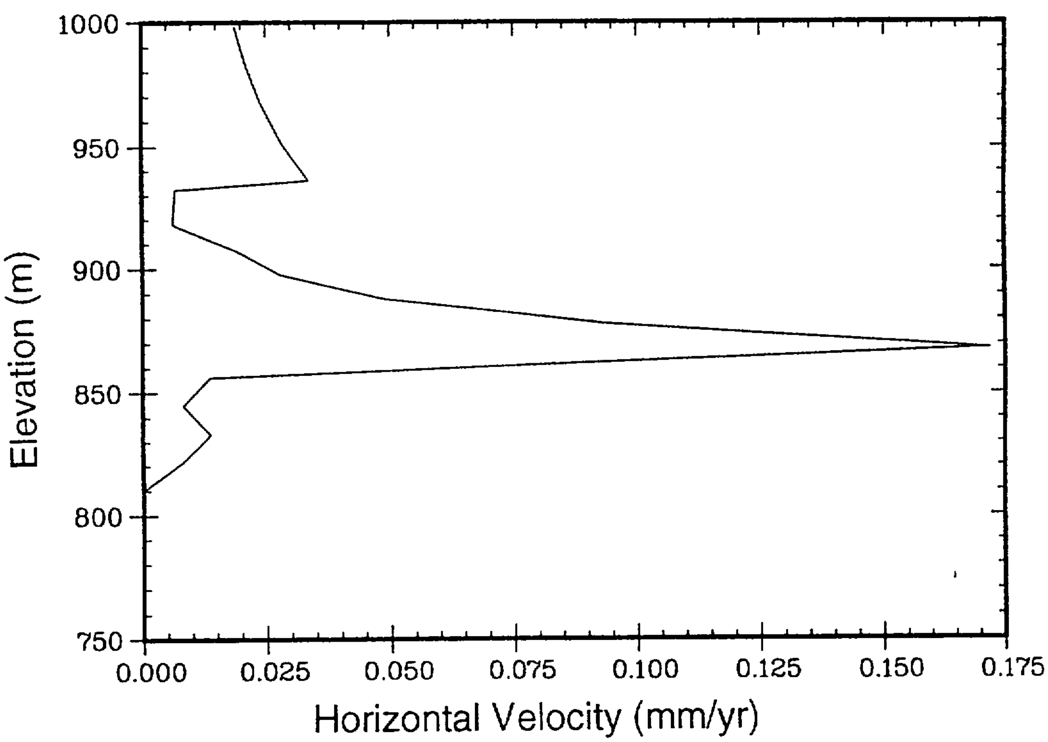

Figure 9-5. Horizontal groundwater velocity at x = 250 m

9.2.2 Other comparisons

When comparing abstracted models with detailed ones, the ranges of applicability of the abstractions must be considered. For example, there are many prior examples of unsaturated-flow analyses where the groundwater does not flow primarily downward. Indeed, the choices of problem domain, boundary conditions, and material properties used in the TSPA may have contributed to the satisfactory relationship between the 1-D and 2-D calculations. One of the areas of future work on abstracted TSPA analyses is to determine the regions of applicability of the models.

9.2.2.1 Saturated-zone calculations

The flow fields used as inputs to the saturated-flow TSPA analysis were separately calculated with the code STAFF2D, rather than being calculated as part of the TSPA analyses. This component of the TSPA has not been independently compared with more detailed models, since we do not have any model with more detail.

9.2.2.2 Human intrusion and basaltic igneous activity

The SNL human-intrusion and basaltic-igneous-activity analyses were abstracted from prior conceptual models. The TSPA analyses are as complex as the supporting calculations for the original conceptual models (e.g., compare Crowe et al., 1983, for the igneous analysis), so there is no comparison that can be made with complex models.

9.2.2.3 Gas transport

The gas-transport TSPA calculations used as the abstracted model the travel times calculated by the TGIF analysis (Ross et al., 1992). In contrast, the PNL analysis* calculated gas flow resulting from the transient thermal and hydrologic response of the unsaturated rock to repository heating. Their model included 2-D geometry, multi-phase transport, and transient thermal and flow conditions. The transport process for the SNL model was advection of $^{14}CO_2$; both advection and diffusion were included in PNL's model. Although both the SNL and PNL analyses used the water percolation rate as a parameter, this factor only affected the source term in the SNL work. Because the PNL work considered two-phase pro-

* A description of the PNL analysis is given in the document by Eslinger et al. listed in the bibliography.

cesses, the percolation rate parameterized every simulation. In the PNL analysis, only results for the 0 mm/yr percolation rate are shown; however, both that rate and a 0.01 mm/yr percolation rate were investigated. The most important factor in the differences between the SNL and PNL results was the value for the air permeability. PNL used a considerably smaller permeability, which had the effect of making their results be diffusion-dominated. The larger permeability value used by SNL resulted in an advection-dominated process for our results. The PNL work found that gas flow was strongly affected by the saturation in the rock; at high saturations, little gas flow could occur. Table 9-3 compares the gas-phase releases for the PNL analysis and the two SNL models.

Table 9-3
Gas-phase releases of ^{14}C
(Adapted from Eslinger et al., 1992b)

Model	Time of Maximum Release (yr)	Release Rate at Surface (Ci/yr)	Cumulative Release at Surface (Ci)
SNL (Composite-Porosity Model)	3550	1.42	3.0
SNL (Weeps Model)	3550	$5.59*10^{-4}$	$4.0*10^{-4}$
PNL (SUMO)	9768	$1.0*10^{-2}$	2.4

The two SNL models predict the same time of maximum release, since they only differ by the mobilization mechanism for the source term (see Chapter 5). The release rates differ by the differing strengths of the two source terms. Both SNL results were calculated with a water flux rate of 1.0 mm/yr. The PNL results shown above were calculated using the 0 mm/yr groundwater flux. Because they used a lower gas permeability, and because of the retarding effect of water saturation arising from repository thermal processes, the PNL results show a longer time to reach maximum release. Given the uncertainties in the calculations, the cumulative releases over 10,000 years are comparable for the SNL and PNL composite-porosity models.

9.3 Success of abstraction

The abstracted results appear to adequately represent our understanding of the results obtained from exercising our currently available detailed models. The two models chosen for the aqueous processes most likely represent extremes of the possible phenomena; although there is little validation of the gas-flow models, the two independent calculations (SNL's and PNL's) produced similar results; the results for igneous activity lie sufficiently far away from regulatory limits that it is unlikely that uncertainties in the model can cause releases to exceed those limits. The responses to variations in the input parameters and to variations in modeling assumptions are reasonable, given our understanding of the processes. The abstraction done for this study probably forces more conservatism into the models than will be included in the more detailed calculations; presumably, additional data will furnish justification for assumptions that in this study were made conservatively simply because of the scarcity of data. Consequently, the results of this TSPA may not accurately reflect the characteristics and behavior of the site as accurately as future assessments will.

9.4 Comments on performance measures

The performance measure specified by EPA is the CCDF. It graphically illustrates the probability of exceeding a release limit (in this case, release of radionuclides to the accessible environment). CCDFs may obscure other aspects of the results, however. For CCDF curves that do not exceed the release limit, there are other ways of displaying the outcomes of analyses that may be more useful in characterizing the performance of the total system. For example, the two disjoint distributions comprising the near misses and direct hits due to drilling are better illustrated by histograms of the releases (see Section 6.6).

The CCDFs representing the total-system performance presented in this report give the probabilities of cumulative release of radionuclides to the accessible environment from all components of the system that were modeled. For the components themselves, other performance measures may be more illuminating. Examples of other performance measures are release rates, or distributions of releases as functions of time or other parameters. Some of these measures may be better for evaluating the performance of the components. Subsystem performance objectives, such as the NRC containment and travel-time requirements, should be viewed as performance measures for the subsystem only; as was shown in Section 4.7, some subsystem performance measures may indicate acceptable total-system behavior while other measures of subsystem performance do not. Similarly, some measures of performance that satisfy regulatory standards based on dose may not meet standards based on releases.

Chapter 10
Conclusions and Summary
(Barnard and Dockery)

10.1 General conclusions

The preliminary total-system performance assessment completed by SNL met the two goals stated in Chapter 1. This TSPA is the first in a series of iterative total-system performance assessments, and as such, contributes to the development of the process for future iterations. We have shown that we can abstract complex processes into more simplified representations, and yet still produce results that retain some degree of sensitivity consistent with our understanding of the processes and that give results consistent with work done using other models and techniques. We have been able to combine the results into a conditional total-system CCDF. Although the process models used in this TSPA are complex, they are located near the top of the hierarchy of models shown in Figure 2-1. Detailed models near the bottom of the hierarchy are needed to form the basis for abstracted models.

Although the scope was limited and the results may not be directly applicable to an evaluation of site suitability, we believe we have demonstrated the success of using these techniques for this type of analysis. Clearly the fundamental approach is sound. The use of abstracted models facilitates the many calculations required in stochastic analyses without sacrificing understanding of the important aspects of the processes being modeled. Indeed, the abstracted models may make it easier to visualize the effects of the processes. However, the process of abstraction is not simple. It requires a very broad and detailed understanding of the operative processes and their effects. The assumptions underlying any abstraction must undergo extensive testing before we can be confident that we have captured all the important elements and their interrelationships.

The results of this TSPA analysis reflect considerable uncertainty and many conservative assumptions. These conditions can be attributed to the current imperfect understanding of the processes, resulting from the lack of site-specific input data. Therefore, they should not be used as the sole basis for any recommendation of higher-level suitability of the Yucca Mountain site, nor should they serve as a baseline for licensing documents, except as an example analysis to illustrate aspects of the form of anticipated later performance assessments. However, to some extent, these results may be useful in guiding near-term site-characterization activities. This preliminary TSPA can aid in assigning priorities to the collection of site-characterization data and can provide an incentive for further field work and research. In future TSPA-style analyses, sensitivity studies on the aqueous- and gaseous-flow components may prove even more useful to testing prioritization. A detailed list of the requirements for improving future calculations is contained in Chapter 11.

Only a few of many possible scenarios have been investigated in this TSPA. Enough scenarios have been modeled to demonstrate the usefulness of the approach. Our current understanding of these scenarios suggests that the suite probably includes the most significant processes that could lead to the release of radionuclides. Nevertheless, to increase confidence in the predictions of the behavior of the repository system, more scenarios must be modeled.

10.2 Technical conclusions and summaries of components

This section will first relate the TSPA estimates of behavior for the entire YMP repository system to the EPA release limits. Following the general discussion of the results of the analyses, a more detailed consideration of each component will be presented.

10.2.1 Overall

Conditional CCDFs representing an overall performance estimate of the total repository system were constructed; they reflect the contributions of all components modeled. Because two alternative conceptual models were used to represent the aqueous transport processes, two overall CCDFs were constructed—one assuming that the flow obeyed the composite model, and the other that the flow followed the weeps model. These CCDFs, along with their constituents, are shown in Figures 10-1 and 10-2. In addition, an "overall" overall CCDF was produced with the contributions from the two flow models weighted equally (refer to Chapter 8, Figure 8-8).

The main contributors to releases calculated in this study were the nominal processes (i.e., aqueous and gaseous flow and transport). Disturbances, such as human intrusion and volcanism, were of much lesser importance. The overall CCDF using the composite-porosity model shows that the releases are almost entirely from ^{14}C. Due to the large gaseous releases, the possibility exists that the EPA limits for releases at the accessible environment are exceeded. The overall CCDF for the weeps model does not exceed the EPA limits. The particular combination of the two CCDFs shown here lies just below the EPA limits. The gaseous-release

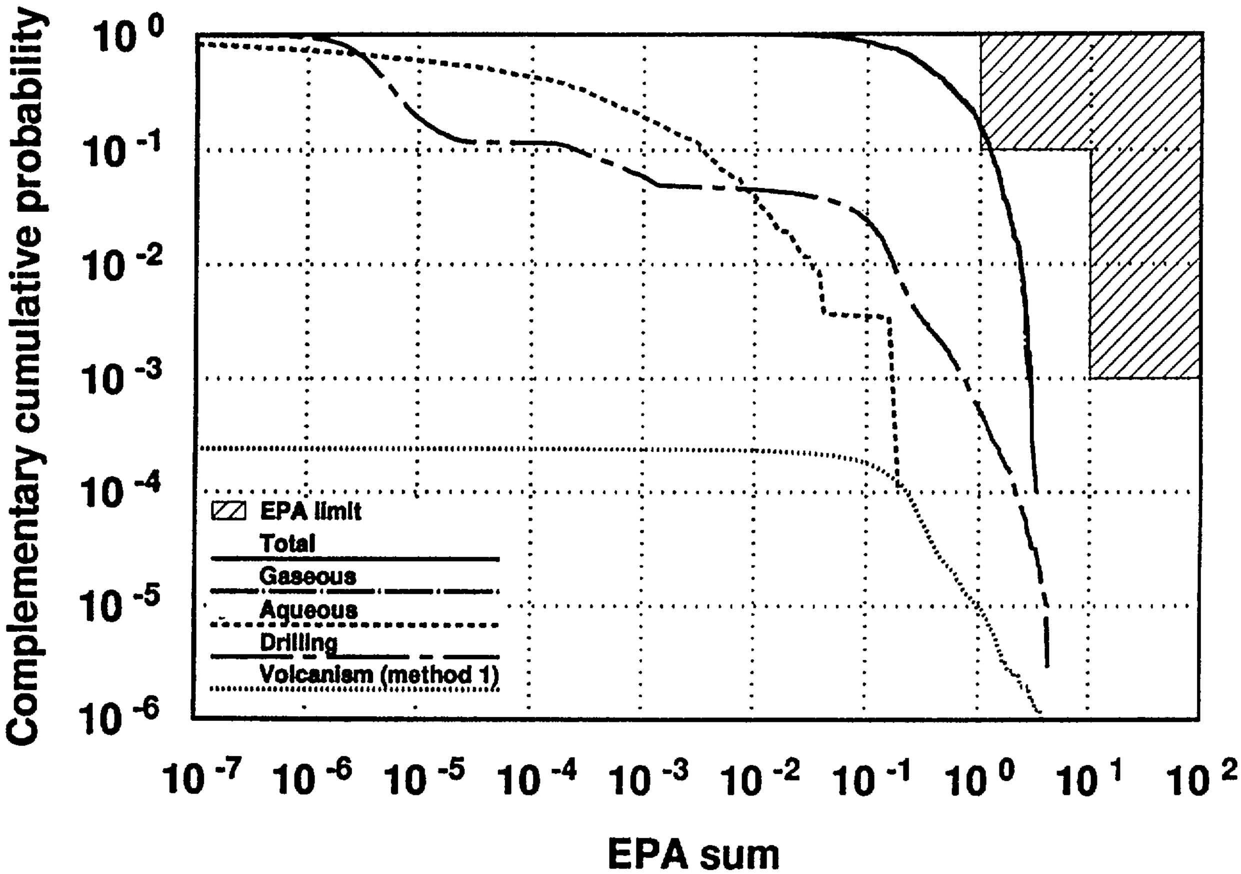

Figure 10-1. Overall CCDF for releases assuming the composite model for aqueous transport

component of the composite-porosity model is the cause for exceeding the limits. However, a number of extremely conservative assumptions are built into the calculations that were used to calculate the noncompliant CCDFs. Primarily, the assumption that the source term does not allow any benefit from the waste container or cladding (after container failure) is obviously not realistic for use in a final total-system assessment. Thus, the fact that our TSPA results show the possibility of noncompliance for these assumptions in no way indicates our belief that the site is inherently unsuitable. The results, particularly for the aqueous- and gaseous-release components, may be construed as an upper bound for waste in an emplacement hole. Future calculations that allow more credit for containment by the EBS will allow a more reasonable approximation of the actual behavior of the repository system.

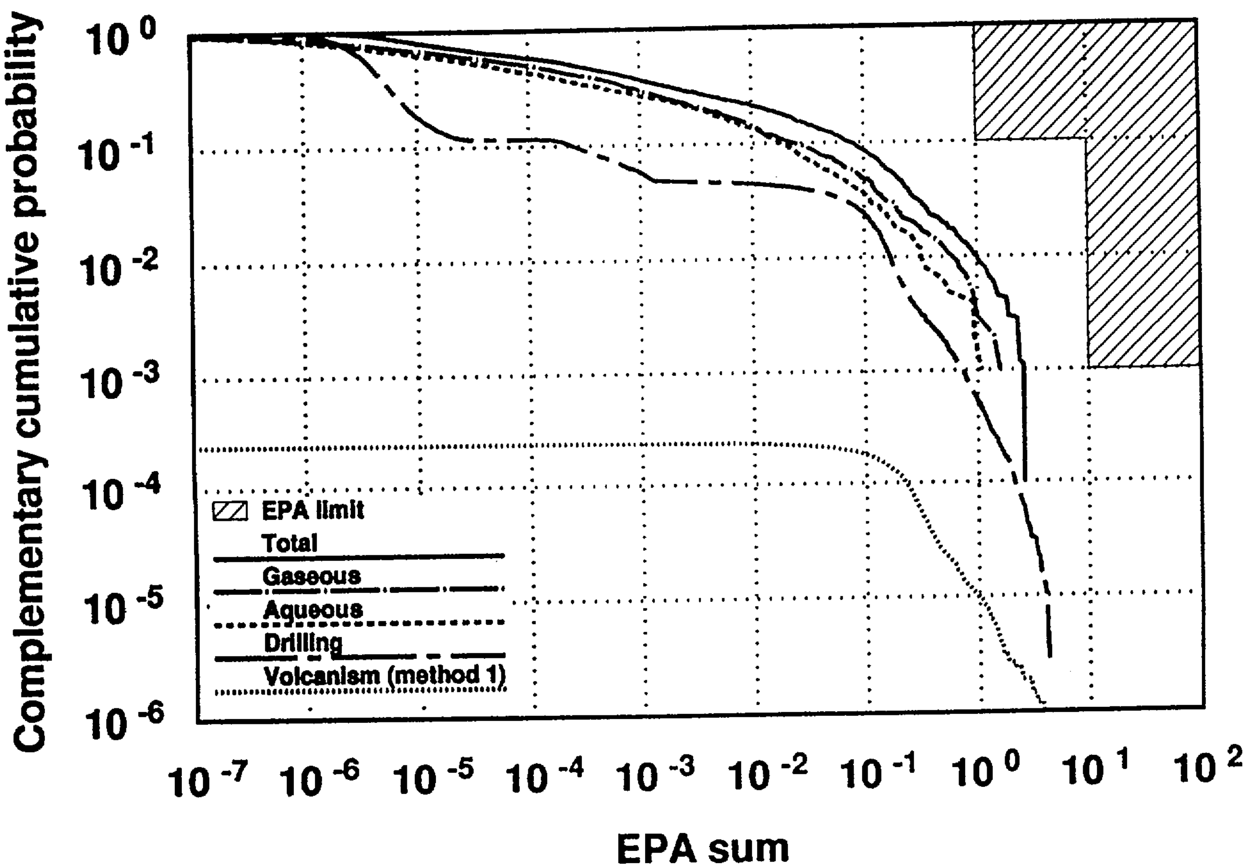

Figure 10-2. Overall CCDF for releases assuming the weeps model for aqueous transport

10.2.2 Data set

As was noted earlier, stochastic analyses incorporate uncertainties in data and model parameters and permit the estimation of uncertainty in the output. For the TSPA analyses, data were sampled from probability density functions for the parameters. Considerable effort was expended on choosing PDFs that were felt to reflect the analysts' degree of knowledge. However, given the uncertainties and sparseness of the data, the exact shape of a PDF may not be too important. As long as the PDF includes the entire range of significant probability, the results will be roughly similar.

10.2.3 Nominal processes

These TSPA components include scenarios for both aqueous and gaseous releases of radionuclides from the potential repository as caused by nominal groundwater-flow and transport processes. Uncertainty in the models has been partially addressed by using two alternative conceptual models of flow in the unsaturated zone—the composite-porosity model and the weeps model. The calculated releases are sensitive to the choice of the flow model; because a sensitivity study has not been done, the most important parameters for nominal conditions cannot be identified.

Of the two nominal processes examined, gaseous releases are found to be the most significant, given the release limits as written in 40 CFR Part 191. The EPA limit for ^{14}C is 0.1 Ci/MTHM. This limit may be conservative for gaseous releases; i.e., the real health effects due to releases at that limit may be so few as to be unobservable. Regardless of the conservatism of the standard, given the use of a more realistic representation of the EBS, it is quite reasonable to assume that the releases would have been in compliance with the limits in 40 CFR Part 191.

For gaseous releases, the composite-porosity model predicts higher releases than the weeps model. This result is largely due to assumptions about how the waste containers fail in the two models. Another factor is that the percolation-rate distribution may be weighted too heavily in the high range, especially for the composite-porosity model.

10.2.3.1 Groundwater flow and transport

The results appear to indicate that there is little difference between the composite porosity and the weeps model concerning of site performance. However, analyses of subsystems of the total system (to compare with the NRC subsystem requirements) show the markedly different behavior of the two models. In calculations using "average" values, the weeps model predicts a largely intact repository after 10,000 years. The composite-porosity model predicts a repository that is actively degrading, with even greater releases at later times. In almost every case, the calculations using average parameter values result in significantly lower releases than the average of the results produced by the Monte Carlo simulations. This effect occurs because combinations of extreme parameter values in probabilistic simulations produce results that outweigh average behavior. This effect is caused by nonlinear problems.

10.2.3.1.1 Composite-porosity model

For the composite-porosity flow model, the calculated aqueous releases at the accessible environment are about two orders of magnitude below the EPA limit. The releases at the water table are well below those from the EBS, indicating that the unsaturated zone is a significant barrier to the release of radionuclides. The processes contributing to this reduction include the generally long groundwater travel time associated with the composite-porosity model (a median of approximately 70,000 years); the close coupling of the matrix and fractures included in this model, which allows significant matrix diffusion of radionuclides; and the retardation of most radionuclides by sorptive minerals. The saturated zone, as modeled, adds little impediment to the radionuclide transport. In contrast to the unsaturated zone, the travel time in the saturated zone is only about 1000 years. However, a more sophisticated treatment of the saturated zone, especially in the tuff aquifer where water may be moving in very complex, nonlinear paths, could cause this travel time to change considerably.

Among the nine radionuclides used in this study, ^{99}Tc and ^{129}I dominate all aqueous releases. They are both highly soluble and are released from the waste form at the highest possible rate consistent with the source-term model—the fuel-matrix-alteration rate. Again, if a more realistic source term is developed for future calculations, the EBS will almost certainly provide a more robust barrier to release. Also, of the radionuclides studied, ^{99}Tc and ^{129}I are considered nonsorbing, and therefore their movement through both the unsaturated and saturated zones is not retarded.

10.2.3.1.2 Weeps model

Aqueous releases from the weeps model, to both the accessible environment and at the EBS boundary, are about one order of magnitude below the EPA limit. This is true even though the assumptions in the modeled conditions are quite conservative. In the analysis, once radionuclides are mobilized from a waste package, most of them are transported from the EBS to the water table instantaneously.

The dominant radionuclides in the release profile are again ^{99}Tc and ^{129}I. Slight contributions are also made by ^{79}Se, ^{234}U, and ^{237}Np, which are relatively weakly sorbed, and thus not strongly retarded in the saturated zone. Yet, the saturated zone still provides a significant barrier for ^{79}Se, ^{234}U, and ^{237}Np, as well as for the other radionuclides considered in this study.

10.2.3.2 Gas flow and transport

Interaction of groundwater with the waste containers plays a major role in the mobilization of ^{14}C. The gaseous-release source term uses the same unsaturated-zone flow models as for aqueous-release analyses—the composite-porosity model and the weeps model. Therefore, in addition to the importance of developing a realistic model for the source term and the near field interactions, identifying the applicable conceptual models of groundwater flow is necessary.

The gaseous releases calculated for the composite-porosity model slightly exceed the EPA standard. This result primarily reflects the extreme conservatism of the assumptions employed for both the source term and the transport. The source-release model used in this exercise ignored the waste container and fuel-rod cladding as barriers to releases after the time of container failure. As soon as the ^{14}C was mobilized, it was considered to be available for transport. In addition, the assumptions concerning alteration-limited releases from the spent-fuel matrix may be conservative.

The CCDFs for releases to the accessible environment for gaseous flow are higher for the composite-porosity model than for the weeps model. This effect is the reverse of that for the aqueous releases. It occurs because the weeps model assumes that only a subset of waste containers is breached by flowing water and release radionuclides. In the composite-porosity model, the flow is assumed to be more uniform, thus nearly all the waste containers are contacted and fail over time. It is possible for all the waste containers in a weeps simulation to fail and release all the ^{14}C, but, with the current parameter distributions, the probability that they will do so is fairly low.

10.2.4 Disturbed conditions

The TSPA modeled two categories of disturbed conditions—human intrusion and basaltic igneous activity. Drilling at the Yucca Mountain site was considered the mechanism for human intrusion, and both surface releases and aqueous releases were modeled. Igneous intrusion considered the effects of a dike passing directly through the repository.

Under the assumptions modeled, human-intrusion surface releases do not exceed the EPA limits. The releases can be made to approach the limits only by substantially increasing (by twenty-fold) the EPA guidance for the maximum number of holes drilled. The likelihood of the occurrence of a human-intrusion event was not incorporated into this problem (i.e., the probability that drilling would occur was assumed to be 1.0). Although more information about the occurrence of attractive natural resources at the site may help us understand the probability of such an event, it will only decrease a CCDF that currently makes very little contribution to overall releases.

Direct releases due to basaltic igneous activity also lie below the EPA limits. A more detailed model of the process would produce releases that probably would be much lower, since a number of extremely conservative estimates were incorporated into the analysis

10.2.4.1 Human intrusion

The conditional CCDFs for the base case in the human-intrusion scenario show that the surface releases do not exceed the EPA limits. Releases due to direct hits on waste packages were about 0.1 of the EPA limit, while releases from bringing contaminated rock to the surface (near misses) were about five orders of magnitude lower. Similarly, aqueous releases due to mechanically transporting the waste to the saturated zone were significantly below the EPA limits.

The magnitudes of direct surface releases were consistently above those of the groundwater-based processes. Releases from the tuff aquifer were about three orders of magnitude below those from the carbonate aquifer, primarily because the lower saturated water velocity and higher retardation assumed for the tuff keep plutonium and americium from reaching the accessible environment within 10,000 years. The composite conditional CCDF for human intrusion is dominated by the surface-release component. Any aqueous contribution is about three orders of magnitude below the maximums created by surface release.

For aqueous scenarios, the maximum releases through the tuff aquifer are produced by carbon, neptunium, and uranium isotopes. Averaged over all realizations, carbon contributes over 60 percent of the radioactive release, with neptunium contributing about 15 percent. Because faster travel times were specified for the carbonate aquifer, the releases are greater. Releases from the carbonate aquifer are over two orders of magnitude higher at the 1 percent probability level. Averaged over all realizations, the two plutonium isotopes contribute over 90 percent of the total. The release of ^{14}C is roughly the same for both aquifers, but the plutonium and americium releases are greatly increased in the carbonate aquifer.

To attempt to more fully test the model, several sensitivity studies were done. For surface releases, the greatest effects occur when the maximum number of boreholes drilled over 10,000 years is increased. For this study, the effects of increasing drilling density were shown for 10 times (170 holes) and 20 times (340 holes) the base case. However, even the twenty-fold increase still does not cause the conditional CCDF to exceed the EPA limit. Other sensitivity studies, such as using multiple-inventory sources instead of a lumped-inventory source, or increasing the diffusion coefficient, or biasing the time distribution for drilling toward the latter part of the 10,000 years, had little effect on the releases. Because of the abstractions used in the drilling model, this model may not be fully representative of the site. Therefore, the results of the sensitivity studies are more properly interpreted as demonstrating the response of the model to parameter variations, rather than the response of the site to those variations.

10.2.4.2 Basaltic igneous activity

Surface releases due to basaltic igneous activity are below the EPA limits. This finding is supported by a consistency check done on prior work. Approximately 90% of the releases come from ^{240}Pu, ^{239}Pu, and ^{241}Am, i.e., those nuclides that are highest in the inventory. However, these releases are based on a very simplistic model using mechanical transport that does not take into account interaction of the waste with heat or reactive chemicals in the magma.

Chapter 11
Areas For Future Work

(Wilson, Dockery, Barnard)

Both the construction of the models and the results of the TSPA have given us a better understanding of the areas that should be investigated for future analyses. Conversely, it has also pointed to areas that may be of lesser immediate concern. Following is a list of topics that we believe should be addressed in future TSPA calculations. Only some of these issues will be addressed in the next iteration; therefore, suggestions from the YMP community may be useful in assigning priorities to these topics.

11.1 General Areas

- We need to work toward an exhaustive set of scenario categories and eventually perform the calculations within one of the two formal methods discussed in Chapter 8. One potentially important scenario category that was not considered at all for this study is seismic events (tectonism).

- We should maintain an ongoing effort to validate the abstractions used in the TSPA.

- New alternative conceptual models must be developed and integrated into the TSA as they arise. We need to study whether to combine existing models and how to combine them (e.g., the composite-porosity model and the weeps model).

- Future TSPA-style analyses should help to guide the site-characterization effort by continuing the identification of data needs begun in this analysis. These studies can begin by examining the data needs documented here.

- New site-characterization data must be analyzed and, where applicable, incorporated into new TSPA-style analyses. For example, groundwater-age data could indicate that weep flow dominates in part of Yucca Mountain (e.g., along Solitario Canyon), while composite-porosity flow dominates in another part. Future total-system analyses would then have to be adjusted to use different conceptual models of flow for different parts of the mountain. As another example, climate data could indicate a significantly wetter (or drier) future at Yucca Mountain, and the analyses would then have to be adjusted to address this finding. If the data help to better define probability density functions, the reduced uncertainty can be useful in providing further guidance for the site-characterization effort.

- The effects of disturbing conditions such as volcanism, tectonism, and human intrusion on nominal flow conditions should be investigated.
- The general thermal effects caused by repository heating should be investigated to better understand potential changes in hydrologic properties (such as permeability), geochemistry, and mechanical properties of the affected host rock.

11.2 Parameters

11.2.1 Data set

- We need to continue to develop alternative interpretations of the Yucca Mountain geohydrologic stratigraphy. Various interpretations of the stratigraphy have included large differences in conductivity between adjacent layers—e.g., the COVE-2A study (Dykhuizen and Barnard, 1992) and the PACE-90 study (Barnard and Dockery, 1991)—or detailed stratigraphy—e.g., the PACE-90 study—or simple stratigraphies—e.g., the HYDROCOIN study (Prindle and Hopkins, 1990) and this TSPA. Each of these has produced different results. Other possibilities include anisotropy or heterogeneity within layers.
- A formal sensitivity study is needed to identify the parameters that are the most important. From the work that has been done so far, certain parameters appear to be important, including container lifetime, gas source terms, fuel-matrix-alteration rate, solubility, the fraction of the waste interacting with the water, percolation rate, matrix/fracture coupling, hydraulic conductivity, porosity, and saturated-zone velocity. A formal sensitivity study can quantify the importance of these parameters, help define what tests might give these data, and help to guide the gathering of those relevant data during site characterization.

- We should refine further the elicitation techniques employed to develop the data set. Elicitations of expert opinion about PDFs were regarded favorably by both the experts and the users of the data. The combination of rapid feedback using our software with more formal elicitation techniques could make the process more effective.

- Parameter distributions should be refined as additional information becomes available. One of the most important parameters, the water percolation flux, is poorly defined; a study of current estimates of percolation and possibilities for future values is needed.

- Correlations among parameters must be analyzed. The little that has been done in this area (Wilson, 1991) has failed to find any correlations that led to significant changes in the CCDFs, but there could potentially be important correlation effects.

- Hydrogeologic and geochemical parameter values for the saturated zone are needed. For this study, most of the emphasis was put on parameter values for the unsaturated zone, while the saturated-zone parameters were developed less thoroughly.

- The effects of scale on the model parameters need to be quantified. The information available on hydrologic parameters typically comes from laboratory measurements on core samples (a scale of a few centimeters). It is known that quantities measured on a small scale are not appropriate for use in large-scale calculations (the calculations in this study have horizontal scales of kilometers and vertical scales of hundreds of meters) without applying some sort of scaling transformation. The appropriate scaling transformation is not known.

- The effects of heterogeneity among the characteristics of the stratigraphic units needs to be investigated both by modeling and by collecting data.

- The validity of the one-dimensional modeling needs to be investigated more thoroughly by additional comparisons with detailed modeling. Such studies may suggest improvements in the one-dimensional modeling, making it better able to represent the results of calculations with multidimensional models.

11.2.2 Source-term

- More accurate, correlated, and defensible parameter distributions are needed. Many of the parameters that were treated as constants in this analysis should be expanded into probability distributions to reflect the uncertainties and variabilities. All distributions should be reexamined, but the required level of accuracy and the justification for each variable could be guided by a sensitivity study. The calculations could be made more realistic if the parameter distributions (especially the container lifetime) were contingent upon the container environment (for example, "moist" containers could take longer to fail than "wet" ones).

- Some aqueous-transport analyses should be performed that include all significant radionuclides (listed in Table 6-4), to be sure that the most important ones have been included. Additional source submodels are needed for those nuclides that are present in the cladding and the fuel-assembly hardware (Wilson, 1991).

- The waste container and the fuel-rod cladding should be included in a more realistic manner as barriers to transport. For example, diffusion would probably not take place across the whole container surface. The effective diffusion surface area could be reduced to account for this, or diffusion through cracks and holes in the container could be modeled as an additional diffusive barrier (apart from the barrier presented by the rubble-filled air gap in the present model). A model of this sort has already been developed by Ueng and O'Connell (1991).

- Submodels are needed for additional release modes; for example, a glass-waste submodel is needed. The submodels already included should be extended to include additional processes; for example, a "bathtub" release mode could be included (see, e.g., O'Connell, 1990, and Apted et al., 1990).

- The validity of the alteration-limited-release model needs to be verified. This model predicts very high release rates for the soluble elements (at least, it does with the parameter values used in this study). The experimental evidence for the alteration effect is ambiguous and could possibly be explained by leaching of the gap/grain-boundary inventory. If the model is found to be valid, a better quantification of the effects of temperature and moisture on the alteration rate is needed.

11.2.3 Geochemistry

- Parameter distributions should be refined as additional information becomes available. The applicability of the "minimum K_d" approach in different scenarios should be examined. For example, were calculations desired for a period longer than 10,000 years, the exact value of K_d can possibly be more important.

- Retardation information is needed for all significant radionuclides (Table 6-4), to be sure that the most important ones are included. Currently, there is little sorption information for some elements with significant inventories (e.g., nickel and zirconium). Little information may be needed if the solubility is known to be low enough to prevent significant source releases, so there is a correlation between sorption data needs and solubility data needs.

- Retardation for transport in fractures should be included if it can be shown to be significant. The enhanced weeps model, discussed below, could test the significance of this issue.

- The effects of colloids—especially of plutonium and americium—must be studied. This requires a source model for formation of colloids and a model for transport of colloids. Because of the large inventory of these elements, even a small fraction that could be transported rapidly because of colloid formation could be important.

- It may be useful to investigate methods for modeling radionuclide transport in addition to the use of K_d values.

11.3 Aqueous flow and transport

11.3.1 Unsaturated flow and transport

- Correlations between the 1-D columns in the composite-porosity calculation should be included. More generally, the effects of spatial correlations need to be studied, using geostatistical techniques.

- Refinement of the weeps model may be useful. The parameter distributions need to be better defined, and some elements of the model (such as the absorption factor) could be quantified using submodels rather than merely sampling from a random distribution. For example, the TSPA weeps model assumes that flow remains in the same fractures or set of fractures. This assumption should be investigated.

- A study of climate change and its effects on percolation flux is needed to determine whether climate change needs to be incorporated directly into the flow models or whether it can be treated adequately by varying the percolation-rate parameter in steady-state calculations, as was done for this study.

- Effects of repository heating on groundwater flow and transport must be investigated. These effects include both redistribution of water during the hot-repository stage and changes in flow and transport parameters (such as fracture and matrix hydraulic conductivity and retardation with temperature).

- Conceptual models which are used as 1-D simulations in the TSPA should be verified with the more complex codes.

11.3.2 Saturated flow and transport

- Coupling of the unsaturated zone and saturated zone can be improved. For example, the composite-porosity columns presently release radionuclides into a generic saturated-zone flow tube; specific saturated-zone flow tubes could be made for each composite-porosity column.

- A better accounting for the uncertainty in saturated-zone travel time (or velocity) is needed. The calculations done for this TSPA used only a single realization of the saturated zone, taken from Czarnecki's regional model. Variations in that model are possible and should be investigated. Furthermore, Czarnecki's model may not be appropriate at all, because it does not actually model the tuff aquifer near Yucca Mountain: the model is a composite of the tuff and carbonate aquifers. A more detailed model for the saturated zone has been proposed by Fridrich et al. (1991) that suggests the possibility of very long travel times through the tuff aquifer. This three-dimensional model of saturated-zone flow should be investigated to elucidate further the interactions between the aquifers and to supply parameters to abstracted models.

- Effects of matrix/fracture coupling in the saturated zone must be investigated. If flow in the tuff aquifer is primarily in a few fracture zones, there may not be time for the matrix and fracture concentrations to equilibrate before the accessible environment is reached. Fracture-water travel times have been estimated to be about 100 to 200 years (DOE, 1986; DOE, 1988), so if the radionuclides were to be transported in fractures with little matrix interaction, the saturated zone could be a negligible barrier to releases of radioactivity to the accessible environment. (Note, however, that Figures 4-36 and 4-41 imply that with the conservative assumptions made in this study the saturated zone was not much of a barrier to releases.)

- Effects on saturated-zone flow due to seismic, tectonic, and volcanic activity should be investigated. The direction and magnitude of regional groundwater flow could change significantly because of such events. These events are likely to be of low probability, but the probability has not been quantified. Changes in the saturated zone are unlikely to affect releases to the accessible environment unless the water-table level were to rise significantly beneath the repository (in worst case, actually inundating the repository). This possibility is considered to be of low probability (Dudley et al., 1989; Carrigan et al., 1991), but there is some controversy (Szymanski, 1987).

11.4 Gaseous flow and transport

- The aqueous and gaseous releases should be calculated together, to avoid the inaccuracy of combining the releases without the proper correlations.

- A better characterization of the gas permeability throughout the unsaturated zone at Yucca Mountain is needed.

- Variations on the permeability contrast between welded and nonwelded tuff should be sampled, so that the uncertainty in that parameter is included.

- Travel-time distributions at additional temperatures should be calculated, so that the "stair steps" in the repository-temperature curve stay closer to the real curve.

- Better characterization of the ^{14}C inventory, its prompt fraction, and its release rate is needed.

- Travel-time distributions should be calculated with a model that couples gas flow and thermal effects so that the cooling during transport can be taken into account. Benjamin Ross and his coworkers have begun developing such a coupled model (Amter et al., 1991). The coupled model would also eliminate the problem of associating an incompatible repository-temperature history with the ^{14}C travel-time distributions.

- Additional work on carbon geochemistry is needed, especially on interactions with the rock.

11.5 Human intrusion

- Further effort should be made to determine the likelihood that commercially attractive natural resources are present at the site. The presence of attractive natural resources would imply that extensive drilling might occur. Since releases were most strongly influenced by the number of holes drilled, resource exploration could increase the likelihood of releases. On the other hand, if no attractive resources are present, the probability that drilling might occur should decrease, thus reducing the importance of human intrusion in the overall CCDF.

- The human-intrusion event tree should be completed to see if there are any scenarios other than drilling that would be of concern.

11.6 Basaltic igneous activity

- The complete event tree for igneous events must be reviewed. Although this analysis showed that direct interactions between an intrusive dike and the repository produce releases below EPA limits, some indirect effects, such as an alteration of the regional groundwater-flow field, could have greater consequences.

- Interactions between magma and waste other than mechanical should be considered. Although direct mechanical transport to the surface appears intuitively to have the potential for highest releases, interactions of hostile magmatic volatiles with the waste may also be important. We have not considered the effects of a sill emplaced in the repository horizon. Neither of these two possible scenarios leads to direct release at the surface. However, they could result in a large number of waste packages being affected underground. This could alter the radionuclide source for aqueous-transport processes.

- Further work should be done to estimate probabilities for igneous activity. Recent work (Valentine et al., 1992) indicates that the probability of occurrence may be increased. In the current interpretation of basaltic igneous activity originating beneath Yucca Mountain, the constraints of the overburden pressure require that any dike injected into rock at the repository horizon continue on to the surface. Field work in surrounding areas indicates that this assumption may not be true and that there may be a number of dikes present in the tuffs underlying Yucca Mountain that are not exposed at the surface. Thus, the numbers derived for the probability of occurrence, which to date have been based on evidence afforded by visible extrusive structures, may change dramatically.

- The interaction depth for wall-rock erosion should be investigated. Although the estimation of interaction volume used in the TSPA probably overestimated the amount of waste available to be entrained, a more accurate estimate of the volume would reduce this uncertainty.

- Another way to reduce the uncertainty concerning the amount of waste mechanically carried to the surface would be to obtain a better understanding of the depth at which vesiculation occurs. If the depth is as shallow as current field observations indicate (Crowe et al., 1983; Valentine et al, 1992), entrainment of any foreign material from depths as great as that of the potential repository could be essentially zero.

11.7 Conclusions

Resolution of the items listed above would greatly improve future total-system performance assessments. Many open issues would be addressed, and subsequent analyses would be enhanced by new models and data. To address the most important items with the rigor commensurate with their potential importance will require a significant effort. To make useful progress on these items, the next cycle of total-system performance assessment analyses will probably need to last 18 to 24 months.

References

Amter, S., N. Lu, and B. Ross, 1991, "Thermally Driven Gas Flow Beneath Yucca Mountain, Nevada," in *Multiphase Transport in Porous Media—1991*, edited by R. R. Eaton, M. Kaviany, M. P. Sharma, K. Vafai, and K. S. Udell, American Society of Mechanical Engineers, New York, NY, pp. 17-23. (NNA.920428.0026)

Anderson, M. P., 1979, "Using Models to Simulate the Movement of Contaminants Through Groundwater Flow Systems," in *CRC Critical Reviews in Environmental Control*, CRC Press, Boca Raton, FL, pp. 97-156. (NNA.920505.0056)

Apostolakis, G., R. L. Bras, L. L. Price, J. Valdes, K. K. Wahi, 1991, "Techniques for Determining Probabilities of Events and Processes Affecting the Performance of Geologic Repositories: Volume II—Suggested Approaches," U.S. Nuclear Regulatory Commission, NUREG/CR-3964, Washington, DC. (NNA.920630.0037)

Apted, M. J., W. J. O'Connell, K. H. Lee, A. T. MacIntyre, T.-S. Ueng, W. W.-L. Lee, and T. H. Pigford, 1990, "Preliminary Calculations of Release Rates of Tc-99, I-129, and Np-237 from Spent Fuel in a Potential Repository in Tuff," LBL-31069, Lawrence Berkeley Laboratory, Berkeley, CA. (NNA.900627.0053)

Barnard, R. W., 1992, "A Six-Step Method for Systematic Performance Assessment," in *Proceedings of the 1992 Annual Meeting*, American Nuclear Society, La Grange Park, IL, pp. 55-57. (NNA.920629.0031)

Barnard, R. W., and H. A. Dockery, editors., 1991, "Technical Summary of the Performance Assessment Calculational Exercises for 1990 (PACE-90), Vol. 1: 'Nominal Configuration' Hydrogeologic Parameters and Calculational Results," *SAND90-2726*, Sandia National Laboratories, Albuquerque, NM. (NNA.910523.0001)

Barr, G. E., R. W. Barnard, H. A. Dockery, E. Dunn, and A. T. MacIntyre, 1991, "Scenario Evolution: Interaction Between Event Tree Construction and Numerical Analyses," in *High Level Radioactive Waste Management: Proceedings of the Second Annual International Conference*, American Nuclear Society, La Grange Park, IL, pp. 1480-1486. (NNA.920427.0049)

Bateman, H., 1910, "The Solution of a System of Differential Equations Occurring in the Theory of Radioactive Transformations," *Proc. Cambridge Phil. Soc.*, **15**, pp. 423-427. (NNA.910128.0150)

Bentley, C. B., 1984, "Geohydrologic Data for Test Well USW G-4, Yucca Mountain Area, Nye County, Nevada," *OFR 84-063*, U.S. Geological Survey, Denver, CO. (NNA.870519.0100)

Bentley, C. B., J. H. Robinson, and R. W. Spengler, 1983, "Geohydrologic Data for Test Well USW H-5, Yucca Mountain Area, Nye County, Nevada," *OFR 83-853*, U.S. Geological Survey, Denver, CO. (NNA.870519.0098)

Bertram-Howery, S. G., M. G. Marietta, R. P. Rechard, P. N. Swift, D. R. Anderson, B. L. Baker, J. E. Bean, Jr., W. Beyeler, K. F. Brinster, R. V. Guzowski, J. C. Helton, R. D. McCurley, D. K. Rudeen, J. D. Schreiber, and P. Vaughn, 1990, "Preliminary Comparison with 40 CFR Part 191, Subpart B for the Waste Isolation Pilot Plant, December 1990," *SAND90-2347*, Sandia National Laboratories, Albuquerque, NM. (NNA.910429.0147)

Bruce, P. M., and H. E. Huppert, 1989, "Thermal Control of Basaltic Fissure Eruptions," *Nature*, **342**, pp. 665-667. (NNA.920505.0058)

Buscheck, T. A., and J. J. Nitao, 1988, "Preliminary Scoping Calculations of Hydrothermal Flow in Variably Saturated, Fractured, Welded Tuff During the Engineered Barrier Design Test at the Yucca Mountain Exploratory Shaft Test Site," *UCID-21571*, Lawrence Livermore National Laboratory, Livermore, CA. (NNA.890224.0009)

Byers, F. M., Jr., W. J. Carr, P. P. Orkild, W. D. Quinlan, and K. A. Sargent, 1976, "Volcanic Suites and Related Cauldrons of Timber Mountain-Oasis Valley Caldera Complex of Southern Nevada," USGS Prof. Paper 919, U.S. Geological Survey, Denver, CO. (NNA.870406.0239)

Campbell, G. S., 1985, *Soil Physics with Basic: Transport Models for Soil-Plant Systems*, Elsevier Press, New York, 150p. (NNA.890906.0198)

Carlos, B. A., 1985, "Minerals in Fractures of the Unsaturated Zone from Drill Core USW G-4, Yucca Mountain, Nye County, Nevada," *LA-10415-MS*, Los Alamos National Laboratory, Los Alamos, NM. (HQS.880517.1112)

Carr, W. J., 1974, "Summary of Tectonic and Structural Evidence for Stress Orientations at the Nevada Test Site," *OFR 74-176*, U.S. Geological Survey, Denver, CO. (NNA.870406.0240)

Carrigan, C. R., G. C. P. King, G. E. Barr, and N. E. Bixler, 1991, "Potential for Water-Table Excursions Induced by Seismic Events at Yucca Mountain, Nevada," *Geology*, **19**, pp. 1157-1160. (NNA.920427.0050)

Carrigan, C. R., and J. Eichelberger, 1990, "Zoning of Magmas by Viscosity in Volcanic Conduits," *Nature*, **343**, pp. 248-251. (NNA.920505.0059)

Carsel, R. F., and R. S. Parrish, 1988, "Developing Joint Probability Distributions of Soil Water Retention Characteristics," *Water Resources Research*, **24** (5), pp. 755-769. (NNA.910128.0146)

Castor, S. B., S. C. Feldman, and J. V. Tingley, 1989, "Mineral Evaluation of the Yucca Mountain Addition, Nye County, Nevada," prepared for Science Applications International Corp., Las Vegas, NV by Nevada Bureau of Mines and Geology, Reno, NV, also published as Nevada Bureau of Mines and Geology OFR 90-4. (NNA.920131.0227)

Chesnut, D. A., 1992, "Characterizing the Altered Zone at Yucca Mountain: The Beginning of a Testing Strategy," in *High Level Radioactive Waste Management: Proceedings of the Third Annual International Conference,* American Nuclear Society, La Grange Park, IL, pp. 1026-1039. (NNA.920505.0062)

Codell, R. B., and W. M. Murphy, 1992, "Geochemical Model for ^{14}C Transport in Unsaturated Rock," in *High Level Radioactive Waste Management: Proceedings of the Third Annual International Conference,* American Nuclear Society, La Grange Park, IL, pp. 1959-1965. (NNA.920505.0063)

Conca, J., 1990, "Diffusion Barrier Transport Properties of Unsaturated Paintbrush Tuff Rubble Backfill," in *Proceedings of the International Topical Meeting on High-Level Radioactive Waste Management,* American Nuclear Society, La Grange Park, IL, pp. 394-401. (NNA.900710.0198)

Crank, J., 1956, *The Mathematics of Diffusion,* Oxford University Press, London, 424p. (NNA.910327.0003)

Crowe, B. M., 1991, "Volcanic Hazard Studies for the Yucca Mountain Site," *Geological Soc. of America Abstracts With Prog., Cordilleran Section,* **23** (5), March 25-27, San Francisco, CA. (NNA.920609.0027)

Crowe, B. M., R. Amos, F. Perry, S. Self, and D. Vaniman, 1982, "Aspects of Possible Magmatic Disruption of a High-Level Waste Repository in Southern Nevada," *LA-9326-MS,* Los Alamos National Laboratory, Los Alamos, NM. (SRX.830418.0062)

Crowe, B. M., S. Self, D. Vaniman, R. Amos, and F. V. Perry, 1983, "Aspects of Potential Magmatic Disruption of a High-Level Radioactive Waste Repository in Southern Nevada," *J. Geol.,* **91**, pp. 259-276. (NNA.870407.0154)

Crowe, B. M., R. Picard, G. A. Valentine, F. V. Perry, 1992, "Recurrence Models of Volcanic Events: Applications to Volcanic Risk Assessment," in *High Level Radioactive Waste Management: Proceedings of the Third Annual International Conference,* American Nuclear Society, La Grange Park, IL, pp. 2344-2355. (NNA.920505.0067)

Czarnecki, J. B., 1985, "Simulated Effects of Increased Recharge on the Ground-Water Flow System of Yucca Mountain and Vicinity, Nevada-California," *USGS/WRI-84-4344,* U.S. Geological Survey, Denver, CO. (NNA.870407.0008)

Czarnecki, J. B., and R. K. Waddell, 1984, "Finite-Element Simulation of Ground-Water Flow in the Vicinity of Yucca Mountain, Nevada-California," *USGS/WRI-84-4349*, U.S. Geological Survey, Denver, CO. (NNA.870407.0173)

Daniels, W. R., K. Wolfsburg, R. S. Rundberg, A. E. Ogard, J. F. Kerrisk, C. J. Duffy, T. W. Newton, J. L. Thompson, B. P. Bayhurst, D. L. Bish, J. D. Blacic, B. M. Crowe, B. R. Erdal, J. F. Griffith, S. D. Knight, F. O. Lawrence, V. L. Rundberg, M. L. Skyes, G. M. Thompson, B. J. Travis, E. N. Treher, R. J. Vidale, G. R. Walter, R. D. Aguilar, M. R. Cisneros, S. Maestas, P. Q. Oliver, N. A. Raybold, and P. L. Wanek, 1982, "Summary Report on the Geochemistry of Yucca Mountain and Environs," *LA-9328-MS*, Los Alamos National Laboratory, Los Alamos, NM. (NNA.870406.0180)

de Marsily, G., 1986, *Quantitative Hydrogeology: Groundwater Hydrology for Engineers*, Academic Press, Orlando, FL, 459 p. (NNA.910207.0116)

Department of Energy (DOE), 1984, "Nuclear Waste Policy Act of 1982; General Guidelines for the Recommendation of Sites for the Nuclear Waste Repositories; Final Siting Guidelines," 10 CFR Part 960, U. S. Department of Energy, Washington, DC. (NNA.870506.0140)

Department of Energy (DOE), 1986, "Nuclear Waste Policy Act (Section 112) Environmental Assessment, Yucca Mountain Site, Nevada Research and Development Area, Nevada," *DOE/RW-0073*, U. S. Department of Energy, Washington, DC. (NNA.890327.0062-.0064)

Department of Energy (DOE), 1987, "Characteristics of Spent Fuel, High-Level Waste, and Other Radioactive Wastes Which May Require Long-Term Isolation," *DOE/RW-184*, U.S. Department of Energy, Washington, DC. (HQO.880121.0001-.0006)

Department of Energy (DOE), 1988, "Site Characterization Plan, Yucca Mountain Site, Nevada Research and Development Area, Nevada," *DOE/RW-0199*, U.S. Department of Energy, Washington, DC. (HQO.881201.0002)

Dudley, A. L., R. R. Peters, J. H. Gauthier, M. L. Wilson, M. S. Tierney, and E. A. Klavetter, 1988, "Total System Performance Assessment Code (TOSPAC), Volume 1: Physical and Mathematical Bases," *SAND85-0002*, Sandia National Laboratories, Albuquerque, NM. (NNA.881202.0211).

Dudley, W. W., Jr., G. E. Barr, D. A. Chesnut, and C. J. Fridrich, editors, 1989, "Review of a Conceptual Model and Evidence for Tectonic Control of the Ground-Water System in the Vicinity of Yucca Mountain, Nevada," U.S. Department of Energy, Yucca Mountain Project Office, Las Vegas, NV. (NNA.890530.0132)

Dykhuizen, R. C., and R. W. Barnard, 1992, "Groundwater Flow Code Verification 'Benchmarking' Activity (COVE-2A): Analysis of Participants' Work," *SAND89-2558*, Sandia National Laboratories, Albuquerque, NM. (NNA.920130.0016)

Eaton, R. R., and P. L. Hopkins, 1992, "LLUVIA-II: A Program for Two-Dimensional, Transient Flow Through Partially Saturated Porous Media," *SAND91-2416*, Sandia National Laboratories, Albuquerque, NM. (NNA.920630.0034)

Eley, D. L., 1990, "Completion of IGIS Job Number 345, Sandia National Laboratories, Albuquerque, NM. (NNA.910131.0085)

Ellis, W. L., and L. E. Magner, 1980, "Compilation of Results of Three-Dimensional Stress Determinations made in Rainier and Aqueduct Mesas, Nevada Test Site, Nevada," *OFR 80-1098*, U.S. Geological Survey, Denver, CO. (HQS.880517.1186)

Environmental Protection Agency (EPA), 1985, "Environmental Radiation Protection Standards for Management and Disposal of Spent Nuclear Fuel, High-Level and Transuranic Radioactive Wastes," *Code of Federal Regulations*, Title 40, Part 191. (HQS.880517.3264).

Eslinger, P. W., and B. Sagar, 1988, "EPASTAT: A Computer Model for Estimating Releases at the Accessible Environment Boundary of a High-Level Nuclear Waste Repository—Mathematical Model and Numerical Methods," *SD-BWI-TA-022*, Rev. 1, Westinghouse Hanford Co., Richland, WA. (NNA.920521.0050)

Fewell, M. E., S. R. Sobolik, and J. H. Gauthier, 1992, "Estimation of the Limitations for Surficial Water Addition above a Potential High Level Radioactive Waste Repository of Yucca Mountain, Nevada," *SAND91-0790*, Sandia National Laboratories, Albuquerque, NM. (NNA.911217.0002)

Flint, A., 1989, "Characterization of Infiltration," in transcript of public meeting of Hydrology & Geochemistry Panel of the U.S. Nuclear Waste Technical Review Board, Denver, Colorado, December 11-12, 1989, U. S. Nuclear Waste Technical Review Board, Arlington, VA. (NNA.920218.0021)

Freeze, R. A., and J. A. Cherry, 1979, *Groundwater*, Prentice-Hall, Inc., Englewood Cliffs, NJ, 604 p. (NNA.870406.0444)

Fridrich, C. J., D. C. Dobson, and W. W. Dudley, Jr., 1991, "A Geologic Hypothesis for the Large Hydraulic Gradient under Yucca Mountain, Nevada," *EOS*, **72** (17) Supplement, American Geophysical Union, Washington, DC, p. 121. (NNA.910919.0013)

Gainer, G., P. G. Kaplan, A. S. Schenker, and H. A. Dockery, 1992, "Model Domains and Hydrogeologic Data Base To Support Early Site Suitability and Total-System Performance Assessment Models," *SAND92-0799*, Sandia National Laboratories, Albuquerque, NM. (NNA.920630.0035)

Gallegos, D. P., S. G. Thoma, and D. M. Smith, 1992, "Impact of Fracture Coatings on the Transfer of Water Across Fracture Faces in Unsaturated Media," in *High Level Radioactive Waste Management: Proceedings of the Third Annual International Conference,* American Nuclear Society, La Grange Park, IL, pp. 738-745. (NNA.920505.0060)

Gauthier, J. H., M. L. Wilson, and F. C. Lauffer, 1992a, "Estimating the Consequences of Significant Fracture Flow at Yucca Mountain," in *High Level Radioactive Waste Management: Proceedings of the Third Annual International Conference,* American Nuclear Society, La Grange Park, IL, pp. 891-898. (NNA.920505.0068)

Gauthier, J. H., M. L. Wilson, R. R. Peters, A. L. Dudley, and L. H. Skinner, 1992b, "Total System Performance Assessment Code (TOSPAC) Volume 2: User's Guide," *SAND85-0004*, Sandia National Laboratories, Albuquerque, NM. (NNA.920623.0013)

Harr, M. E., 1977, *Mechanics of Particulate Media: A Probabilistic Approach,* McGraw-Hill Book Co., New York, NY, pp. 495-496. (NNA.900727.0310)

Harr, M. E., 1987, *Reliability-Based Design in Civil Engineering,* McGraw-Hill Book Co., New York, NY, 301 p. (NNA.890713.0149)

Ho, C.-H, 1991, "Time Trend Analysis of Basaltic Volcanism for the Yucca Mountain Site," *Jour. Volcanol. Geotherm. Res.,* **46,** pp. 61-72. (NNA. 920610.0025)

Hopkins, P. L., R. R. Eaton, and N. E. Bixler, 1991, "NORIA-SP—A Finite Element Computer Program for Analyzing Liquid Water Transport in Porous Media," *SAND90-2542*, Sandia National Laboratories, Albuquerque, NM. (NNA.911202.0031)

Huyakorn, P. S., H. O. White Jr., and S. Panday, 1991, "STAFF2D, Version 3.2, A Two-Dimensional Finite-Element Code for Simulating Fluid Flow and Transport of Radionuclides in Fractured Porous Media with Water Table Boundary Conditions," HydroGeoLogic, Inc., Herndon, VA. (NNA.920630.0036)

Iman, R. L., and M. J. Shortencarrier, 1984, "A FORTRAN-77 Program and User's Guide for the Generation of Latin Hypercube and Random Samples for Use with Computer Models," *SAND83-2365, NUREG/CR-3624*, Sandia National Laboratories, Albuquerque, NM. (NNA.900117.0157)

Jaynes, E. T., 1957, "Information Theory and Statistical Mechanics II" *Phys. Rev.*, **108**, pp. 171-190. (NNA.910306.0127)

Johnson, G. L., and D. N. Montan, 1990, "Thermal Calculations Pertaining to a Proposed Yucca Mountain Nuclear Waste Repository," *UCRL-ID-103534*, Lawrence Livermore National Laboratory, Livermore, CA. (NNA.900925.0060)

Kaplan, P. G., 1991, "A Formalism to Generate Probability Distributions for Performance Assessment Modeling," in *High Level Radioactive Waste Management: Proceedings of the Second Annual International Conference,* American Nuclear Society, La Grange Park, IL, pp. 1487-1490. (NNA.910819.0005)

Kaplan, P. G., and L. Yarrington, 1989, "Modeling the Uncertainties in the Parameter Values of a Layered, Variably Saturated Column of Volcanic Tuff Using the Beta Probability Distribution," in *Solving Ground Water Problems with Models*, National Well Water Association, Dublin, OH. (NNA.890324.0118)

Klavetter, E. A., and R. R. Peters, 1986, "Fluid Flow in a Fractured Rock Mass," *SAND85-0855*, Sandia National Laboratories, Albuquerque, NM. (NNA.870721.0004)

Lappin, A. R., R. L. Hunter, D. P. Garber, and P. B. Davies, editors, 1989, "Systems Analysis, Long-Term Radionuclide Transport, and Dose Assessments, Waste Isolation Pilot Plant (WIPP), Southeastern New Mexico; March 1989," *SAND89-0462*, Sandia National Laboratories, Albuquerque, NM. (NNA.920427.0052)

Light, W. B., E. D. Zwahlen, T. H. Pigford, P. L. Chambré, and W. W.-L. Lee, 1990, "C-14 Release and Transport from a Nuclear Waste Repository in an Unsaturated Medium," *LBL-28923*, Lawrence Berkeley Laboratory, Berkeley, CA. (NNA.900709.0481)

Lu, N., S. Amter, and B. Ross, 1991, "Effect of a Low-Permeability Layer on Calculated Gas Flow at Yucca Mountain," in *High Level Radioactive Waste Management: Proceedings of the Second Annual International Conference,* American Nuclear Society, La Grange Park, IL, pp. 853-860. (NNA.910819.0010)

MacDougall, H. J., L. W. Scully, and J. R. Tillerson, 1987, "Site Characterization Plan Conceptual Design Report," *SAND84-2641*, Sandia National Laboratories, Albuquerque, NM. (NN1.880902.0014-.0019)

MacLean, S. C., D. G. Coles, and H. C. Weed, 1978, "The Measurement of Sorption Ratios for Selected Radionuclides on Various Geologic Media," *UCID-17928*, Lawrence Livermore National Laboratory, Livermore, CA. (NNA.900904.0131)

McGraw, M. A., K. W. Burdick, and P. W. Eslinger, 1991, "One-Dimensional Human Intrusion Analysis of the Paleozoic Aquifer, as Part of the Site Suitability Effort at Yucca Mountain, Nevada," *PNL-7774*, Pacific Northwest Laboratory, Richland, WA. (NNA.920505.0055)

McGuire, R. K., D. B. Bullen, N. Cook, K. J. Coppersmith, J. Kemeny, A. Long, F. J. Pearson, Jr., F. Schwartz, M. Sheridan, and R. R. Youngs, 1990, "Demonstration of a Risk-Based Approach to High-Level Waste Repository Evaluation," *EPRI NP-7057*, Electric Power Research Institute, Palo Alto, CA. (NNA.910813.0004)

Meijer, A., 1990, "Yucca Mountain Project Far-Field Sorption Studies and Data Needs," *LA-11671-MS*, Los Alamos National Laboratory, Los Alamos, NM. (NNA.920131.0363)

Meijer, A., 1991, "A Strategy for the Derivation and Use of Sorption Coefficients in Performance Assessment Calculations for the Yucca Mountain Site," in *Proceedings of Workshop on Radionuclide Adsorption* held in Los Alamos, NM, September 11-12, 1990," *LA-UR-91-3747*, Los Alamos National Laboratory, Los Alamos, NM. (NNA.920610.0024)

Miller I., R. Kossik, and M. Cunnane, 1992, "A New Methodology for Repository Site Suitability Evaluation," in *High Level Radioactive Waste Management: Proceedings of the Third Annual International Conference,* American Nuclear Society, La Grange Park, IL, pp. 494-501. (NNA.920505.0064)

Montazer, P., and W. E. Wilson, 1984, "Conceptual Hydrologic Model of Flow in the Unsaturated Zone, Yucca Mountain, Nevada," *USGS/WRIR 84-4345*, U. S. Geological Survey, Lakewood, CO. (NNA.890327.0051)

Montazer, P., E. P. Weeks, F. Thamir, S. N. Yard, and P. B. Hofrichter, 1986, "Monitoring the Vadose Zone in Fractured Tuff, Yucca Mountain, Nevada," in *Proceedings of the NWWA Conference on Characterization and Monitoring of the Vadose (Unsaturated) Zone*, National Water Well Association, Worthington, OH, pp. 439-469. (HQS.880517.1797)

Napier, B. A., R. A. Peloquin, D. L. Strenge, and J. V. Ramsdell, 1988, "Hanford Environmental Dosimetry Upgrade Project. GENII—The Hanford Environmental Radiation Dosimetry Software System," Volume 1: Conceptual Representation, Volume 2: Users' Manual, Volume 3: Code Maintenance Manual, *PNL-6584* Vols. 1, 2, and 3, Pacific Northwest Laboratory, Richland, Washington. (NNA.920626.0034) (NNA.920626.0036) (NNA.920626.0041)

Norris, A. E., 1990, "The Use of Chlorine Iostope Measurements to Trace Water Movements at Yucca Mountain," in *Proceedings of the Topical Meeting on Nuclear Waste Isolation in the Unsaturated Zone, Focus '89,* American Nuclear Society, La Grange Park, IL, pp. 400-405. (NNA.920218.0022)

Nuclear Regulatory Commission (NRC), 1983, "Disposal of High-Level Radioactive Wastes in Geologic Repositories," *Code of Federal Regulations*, Title 10, Part 60, pp. 28194-28220. (NNA.900727.0307)

Nuclear Regulatory Commission (NRC), 1989, "NRC Staff Site Characterization Analysis of the Department of Energy's Site Characterization Plan, Yucca Mountain Site, Nevada," *NUREG-1347*, U. S. Nuclear Regulatory Commission, Washington, DC. (NNA.891020.0161)

O'Connell, W. J., 1990, "Status of Integrated Performance Assessment of the Waste Packages and Engineering Barrier System," *UCRL-10214*, Lawrence Livermore National Laboratory, Livermore, CA. (NNA.900607.0215)

O'Connell, W. J., 1992, "Simplified Source Term Model for Total System Performance Assessment," UCRL-110511, Lawrence Livermore National Laboratory, Livermore, CA. (NNA.920505.0309)

Organisation for Economic Co-operation and Development (OECD), 1992, *Safety Assessment of Radioactive Waste Repositories, Systematic Approaches to Scenario Development*, Nuclear Energy Agency, Paris, France, 76 p. (NNA.920610.0027)

Park, U. S., and C. G. Pflum, 1990, "Requirements for Controlling a Repository's Releases of Carbon-14 Dioxide; the High Costs and Negligible Benefits," in *Proceedings of the International Topical Meeting on High Level Radioactive Waste Management*, American Nuclear Society, La Grange Park, IL, pp. 1158-1164. (NNA.900615.0185)

Pescatore, C., 1990, "^{14}C Release from Failed Spent Fuel Containers," in *Proceedings of the International Topical Meeting on High Level Radioactive Waste Management*, American Nuclear Society, La Grange Park, IL, pp. 426-429. (NNA.910410.0182)

Peters, R. R., and E. A. Klavetter, 1988, "A Continuum Model for Water Movement in an Unsaturated Fractured Rock Mass," *Water Resources Research*, **24**, pp. 416-430. (NNA.890523.0139)

Peters, R. R., E. A. Klavetter, I. J. Hall, S. C. Blair, P. R. Heller, and G. W. Gee, 1984, "Fracture and Matrix Hydrologic Characteristics of Tuffaceous Materials From Yucca Mountain, Nye County, Nevada," *SAND84-1471*, Sandia National Laboratories, Albuquerque, NM. (NNA.870407.0036)

Prindle, R. W., and P. L. Hopkins, 1990, "On Conditions and Parameters Important to Model Sensitivity for Unsaturated Flow Through Layered, Fractured Tuff: Results of Analyses for HYDROCOIN Level 3 Case 2," *SAND89-0652*, Sandia National Laboratories Albuquerque, NM. (NNA.900523.0211)

Pruess, K., 1987, "TOUGH Users' Guide," *LBL-20700/SAND86-7104*, Lawrence Berkeley Laboratory, University of California, Berkeley, CA. (NNA.890315.0010)

Rasmussen, T. C., D. D. Evans, P. J. Sheets, and J. H. Blanford, 1990, "Unsaturated Fractured Rock Characterization Methods and Data Sets at the Apache Leap Tuff Site," *NUREG/CR-5596*, U.S. Nuclear Regulatory Commission, Washington, DC. (NNA.910306.0155)

Rautman, C. A., B. C. Whittet, and D. L. South, 1987, "Definitions of Reference Boundaries for the Proposed Geologic Repository at Yucca Mountain, Nevada," *SAND86-2157*, Sandia National Laboratories, Albuquerque, NM. (NNA.890123.0066)

Rautman, C. A., and A. Flint, 1992, "Deterministic Geologic Processes and Stochastic Modeling," in *High Level Radioactive Waste Management: Proceedings of the Third Annual International Conference,* Las Vegas, NV, American Nuclear Society, La Grange Park, IL, pp. 1617-1624. (NNA.920505.0069)

Rechard, R. P., H. Iuzzolino, and J. S. Sandha, 1990, "Data Used in Preliminary Performance Assessment of the Waste Isolation Pilot Plant (1990)," *SAND89-2408*, Sandia National Laboratories, Albuquerque, NM. (NNA.920428.0028)

Roddy, J. W., H. C. Claiborne, R. C. Ashline, P. J. Johnson, and B. T. Rhyne, 1986, "Physical and Decay Characteristics of Commercial LWR Spent Fuel," *ORNL/TM-9591/V1&R1*, Oak Ridge National Laboratory, Oak Ridge, TN. (NNA.891016.0145)

Ross, B., 1990, "Quasi-Linear Analysis of Water Flow in the Unsaturated Zone at Yucca Mountain, Nevada, USA," in *Water Resources in Mountainous Regions*, Memoires of the 22nd Congress of the International Association of Hydrogeologists, edited by A. Parriaux, International Association of Hydrogeologists, Lausanne, Switzerland, pp. 166-173. (NNA.920207.0007)

Ross, B., S. Amter, and N. Lu, 1992, "Numerical Studies of Rock-Gas Flow in Yucca Mountain," *SAND91-7034*, Sandia National Laboratories, Albuquerque, NM. (NNA.920205.0062)

Russell, J. D., E. Paterson, A. R. Fraser, and V. C. Farmer, 1975, "Adsorption of Carbon Dioxide on Goethite (α-FeOOH) Surfaces, and its Implications for Anion Adsorption," *Journal of the Chemical Society, Faraday Transactions I*, **71**, pp. 1623-1630. (NNA.920505.0065)

Schulthess, C. P., and J. F. McCarthy, 1990, "Competitive Adsorption of Aqueous Carbonic and Acetic Acids by an Aluminum Oxide," *Soil Science Society of America Journal*, **54**, pp. 688-694. (NNA.920505.0057)

Shannon, C. E., 1948, "A Mathematical Theory of Communication," *Bell Sys. Tech. J.*, **27**, pp. 379-423. (NNA.910306.0126)

Shaw, R., J. C. Stepp, R. F. Williams, and R. K. McGuire, 1992, "Performance Assessment for a High-Level Waste Repository at Yucca Mountain," in *High Level Radioactive Waste Management: Proceedings of the Third Annual International Conference,* Las Vegas, American Nuclear Society, La Grange Park, IL, pp. 869-873. (NNA.920505.0066)

Sinnock, S., Y. T. Lin, and J. P. Brannen, 1984, "Preliminary Bounds on the Postclosure Performance of the Yucca Mountain Repository Site, Southern Nevada," *SAND84-1492,* Sandia National Laboratories, Albuquerque, NM. (NNA.870519.0076)

Spengler, R. W., and M. P. Chornack, 1984, "Stratigraphic and Structural Characteristics of Volcanic Rocks in Core Hole USW G-4, Yucca Mountain, Nye County, Nevada," *OFR 84-789,* U.S. Geological Survey, Denver, CO. (NNA.870519.0105)

Spengler, R. W., D. C. Muller, and R. B. Livermore, 1979, "Preliminary Report on the Geology and Geophysics of Drill Hole Ue25a-1, Yucca Mountain, Nevada Test Site," *OFR 79-1244,* U.S. Geological Survey, Denver, CO. (HQS.880517.1491)

Stock, J. M., J. H. Healy, S. H. Hickman, and M. D. Zoback, 1985, "Hydraulic Fracturing Stress Measurements at Yucca Mountain, Nevada, and Relationship to the Regional Stress Field," *Journal of Geophysical Research,* **90**(B10), pp. 8691-8706. (HQS.880517.1509)

Syzmanski, J., 1987, "Conceptual Considerations of the Death Valley Groundwater System with Special Emphasis on the Adequacy of this System to Accommodate the High-Level Nuclear Waste Repository," U.S. Department of Energy, Nevada Operations Office, Waste Management Project Office, Las Vegas, NV, 321p. (NNA.871204.0065)

Thomas, K. W., 1987, "Summary of Sorption Measurements Performed with Yucca Mountain, Nevada, Tuff Samples and Water from Well J-13," *LA-10960-MS,* Los Alamos National Laboratory, Los Alamos, NM. (NNA.890602.0026)

Thordarson, W., 1983, "Geohydrologic Data and Test Results from Well J-13, Nevada Test Site, Nye County, Nevada," *USGS/WRI-83-4171,* U.S. Geological Survey, Denver, CO. (HQS.880517.1849)

Thorstenson, D. C., 1991, "The Composition and CO_2 Carbon Isotope Signature of Gases from Borehole USW UZ-6, Yucca Mountain, Nevada," presented at Workshop on Unsaturated Flow and Transport, January 7-10, 1991, Tucson, AZ. (NNA.911004.0004)

Tierney, M. S., 1991, "Combining Scenarios in a Calculation of the Overall Probability Distribution of Cumulative Releases of Radioactivity From the Waste Isolation Pilot Plant, Southeastern New Mexico," *SAND90-0838*, Sandia National Laboratories, Albuquerque, NM. (NNA.920427.0053)

Tipton, G. D., 1991, "Site and Engineering Properties Database, Product No. SEP0102," Sandia National Laboratories, Albuquerque, NM. (NNA.911029.0109)

Travis, B. J., S. W. Hodson, H. E. Nuttal, T. L. Cook, and R. S. Rundberg, 1984, "Preliminary Estimates of Water Flow and Radionuclide Transport in Yucca Mountain," *LA-UR-84-40* (Rev.), Los Alamos National Laboratory, Los Alamos, NM. (HQS.880517.1909)

Tsang, Y. W., and K. Pruess, 1987, "A Study of Thermally Induced Convection Near a High-Level Nuclear Waste Repository in Partially Saturated Fractured Tuff," *Water Resources Research*, **23**, pp. 1958-1966. (NNA.890522.0273)

Ueng, T.-S., and W. J. O'Connell, 1992, "Diffusive Barrier Simplified Analysis—Design and Sensitivity Applications," in *Proceedings of the Topical Meeting on Nuclear Waste Packaging, Focus '91*, American Nuclear Society, La Grange Park, IL, pp. 277-284. (NNA.920629.0128)

Valentine, G. A., B. M. Crowe, F. V. Perry, 1992, "Physical Processes and Effects of Magmatism in the Yucca Mountain Region," in *High Level Radioactive Waste Management: Proceedings of the Third Annual International Conference,* Las Vegas NV, pp. 2014-2024. (NNA.920505.0070)

van Genuchten, M. Th., 1980, "A Closed-Form Equation for Predicting the Hydraulic Conductivity of Unsaturated Soils," *Soil Science Society of America Journal*, **44**, pp. 892-898. (NNA.890522.0287)

Van Konynenburg, R. A., 1989, "Review of Gaseous Isotopes," in transcript of public meeting of Hydrology & Geochemistry Panel of the U.S. Nuclear Waste Technical Review Board, Denver, Colorado, December 11-12, 1989, U.S. Nuclear Waste Technical Review Board, Arlington, VA, pp. 194-205. (NNA.910405.0049)

Van Konynenburg, R. A., 1991, "Gaseous Release of Carbon-14: Why the High Level Waste Regulations Should be Changed," in *High Level Radioactive Waste Management: Proceedings of the Second Annual International Conference,* American Nuclear Society, La Grange Park, IL, pp. 313-319. (NNA.910410.0187)

Van Konynenburg, R. A., C. F. Smith, H. W. Culham, and C. H. Otto, Jr., 1985, "Behavior of Carbon-14 in Waste Packages for Spent Fuel in a Repository in Tuff," in *Scientific Basis for Nuclear Waste Management VIII*, edited by C. M. Jantzen, J. A. Stone, and R. C. Ewing, Materials Research Society, Pittsburgh, PA, pp. 405-412. (NNA.901320.0150)

Van Konynenburg, R. A., C. F. Smith, H. W. Culham, and H. D. Smith, 1987, "Carbon-14 in Waste Packages for Spent Fuel in a Tuff Repository," in *Scientific Basis for Nuclear Waste Management X,* edited by J. K. Bates and W. B. Seefeld, Materials Research Society, Pittsburgh, PA, pp. 185-196. (HQS.880517.2562)

Waddell, R. K., 1982, "Two-Dimensional, Steady-State Model of Ground-Water Flow, Nevada Test Site and Vicinity, Nevada-California," *USGS/WRI-82-4085,* U.S. Geological Survey, Denver, CO. (NNA.870518.0055)

Ward, J. C., 1964, "Turbulent Flow in Porous Media," *Journal of the Hydraulics Division, Proceedings of the American Society of Civil Engineers,* **90** (HY5), pp. 1-12. (NNA.910923.0005)

Whitfield, M. S., W. Thordarson, and D. P. Hammermeister, 1990, "Drilling and Geohydrologic Data for Test Hole USW UZ-1, Yucca Mountain, Nye County, Nevada," *OFR 90-354,* U.S. Geological Survey, Denver CO. (NNA.900622.0450)

Wilson, C. N., 1987, "Results From Cycles 1 and 2 of NNWSI Series 2 Spent Fuel Dissolutions Tests," *HEDL-TME 85-22,* Hanford Engineering Development Laboratory, Richland, WA. (HQS.880517.2581)

Wilson, C. N., 1990a, "Results From NNWSI Series 2 Bare Fuel Dissolution Tests," *PNL-7169,* Pacific Northwest Laboratory, Richland, WA. (NNA.900814.0048)

Wilson, C. N., 1990b, "Results From NNWSI Series 3 Spent Fuel Dissolution Tests," *PNL-7170,* Pacific Northwest Laboratory, Richland, WA. (NNA.900329.0142)

Wilson, C. N., and C. J. Bruton, 1989, "Studies on Spent Fuel Dissolution Behavior Under Yucca Mountain Repository Conditions," *PNL-SA-16832,* Pacific Northwest Laboratory, Richland, WA. (NNA.890905.0053)

Wilson, M. L., 1991, "A Simplified Radionuclide Source Term for Total-System Performance Assessment," *SAND91-0155,* Sandia National Laboratories, Albuquerque, NM. (NNA.911118.0079)

Wilson, M. L., 1992, "Comparison of Two Conceptual Models of Flow Using the TSA," in *High Level Radioactive Waste Management: Proceedings of the Third Annual International Conference,* American Nuclear Society, La Grange Park, IL, pp. 882-890. (NNA.920505.0061)

Wilson, M. L., F. C. Lauffer, J. C. Cummings, and N. B. Zieman, 1991, "Total-System Analyzer for Performance Assessment of Yucca Mountain," in *High Level Radioactive Waste Management: Proceedings of the Second Annual International Conference,* American Nuclear Society, La Grange Park, IL, pp. 1734-1743. (NNA.920427.0051)

Younker, J., W. Andrews, G. Fasano, C. Herrington, S. Mattson, R. Murray, L. Ballou, M. Revelli, A. DuCharme, L. Shephard, W. Dudley, D. Hoxie, R. Herbst, E. Patera, B. Judd, J. Docka, and L. Rickertsen, 1992, "Report of Early Site Suitability Evaluation of the Potential Repository Site at Yucca Mountain, Nevada," *SAIC-91/8000*, Science Applications International Corporation, Las Vegas, NV. (NNA.910708.0111)

Zimmerman, R. M., and W. C. Vollendorf, 1982, "Geotechnical Field Measurements, G-Tunnel, Nevada Test Site," *SAND81-1971*, Sandia National Laboratories, Albuquerque, NM. (HQS.880517.1720)

Zimmerman, R. M., R. A. Bellman Jr., K. L. Mann, D. P. Zerga, M. Fowler, and R. L. Johnson, 1988, "G-Tunnel Welded Tuff Mining Experiment Evaluations," *SAND87-1433*, Sandia National Laboratories, Albuquerque, NM. (HQS.880517.3224)

Bibliography

The following documents are not cited in this report, but may be of interest to readers wishing further information. The documents are all in draft stage at the time of printing of this report.

Eslinger, P. W., L. A. Doremus, D. W. Engel, T. B. Miley, M. T. Murphy, W. E. Nichols, M. D. White, in preparation, "Preliminary Total-Systems Analysis of a Potential High-Level Nuclear Waste Repository at Yucca Mountain," *PNL-XXXX*, Pacific Northwest Laboratory, Richland, Washington.

Eslinger, P. W., T. B. Miley, and D. W. Engel, in review, "SUMO—System Performance Assessment for a High-Level Nuclear Waste Repository: Mathematical Models," *PNL-7581*, Pacific Northwest Laboratory, Richland, Washington.

Wang, J.S.Y., and T. N. Narasimhan, in review, "Processes, Mechanisms, and Parameters Governing Partially Saturated Flow in Soil and Rock Media," *SAND88-7054*, Sandia National Laboratories, Albuquerque, NM.

Appendix I
Calculation of Probabilities for Intersecting Waste Packages

Sandia National Laboratories

Albuquerque, New Mexico 87185

date: February 20, 1991

to: R.W. Barnard (6313) and H.A. Dockery (6312)

from: D.P. Gallegos (6416)

subject: Probability of Intersecting a Waste Package Based on Geometric Considerations (Calculations conducted in support of site suitability evaluation)

Introduction

An estimate of the probability of hitting a waste package given certain geometric constraints and assumptions has been derived. These human intrusion scenario calculations are based on and are limited to exploratory borehole drilling at the site. In the calculations presented here, the number of boreholes drilled is assumed to be the maximum that will occur at the Yucca Mountain site over 10,000 years. Both vertical and horizontal emplacement of waste packages has been considered. In an alternative calculation presented here, the number of boreholes drilled is assumed to be the mean number drilled over 10,000 years, and the frequency of drilling is assumed to follow a Poisson distribution. For both cases, the frequency of hitting a waste canister during the drilling process is assumed to follow a binomial distribution. From the binomial distribution, the chances of a given number of hits can be derived. The probability of hitting a waste canister is based on the normal fractional area of the repository covered by waste packages, as seen by a vertical borehole. In doing the calculations, a number of assumptions must be made regarding waste package emplacement, drilling techniques and frequency, and general repository characteristics. Although these assumptions have been identified, because of the nature of the problem, justification cannot be provided for all of them. In a second alternative calculation, the work conducted by Bob Wilems of Rogers and Associates Engineering is summarized.

Discussion of Assumptions

The waste canisters in the repository are assumed to be emplaced either vertically or horizontally. The orientation of any borehole that will be drilled at or near the repository area as part of this human intrusion scenario calculation is assumed to be vertical. Diagonal boreholes entering the underground facility that originate from outside the repository land surface area have not been considered. In the current repository design, the repository follows the dip of the geologic units. The dip of the units is approximately 6 degrees. If the waste packages are emplaced perpendicular to the drift floor, then they will be at about a 6 degree tilt from vertical. This would increase the normal waste package area as viewed from the surface looking vertically downward. However, this slight tilt has not been considered in the calculations because the packages are expected to be emplaced vertically. These assumptions result in an effective waste package area equal to the cross sectional area of the waste canisters. Therefore, the calculations essentially consider only the two-dimensional x-y plane. Therefore, for vertically emplaced canisters, the length of the waste packages does not play a role. Under horizontal emplacement however, the length of the waste packages becomes important. Spacing of waste packages in both cases is expected to be such (5 m between centers [DOE, 1988]) that a single vertical borehole would not intersect two waste canisters simultaneously.

The calculations included herein assume that 20th century rotary drilling technology will continue to be used over the regulatory period (10,000 years), or at least the results of the drilling activity are similar to results from 20th century drilling techniques (i.e., drilling will result in a cylindrical borehole).

As shown in Figure 1, the topography above the repository is quite variable. As a result, some areas on the land surface may provide better locations for drilling machinery than others. If these preferential locations coincided with the underground repository configuration and geometry, then the chances of hitting a waste canister would change accordingly. For instance, if a plateau feature on the surface was chosen as a preferential drill site and this plateau was located directly over an emplacement drift, then the probability of hitting a waste canister would correspondingly increase. However, for these calculations, drilling technology is assumed to be such that the location of a drill rig on the surface can be randomly chosen. Therefore, the configuration of the underground facility will not play a role in determining the probability of hitting a waste package.

Perhaps the most uncertain parameter to consider is the number of boreholes that will be drilled over the repository area over 10,000 years. The Environmental Protection Agency (EPA) in 40 CFR Part 191, Appendix C [EPA, 1985] has provided guidelines for the maximum numbers of boreholes for repositories in the proximity of both sedimentary and non-sedimentary geologic formations. For sedimentary rock, the EPA guideline specifies that the maximum number of boreholes per square kilometer per 10,000 years is 30. For repositories not in the proximity of sedimentary rock, the EPA arbitrarily assumed the drilling rate to be one-tenth (3 boreholes/km^2/10,000 yrs) the rate given for drilling near sedimentary rock. These estimates come from the work conducted by Little [1980] for the EPA, and are based on oil and gas exploration. Apostolakis et al. [1991] give estimates of drilling rates ranging from a single borehole per square kilometer per 10,000 years to thousands of boreholes per square kilometer per 10,000 years. Most of the estimates are, however, less than fifty boreholes/km^2/10,000 years. Their estimates draw from a number of studies and are based oil and gas, water, and gold exploration. Even though it does not have a solid foundation, we will assume, for the time being that the EPA estimate for drilling near non-sedimentary rock is a reasonable estimate for the drilling rate at Yucca Mountain, and this number will be used in the calculations that follow. Based on current drilling rates for oil and gas in igneous rock [Apostolakis et al., 1991], this is probably not a bad estimate. Perhaps the working group tasked with conducting resource evaluations of Yucca Mountain can provide better guidance as to the potential number of boreholes that will be drilled.

The locations of the boreholes are assumed to occur randomly with the location of each new borehole being independent of all others that precede it. This precludes the use of so-called "wildcat" or "Great Basin" style of drilling for resource exploration. In this style of drilling, once a valuable resource has been detected in an exploratory drill hole, several (perhaps hundreds) of additional exploratory boreholes are drilled in the vicinity of the initial hole. Conversely, this assumption also implies that if a borehole hits a waste package, the knowledge of such an event is not passed on to the next drilling activity.

Data and Calculations

The calculations performed to estimate the probability of hitting a waste package given the above assumptions, and the data contained therein, are presented in this section.

The repository area has been calculated by Rautman et al. [1987] to be 5.61×10^6 m^2. This is consistent with the area estimated in the Yucca Mountain Site Characterization Plan (SCP) [DOE, 1988] of 5.75×10^6 m^2 $\pm$ 8.5×10^5 m^2, which is based on an allowable areal power density of 57 kW/acre [DOE, 1988]. The total amount of waste expected to be received by the facility is 70,000 MTHM [DOE, 1988]. This consists of 62,000 MTHM of spent fuel and 8,000 MTHM of West Valley and defense high-level wastes (HLW). Both the reference spent fuel and the HLW waste canisters have a diameter of 0.66 m [DOE, 1988]. The alternative spent fuel canister has a diameter of 0.71 m [DOE, 1988]. The length of both the reference and alternative spent fuel canisters is 4.76 m, and the length of the West Valley and defense HLW package is 3.28 m. However, only a canister with dimensions of the reference canister is considered in the calculations presented here. The average quantity of waste per canister has been given by the PACE90 Working Group 2 to be 2.1 MTHM.[1] Therefore, the total number of waste packages is calculated to be 33,333 (70,000 MTHM/ 2.1 MTHM).

Using the guidance provided by the EPA [1985] in 40 CFR 191, Appendix C, the number of exploratory boreholes is taken to be 3 boreholes/km^2/10,000 yrs. The diameter of an exploratory borehole at repository level is conservatively assumed to be 0.61 m, based on discussions with exploratory drilling experts. The expected number of boreholes over 10,000 years will be the number of boreholes per square-kilometer multiplied by the repository area. This will be approximately equal to 17 boreholes/10,000 yrs (that is, 5.61 km^2 x 3 bh/km^2/10,000 yrs = 17 boreholes/10,000 yrs). In the calculation presented below, 17 boreholes/10,000 yrs will be assumed to be the maximum number of boreholes. In a subsequent, alternative calculation, it will be assumed to be the mean number of boreholes.

---

[1] Working Group 2, 1990. PACE90 Working Group 2 Final Report.

For these calculations, the area of a waste package is not simply the normal cross sectional area of the waste canister, but must also include the cross sectional area of the drill hole. That is, for a given distance away from a waste canister, a larger drill hole has a greater chance of hitting the waste canister than a smaller drill hole. Therefore, the "enhanced" area of a single, vertically emplaced canister can be expressed as:

$$Enhanced\ Area\ of\ Canister = \pi\,(r_{wp} + r_{bh})^2 \tag{1}$$

where r is radius. The subscripts *wp* and *bh* represent waste package and borehole respectively. For a single horizontally emplaced canister, the enhanced area is given as:

$$Enhanced\ Area\ of\ Canister = (D_{wp} + D_{bh}) \cdot (L_{wp} + D_{bh}) \tag{2}$$

where D is diameter and L is length.

The probability of hitting a waste canister given a single drilling event is directly proportional to the fractional area of the repository area covered by waste canisters. To repeat, the area of the repository and the waste canisters is the area as viewed from the land surface looking vertically downward (i.e., cross-sectional area). The areal-based probability of a hit given a single drilling event, and for vertically emplaced waste packages, is then given by:

$$\begin{aligned} P_{hit} &= \frac{enhanced\ area\ of\ all\ canisters}{area\ of\ repository} \\ &= \frac{N_{wp}\,[\pi\,(r_{wp} + r_{bh})^2]}{area\ of\ repository} \\ &= \frac{33{,}333\,[\pi\,(0.33 + 0.305)^2]}{5.61x10^6} \\ &= 0.0075 \end{aligned} \tag{3}$$

Similarly, the probability of a hit given a single drilling event, and for horizontally emplaced waste packages is given by:

$$\begin{aligned} P_{hit} &= \frac{enhanced\ area\ of\ all\ canisters}{area\ of\ repository} \\ &= \frac{N_{wp}\,[(D_{wp} + D_{bh}) \cdot (L_{wp} + D_{bh})]}{area\ of\ repository} \\ &= \frac{33{,}333\,[(0.66 + 0.61)\,x\,(4.6 + 0.61]}{5.61x10^6} \\ &= 0.0393 \end{aligned} \tag{4}$$

The length of the waste package used in the Equation 4 calculation is a weighted average based on the number of spent fuel and HLW packages.

A rough guess at the probability of hitting a canister over 10,000 years can be calculated by simply multiplying P_{hit} times the expected number of boreholes over 10,000 years. Assuming a maximum of 17 boreholes are drilled and vertical waste package emplacement, this results in a probability of hitting a waste package of 0.128 (12.8% chance of one hit in 10,000 years). However, the frequency of hitting a waste canister during the drilling process can be assumed to follow a binomial distribution, in which the probability of a hit given a single drilling event is given by Equation 2. A binomial distribution is chosen because it describes "yes-or-no" (or in this case, "hit-or-miss") type behavior. The resulting probability distribution of hits for vertically emplaced waste packages is given in Table 1:

Table 1. Probability Distribution of Hits for 17 Drilling Events and Vertically Emplaced Waste Packages

Number of Hits/Total Number of Drilling Events	Probability	Cumulative Probability
0	0.880	0.880
1	0.113	0.993
2	0.683×10^{-2}	0.9997
3	0.258×10^{-3}	0.999993

There is an 88% chance that no waste canisters will be hit over 10,000 years with 17 drilling events. There is an 11.3% chance that 1 waste canister will be hit during that period. The probability of 1 or less hits is accordingly 99.3%. Although the binomial distribution calculation results in a similar estimate for a single hit as the simple calculation of multiplying the probability of a hit given a single drilling event by the number of events, the binomial distribution provides additional information about the possibility of more than one hit. The probability of multiple hits drops off rapidly after 1 hit because of the small probability of a hit given a single drilling event. There is less than a 1% chance that 2 waste packages will be hit. The probability of hits beyond 3 is included in the attachments to this memo.

The resulting probability distribution for hits, given horizontally emplaced waste packages is given in Table 2:

Table 2. Probability Distribution of Hits for 17 Drilling Events and Horizontally Emplaced Waste Packages

Number of Hits/Total Number of Drilling Events	Probability	Cumulative Probability
0	0.506	0.506
1	0.352	0.858
2	0.115	0.973
3	0.235×10^{-1}	0.996
4	0.337×10^{-2}	0.9996
5	0.359×10^{-3}	0.99997

The probability of hits is markedly greater for the horizontal emplacement case, because of the increase in the cross-sectional area of the waste packages under this configuration. The probability of hits beyond 5 for the horizontal emplacement case is included in the attachments to this memo.

Note that because of the way the waste canister area was calculated, "hit" does not necessarily imply a direct hit. Rather, a hit is such that the waste canister is at the least, touched by the drill bit.

Alternative Calculation 1

The above calculation has assumed that the specified number of boreholes is the maximum that would occur. However, it is fair to assume that some uncertainty is associated with this maximum. In this alternative calculation, the 17 boreholes is assumed to be the mean number of boreholes drilled and the frequency of drilling at the site is assumed to follow a Poisson distribution. Given these assumptions, the cumulative probability function of the Poisson distribution indicates that there is a 99.9% chance that 31 or fewer boreholes will be drilled inside the repository area over 10,000 years. There is a 99.99% chance that 34 or fewer will be drilled in that time. As discussed above, the frequency of hits is still assumed to follow a binomial distribution. Therefore, the probability of *n* hits, for *N* boreholes, is given by:

$$P(n\ hits) = \sum_{N=n}^{\infty} P(N) \cdot P(n|N) \qquad (5)$$

where $P(N)$ is described by the Poisson distribution for the number of boreholes, given a mean number of boreholes, μ, of 17. $P(n|N)$ is described by a binomial distribution for the number of hits given N boreholes. Equation 5 can be further written as:

$$P(n\ hits) = \sum_{N=n}^{\infty} \frac{\mu^N e^{-\mu}}{N!} \cdot \frac{N!}{(N-n)!\,n!} P_{hit}^n (1-P_{hit})^{N-n} \tag{6}$$

This can be simplified and written as

$$P(n\ hits) = \frac{(\mu P_{hit})^n}{n!} e^{-\mu P_{hit}} \tag{7}$$

Therefore, the number of hits in this case is also Poisson, with the expected number of hits given by μP_{hit}. The corresponding probability distribution of hits for this case, with a mean of 17 drilling events and vertically emplaced waste packages is summarized in Table 3.

Table 3. Probability Distribution of Hits for a Mean Number of Hits Equal to 17 and Vertically Emplaced Waste Packages

Number of Hits/Total Number of Drilling Events	Probability	Cumulative Probability
0	0.880	0.880
1	0.112	0.993
2	0.716×10^{-2}	0.9997
3	0.304×10^{-3}	0.999990

Note that the probabilities of n hits for this case are very similar to those for the initial calculations. For horizontally emplaced waste packages, the probability distribution of hits is given in Table 4.

Table 4. Probability Distribution of Hits for a Mean Number of Hits Equal to 17 and Horizontally Emplaced Waste Packages

Number of Hits/Total Number of Drilling Events	Probability	Cumulative Probability
0	0.513	0.513
1	0.343	0.855
2	0.114	0.970
3	0.255×10^{-1}	0.995
4	0.426×10^{-2}	0.9994
5	0.569×10^{-3}	0.99993

Again note that the probabilities of *n* hits for this case are very similar to those for the initial calculations.

As a further alternative to these calculations, one could perhaps assume, conservatively, that 31 is the maximum number of boreholes drilled (based on the Poisson distribution with mean of 17) and subsequently calculate the probability of a hit using 31 as the number of observations for the binomial distribution. The probability of a hit given a single drilling event would remain constant.

Alternative Calculation 2

R. Wilems [1990][2] conducted similar calculations to the initial ones presented above. The primary difference between Wilems calculations and those presented above was in the calculation of the cross sectional area of waste packages in the repository. The difference arose from different numbers and types of waste packages considered. The probabilities of hitting a waste package have been recalculated using the Wilems' waste package cross-sectional areas and the repository area in Rautman et al. [1987]. The results are presented below.

[2] Memo from Bob Wilems (Rogers and Associates Engineering Corporation) to PA Working Group 2 on the subject of Probability of Borehole Intersection of Waste Packages, dated April 19, 1990 (amended May 3, 1990).

Table 5. Probability Distribution of Hits for 17 Drilling Events
and Vertically Emplaced Waste Packages
(Waste Package Area taken from Wilems [1990])

Number of Hits/Total Number of Drilling Events	Probability	Cumulative Probability
0	0.917	0.917
1	0.799×10^{-1}	0.997
2	0.328×10^{-2}	0.99991
3	0.840×10^{-4}	0.999998

Table 6. Probability Distribution of Hits for 17 Drilling Events
and Horizontally Emplaced Waste Packages
(Waste Package Area taken from Wilems [1990])

Number of Hits/Total Number of Drilling Events	Probability	Cumulative Probability
0	0.571	0.571
1	0.325	0.896
2	0.871×10^{-1}	0.984
3	0.146×10^{-1}	0.998
4	0.171×10^{-2}	0.9998
5	0.149×10^{-3}	0.99999

Wilems also conducted the same calculations for the alternative spent fuel waste package. These results are presented below.

Table 7. Probability Distribution of Hits for 17 Drilling Events and Horizontally Emplaced Waste Packages (Waste Package Area taken from Wilems [1990] using Alternative Spent Fuel Package)

Number of Hits/Total Number of Drilling Events	Probability	Cumulative Probability
0	0.947	0.947
1	0.517×10^{-1}	0.953
2	0.133×10^{-2}	0.99997
3	0.213×10^{-4}	0.9999998

Table 8. Probability Distribution of Hits for 17 Drilling Events and Horizontally Emplaced Waste Packages (Waste Package Area taken from Wilems [1990] using Alternative Spent Fuel Package)

Number of Hits/Total Number of Drilling Events	Probability	Cumulative Probability
0	0.702	0.702
1	0.251	0.953
2	0.422×10^{-1}	0.995
3	0.444×10^{-2}	0.9996
4	0.327×10^{-3}	0.99998

Data used by Wilems [1990] are attached to this memo. Note that the results in the attachment will not agree exactly with those presented above because Wilems used a repository area of 5.75×10^6 m^2.

Summary
Calculations have been conducted to estimate the probability of hitting a waste canister at the Yucca Mountain site, based on geometric considerations, site characteristics, and other assumptions with regard to drilling techniques and frequency. Obviously, these calculations are only meaningful if the assumptions made are reasonable. Those assumptions that will need further investigation include (1) the estimated frequency of drilling at the site over 10,000 years, (2) the techniques used for drilling over that time period, (3) waste emplacement configurations including the number and type of waste packages, and (4) preferential drilling locations and their coincidence with the underground repository configuration.

Provided in this memo is a simple procedure that can be followed to calculate the probability of hitting a waste package during a drilling operation at a given repository over 10,000 years. The procedure requires knowledge of the repository characteristics, drilling characteristics, and information about frequency and location of drilling. The calculations presented in this memo are supported by limited information, and should therefore be interpreted with that in mind.

Acknowledgement
Valuable technical review comments on a draft of this memo were provided by M.L. Wilson (6312), particularly for Alternative Calculation 1.

References

Apostolakis, G., Bras, R.L., Price, L.L., Valdes, J., Wahi, K.K., 1991. Techniques for Determining Probabilities of Events and Processes Affecting the Performance of Geologic Repositories: Volume II - Suggested Approaches. U.S. Nuclear Regulatory Commission, NUREG/CR-3964, Washington, DC, and Sandia National Laboratories, SAND86-0196, Albuquerque, NM, Draft Report.

DOE (Department of Energy), 1988. Site Characterization Plan: Yucca Mountain Site, Nevada Research and Development Area, Nevada. U.S. Department of Energy, DOE/RW-0199, U.S. Government Printing Office.

EPA (Environmental Protection Agency), 1985. Environmental Standards for the Management and Disposal of Spent Nuclear Fuel, High-Level and Transuranic Radioactive Wastes. Code of Federal Regulations, Title 40, Part 191, U.S. Government Printing Office, Washington, DC.

Little, A.D., 1980. Technical Support of Standards for High-Level Radioactive Waste Management, Volume D, Release Mechanisms. EPA 520/4-79-007D, PB81-106254, Office of Radiation Protection Programs, Environmental Protection Agency, Washington, DC.

Rautman, C.A., Whittet, B.C., South, D.L., 1987. Definition of Reference Boundaries for the Proposed Geologic Repository at Yucca Mountain, Nevada. Sandia National Laboratories, SAND86-2157, Albuquerque, NM.

Copy to (w/ attachments):
6312 F.W. Bingham, Actg.
6312 F.C. Lauffer
6312 M.L. Wilson
6313 J.H. Gauthier
6313 L.E. Shephard, Actg.
6313 M.E. Fewell
6416 E.J. Bonano
6416 D.P. Gallegos

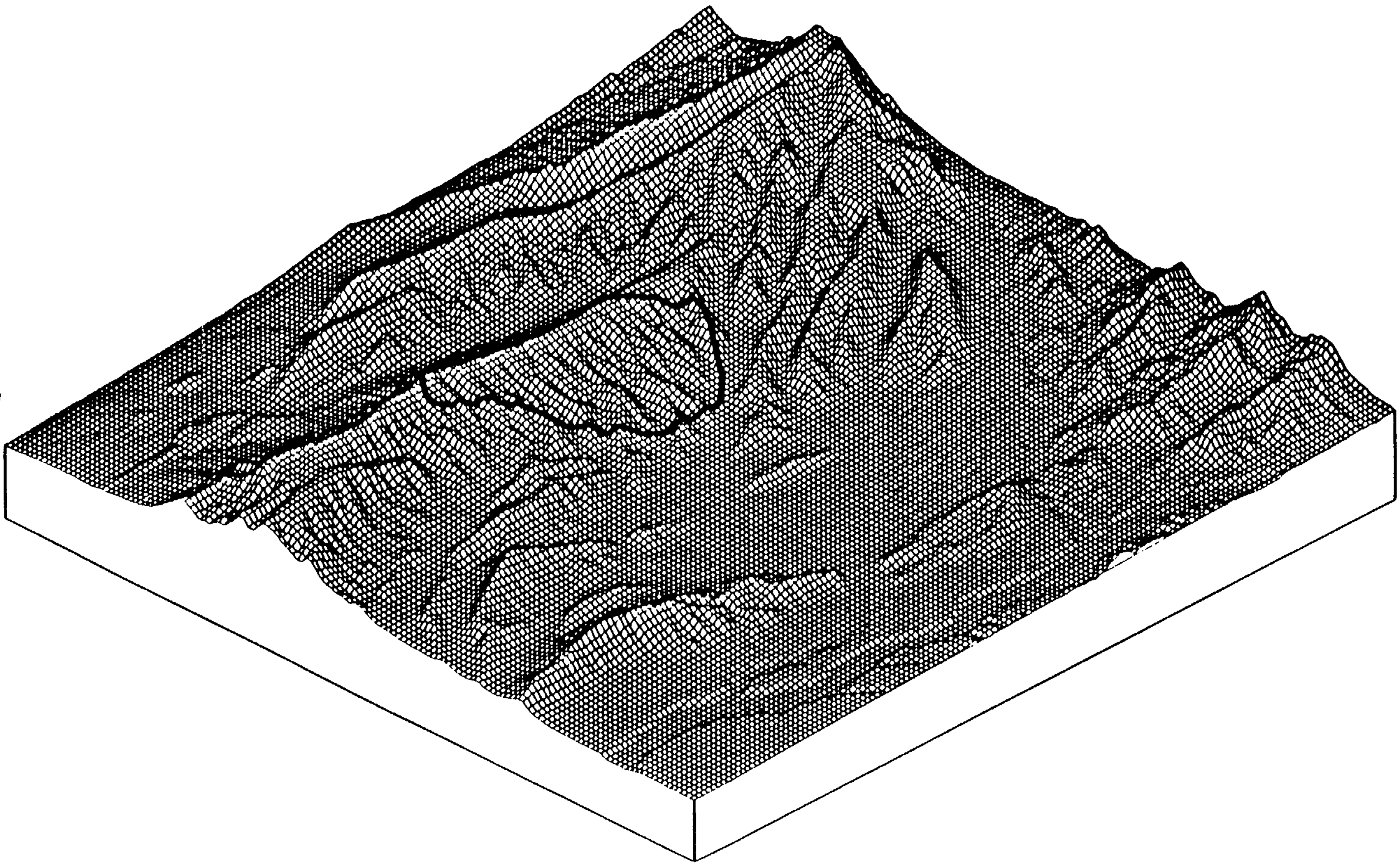

Figure 1.

nter total number of **observations**: 17

Enter probability of **affirmative event** (0<p<1): 0.0075

vation	Probability	**Cumulative probability**
0.000000	0.879870510801553	0.879870510801553
1.00000	0.113031227641710	0.992901738443263
2.00000	0.683312207405805D-002	0.999734860517321
3.00000	0.258178404574787D-003	0.999993038921896
4.00000	0.682839593035564D-005	0.999999867317827
5.00000	0.134159920042252D-006	1.00000000147775
6.00000	0.202760584446728D-008	1.00000000350535
7.00000	0.240773633923787D-010	1.00000000352943
8.00000	0.227431014411637D-012	1.00000000352966
9.00000	0.171862227515091D-014	1.00000000352966
10.0000	0.103896560714413D-016	1.00000000352966
11.0000	0.499617076941302D-019	1.00000000352966
12.0000	0.188772195317872D-021	1.00000000352966
13.0000	0.548650054208116D-024	1.00000000352966
14.0000	0.118456293723725D-026	1.00000000352966
15.0000	0.179027152017518D-029	1.00000000352966
16.0000	0.169106251905716D-032	1.00000000352966
17.0000	0.751694681821390D-036	1.00000000352966

Vertical Emplacement
(Addendum to Table 1)

E:\MATH\DPGMATH>

Enter total number of **observations**: 17

Enter probability of **affirmative event** (0<p<1): 0.0393

Observation	Probability	**Cumulative probability**
0.000000	0.505815859160861	0.505815859160861
1.00000	0.351759743382744	0.857575602543605
2.00000	0.115117376204366	0.972692978747972
3.00000	0.235459180099962D-001	0.996238896757968
4.00000	0.337123029685666D-002	0.999610127054825
5.00000	0.358563871898421D-003	0.999968690926723
6.00000	0.293360261592754D-004	0.999998026952882
7.00000	0.188582196146482D-005	0.999999912774844
8.00000	0.964307316092009D-007	1.00000000920558
9.00000	0.394475669016508D-008	1.00000001315033
10.0000	0.129096648629947D-009	1.00000001327943
11.0000	0.336066391344365D-011	1.00000001328279
12.0000	0.687384676789505D-013	1.00000001328286
13.0000	0.108151179019415D-014	1.00000001328286
14.0000	0.126406085899044D-016	1.00000001328286
15.0000	0.103419577259875D-018	1.00000001328286
16.0000	0.528831761516745D-021	1.00000001328286
17.0000	0.127254560797685D-023	1.00000001328286

Horizontal Emplacement

(Addendum to Table 2)

E:\MATH\DPGMATH>

:\MATH\DPGMATH>up poisson
Copyright (c) 1990 Ergo Computing (OS 2.1.04; CP 5.33)

Enter mean: 0.1275

Enter maximum value: 13

Number	Probability	Cumul. prob.
0	0.880293415834221	0.880293415834221
1	0.112237410518863	0.992530826353084
2	0.715513492057753D-002	0.999685961273662
3	0.304093234124545D-003	0.999990054507786
4	0.969297183771987D-005	0.999999747479624
5	0.247170781861857D-006	0.999999994650406
6	0.525237911456446D-008	0.999999999902785
7	0.956683338724240D-010	0.999999999998453
8	0.152471407109176D-011	0.999999999999978
9	0.216001160071332D-013	1.00000000000000
10	0.275401479090949D-015	1.00000000000000
11	0.319215350764509D-017	1.00000000000000
12	0.339166310187291D-019	1.00000000000000
13	0.332643881145227D-021	1.00000000000000

E:\MATH\DPGMATH>

Vertical Emplacement
(Addendum to Table 3)

E:\MATH\DPGMATH>up poisson
Copyright (c) 1990 Ergo Computing (OS 2.1.04; CP 5.33)

Enter mean: 0.6681

Enter maximum value: 13

Number	Probability	Cumul. prob.
0	0.512681748303566	0.512681748303566
1	0.342522676041612	0.855204424345178
2	0.114419699931701	0.969624124276879
3	0.254812671747897D-001	0.995105391451669
4	0.425600864986926D-002	0.999361400101538
5	0.568687875795530D-003	0.999930087977334
6	0.633233949698323D-004	0.999993411372303
7	0.604376573990642D-005	0.999999455138043
8	0.504729986353935D-006	0.999999959868030
9	0.374677893203404D-007	0.999999997335819
10	0.250322300449194D-008	0.999999999839042
11	0.152036662663733D-009	0.999999999991079
12	0.846464119380336D-011	0.999999999999543
13	0.435017444736925D-012	0.999999999999978

E:\MATH\DPGMATH>

Horizontal Emplacement
(Addendum to Table 4)

DATA & RESULTS FROM WILEMS [1990]

CASE 1. SCENARIO WITH SCP ALTERNATE SF PACKAGES AND DHLW PACKAGES

	ALT. SF PACKAGE	DHLW PACKAGE	TOTAL REPOS
AREA OF REPOSITORY (SQ KM)	5.75	5.75	5.75
# OF PACKAGES IN REPOSITORY	30000	14000	
# OF BOREHOLES/SQ KM OVER 10,000 YEARS	3.00	3.00	3.00
# OF BOREHOLES IN AREA - 10,000 YEARS	17.00	17.00	17.00
BOREHOLE DIAMETER (M)	0.22	0.22	
WASTE PACKAGE LENGTH (M)	4.76	3.28	
WASTE PACKAGE WIDTH OR DIAMETER (M)	0.71	0.66	
WASTE PACKAGE RADIUS (M)	0.36	0.33	
HORIZ. WASTE PKG-BOREHOLE AREA (SQ M)	4.63	3.08	7.70
TOTAL AREA - HORIZ PKGS-BOREHOLES (SQ KM)	0.1388	0.0431	0.1819
PROB. OF HIT - HORIZONTAL PACKAGE	0.0241	0.0075	0.0316
PROB. OF MISS - HORIZONTAL PACKAGE	0.9759	0.9925	0.9684
PROB. OF 1 OR MORE HITS - HORIZ. PACKAGES	0.3400	0.1200	0.4210
PROB. OF NO HITS - HORIZ. PACKAGES	0.6600	0.8800	0.5790
PROB. OF 1 AND ONLY 1 HIT - HORIZ. PKGS.	0.2776	0.1129	0.3215
PROB. OF 2 AND ONLY 2 HITS - HORIZ. PKGS.	0.0550	0.0068	0.0840
PROB. OF 3 AND ONLY 3 HITS - HORIZ. PKGS.	0.0068	0.0003	0.0137
PROB. OF 4 AND ONLY 4 HITS - HORIZ. PKGS.	0.0006	<0.0001	0.0016
PROB. OF 5 AND ONLY 5 HITS - HORIZ. PKGS.	<0.0001	<0.0001	0.0001
PROB. OF 6 OR MORE HITS - HORIZ. PACKAGES	<0.0001	<0.0001	<0.0001
VERT. WASTE PKG-BOREHOLE AREA (SQ M)	0.68	0.61	1.28
TOTAL AREA - VERT. PKGS-BOREHOLES (SQ KM)	0.0203	0.0085	0.0288
PROB. OF HIT - VERTICAL PACKAGE	0.0035	0.0015	0.0050
PROB. OF MISS - VERTICAL PACKAGE	0.9965	0.9985	0.9950
PROB. OF 1 OR MORE HITS - VERT. PACKAGES	0.0585	0.0248	0.0819
PROB. OF NO HITS - VERT. PACKAGES	0.9415	0.9752	0.9181
PROB. OF 1 AND ONLY 1 HIT - VERT. PKGS.	0.0568	0.0245	0.0787
PROB. OF 2 AND ONLY 2 HITS - VERT. PKGS.	0.0016	0.0003	0.0032
PROB. OF 3 AND ONLY 3 HITS - VERT. PKGS.	0.0001	<0.0001	0.0003
PROB. OF 4 OR MORE HITS - VERT. PACKAGES	<0.0001	<0.0001	<0.0001

CASE 1. SCENARIO WITH SCP ALTERNATE SF PACKAGES AND DHLW PACKAGES

	REFERENCES
AREA OF REPOSITORY (SQ KM)	SCP, page 6-224
# OF PACKAGES IN REPOSITORY	JARDINE NWTRB PAPER, 1/18/90
# OF BOREHOLES/SQ KM OVER 10,000 YEARS	EPA, 40 CFR PART 191
# OF BOREHOLES IN AREA - 10,000 YEARS	
BOREHOLE DIAMETER (M)	
WASTE PACKAGE LENGTH (M)	SCP, page 7-30,33
WASTE PACKAGE WIDTH OR DIAMETER (M)	SCP, page 7-30,33
WASTE PACKAGE RADIUS (M)	SCP, page 7-30,33

HORIZ. WASTE PKG-BOREHOLE AREA (SQ M)
TOTAL AREA - HORIZ PKGS-BOREHOLES (SQ KM)

PROB. OF HIT - HORIZONTAL PACKAGE
PROB. OF MISS - HORIZONTAL PACKAGE
PROB. OF 1 OR MORE HITS - HORIZ. PACKAGES

PROB. OF NO HITS - HORIZ. PACKAGES
PROB. OF 1 AND ONLY 1 HIT - HORIZ. PKGS.
PROB. OF 2 AND ONLY 2 HITS - HORIZ. PKGS.
PROB. OF 3 AND ONLY 3 HITS - HORIZ. PKGS.
PROB. OF 4 AND ONLY 4 HITS - HORIZ. PKGS.
PROB. OF 5 AND ONLY 5 HITS - HORIZ. PKGS.
PROB. OF 6 OR MORE HITS - HORIZ. PACKAGES

VERT. WASTE PKG-BOREHOLE AREA (SQ M)
TOTAL AREA - VERT. PKGS-BOREHOLES (SQ KM)

PROB. OF HIT - VERTICAL PACKAGE
PROB. OF MISS - VERTICAL PACKAGE
PROB. OF 1 OR MORE HITS - VERT. PACKAGES

PROB. OF NO HITS - VERT. PACKAGES
PROB. OF 1 AND ONLY 1 HIT - VERT. PKGS.
PROB. OF 2 AND ONLY 2 HITS - VERT. PKGS.
PROB. OF 3 AND ONLY 3 HITS - VERT. PKGS.
PROB. OF 4 OR MORE HITS - VERT. PACKAGES

CASE 2. SCENARIO WITH SCP REFERENCE SF PACKAGES AND DHLW PACKAGES

	REF SF PACKAGE	DHLW PACKAGE	TOTAL REPOS
AREA OF REPOSITORY (SQ KM)	5.75	5.75	5.75
# OF PACKAGES IN REPOSITORY	18000	12000	
# OF BOREHOLES/SQ KM OVER 10,000 YEARS	3.00	3.00	3.00
# OF BOREHOLES IN AREA - 10,000 YEARS	17.00	17.00	17.00
BOREHOLE DIAMETER (M)	0.22	0.22	
WASTE PACKAGE LENGTH (M)	4.76	3.28	
WASTE PACKAGE WIDTH (M)	0.66	0.66	
WASTE PACKAGE RADIUS (M)	0.33	0.33	
HORIZ. WASTE PKG-BOREHOLE AREA (SQ M)	4.38	3.08	7.45
TOTAL AREA - HORIZ PKGS-BOREHOLES (SQ KM)	0.0788	0.0369	0.1157
PROB. OF HIT - HORIZONTAL PACKAGE	0.0137	0.0064	0.0201
PROB. OF MISS - HORIZONTAL PACKAGE	0.9863	0.9936	0.9799
PROB. OF 1 OR MORE HITS - HORIZ. PACKAGES	0.2091	0.1037	0.2922
PROB. OF NO HITS - HORIZ. PACKAGES	0.7909	0.8963	0.7078
PROB. OF 1 AND ONLY 1 HIT - HORIZ. PKGS.	0.1869	0.0984	0.2471
PROB. OF 2 AND ONLY 2 HITS - HORIZ. PKGS.	0.0208	0.0051	0.0406
PROB. OF 3 AND ONLY 3 HITS - HORIZ. PKGS.	0.0014	0.0002	0.0042
PROB. OF 4 OR MORE HITS - HORIZ. PACKAGES	<0.0001	<0.0001	0.0003
PROB. OF 5 OR MORE HITS - HORIZ. PACKAGES	<0.0001	<0.0001	<0.0001
VERT. WASTE PKG-BOREHOLE AREA (SQ M)	0.61	0.61	1.21
TOTAL AREA - VERT. PKGS-BOREHOLES (SQ KM)	0.0109	0.0073	0.0182
PROB. OF HIT - VERTICAL PACKAGE	0.0019	0.0013	0.0032
PROB. OF MISS - VERTICAL PACKAGE	0.9981	0.9987	0.9968
PROB. OF 1 OR MORE HITS - VERT. PACKAGES	0.0318	0.0213	0.0525
PROB. OF NO HITS - VERT. PACKAGES	0.9682	0.9787	0.9475
PROB. OF 1 AND ONLY 1 HIT - VERT. PKGS.	0.0313	0.0211	0.0512
PROB. OF 2 AND ONLY 2 HITS - VERT. PKGS.	0.0005	0.0002	0.0013
PROB. OF 3 AND ONLY 3 HITS - VERT. PKGS.	<0.0001	<0.0001	0.0001
PROB. OF 4 OR MORE HITS - VERT. PKGS.	<0.0001	<0.0001	<0.0001

CASE 2. SCENARIO WITH SCP REFERENCE SF PACKAGES AND DHLW PACKAGES

	REFERENCES
AREA OF REPOSITORY (SQ KM)	SCP, page 6-224
# OF PACKAGES IN REPOSITORY	
# OF BOREHOLES/SQ KM OVER 10,000 YEARS	EPA, 40 CFR PART 191
# OF BOREHOLES IN AREA - 10,000 YEARS	
BOREHOLE DIAMETER (M)	
WASTE PACKAGE LENGTH (M)	SCP, page 7-28,30,33
WASTE PACKAGE WIDTH (M)	SCP, page 7-28,30,33
WASTE PACKAGE RADIUS (M)	SCP, page 7-28,30,33

HORIZ. WASTE PKG-BOREHOLE AREA (SQ M)
TOTAL AREA - HORIZ PKGS-BOREHOLES (SQ KM)

PROB. OF HIT - HORIZONTAL PACKAGE
PROB. OF MISS - HORIZONTAL PACKAGE
PROB. OF 1 OR MORE HITS - HORIZ. PACKAGES

PROB. OF NO HITS - HORIZ. PACKAGES
PROB. OF 1 AND ONLY 1 HIT - HORIZ. PKGS.
PROB. OF 2 AND ONLY 2 HITS - HORIZ. PKGS.
PROB. OF 3 AND ONLY 3 HITS - HORIZ. PKGS.
PROB. OF 4 OR MORE HITS - HORIZ. PACKAGES
PROB. OF 5 OR MORE HITS - HORIZ. PACKAGES

VERT. WASTE PKG-BOREHOLE AREA (SQ M)
TOTAL AREA - VERT. PKGS-BOREHOLES (SQ KM)

PROB. OF HIT - VERTICAL PACKAGE
PROB. OF MISS - VERTICAL PACKAGE
PROB. OF 1 OR MORE HITS - VERT. PACKAGES

PROB. OF NO HITS - VERT. PACKAGES
PROB. OF 1 AND ONLY 1 HIT - VERT. PKGS.
PROB. OF 2 AND ONLY 2 HITS - VERT. PKGS.
PROB. OF 3 AND ONLY 3 HITS - VERT. PKGS.
PROB. OF 4 OR MORE HITS - VERT. PKGS.

Appendix II
Setup for 2-D Groundwater-Flow Analyses

(Barnard, Eaton)

As part of the effort to evaluate the applicability of the use of abstracted models for unsaturated groundwater flow, independent calculations were made using the finite-element code NORIA-SP (Hopkins et al., 1991) and the finite-difference code LLUVIA-II (Eaton and Hopkins, 1992). These calculations used two-dimensional models of groundwater flow (no radionuclide transport was done) to provide results from the lower part of the modeling hierarchy (Figure 2-1), to be compared with the TSPA results from the top of the modeling pyramid.

II.1 Geometry and numerical grid

A subregion of the TSPA problem domain was used for these analyses. Figure II-1 shows an outline of the geometry used for the NORIA-SP calculations. The horizontal extent of the problem domain was shortened from the one specified for the TSPA to 1200 m, ending between the Ghost Dance Fault and drillhole USW G-4. The domain extends vertically from the repository level to the water table. Included in the region are five fractured geologic layers and a fault. A total of 630 eight-node, biquadratic finite elements were used with the NORIA-SP code (Figure II-2). The 2-D analyses were run using the mean values of the material properties for the matrix and fractures (developed in Chapter 3). The parameters are shown in Table II-1. The values listed for the fractures are consistent with an effective fracture aperture of 99 μm, as discussed in Chapter 3. The NORIA calculation was run at 3.0 mm/yr.

Table II-1
Material properties for 2-D problems.

Layer	Total Porosity	K_s (m/s)	Alpha (m^{-1})	Beta	S_r	Fractures ($1/m^3$)
1	0.11	$2.0*10^{-11}$	0.00567	1.798	0.080	28.3
2	0.09	$3.0*10^{-12}$	0.0033	1.798	0.052	35.6
3	0.21	$8.0*10^{-11}$	0.0265	2.223	0.164	2.0
4	0.41	$3.0*10^{-12}$	0.0220	1.236	0.010	1.6
5	0.24	$1.4*10^{-8}$	0.0140	2.640	0.066	4.4
Fractures	0.43	$8.25*10^{-5}$	14.5	2.68	0.045	——

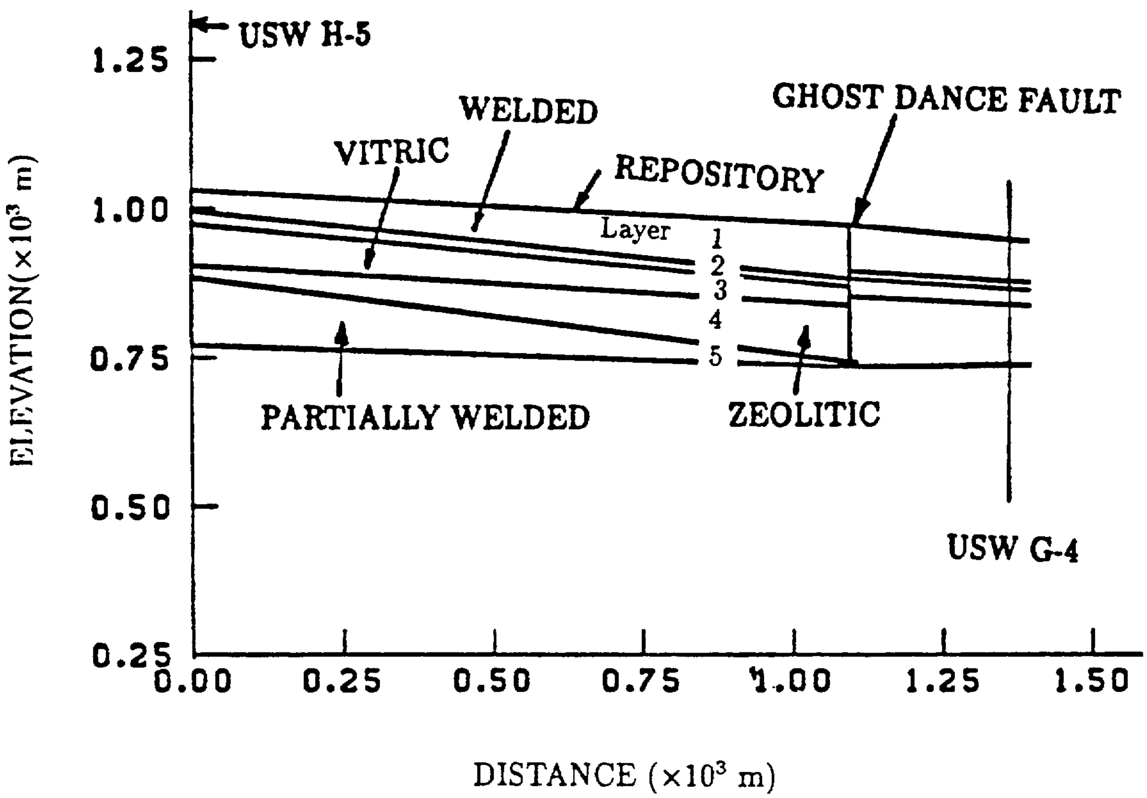

Figure II-1. Problem domain for 2-D NORIA-SP analysis

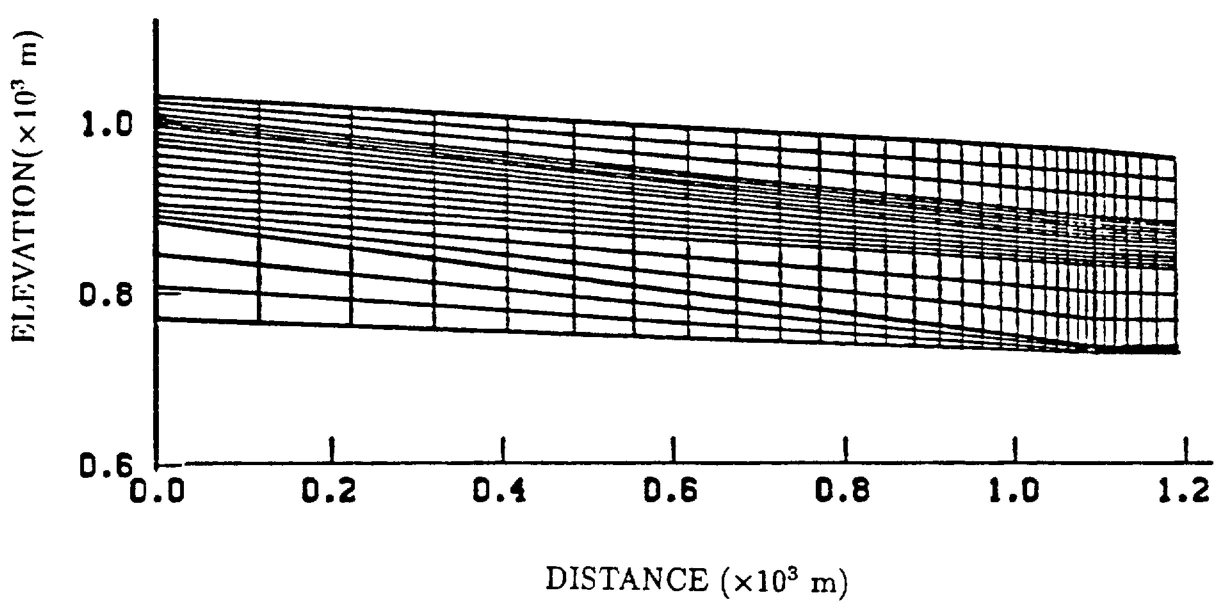

Figure II-2. NORIA-SP computational mesh

Because of the considerably shorter execution times required by LLUVIA-II, this code was used to calculate the water flow patterns for fluxes of 0.01, 0.1, and 1.0 mm/yr. The LLUVIA-II problem domain was set up as a rectangular grid, with the dip of the geologic units approximated by rotating the gravitational-force vector by 6.25 degrees. This effectively rotated the water table by 6.25°. The actual dip angle given for the water table was 2.03°. Thus, lateral diversion of water at the bottom boundary would be overstated. However, as the results will show, lateral motion at the bottom boundary is nearly zero. The five geologic units were approximated as constant thicknesses using the average values of each unit given in Table 3-1. A horizontal domain of 500 m was used, starting approximately 500 m east of drillhole USW H-5. The Ghost Dance Fault was not included in this domain (Figure II-3).

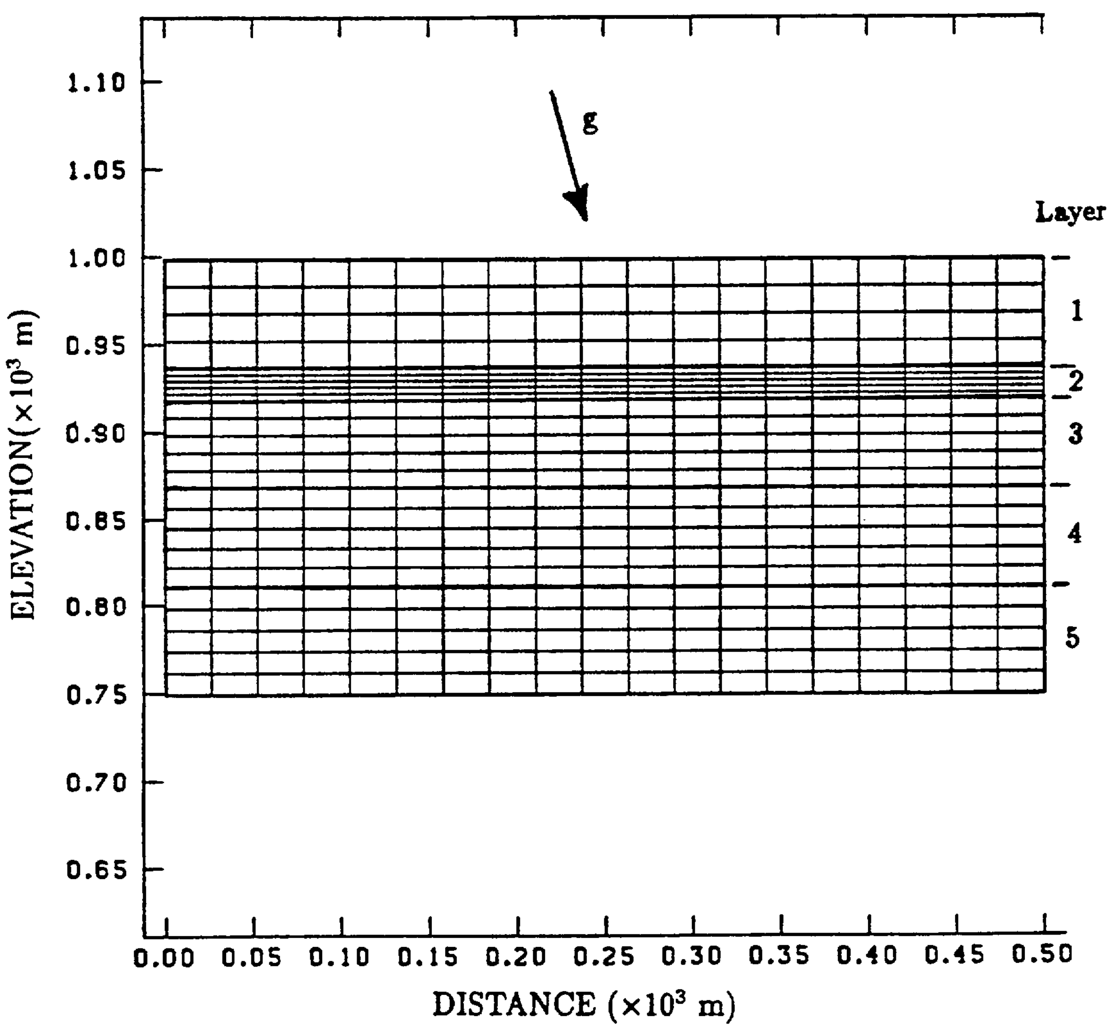

Figure II-3. LLUVIA-II computational mesh

II.2 Boundary and initial conditions

The calculations were run for four water percolation rates—0.01, 0.1, 1.0, and 3.0 mm/yr. A steady water-flux rate (q_i) of 3.0 mm/yr was evenly distributed along the top boundary for the NORIA-SP calculations. Evenly distributed steady fluxes of 0.01, 0.1, and 1.0 mm/yr were used for the LLUVIA-II calculations. Zero horizontal flow was specified at the right and left boundaries. The bottom boundary was located at the water table and was therefore held at a constant pressure head of zero. At time zero, a constant effective pressure was applied everywhere within the flow region, resulting in zero initial water velocity. The codes were run until the results approached steady state.

Appendix III
RIB/SEPDB Data

Most of the data used in this analysis were not taken from the RIB. The RIB contains average values for parameters, which generally speaking represent judgments by the submittors of the data. For this analysis we did not want to impose any biases on the data which we could not clearly identify. The sources of the data are identified in the text of the report. All data should be considered to be Quality Assurance level NQ.

Some of these data may be submitted to the SEPDB and/or the RIB. The Gainer et al. (1992) report describes the development of the geohydrologic data, and is the more appropriate source for submitting data to the RIB/SEPDB.

DISTRIBUTION LIST

1 J. W. Bartlett, Director (RW-1)
Office of Civilian Radioactive
Waste Management
U.S. Department of Energy
1000 Independence Avenue, S.W.
Washington, DC 20585

1 F. G. Peters, Deputy Director (RW-2)
Office of Civilian Radioactive
Waste Management
U.S. Department of Energy
1000 Independence Avenue, S.W.
Washington, DC 20585

1 T. H. Isaacs (RW-4)
Office of Strategic Planning
and International Programs
Office of Civilian Radioactive
Waste Management
U.S. Department of Energy
1000 Independence Avenue, S.W.
Washington, DC 20585

1 J. D. Saltzman (RW-5)
Office of External Relations
Office of Civilian Radioactive
Waste Management
U.S. Department of Energy
1000 Independence Avenue, S.W.
Washington, DC 20585

1 Samuel Rousso (RW-10)
Office of Program and Resources
Management
Office of Civilian Radioactive
Waste Management
U.S. Department of Energy
1000 Independence Avenue, S.W.
Washington, DC 20585

1 J. C. Bresee (RW-10)
Office of Civilian Radioactive
Waste Management
U.S. Department of Energy
1000 Independence Avenue, S.W.
Washington, DC 20585

1 C. P. Gertz (RW-20)
Office of Geologic Disposal
Office of Civilian Radioactive
Waste Management
U.S. Department of Energy
1000 Independence Avenue, S.W.
Washington, DC 20585

1 S. J. Brocoum (RW-22)
Analysis and Verification Division
Office of Civilian Radioactive
Waste Management
U.S. Department of Energy
1000 Independence Avenue, S.W.
Washington, DC 20585

1 J. Roberts, Acting Assoc. Dir.
(RW-30)
Office of Systems and Compliance
Office of Civilian Radioactive
Waste Management
U.S. Department of Energy
1000 Independence Avenue, S.W.
Washington, DC 20585

1 J. Roberts (RW-33)
Director, Regulatory Compliance
Division
Office of Civilian Radioactive
Waste Management
U.S. Department of Energy
1000 Independence Avenue, S.W.
Washington, DC 20585

1 G. J. Parker (RW-332)
Office of Civilian Radioactive
Waste Management
U.S. Department of Energy
1000 Independence Avenue, S.W.
Washington, DC 20585

1 R. A. Milner (RW-40)
Office of Storage & Transportation
Office of Civilian Radioactive
Waste Management
U.S. Department of Energy
1000 Independence Avenue, S.W.
Washington, DC 20585

1 S. Rousso, Acting Assoc. Director
(RW-50)
Office of Contract Business
Management
Office of Civilian Radioactive
Waste Management
U.S. Department of Energy
1000 Independence Avenue, S.W.
Washington, DC 20585

1 Trudy Wood (RW-52)
Director, M&O Management Div.
Office of Civilian Radioactive
Waste Management
U.S. Department of Energy
1000 Independence Avenue, S.W.
Washington, DC 20585

1 John E. Cantlon, Chairman
Nuclear Waste Technical
Review Board
1795 Bramble Dr.
East Lansing, MI 48823

1 Clarence R. Allen
Nuclear Waste Technical
Review Board
1000 E. California Blvd.
Pasadena, CA 91106

1 Garry D. Brewer
Nuclear Waste Technical Review
Board
Univ. of Michigan
Dana Bldg., Rm 3516
Ann Arbor, Michigan 48109-1115

1 Pat Domenico
Nuclear Waste Technical Review
Board
1100 Wilson Boulevard, Suite 910
Arlington, VA 22209

1 Donald Langmuir
Nuclear Waste Technical
Review Board
109 So. Lookout Mountain Cr.
Golden, CO 80401

1 John J. McKetta
Nuclear Waste Technical
Review Board
Dept. of Chemical Engineering
CRE Bldg. 1.450
Austin, TX 78712-1062

1 D. Warner North
Nuclear Waste Technical
Review Board
Decision Focus, Inc.
4984 El Camino Real
Los Altos, CA 94062

1 Dennis L. Price
Nuclear Wast Technical
Review Board
1011 Evergreen Way
Blacksburg, VA 24060

1 Ellis D. Verink
Nuclear Waste Technical
Review Board
4401 N.W. 18th Place
Gainesville, FL 32605

5 C. P. Gertz, Project Manager
Yucca Mountain Site Characterization Project Office
U.S. Department of Energy
P.O. Box 98608--MS 523
Las Vegas, NV 89193-8608

1 C. L. West, Director
Office of External Affairs
DOE Field Office, Nevada
U.S. Department of Energy
P.O. Box 98518
Las Vegas, NV 89193-8518

12 Technical Information Officer
DOE Nevada Field Office
U.S. Department of Energy
P.O. Box 98518
Las Vegas, NV 89193-8518

1 P. K. Fitzsimmons, Technical Advisor
Office of Assistant Manager for Environmental Safety and Health
DOE Field Office, Nevada
U.S. Department of Energy
P.O. Box 98518
Las Vegas, NV 89193-8518

1 D. R. Elle, Director
Environmental Protection Division
DOE Nevada Field Office
U.S. Department of Energy
P.O. Box 98518
Las Vegas, NV 89193-8518

1 Repository Licensing & Quality Assurance
Project Directorate
Division of Waste Management
U.S. Nuclear Regulatory Commission
Washington, DC 20555

1 Senior Project Manager for Yucca Mountain
Repository Project Branch
Division of Waste Management
U.S. Nuclear Regulatory Commission
Washington, DC 20555

1 NRC Document Control Desk
Division of Waste Management
U.S. Nuclear Regulatory Commission
Washington, DC 20555

1 P. T. Prestholt
NRC Site Representative
301 E. Stewart Ave., Room 203
Las Vegas, NV 89101

1 E. P. Binnall
Field Systems Group Leader
Building 50B/4235
Lawrence Berkeley Laboratory
Berkeley, CA 94720

1 Center for Nuclear Waste Regulatory Analyses
6220 Culebra Road
Drawer 28510
San Antonio, TX 78284

3 W. L. Clarke
Technical Project Officer for YMP
Attn: YMP/LRC
Lawrence Livermore National Laboratory
P.O. Box 5514
Livermore, CA 94551

4 J. Canepa
Technical Project Officer for YMP
N-5, Mail Stop J521
Los Alamos National Laboratory
P.O. Box 1663
Los Alamos, NM 87545

1 H. N. Kalia
Exploratory Shaft Test Manager
Los Alamos National Laboratory
Mail Stop 527
101 Convention Center Dr
Suite 820
Las Vegas, NV 89109

1 J. F. Divine
Assistant Director for
Engineering Geology
U.S. Geological Survey
106 National Center
12201 Sunrise Valley Dr.
Reston, VA 22092

6 L. R. Hayes
Technical Project Officer
Yucca Mountain Project Branch
MS 425
U.S. Geological Survey
P.O. Box 25046
Denver, CO 80225

1 V. R. Schneider
Asst. Chief Hydrologist--MS 414
Office of Program Coordination &
Technical Support
U.S. Geological Survey
12201 Sunrise Valley Drive
Reston, VA 22092

1 J. S. Stuckless
Geological Division Coordinator
MS 913
Yucca Mountain Project
U.S. Geological Survey
P.O. Box 25046
Denver, CO 80225

1 D. H. Appel, Chief
Hydrologic Investigations Program
MS 421
U.S. Geological Survey
P.O. Box 25046
Denver, CO 80225

1 E. J. Helley
Branch of Western Regional Geology
MS 427
U.S. Geological Survey
345 Middlefield Road
Menlo Park, CA 94025

1 R. W. Craig, Chief
Nevada Operations Office
U.S. Geological Survey
101 Convention Center Drive
Suite 860, MS 509
Las Vegas, NV 89109

1 D. Zesiger
U.S. Geological Survey
101 Convention Center Dr.
Suite 860 - MS 509
Las Vegas, NV 89109

1 R. V. Watkins, Chief
Project Planning and Management
U.S. Geological Survey
P.O. Box 25046
421 Federal Center
Denver, CO 80225

1 A. L. Flint
U.S. Geological Survey
MS 721
P.O. Box 327
Mercury, NV 89023

1 D. A. Beck
U.S. Geological Survey
1500 E. Tropicana, Suite 201
Las Vegas, NV 89119

1 P. A. Glancy
U.S. Geological Survey
Federal Building, Room 224
Carson City, NV 89701

1 Sherman S. C. Wu
Branch of Astrogeology
U.S. Geological Survey
2255 N. Gemini Dr.
Flagstaff, AZ 86001

1 J. H. Sass
Branch of Tectonophysics
U.S. Geological Survey
2255 N. Gemini Dr.
Flagstaff, AZ 86001

1 DeWayne A. Campbell
Technical Project Officer for YMP
U.S. Bureau of Reclamation
Code D-3790
P.O. Box 25007
Denver, CO 80225

1 K. W. Causseaux
NHP Reports Chief
U.S. Geological Survey
421 Federal Center
P.O. Box 25046
Denver, CO 80225

1 W. R. Keefer
U.S. Geological Survey
913 Federal Center
P.O. Box 25046
Denver, CO 80225

1 M. D. Voegele
Technical Project Officer for YMP
Science Applications International Corp.
101 Convention Center Dr.
Suite 407
Las Vegas, NV 89109

2 SAIC-T&MSS Library
Science Applications International Corp.
101 Convention Center Dr.
Suite 407
Las Vegas, NV 89109

2 L. D. Foust
Nevada Site Manager
TRW Environmental Safety Systems
101 Convention Center Drive
Suite 540, MS 423
Las Vegas, NV 89109

1 C. E. Ezra
YMP Support Project Manager
EG&G Energy Measurements, Inc.
MS V-02
P.O. Box 1912
Las Vegas, NV 89125

1 R. E. Jackson, Program Manager
Roy F. Weston, Inc.
955 L'Enfant Plaza, Southwest
Washington, DC 20024

1 Technical Information Center
Roy F. Weston, Inc.
955 L'Enfant Plaza, Southwest
Washington, DC 20024

1 D. Hedges, Vice President,
Quality Assurance
Roy F. Weston, Inc.
4425 Spring Mountain Road
Suite 300
Las Vegas, NV 89102

1 D. L. Fraser, General Manager
Reynolds Electrical & Engineering Co.
Mail Stop 555
P.O. Box 98521
Las Vegas, NV 89193-8521

1 R. F. Pritchett
Technical Project Officer for YMP
Reynolds Electrical & Engineering Co.
MS 408
P.O. Box 98521
Las Vegas, NV 89193-8521

1 B. W. Colston
President/General Manager
Las Vegas Branch
Raytheon Services Nevada
MS 416
P.O. Box 95487
Las Vegas, NV 89193-5487

1 R. L. Bullock
Technical Project Officer for YMP
Raytheon Services Nevada
Suite P250, MS 403
101 Convention Center Dr.
Las Vegas, NV 89109

1 R. E. Lowder
Technical Project Officer for YMP
MAC Technical Services
101 Convention Center Drive
Suite 1100
Las Vegas, NV 89109

1 Paul Eslinger, Manager
PASS Program
Pacific Northwest Laboratory
P.O. Box 999
Richland, WA 99352

1 A. T. Tamura
Science and Technology Division
Office of Scientific and Technical
Information
U.S. Department of Energy
P.O. Box 62
Oak Ridge, TN 37831

1 Carlos G. Bell, Jr.
Professor of Civil Engineering
Civil and Mechanical Engineering
Department
University of Nevada, Las Vegas
4505 South Maryland Parkway
Las Vegas, NV 89193-3478

1 C. F. Costa, Director
Nuclear Radiation Assessment
Division
U.S. Environmental Protection
Agency
Environmental Monitoring Systems
Laboratory
P.O. Box 93478
Las Vegas, NV 89193-3478

1 ONWI Library
Battelle Columbus Laboratory
Office of Nuclear Waste Isolation
505 King Avenue
Columbus, OH 43201

1 T. Hay, Executive Assistant
Office of the Governor
State of Nevada
Capitol Complex
Carson City, NV 89710

3 R. R. Loux, Jr.
Executive Director
Nuclear Waste Project Office
State of Nevada
Evergreen Center, Suite 252
1802 North Carson Street
Carson City, NV 89710

1 C. H. Johnson
Technical Program Manager
Nuclear Waste Project Office
State of Nevada
Evergreen Center, Suite 252
1802 North Carson Street
Carson City, NV 89710

1 John Fordham
Water Resources Center
Desert Research Institute
P.O. Box 60220
Reno, NV 89506

1 Dr. Martin Mifflin
Water Resources Center
Desert Research Institute
2505 Chandler Avenue, Suite 1
Las Vegas, NV 89120

1 Eric Anderson
Mountain West Research-
Southwest Inc.
2901 N. Central Ave. #1000
Phoenix, AZ 85012-2730

1 Department of Comprehensive
Planning
Clark County
225 Bridger Avenue, 7th Floor
Las Vegas, NV 89155

1 Planning Department
Nye County
P.O. Box 153
Tonopah, NV 89049

1 Lincoln County Commission
Lincoln County
P.O. Box 90
Pioche, NV 89043

5 Judy Foremaster
City of Caliente
P.O. Box 158
Caliente, NV 89008

1 Economic Development
Department
City of Las Vegas
400 East Stewart Avenue
Las Vegas, NV 89101

1 Community Planning &
Development
City of North Las Vegas
P.O. Box 4086
North Las Vegas, NV 89030

1 Director of Community Planning
City of Boulder City
P.O. Box 367
Boulder City, NV 89005

1 Commission of the European
Communities
200 Rue de la Loi
B-1049 Brussels
BELGIUM

2 M. J. Dorsey, Librarian
YMP Research and Study Center
Reynolds Electrical & Engineering
Co., Inc.
MS 407
P.O. Box 98521
Las Vegas, NV 89193-8521

1 Amy Anderson
Argonne National Laboratory
Building 362
9700 So. Cass Ave.
Argonne, IL 60439

1 Steve Bradhurst
P.O. Box 1510
Reno, NV 89505

1 Vernon Poe
P.O. Box 1026
Hawthorne, NV 89415

1 Jason Pitts
Lincoln County Courthouse
Pioche, NV 89043

1 Michael L. Baughman
35 Clark Road
Fiskdale, MA 01518

1 Glenn Van Roekel
Director of Community
Development
P.O. Box 158
Caliente, NV 89008

1 Ray Williams, Jr.
P.O. Box 10
Austin, NV 89310

1 Leonard J. Fiorenzi
P.O. Box 257
Eureka, NV 89316

1 Brad Mettam
P.O. Box 539
Goldfield, NV 89013

1 Bjorn Selinder
190 W. First St.
Fallon, NV 89406

1 Charles Thistlethwaite, AICP
Associate Planner
Planning Department
Drawer L
Independence, CA 93526

1 Richard Codell
U.S. Nuclear Regulatory
Commission
M/S 4-H-3
Washington, DC 20555

1 Seth M. Coplan
U.S. Nuclear Regulatory
Commission
M/S 4-H-3
Washington, DC 20555

1 Norman A. Eisenberg
U.S. Nuclear Regulatory
Commission
M/S 4-H-3
Washington, DC 20555

1 A. B. Gureghian
CNWRA
6220 Culebra Road
San Antonio, TX 78228-0510

1 Phil Justus
U. S. Nuclear Regulatory
Commission
M/S 4-H-3
Washington, DC 20555

1 Johan Andersson
SKI
Division of Nuclear Waste
Sehlstedtgatan II
Box 27106
S-102 52 Stockholm
SWEDEN

1 Michael J. Apted
Intera Sciences
3609 S. Wadsworth Blvd., 5th Fl.
Denver, CO 80235

1 Daniel B. Bullen
Iowa State University
P.O. Box 1768
Ames, IA 50010

1 Kevin Coppersmith
Geomatrix Consutants
100 Pine Street, 10th Floor
San Francisco, CA 94111

1 Allen G. Croff
Associate Director of Waste & Environmental Programs
Chemical Technology Division
Oak Ridge National Laboratory
Oak Ridge, TN 37831

2 A. L. Dudley
SPECTRA Research Institute
1603 University NE
Albuquerque, NM 87102

1 M.E. Harr
School of Civil Engineering
Pudue University
1284 Civing Engineering Building
West Lafayette, IN 47907-1284

1 Edwin E. Kinter
Bradley Hill Road
P.O. Box 682
Norwich, VT 05055

1 Robert Luce
Nuclear Waste Technical Review Board
1100 Wilson Blvd., Suite 910
Arlington, VA 22209

1 Edward A. Mason
Amoco Resource Center
P.O. Box 451
46 Admirals Lane
Osterville, MA 02655-0451

1 Russell McFarland
Nuclear Waste Technical Review Board
1100 Wilson Blvd., Suite 910
Arlington, VA 22209

1 Robin McGuire
Risk Engineering, Inc.
5255 Pine Ridge Road
Golden, CO 80403

1 Ian McKinley
NAGRA
Hardstrasse 73
Wettingen, CH-5430
SWITZERLAND

1 Fred W. McLafferty
Department of Chemistry
Cornell University
2600 Baker Laboratory
Ithaca, NY 14853-1301

1 Brad R. Mettam
Project Coordinator
County of Inyo
Yucca Mountain Repository Assessment Office
P.O. Drawer L
Independence, CA 93526

1 Ian Miller
Golder Associates, Inc.
4104 148th Avenue, N.E.
Redmond, WA 98052

1 F. Joseph Pearson, Jr.
1304 Walnut Hill La.
Suite 210
Irving, TX 75038

1 T. H. Pigford
University of California
Department of Nuclear Engineering
Berkeley, CA 94720

1 Norman C. Rasmussen
Massachusetts Institute of Technology
Department of Nuclear Engineering
Bldg. 24-205
Cambridge, MA 02139

1 Leon Reiter
Nuclear Waste Technical Review Board
1100 Wilson Blvd., Suite 910
Arlington, VA 22209-2297

1 Larry Rickertsen
TRW Environmental Safety Systems
2650 Park Tower Drive
Fairfax, VA 22033

1 Benjamin Ross
Disposal Safety, Inc.
1660 L Street, N.W., Suite 314
Washington, DC 20036

1 Frank W. Schwartz
195 Thornbury La.
Powell, OH 43065

1 Robert Shaw
Electric Power Research Institute
3412 Hillview Avenue
Palo Alto, CA 94304

1 Roger Staehle
University of Minnesota
Dept. of Chemical Engineering and Materials Science
22 Red Fox Road
North Oaks, MN 55127

1 Jane Stockey
U.S. Department of Energy
Forrestal RW-22, 7F-091/FORS
Washington, DC 20555

1 K. T. Thomas
National Academy of Science
2001 Wisconsin Ave., N.W.
Harris Bldg., Room 456
Washington, DC 20007

1 Robert F. Williams
EPRI, Nuclear Power Div.
P.O. Box 10412
3412 Hillview Ave.
Palo Alto, CA 94303

1 Tom Bjerstedt
Yucca Mountain Project Office
U.S. Department of Energy
P.O. Box 98608
M/S 523
Las Vegas, NV 89193-8518

1 Maxwell Blanchard
Yucca Mountain Project Office
P.O. Box 98608
M/S 523
Las Vegas, NV 89193-8518

5 Jeremy Boak
Yucca Mountain Project Office
U.S. Department of Energy
P.O. Box 98608
M/S 523
Las Vegas, NV 89193-8518

1 Scott Borg
Yucca Mountain Project Office
U.S. Department of Energy
P.O. Box 98608
M/S 523
Las Vegas, NV 89193-8518

1 J. Russell Dyer
Yucca Mountain Project Office
U.S. Department of Energy
P.O. Box 98608
M/S 523
Las Vegas, NV 89193-8518

1 Claudia Newbury
Yucca Mountain Project Office
U.S. Department of Energy
P.O. Box 98608
M/S 523
Las Vegas, NV 89193-8518

1 Ardyth Simmons
Yucca Mountain Project Office
U.S. Department of Energy
P.O. Box 98608
M/S 523
Las Vegas, NV 89193-8518

1 Scott Sinnock
TRW Environmental Safety Systems
101 Convention Center Drive
Suite P110
Las Vegas, NV 89109

1 Jean Younker
TRW Environmental Safety Systems
101 Convention Center Drive
Suite P110
Las Vegas, NV 89109

1 R. W. Nelson
INTERA-M&O
101 Convention Center Drive
Suite P110
Las Vegas, NV 89109

1 Suresh Pahwa
INTERA
6850 Austin Center Blvd.
Suite 300
Austin, TX 78731

1 Abraham Van Luik
INTERA-M&O
101 Convention Center Drive
Suite # P110
Las Vegas, NV 89109

1 W. W.-L. Lee
Lawrence Berkeley Laboratory
Earth Sciences Division
1 Cyclotron Road
Berkeley, CA 94720

1 T. N. Narasimhan
Lawrence Berkeley Laboratory
Earth Sciences Division
1 Cyclotron Road
Berkeley, CA 94720

1 Karsten Pruess
Lawrence Berkeley Laboratory
Earth Sciences Division
1 Cyclotron Road
Berkeley, CA 94720

1 C. F. Tsang
Lawrence Berkeley Laboratory
Earth Sciences Division
1 Cyclotron Road
Berkeley, CA 94720

1 Joseph Wang
Lawrence Berkeley Laboratory
Earth Sciences Division
1 Cyclotron Road
Berkeley, CA 94720

1 Thomas A. Buscheck
Lawrence Livermore National Laboratory
P.O. Box 808
M/S L206
Livermore, CA 94550

1 Dwayne Chesnut
Lawrence Livermore National Laboratory
P.O. Box 808
M/S L202
Livermore, CA 94551

1 William G. Halsey
Lawrence Livermore National Laboratory
P.O. Box 808
M/S L-204
Livermore, CA 94551

1 Annette MacIntyre
Lawrence Livermore National Laboratory
P.O. Box 808
M/S L-194
Livermore, CA 94551

1 William J. O'Connell
Lawrence Livermore National Laboratory
P.O. Box 808
M/S L-195
Livermore, CA 94551

1 Michael Revelli
Lawrence Livermore National Laboratory
P.O. Box 808
M/S L-206
Livermore, CA 94551

1 Richard Van Konynenburg
Lawrence Livermore National Laboratory
P.O. Box 808
Livermore, CA 94551

1 Bruce M. Crowe
Los Alamos National Laboratory/LV
101 Convention Center Drive
Suite 820
Las Vegas, NV 89109

1 Arend Meijer
Los Alamos National Laboratory
P.O. Box 1663
M/S J514
Los Alamos, NM 87545

1 Everett Springer
Los Alamos National Laboratory
P.O. Box 1663
M/S J495
Los Alamos, NM 87545

1 Aaron Thode
Los Alamos National Laboratory
M/S F607
P.O. Box 1663
Los Alamos, NM 87545

1 Greg Valentine
Los Alamos National Laboratory
P.O. Box 1663
M/S F665
Los Alamos, NM 87545

1 L. A. Doremus
Pacific Northwest Laboratory
P.O. Box 999
M/S K6-96
Richland, WA 99352

1 D. W. Engel
Pacific Northwest Laboratory
P.O. Box 999
M/S K7-34
Richland, WA 99352

1 T. B. Miley
Pacific Northwest Laboratory
P.O. Box 999
M/S K7-34
Richland, WA 99352

1 M. T. Murphy
Pacific Northwest Laboratory
P.O. Box 999
M/S K6-84
Richland, WA 99352

1 Will Nichols
Pacific Northwest Laboratory
P.O. Box 999
M/S K6-77
Richland, WA 99352

1 M. D. White
Pacific Northwest Laboratory
P.O. Box 999
M/S K6-77
Richland, WA 99352

1 U-S. Park
Science Applications International Corporation
101 Convention Center Drive
Las Vegas, NV 89109

1 Chris Pflum
Science Applications International Corporation
101 Convention Center Drive
Las Vegas, NV 89109

1 William Dudley
U.S. Geological Survey
P.O. Box 25046
M/S 425
Denver, CO 80225

1 Dwight Hoxie
U.S. Geological Survey
101 Convention Center Drive
Suite 860
Las Vegas, NV 89109

1 Ed Weeks
U. S. Geological Survey
P.O. Box 25046
Federal Center, M/S 413
Lakewood, CO 80225

1	6300	D. E. Miller
1	6302	T. E. Blejwas
2	6318	R. J. Macer for 100/12141/SAND91-2795/QA
1	6319	R. R. Richards
1	1502	J. C. Cummings
1	1511	J. S. Rottler
1	1511	P. L. Hopkins
1	1511	M. J. Martinez
1	1513	R. C. Dykhuizen
1	1513	R. R. Eaton
1	1513	R. D. Skocypec
1	6115	P. J. Hommert, Acting
1	6115	J. A. Fernandez
1	6115	R. J. Glass
1	6115	C. A. Rautman
1	6115	M. D. Siegel
1	6115	V. C. Tidwell
1	6312	F. W. Bingham
50	6312	R. W. Barnard
1	6312	G. E. Barr

1	6312	W. F. Chambers
10	6312	H. A. Dockery
1	6312	E. Dunn
3	6312	J. H. Gauthier
1	6312	P. G. Kaplan
1	6312	T. H. Robey
1	6312	K. C. Sanchez
1	6312	L. H. Skinner
10	6312	M. L. Wilson
1	6313	L. S. Costin
1	6313	M. E. Fewell
1	6313	E. E. Ryder
1	6313	S. R. Sobolik
1	6313	A. H. Treadway
1	6900	T. O. Hunter
5	7141	S. A. Landenberger
3	7151	G. C. Claycomb
8	7613-2	Document Processing for DOE/OSTI
1	7723	F. C. Lauffer
20	6341	WMT Library
1	6410	D. A. Dahlgren
1	8523-2	Central Technical Files

☆ U.S. GOVERNMENT PRINTING OFFICE: 1992—673-122/60163

SAND91-2795

The number in the lower right-hand corner is an accession number used for Office of Civilian Radioactive Waste Management purposes only. It should not be used when ordering this publication.

Org.	Bldg.	Name	Rec'd by	Org.	Bldg.	Name	Rec'd by

Sandia National Laboratories